Towards the Development of a Robotic Dexterity Assessment Framework

---

Mark W. Culleton

Department of Mechanical & Manufacturing Engineering

Parsons Building

Trinity College Dublin

The University of Dublin

Dublin 2

Ireland

July 2017

A thesis submitted to the University of Dublin in partial

fulfilment of the requirements for the degree of:

Doctor of Philosophy

Declaration

I declare that this thesis has not been submitted as an exercise for a degree at this or any other university and it is entirely my own work.

I agree to deposit this thesis in the University's open access institutional repository or allow the library to do so on my behalf, subject to Irish Copyright Legislation and Trinity College Library conditions of use and acknowledgement.

<div style="text-align: right;">

Mark Culleton,   July 2017

</div>

Abstract

The importance of flexible manufacturing processes and small-scale assembly is growing due to the increased pace of globalisation and greater consumer demands for product customisation. To address this trend, there has been increased interest in collaborative industrial robots that are better suited to work alongside humans in this changing environment. However, adoption of these robots within flexible manufacturing processes has been relatively slow, which can be, as demonstrated in this thesis, attributed to the current uncertainty around robotic dexterity. Dexterity is a key requirement if collaborative industrial robotics is to be useful within flexible manufacturing processes. However, an effective method for defining and measuring robotic dexterity is currently lacking, which has made it difficult for robotic integrators to introduce collaborative robots in these processes due to challenges in mapping their performance to the task assembly requirements.

The core hypothesis that underlies this work is that the adoption of industrial robots within flexible manufacturing processes can be facilitated by the development of a framework which comprehensively assesses robotic dexterity. This framework should consider the range of dexterous requirements within flexible manufacturing processes, and compliment current manufacturing assessment methods in order to maximise its scope and ease-of-use within the area.

To develop such a framework, this work explores and defines robotic dexterity within flexible manufacturing by abstracting influences from both the human and robotic dexterity literature. The demand for robotic dexterity is found to stem from the surrounding environment, and the classification tables within the Boothroyd-Dewhurst (B-D) design-for-assembly method are shown to comprehensively represent the range of possible operations within flexible manufacturing processes. Accordingly, this work

demonstrates that the dexterity of a robotic system within flexible manufacturing can be captured by considering the robotic system's ability to perform the operations identified within the B-D classification tables.

From this consideration of dexterity, the B-D tables are used to compose a robotic dexterity assessment framework that measures a robotic systems dexterity and determines its potential within flexible manufacturing operations. The framework develops robotic performance metrics which supersede supplier specifications and provide a greater insight into the dexterous ability of industrial robot systems. These metrics consider the dexterous requirements identified by the B-D tables, and their links to these tables simplify robotic integration within flexible manufacturing processes.

The capability of the developed framework is demonstrated using three scenarios commonly encountered within small-scale assembly. For each scenario, the framework provides a structured approach for analysing the scenario and evaluating robotic systems. An initial set of performance metrics is used to estimate the performance of different robotic systems, and physical testing is performed to validate the estimated results. In all scenarios, the developed framework provides an accurate estimate of the robot system's probability of success (PS) and task completion time (CT), which combine to characterise the dexterity of the robot system. These values are compared to normative data from B-D tables to determine the viability of each robotic system relative to human operators. Use of the framework demonstrates that a human operator is the most suitable choice in the majority of the considered scenarios, which supports the current dominance of manual labour within flexible manufacturing processes. Furthermore, the framework permits direct robotic system comparisons and helps to quantify the current gap between human and robot dexterity, which is an invaluable tool for robotic integrators and highlights the framework's potential for adoption within flexible manufacturing.

Acknowledgements

Firstly, I would like to express my sincerest thanks to my advisor Prof. Kevin Kelly for his continual support over the duration of my Ph.D. and related research. His patience, motivation, knowledge and guidance have helped me throughout my research and writing of this thesis. I could not have imagined having a better advisor and mentor.

A special thanks must be given to Elena Messina for the amazing opportunity to visit the National Institute of Standards and Technology (NIST) as a guest researcher during my research. I really appreciate the invitation and the organising that was required in order to make the visit happen. During my time at NIST, I worked within the Intelligent Systems Division and got to meet some amazing people. They made my time at NIST very enjoyable, and I thank them for the memories and lasting friendships. In particular I would like to extend my thanks to Joe Falco, Jeremy Marvel, Karl Van Wyk, and Rick Norcross. Without their stimulating discussions and continual support I would not have been able to conduct the research presented within this thesis.

In addition to visiting NIST, I also had the privilege of spending some time at Queen's University Belfast (QUB) under the guidance of Dr. Yan Jin. This collaboration opened up possibilities that were not possible within my home university, so I am truly grateful for the opportunity. During my time at QUB, Dr. Jin always made himself available to me and provided me with support when needed, so I extend him my sincerest gratitude.

Within my department, I would like to thank Prof. John Monaghan, Dr. Rocco Lupoi, Dr. Garret O'Donnell, Dr. Gareth Bennett, and Mr. Paul Normoyle for their guidance and assistance during my time in the Department of Mechanical and

Manufacturing Engineering. I would also like to extend a special gratitude to Dr. Conor McGinn for his dedicated support and tutelage throughout my research. His interest and work in robotics has helped to establish a robotics research group within the department, and I am truly appreciative of everything that he has done.

I have had the opportunity to work alongside a number of talented researchers during my Ph.D. and related research, and I would like to thank them for their continued friendship and input. In this regard, a special acknowledgement is given to Michael Cullinan, Aran Sena, Mark O'Regan Murphy, and Dr. Eoin Parle.

Outside of academia, I must also express my sincerest thanks to my housemates Jonathan Moran and Karen Mulligan. Their friendship and understanding throughout my research and write-up was invaluable, and I hope I can return the favour as they complete their own postgraduate degrees.

Last but by no means least, I would like to thank my family; my parents Martin and Eileen, my brothers Shane and Darragh, and my sister Helena for their endless love and kindness. In particular, I am forever indebted to my parents for their unfaltering belief and support throughout my life and these challenging few years. They have shaped me into the person I am today, which is why I would like to dedicate this thesis to them both.

Contents

List of Figures

List of Tables

Abbreviations

AGO Allegro Robotic Hand

BAX Baxter Robotic Manipulator

$B-D$ Boothroyd-Dewhurst

C Cognex Initialisation Approach

CL Confidence Level

CR Cognex + Registration Initialisation Approach

CT Completion Time

DFA Design-For-Assembly

DOF Degrees Of Freedom

H_0 Null Hypothesis

H_a Alternative Hypothesis

$HDAT$ Human Dexterity Assessment Tests

KGG Schunk KGG 80-30 Gripper

$LWR4$ KUKA LWR4 Robotic Manipulator

$MRMT$ Minnesota Rate of Manipulation Test

MTM Methods-Time Measurement

NSV Net Selling Value

$NIST$ National Institute of Standards and Technology

PAP Primary Assembly Process

PB Payback Period

POV Program Override Value

PS Probability of Success

R Robot Registration Initialisation Approach

$_r$ Random Search Strategy

RCC Remote Centre Compliance

RIQ Robotiq 3-Fingered Gripper

$_s$ Spiral Search Strategy

S Simulated Perception Error

SAP Secondary Assembly Process

$SMEs$ Small and Medium Sized Enterprises

T Teach Programming Initialisation Approach

TCP Tool Centre Point

$_q$ Quasi-Random Search Strategy

VAC Baxter Vacuum Gripper

YCB Yale - Carnegie Mellon - Berkeley

Operators

α — Significance level

$BINCDF$ — Binomial cumulative distribution function

d_{traj} — Linear trajectory distance of robot arm

d_{thresh} — Threshold trajectory distance at which a robotic arm reaches v_{prog}

E_a — Efficiency of an assembly process

e_x — Positional error in the x-direction

$invNorm$ — Inverse of the cumulative normal distribution function

μ — Population mean

s — Sample standard deviation

σ — Population standard deviation

Σ — Population covariance matrix

t_{traj} — Trajectory completion time of robot arm

v_{prog} Programmed linear velocity of a robotic manipulator

v_{traj} Linear velocity achieved by a robotic manipulator during a trajectory

$\bar{x}$ Sample mean

$z_{\alpha/2}$ Two-tailed z-score for a $(1 - \alpha)$ confidence level

Glossary

Agile Manufacturing Agile manufacturing is a manufacturing approach whereby a company's processes and structure are organised to enable a swift response to changing consumer needs and markets.

Alternative Hypothesis (H_a) The alternative hypothesis is used within statistical tests and is the opposing hypothesis to the null hypothesis. The alternative hypothesis is usually taken to be that there is a significant difference between the samples being considered due to a real effect during testing. In general H_a is the hypothesis that a statistical test is trying to prove.

Boothroyd-Dewhurst (B-D) Method The Boothroyd-Dewhurst (B-D) method is a design-for-assembly (DFA) method used to optimise and assembly process within manufacturing. The B-D method is the most commonly used DFA method, and optimises an assembly by minimising the number of parts, number of operations and their complexity.

Collaborative Robot   Within industry, collaborative robots refer to robotic systems that are able to share a workspace with humans. Since collaborative robots need to work alongside and/or with human co-workers, collaborate robots are designed to be inherently safe through mechanical design, smart control or a combination of both. The majority of collaborative robots are low payload and are easily programmable and transportable to facilitate their use within flexible manufacturing.

Completion Time (*CT*)   Robotic performance metric which corresponds to the time required by the robotic system to perform a given task successfully and in full.

Confidence Level (*CL*)   Within statistics, the confidence level is the probability that the value of a parameter falls within a specified range of values known as a confidence interval. While somewhat arbitrary, a 95% confidence level is commonly used within statistics and industry, which implies that you can be 95% certain that the corresponding confidence interval contains the true mean of a population.

Confidence Interval (*CI*)   See *Confidence Level (CL)*.

Design-for-assembly (DFA)   Design-for-assembly (DFA) methods are used within industry to optimize an assembly process. DFA methods reduce the overall cost of an assembly process by minimising the number of discrete operations, the number of parts, and the complexity of the remaining operations.

Dexterity   See *Robotic Dexterity*.

Degrees of freedom (DOF) The degrees of freedom (DOF) of a system are the number of independent parameters that describe its configuration. The degrees of freedom of a robot typically corresponds with the number of actuated joints or controllable degrees of freedom it possesses.

Flexible Manufacturing Flexible manufacturing refers to manufacturing processes that that incur changes at the macro level (e.g. in product volume and mix) and/or the micro level (e.g. disturbances in product geometry or material properties). Flexible manufacturing is part of the agile manufacturing approach, but its scope limited to the production of features, workpieces, and sub-products within manufacturing stations, cells, and/or segments.

Foreign Direct Investment (FDI) Foreign direct investment (FDI) occurs when a corporation invests in a foreign country by establishing a business operation or acquiring business assets (such as ownership or controlling interest in a local company).

Industrial Development Agency (IDA) Ireland Industrial Development Agency (IDA) Ireland is a Irish Government State Agency that focuses exclusively on the promotion and generation of high-quality Foreign Direct Investment (FDI) in Ireland.

Initialisation Time Robotic performance metric which corresponds to the time required to change a robotic system between one operation and another. This metric does not consider the initial development of the control program(s), but rather focuses on the time required to reprogram and/or teach the robotic system during integration.

Kolmogorov-Conover (KC) test
The Kolmogorov-Conover (KC) test is an extension of the KS test, and is used to determine if two discontinuous data sets belong to the same population.

Kolmogorov-Smirnov (KS) two-sample test
The Kolmogorov-Smirnov (KS) test is a non-parametric hypothesis test that is used to determine if two sets belong to the same population by measuring the maximum difference between the two cumulative distributions of the samples.

Margin of Error (E)
Margin of error (or tolerable error) refers to the sampling error present during testing and represents the maximum expected difference between a sample estimated parameter and the true population parameter. In statistics, the margin of error is usually defined as half the width of the confidence interval.

Methods-Time Measurement (MTM)
Methods-Time Measurement (MTM) is a predetermined motion time system that is used to identify the basic motions required during a manual assembly and quantify their time based on the motion's nature and the conditions of the motion.

Minnesota Rate of Manipulation Test (MRMT)
The MRMT is a standardised human dexterity assessment test used to analyse gross coordination and bilateral manual dexterity. The test has five subtests which require the subject to manipulate cylindrical blocks within and a perforated wooden board.

Net Selling Value
Net selling value (NSV) is the net amount (excluding VAT) invoiced to customers during product sales. This value includes amounts charged by enterprises to customers for transport of goods by their own vehicles and packaging costs.

Normal Distribution
A probability distribution that represents the distribution of a data set. A normal (or Gaussian) distribution is bell-shaped, where most values cluster around the mean and taper off symmetrically towards either extreme.

Null Hypothesis (H_0)
The null hypothesis is used within statistical tests and states that samples being considered are from the same population. Acceptance of the null hypothesis suggests that there is no statistical difference between the samples, and any differences can be attributed to random sampling error.

Payback Period (PB)
Within industry, the payback period refers to the elapsed time before the cost of an investment is recovered from the revenue or free cash flow it generates.

Primary Assembly Process (PAP)
A primary assembly process (PAP) is a process which directly contributes to the formation of a product e.g. part mating, energy costs and items of information.

Probability of Success (PS)
A robotic metric that indicates the likelihood that the robotic system will perform the task successfully. During testing, the PS can be determined for a given confidence level (CL) based on the number of successes and the number of independent trials.

Program Override Value (POV)
The program override value (POV) limits the velocity of a robotic arm during program execution, and is specified as a percentage of the robot's programmed velocity.

Remove Centre Compliance (RCC) — A remove centre compliance (RCC) is a mechanical device that is included between a robotic manipulator's wrist and tool to provide the tool with rotational and translational compliance.

Robotic Dexterity — Specific to flexible manufacturing, robotic dexterity refers to the ability of a robotic system to perform and adapt to the operations identified within the Boothroyd-Dewhurst classification tables in adequate time and in the presence of uncertainty. For each operation, the dexterity of a robotic system can be captured by considering its probability of success, initialisation time, and completion time. The probability of success identifies if the robotic system is dexterous enough to perform the operation based on the uncertainty present, while the initialisation and completion times represent the robotic system's level of dexterity. This level of dexterity is relative, and can be compared to the average human times tabulated within the B-D tables.

Secondary Assembly Process (SAP) — A secondary assembly process (SAP) is a process that is required during an assembly but does not directly contribute to the final product's realisation e.g. material handling, transfers, re-grasping, etc.

Small and Medium Sized Enterprises (SMEs) — Small and medium sized enterprises (SMEs) is a term which incorporates companies categorized as micro (employs fewer than 10 employees and whose annual turnover and/or annual balance sheet total does not exceed €2m), small (employs fewer than 50 employees and whose annual turnover and/or annual balance sheet total does not exceed €10m), and medium-sized (employs fewer than 250 employees and whose annual turnover and/or annual balance sheet total does not exceed €50m).

Tool Centre Point   The tool centre point (TCP) is the location on the tool of a
(TCP)   robotic manipulator whose position and orientation define the
                          tools coordinate system. Robotic velocities and positioning is
                          typically defined in relation to the TCP.

Workspace   The space within which a robotic system operates. This space
                          is defined by the set of points that the robotic system can reach.

Chapter 1

Introduction

1.1 Motivation and Challenges

Industrial robots are highly valued within industry due to their speed, repeatability, and lift capabilities [1]. Similar to other automated machines, industrial robots can operate continuously with high reliability and low cost. Consequently, these robots can greatly increase the output and efficiency of a manufacturing process, and their adoption within industry has allowed companies to stay competitive in an increasingly challenging global market.

While having many advantages, industrial robots traditionally required significant investment and dedicated assembly lines, which primarily made them suited for large-scale, high-volume manufacturing. However, with a growing importance in flexible manufacturing processes that can meet more stringent consumer demands [2], there has been an increased interest in industrial robots which can operate within this environment.

Low-payload, collaborate industrial robots have been introduced by robotic suppliers to address this demand. Unlike traditional robots, collaborative robots prioritise a different set of performance parameters which make them more suited to flexible manufacturing processes. Safety is the key requirement, as it allows the robot to work alongside human co-workers within a shared workspace. This opens robotics up to smaller scale manufacturing, which is an area that has seen little robotic integration to-date. Since the same benefits apply to collaborative robots, there is significant potential for the introduction of collaborative robots within this area. This is emphasised by the projected growth of collaborative robotics sector, which is

expected to increase from US $95 million in 2015 to over US $1 billion [3] in 2020. While a range of collaborative industrial robots are commercially available, their adoption within flexible manufacturing has been relatively slow. A primary reason for this is that the performance of collaborative robots within this area is unclear. Current robotic performance metrics were developed for traditional robots, and are consequently insufficient for determining the performance of robots within flexible manufacturing environments. This has made it difficult for companies to identify suitable robotic systems for a given task.

A key enabler of robotic integration within flexible manufacturing is robotic dexterity, as this helps to determine the range of operations that the robotic system can perform. However, robotic dexterity is difficult to comprehensively define and measure, which has led to ambiguity within the area. Without accepted measures, robotic dexterity is typically described qualitatively or using in-house (i.e. robot manufacturer) measurements. Consequently, it is currently challenging to identify and compare the dexterity of different robotic systems.

Motivated by these challenges, this work focuses on a framework for defining and measuring robotic dexterity within flexible manufacturing. The development of a dexterity assessment framework presents many additional challenges, as the framework needs to bridge the gap that currently exists between robotics research and industrial use. The framework must be comprehensive enough to capture the full extent of robotic dexterity, yet simple enough to be adopted by those within industry. In particular, the framework should provide dexterity measurements that are meaningful to those within industry and require minimal effort to use and/or understand.

An initial but important challenge for this framework is to clearly define dexterity and its contributing factors. This helps to identify the key components that need to be considered for a thorough yet concise assessment of dexterity. Based on these components, the framework must develop robotic performance metrics that are better suited for collaborative robots operating within flexible environments. These metrics need to be easily measured across the range of industrial robotic systems available, which requires the development of standardised test methods and artefacts. An additional challenge is that the resulting measures need be both informative and

easily related to flexible manufacturing processes if the framework is to simplify the robot selection process and facilitate the benchmarking of robotic systems.

1.2   Research Objectives

The overall objective of this work was to develop a dexterity assessment framework for robotic systems within flexible manufacturing that is both comprehensive and beneficial to those within industry. The core hypothesis that directed this objective was that the development of a suitable dexterity framework can facilitate the increased adoption of industrial robots within smaller scale manufacturing by establishing a link between robotic performance and flexible manufacturing processes.

To meet this objective, this work aimed to design and develop a dexterity assessment framework based on an in-depth analysis of both human and robotic dexterity. This analysis considered the range of dexterous requirements within flexible manufacturing processes, as their identification helped in the design of a suitable framework that compliments other manufacturing assessment tools and maximises its scope and usability. In addition, the resulting framework accounted for the challenges outlined above by designing and incorporating a number of standardised performance metrics and test methods. These performance metrics provided a greater insight into the dexterous ability of industrial robots within flexible manufacturing processes.

To validate the hypothesis, the developed framework was used to consider a number of robotic systems within flexible manufacturing scenarios. Each robotic system was analysed using the developed performance metrics, and their results incorporated within the developed framework to estimate the system's performance in the given scenarios. The objective in this instance was to calculate the dexterity of the robotic systems and identify their capability and suitability for each scenario. Equally important was to perform actual testing with each robotic system in order to quantify the accuracy of the estimated results and evaluate the usefulness of the developed framework.

1.3   Contribution of Thesis

The work presented within this thesis provides a novel contribution to the industrial robotics sector by developing a framework for assessing industrial robots and identifying their dexterity within flexible manufacturing. In the development of this framework, the following key contributions are made:

1. The Boothroyd-Dewhurst design-for-assembly method, an accepted standard for analysing manufacturing assembly, is extended and used to analyse dexterity assessments within robotics. This method is subsequently incorporated within a functional definition of robotic dexterity and is used to classify the dexterous requirements within flexible manufacturing processes.

2. Dexterity is explored from both human and robotic perspectives. This in-depth analysis identifies the scope of dexterity and addresses the current difficulty in defining the term and its contributing factors. A definition for robot dexterity within flexible manufacturing is presented, which identifies robotic dexterity as the ability of a robotic system to perform and adapt to the operations identified within the B-D tables in adequate time and in the presence of uncertainty. This functional definition is beneficial to both researchers and manufacturers as it encourages dexterity measurements that are more targeted and informative.

3. A framework for assessing the suitability of a robotic system within flexible manufacturing processes is developed. This framework incorporates the DFA method to aid in the development of relevant performance metrics and ensure a comprehensive dexterity assessment framework. The framework establishes a direct link between manufacturing operations and robot performance metrics, which addresses the current integration challenge and highlights the framework's potential within the manufacturing sector.

4. Test scenarios are proposed to benchmark robotic performance within flexible manufacturing and to validate the developed framework. These scenarios incorporate standardised test methods, artefacts and data analysis tools to facilitate the analysis and comparison of robotic systems. The benchmark tests

are used to assess a number of collaborative industrial robots. The numerical results provide an insight into the dexterity of each robotic system, and help to quantify the current gap between human and robotic dexterity which must be reduced if collaborate robots are to become a viable option within flexible manufacturing processes.

Chapter 2

Background and Literature Review

2.1 Preliminary Note

As noted in Section 1.3, one of the key contributions of this work is the exploration of dexterity and the development of a definition and measurement of robotic dexterity within flexible manufacturing. However, it useful at this stage to present a preliminary definition of flexible manufacturing and dexterity, as an understanding of these will assist the reader as they advance through the remainder of this chapter.

In this work, flexible manufacturing refers to manufacturing processes that incur changes at the macro level (e.g. in product volume and mix) and/or the micro level (e.g. disturbances in product geometry or material properties). It is a part of the agile manufacturing approach, whereby a company's processes and structure are organised to enable a swift response to changing consumer needs and markets. While agile manufacturing is employed at all stages of production, the scope of flexible manufacturing is limited to the production of features, workpieces, and sub-products within manufacturing stations, cells, and/or segments.

In general terms, dexterity refers to the ability of a system to "find a motor solution for any situation and in any condition" [4]. While this definition can refer to systems of varying scale, this work focuses on the dexterity of the hand and arm. Accordingly, robotic dexterity within flexible manufacturing can be defined at this stage as the ability of a robotic system to perform the range of operations within flexible manufacturing while overcoming any uncertainties that arise. As noted, this

is only a preliminary definition of robotic dexterity and will be updated in Chapter 3 based on the more in-depth analysis of dexterity performed in Section 2.5.

2.2 Manufacturing Overview

2.2.1 Manufacturing Sector

Manufacturing is a secondary economic activity that involves the value-added conversion of raw materials into finished goods through the use of labour, tools, machines, and other processes. It is a wealth producing activity, and accordingly is a key contributor to a country's economy during development and industrialisation. For modern-day societies with higher levels of socio-economic development, secondary activities typically account for 15% to 20% of the society's workforce distribution (see Figure 2.1).

2.2.2 Manufacturing within Ireland

Manufacturing is an important activity for ensuring Ireland's economic stability. In 2014, manufacturing supported the direct employment of 218,500 people and close to double that number when including indirect employment [7], [8]. The area amounted to 19.55% of Ireland's Gross Domestic Product (GDP) in 2013, and is a key driver of Research and Development (R&D) within Irish based firms. Action plans developed
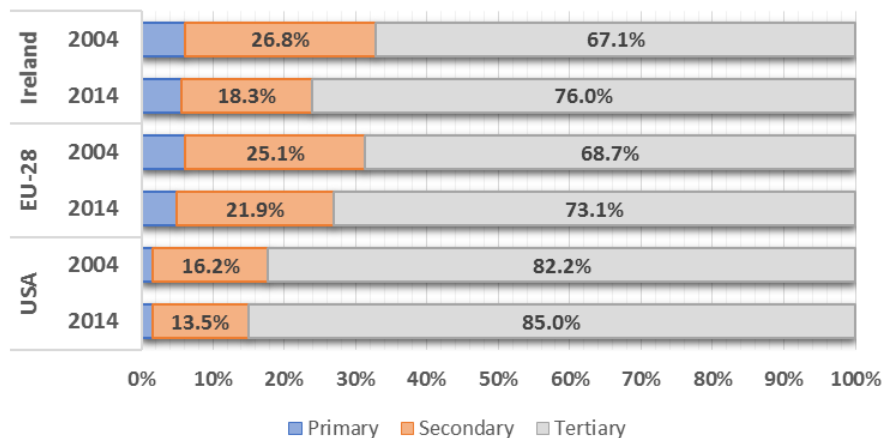
Figure 2.1: Persons in employment by economic activity (% of total employment). Data taken from [5], [6].

by the Government [9] and state agencies such as the Industrial Development Agency (IDA) Ireland [10] identify manufacturing as an important area for job generation and development within Ireland. This highlighted by the 10,000 jobs that were created during the two year period between 2012 and 2014 [8], [9] and IDA Ireland's plan to create 80,000 new jobs within manufacturing between 2015 and 2019 [11].

The primary sectors in which manufacturing firms operate within Ireland are shown in Figure 2.2. Of these sectors, Ireland has identified the food, medical technologies, (bio-)pharmaceutical, ICT, and engineering sectors as key areas for ensuring success in the future. Focus has been placed on these sectors as they address global trends and issues such as globalisation, ageing populations, environmental concerns, and changing consumption behaviours [9].

To establish Ireland as an advanced manufacturing centre within Europe, the Irish government are investing heavily within the manufacturing sector. For example, 20.7% of the total money spent by the government on R&D in 2014 (equivalent to €150.3m) was directly invested in industrial production and technology [13]. Furthermore, six of the fourteen key focus areas for competitive public research funding (as identified by the Research Prioritisation Steering Group) are directly related to manufacturing sector [14].
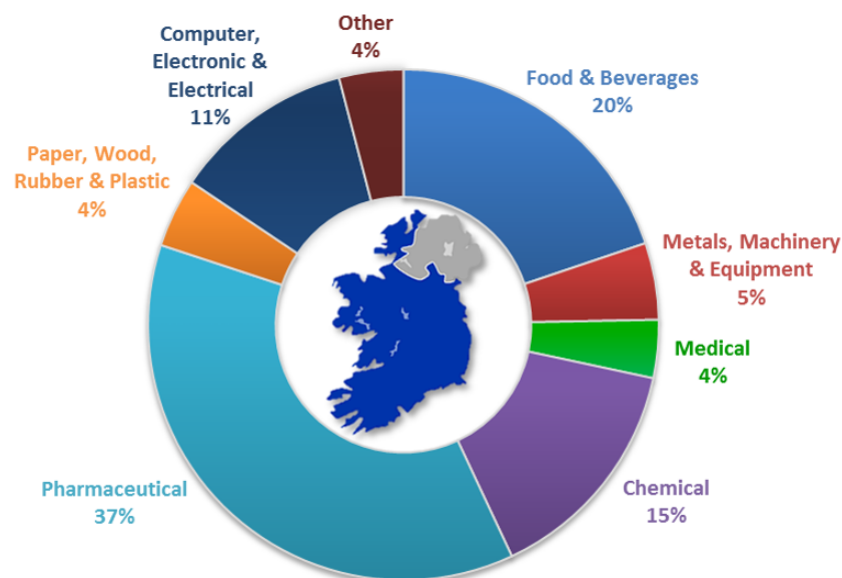
Figure 2.2: Breakdown of the total Net Selling Value (NSV) of Ireland's production by sector in 2015 (data from [12]).

While interest in manufacturing is growing, the level of robotic automation within Ireland is relatively low. One reason for this is the dominance of small and medium enterprises (SMEs), which account for 99.8% of the total number of enterprises within Ireland (see Figure 2.3) [15]. Due to their size, SMEs tend to utilise more flexible manufacturing processes that have traditionally favoured manual assembly over automation. However, as robotic technologies advance and more flexible and collaborative industrial robots are developed, there is significant potential for the adoption of industrial robots within these enterprises. This will be discussed in greater detail in Section 2.4.2.
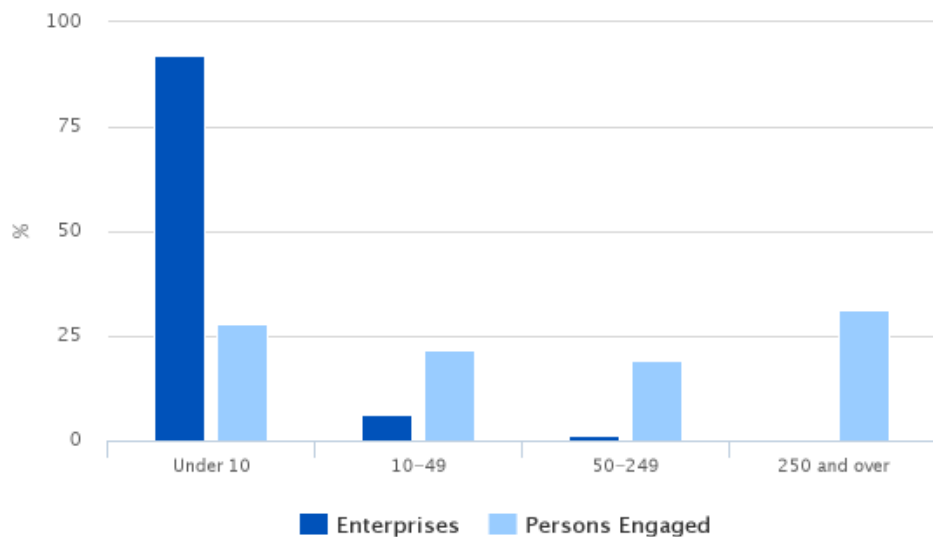
Figure 2.3: Distribution of enterprises and persons engaged within Ireland in 2014 (taken from [15]).

2.2.3   Manufacturing Processes

Within manufacturing, processes are classified according to six major groups [16]:

1. *Primary Shaping Processes:* The initial shaping of a product from an amorphous material. These processes form the general product shape e.g. casting, forging, and rolling.

2. *Secondary or Machining Processes:* Subsequent processes after primary processing which improve the basic shape and ensure it meets some of the products specifications e.g. milling, turning, and drilling.

3. *Metal Forming Processes:* The deformation and displacement of the metal to the required final shape. Achieved using suitable forces, pressures, and/or stresses at temperatures above (hot working) or below (cold working) the metal's recrystallisation temperature e.g. forging, rolling, extrusion, and drawing.

4. *Joining Processes:* The joining of parts together to form the product. Processes can result in a temporary, semi-permanent, or permanent joint, and are widely used within fabrication and assembly e.g. welding, soldering, adhesive bonding, and mechanical fastening.

5. *Surface Finishing Processes:* Processes which impart the specified surface finish by negligible material removal / addition e.g. polishing, grinding, and painting.

6. *Property Altering Processes:* Processes which change the material's microstructure to alter its mechanical properties e.g. annealing, tempering, and shot peening.

2.2.4   Manufacturing Systems

In general, a manufacturing process can be performed using manual labour, fixed automation, flexible automation, or some combination of these. With reference to Figures 2.4 and 2.5, the most suitable system for a manufacturer is dependent on a number of factors including:

- Availability and cost of labour
- Available capital
- Product variability
- Product life cycle
- Production volume

2.2.4.1   Manual Labour

A manual manufacturing system is performed by human operators with or without the aid of mechanical tools. Manual labour is particularly suited to production lines with high variability due to our natural problem solving ability and high levels of dexterity. This combined with low initialisation costs means that manual labour is typically used to meet low-volume production requirements of SMEs. However manual labour has its drawbacks, such as high operation costs and a human's inability to work consistently or continuously.

2.2.4.2   Fixed Automation

Fixed automation refers to specialised manufacturing systems that utilise special-purpose equipment to automate a sequence of operations. Since fixed automation is only efficient if the full manufacturing process is automated, individual operations are often performed by custom-engineered equipment to ensure constant and continuous production. Since the performable operations are restricted by the configuration of this equipment, fixed automation is relatively inflexible to changes to the production process. However, this system supports high production rates, which makes it particularly suited for manufacturing products with very high demands and volumes. Since a custom-engineered and dedicated manufacturing system requires significant initial investment, flexible automation only becomes an economically viable option
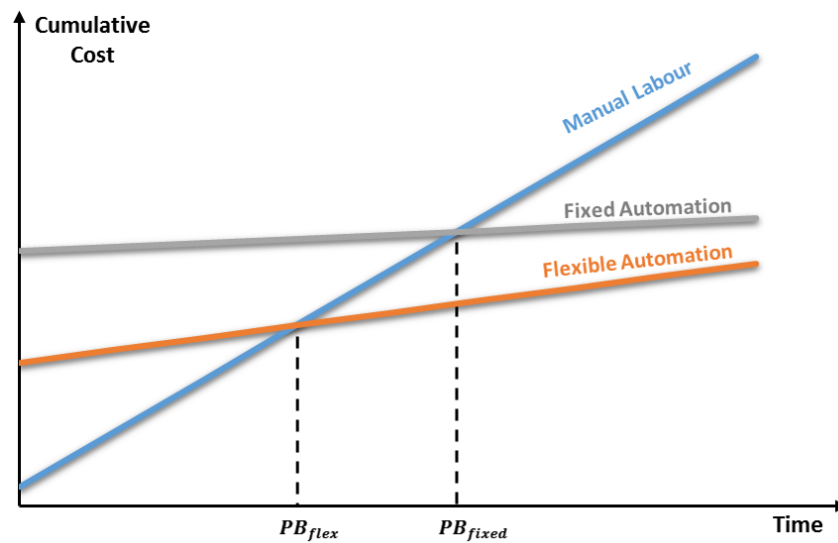
Figure 2.4: Example of cumulative cost (investment + labour + operating cost) for different types of production, showing the high initial investment required for automation and continual cost of manual labour. The time it takes to recover the cost of the investment is known as the payback period (PB) (generated with reference to [17]).

at these large production volumes thanks to economies of scale. Examples of fixed automation include the machining transfer lines commonly seen within the automotive sector and automatic assembly machines [18].

2.2.4.3 Programmable Automation

Programmable automation refers to productions which utilise equipment that are capable of changing the sequence of operations to accommodate product variations. As its name suggests, the operation sequence is controlled by a program which can be re-coded as necessary. Programmable automation has a relatively low production rate (compared to fixed automation), but is much more susceptible to variations in the production process. While the use of general-purpose equipment requires initial investment, programmable automation is typically used in low- and medium-volume batch production that require program and tool alterations between runs. This changeover means that downtime between batches is a feature of programmable automation. Examples of programmable automation includes computer numerical control (CNC) machines and industrial robots.
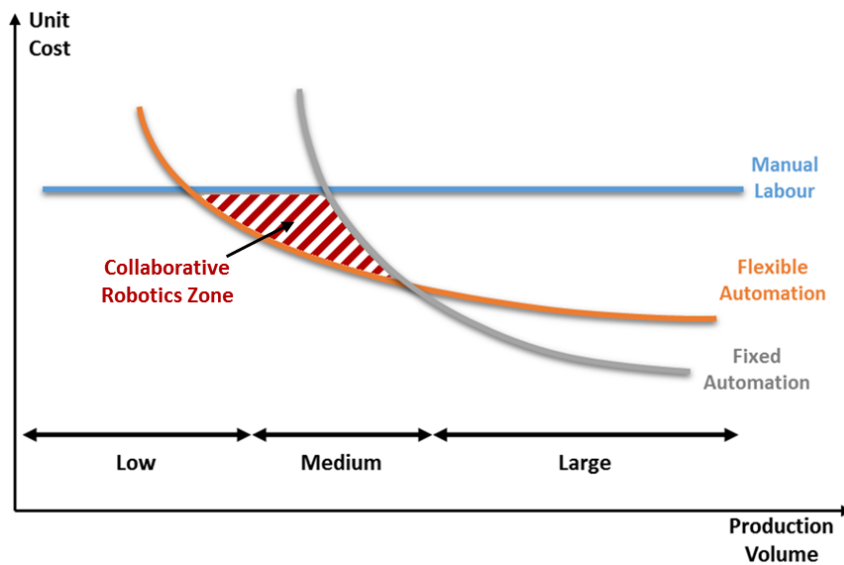
Figure 2.5: Example unit assembly cost for different types of production in relation to annual production volume (generated with reference to [19]). The highlighted zone shows the production volumes at which collaborative robots become a financially viable option.

2.2.4.4   Flexible Automation

Flexible automation is an extension of programmable automation. While flexible automation is a relatively new concept and its principles are still evolving, it is currently distinguishable from programmable automation in that it has the capability to switch between part programs and alter its physical setup with no loss in production time. Accordingly, flexible automation facilitates the continuous production of different product ranges or variations.

Similar to the other forms of automation, flexible automation requires high initial investment in order to procure the necessary equipment. However, its elimination of downtime allows flexible automation to achieve better production rates than programmable automation (but still not comparable to fixed automation). This makes flexible automation particularly suited to lower volume production, as highlighted in Figure 2.5. Examples of flexible automation are the flexible manufacturing systems (FMS) for performing machining operations and collaborative industrial robots.

2.2.5   Flexible Manufacturing

Due to global trends such as the increased pace of globalisation, growing competition, reduced product life cycles, and consumer demands for greater product customisation [1], [2], [9], [20] there is an increased interest in smart factories which will adopt more flexible manufacturing processes to improve their customisation capabilities and responsiveness to change.

As shown in Figure 2.6, manufacturing flexibility can be considered a part of agile manufacturing, which refers to the organisation of company's processes and structures to enable a swift response to changing consumer needs and markets. Within this hierarchy, flexibility incorporates the production of pieces and components within workstations, cells, and factory segments. In this sense, flexibility within manufacturing has been defined as the, *"operative ability of a manufacturing or assembly system to switch with minimal effort and delay within a pre-defined family of work pieces or sub-assemblies by re-programming, re-routing, or re-scheduling the same system"* [21]. Similarly in other work, manufacturing flexibility has been described as the ability to adaptively respond to changing circumstances or environmental uncertainty with minimal impact on time, effort, or performance [22]–[25].

As summarised by Jonsson in [25], manufacturing flexibility can be further broken
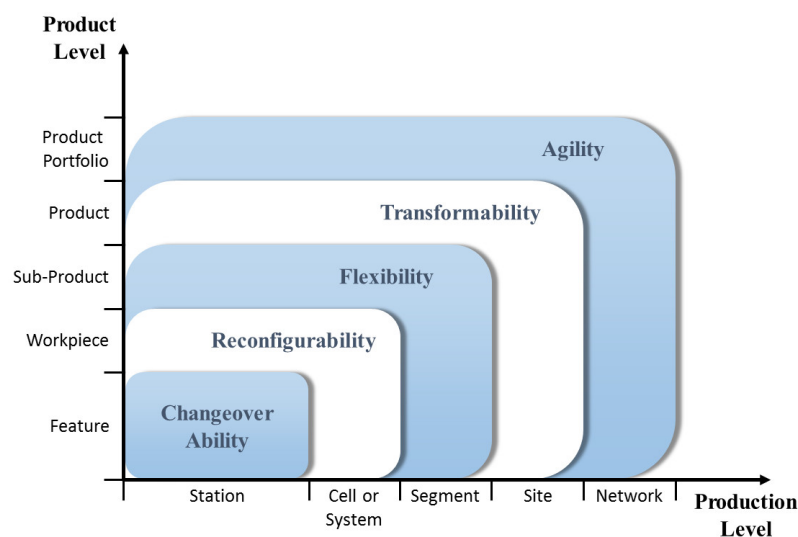
Figure 2.6: The hierarchy of production levels showing the relationship between changeover ability, reconfigurability, flexibility, transformability, and agility (adapted from [26]).

down by phases (e.g. value chain), hierarchy (e.g. machine level), or objects (e.g. products). Regardless of the type, flexibility has three elements [24], [25], [27]:

- Range: The range of products that can be produced by the manufacturing system

- Response: The ease (time, cost, etc.) at which the manufacturing system can respond to each product within this range

- Uniformity: The ability of the system to handle changes without impacting performance (e.g. quality and profitability)

Within this thesis, flexible manufacturing is the term used for a manufacturing environment that requires all or some of the three elements identified above. Accordingly, to perform within this environment a manufacturing system must be capable of responding to changes at the macro level (e.g. in product volume and mix) and micro level (e.g. disturbances in product geometry or material properties) [25]. With reference to Figure 2.6, flexible manufacturing requires flexibility, reconfigurability and changeover ability to enable the production of sub-products at station, cell, or segment level.

2.2.6 Manufacturing Assembly

Assembly is a particularly prevalent and important part of flexible manufacturing as it accounts for up to 30% of a product's manufacturing costs and 50% of its manufacturing time [28]. Of the different manufacturing systems presented in Section 2.2.4, manual labour is best suited for production lines with high variability and consequently is the most widely used assembly approach within this area. This is particularly true within SMEs, as small-scale, low-volume production currently makes manual assembly the most economically viable choice.

Within manual assembly, there are eight layouts commonly used which help to categorise the assembly process (see Figure 2.7). These layouts are dependent on the size of the parts being assembled and the tools required, but in general their floor space is minimised in order to optimise the assembly by reducing transport costs.
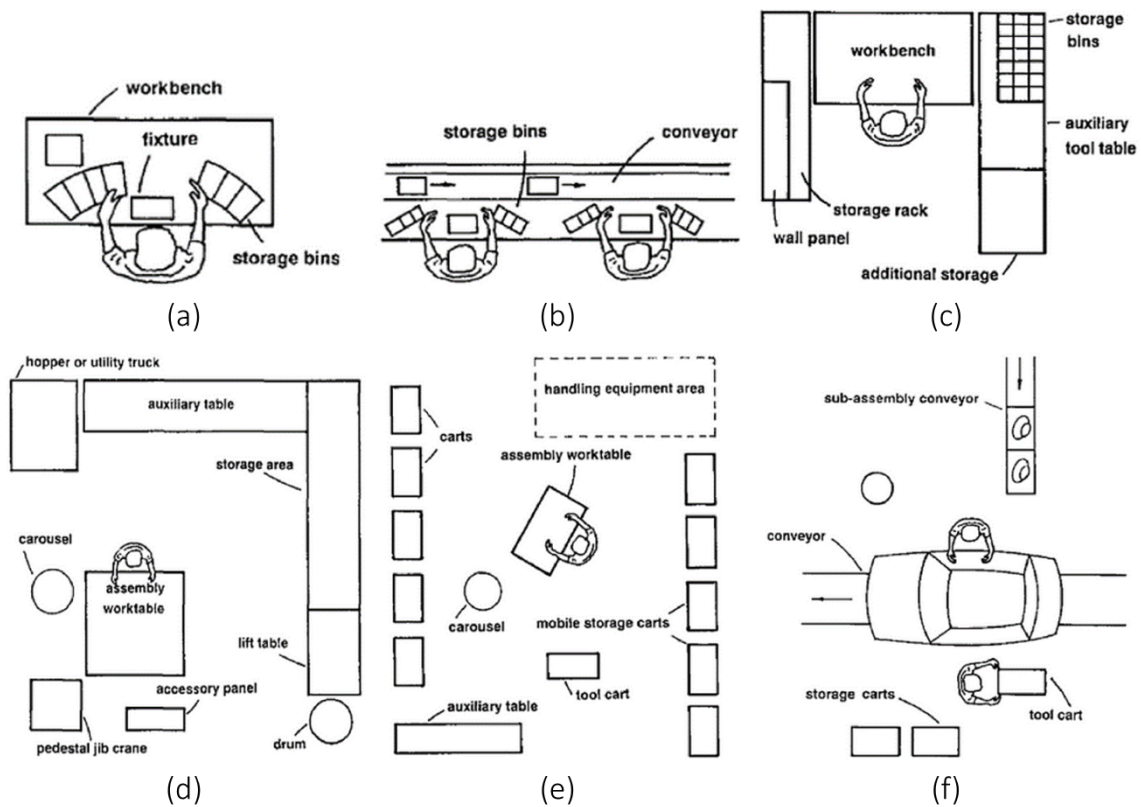
Figure 2.7: Assembly layouts defined by Boothroyd [29] (small to large scale): (a) Bench layout, (b) multi-station layout, (c) modular assembly layout, (d) custom assembly layout, (e) flexible assembly layout and (f) large multi-station layout. Other assembly layouts not shown are the very small assembly layout (e.g. clean room assembly) and assembly on site.

Accordingly, small-scale assemblies typically utilise the bench and multi-station layouts that do not require bending, turning, or walking during the process, while large-scale assemblies utilise the flexible and large multi-station layouts that allow parts to be stored, oriented, and fabricated with greater ease. Large-scale assemblies tend to require additional tools for transport and alignment, which further increases their required footprint. An assembly line is most commonly used within manual assembly. In this setup, the product moves along an automated line while operators perform their assembly tasks at designated workstations (i.e. multi-station layout). To optimise a manual assembly's layout, the complete process can be decomposed into Primary Assembly Processes (PAP) and Secondary Assembly Processes (SAP) [30]. The former refers to all operations which directly contribute to the formation of the product i.e. part mating, energy costs and items of information, while the
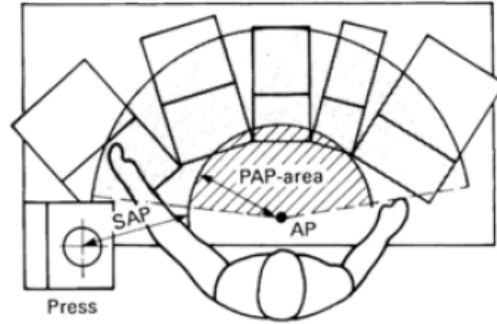
Figure 2.8: Bench assembly layout showing an operator's *PAP* and *SAP* areas based on the assembly position (AP). For assembly of relatively small parts, the *PAP* area has a radius of 35 cm (taken from [30]).

later refers to those operations which are required during an assembly but do not directly contribute to the final product's realisation e.g. material handling, transfers, re-grasping, etc. From [30], a distance threshold exists which identifies movements as either *PAP* or *SAP*. Figure 2.8 shows this distance threshold within a typical bench assembly layout. This transition point occurs at a distance of 35 cm for small-scale assemblies and 45 cm for large-scale assemblies. *PAP* and *SAP* are typically measured using time, and can be used to define the efficiency of an assembly process:

$$E_a = \frac{PAP}{PAP + SAP} \; x \; 100 \; (\%) \tag{2.1}$$

In addition to optimising an assembly's layout, the product being assembled and the operations being performed can be optimised to minimise assembly time and maximise profits. One valid approach to achieving this is to utilise established Design for Assembly (DFA) methods.

2.3   Design for Assembly

DFA methods aim to reduce the overall cost of an assembly process by minimising the number of discrete operations, the number of parts, and the complexity of the remaining operations. To optimise the assembly process, DFA methods typically assess each assembly operation and assign it a cost metric based on part shape, orientation, insertion direction, fastening processes and other conditions [31]. Consequently, one result of a DFA analysis is that an overall assembly is broken into its fundamental operations.

A number of DFA methods exist within industry today, including the Lucas DFA Method, the Hitachi Assembly Evaluation Method, the Modified Westinghouse Method, and the Boothroyd-Dewhurst (B-D) DFA Method.

The Hitachi Assembly Evaluation Method was developed by Hitachi Ltd. to rate the *assemblability* of a proposed design. The evaluation method focuses on 20 elements prevalent during fastening and insertion, and determines a design's suitability to assembly by calculating an *assemblability evaluation score (E)* and an *assembly cost ratio (K)*. The former represents the efficiency of an assembly which is calculated by reducing a score out of 100 for every assembly motion that is unnecessary or differs from a simple downward motion, while the latter represents the assembly cost improvements achieved through use of the evaluatoin method [32].

The Lucas DFA Method utilises penalty factors developed by researchers from Lucas and the University of Hull to give a relative measure of the assembly difficulty. Penalties are assigned during an in-depth product analysis and combined to calculate the overall design efficiency, feeding ratio, and fitting ratio of the assembly [31]. The use of penalty factors is similar to the Hitachi Assembly Evaluation Method, but their wider range facilitates the analysis of both handling and insertion operations.

The Modified Westinghouse Method was developed by Sturges [33] in Westinghouse Electric Corporation. This method includes a DFA calculator which considers nine factors to estimate the index of difficulty of a given assembly. This index of difficulty is combined with typical human motor responses in order to estimate the time required for each assembly operation. Building on the other DFA methods, the

factors are used to consider both acquisition (handling) difficulty and assembly (insertion) difficulty.

While the above methods are used within industry, the most widely used and accepted DFA method is the Boothroyd-Dewhurst DFA method [34], which builds on outcomes from the Methods-Time Measurement (*MTM*) system.

2.3.1 Methods-Time Measurement System

Methods-Time Measurement (*MTM*) is a predetermined motion time system that is used to identify the basic motions required during a manual assembly and quantify their time based on the motion's nature and the conditions of the motion. While a number of *MTM* system variations have been developed, the most commonly used and well-established system is the *MTM-1* system. For this system, time is measured using *TMU* (Time Measurement Unit), where:

$$1\,TMU = 10^{-6}\,hr = 0.036\,s \qquad (2.2)$$

The *MTM-1* system identifies five basic movements which have been shown to form 85% of variable operations within manufacturing assembly; reach, grasp, move, position, and release [30], [35]. A description of these movements and their corresponding lookup tables are given in Appendix A. The times given in these tables have been generated based on the human grasping range and from practical experience. For example, Figure 2.9 shows the recorded relationship between completion time and travel distance when performing a *Case B* reach movement. This type of reach movement is most common within manual assembly, and occurs when handling single objects whose location can vary slightly (refer to Appendix A).

By identifying the basic motions of an assembly and estimating their required time, the MTM-1 system enables designers to optimise an assembly process by removing unnecessary or lengthy motions.
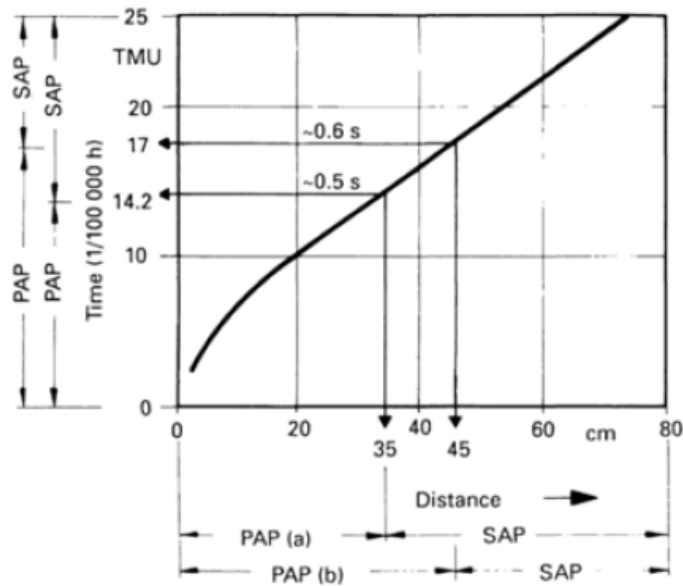
Figure 2.9: Time requirement for a reach (*Case B*) movement in relation to distance. Shown is the differentiation between *PAP* and *SAP* when (a) handling relatively small parts, and (b) handling relatively large parts (taken from [30]).

2.3.2 Boothroyd-Dewhurst DFA Method

The Boothroyd-Dewhurst (B-D) DFA method is used to minimise assembly times and costs by reducing the number of individual part components and optimising their design for handling and insertion [36]. As part of its optimisation approach, the B-D DFA method identifies the fundamental operations within manufacturing assembly and quantifies their difficulty using human completion times derived through empirical testing [29]. The results have been consolidated into two tables known as the B-D manual handling table and the B-D manual insertion table. A more in-depth discussion of these tables and their influential factors is given in [29], but an extract from the manual handling and insertion tables is shown in Figures 2.10 and 2.12 for reference. A summary of the factors given in [29] is given below.

Handling Factors

1. *Requirement:* The handling required to grasp and manipulate the object, which is dependent on the object's size, weight, and handling difficulty.

2. *Part Handling Difficulty:* Ease at which the part can be handled. Parts can present handling difficulties if they nest or tangle, stick together, are fragile, slippery, or require caution during handling.

3. *Part Symmetry:* Total rotational symmetry of a part $(\alpha + \beta)$. Alpha and beta equal the rotational symmetry of the part about an axis perpendicular and parallel to the axis of insertion (see Figure 2.11).

4. *Part Size:* Length of the longest side of the minimum bounding prism that encloses the part.

5. *Part Thickness:* Length of the shortest side of the minimum bounding prism that encloses the part.

6. *Part Weight:* Weight of the object to be manipulated. Becomes a factor when part is too heavy to be grasped and transported with one hand.

MANUAL HANDLING-ESTIMATED TIMES (s)

			Parts are easy to grasp and manipulate					Parts present handling difficulties (1)				
			Thickness >2 mm			Thickness ≤2 mm		Thickness >2 mm			Thickness ≤2 mm	
			Size >15 mm	6 mm ≤ size >15 mm	Size <6 mm	Size >6 mm	Size ≤6 mm	Size >15 mm	6 mm ≤ size ≤15 mm	Size <6 mm	Size >6 mm	Size ≤6 mm
			0	1	2	3	4	5	6	7	8	9
$(\alpha+\beta) < 360°$		0	1.13	1.43	1.88	1.69	2.18	1.84	2.17	2.65	2.45	2.98
$360° \leq (\alpha+\beta) < 540°$		1	1.5	1.8	2.25	2.06	2.55	2.25	2.57	3.06	3	3.38
$540° \leq (\alpha+\beta) < 720°$		2	1.8	2.1	2.55	2.36	2.85	2.57	2.9	3.38	3.18	3.7
$(\alpha+\beta) = 720°$		3	1.95	2.25	2.7	2.51	3	2.73	3.06	3.55	3.34	4

Key: One hand

Parts can be grasped and manipulated by one hand without the aid of grasping tools

Figure 2.10: Extract from the Boothroyd-Dewhurst manual handling tables, showing a number of factors which influence an operator's completion time during a one handed handling operation (© 1999 Boothroyd Dewhurst, Inc.).

α	0	180	180	90	360	360
β	0	0	90	180	0	360
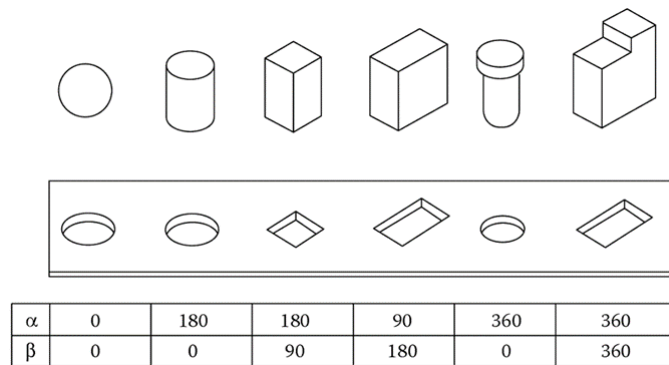
Figure 2.11: Alpha and beta rotational symmetries for various parts (taken from [29]).

Insertion Factors

1. *Ease of Reach:* Ease at which the parts and associated tool (including hands) can reach the desired location. Obstructed access means that the space available for the insertion causes a significant increase in the assembly time. Restricted vision means the operator has to rely mainly on tactile sensing during insertion.

2. *Insertion Resistance:* Resistance encountered during part insertion. Resistance can be due to small clearances, jamming or wedging, hang-up conditions, or insertion against a large force.

3. *Alignment & Positioning:* Parts are easy to align and position if the position of the part is established by locating features on the part or its mating part, and if insertion is aided by well-designed chamfers or similar features.

4. *Holding Requirement:* Holding down required means that the part is unstable after insertion and will require gripping, realignment or holding down in subsequent operations before it is finally secured.

5. *Fastening Processes:* How the parts are finally secured, which can be done either immediately after insertion or as a separate operation.

MANUAL INSERTION-ESTIMATED TIMES (s)

			Alter assembly no holding down required to maintain orientation and location (3)				Holding down required during subsequent processes to maintain orientation at location (3)			
			Easy to align and position during assembly (4)		Not easy to align or position during assembly		Easy to align and position during assembly (4)		Not easy to align or position during assembly	
			No resistance to insertion	Resistance to insertion (5)	No resistance to insertion	Resistance to insertion (5)	No resistance to insertion	Resistance to insertion (5)	No resistance to insertion	Resistance to insertion (5)
			0	1	2	3	6	7	8	9
	Part and associated tool (including hands) can easily reach the desired location	0	1.5	2.5	2.5	3.5	5.5	6.5	6.5	7.5
		1	4	5	5	6	8	9	9	10
	Due to obstructed access or restricted vision (2)	2	5.5	6.5	6.5	7.5	9.5	10.5	10.5	11.5

Key: Part added but not secured

Addition of any part (1) where neither the part itself not any other part is finally secured immediately

Part and associated tool (including hands) cannot easily reach the desired location

Due to obstructed access and restricted vision (2)

Figure 2.12: Extract from the Boothroyd-Dewhurst manual insertion tables, showing a number of factors which influence an operator's completion time during the joining of parts (© 1999 Boothroyd Dewhurst, Inc.).

Within the B-D DFA method, manual assembly efficiency (E_{ma}) is calculated using the equation [29]:

$$E_{ma} = N_{min}t_a/t_{ma} \tag{2.3}$$

where N_{min} is the theoretical minimum number of parts, t_a is the ideal assembly time for one part, and t_{ma} is the estimated time of the complete assembly process. The ideal assembly time refers to the minimum time necessary to assemble a part with no handling, insertion or fastening difficulties, and from Figures 2.10 and 2.12 corresponds to a combined assembly time of 3 s [29]. The theoretical minimum number of parts is determined based on the requirement that each added part must either move relative to all other parts assembled, be of a different material, or be separate to permit assembly [29], [37].

The manual handling times represent the time required by an operator to grasp, orient, and move a part to its receptacle, while the manual insertion times represent the time required to begin an insertion, pick up the tool (if required), complete the assembly operation, and replace the tool. When tools are required during an operation, the tabulated times assume that the most suitable tool is selected. This

includes the use of power tools where applicable. The time penalties associated with each individual factor are not necessarily additive. For example, if a part needs to be moved during mating, then it can probably be orientated during the move. This is accounted for within the tabulated times.

As noted, the times presented within the manual handling and insertion tables are based on empirical data. This data was collected over a period of years through experimentation [38] and represents the average time taken by a human to perform each classified operation. The number of parts and scenarios that fall into each operation classification can be quite large, which suggests that the tabulated times have a high variance. A study by MIT students has quantified this varience. While the study does not account for task proficiency, it still reports that the tabulated times are accurate to within about 10% [38]. The variance in operation completion time is acknowledged by Boothroyd and Dewhurst [29], but they note that any errors in using average time tend to cancel when analysing a full assembly process due to equal likelihood of overestimates and underestimates.

The B-D manual handling and insertion tables were generated for small-scale assembly which means that the tabulated times assume that all tools and parts are located within arm's reach of the operator and that no major body motions are required during the assembly process. Accordingly, the use of these tables is only valid when considering bench and multi-station assemblies. However, supplementary tables can be used when considering larger assembly layouts in order to account for acquisition time [29].

While the B-D DFA method is mainly used within manual assembly, it can also be used to analyse high-speed and general-purpose (robotic) automation assemblies. In these scenarios, the B-D method identifies the overall assembly cost by considering the cost of feeding and orienting individual parts and the cost of automatically inserting those parts [39]. The former is achieved by estimating orienting efficiency and relative feeder cost based on each part's symmetry and defining features, while the latter is achieved by estimating the relative costs, times and penalties that stem from the base robot, gripper / tool selection, and insertion operation. As before, Boothroyd and Dewhurst develop classification tables to assist in the analysis of these automated

assemblies, however the tabulated values are only relative and are therefore of limited use without full knowledge of the assembly equipment and production strategy. In addition, the tables were first published in 1986 [39] and so were developed with traditional fixed and flexible automation in mind. As a consequence, the generated classification tables assume the presence of dedicated assembly lines and axillary equipment such as feed tracks and part placement mechanisms. These assumptions limit the usefulness of the automated classification tables when considering robotic systems within flexible manufacturing.

2.4   Robotics Overview

2.4.1   Brief History of Robotics

Karel Čapek first coined the term *'robot'* during his science-fiction play *R.U.R.* (*Rossumovi Univerzální Roboti* or *Rossum's Universal Robots*). The term stems from the Czech word *'robota'*, which was used at that time to describe a serf or forced agricultural labourer [40], [41]. The robots within *R.U.R.* were biological beings that were developed by Rossum as subservient workers. However, the robots came to realise that they were stronger than their masters and eventually rose up against them.

Čapek's play was important as it helped to shape the notion of robot. The themes explored within *R.U.R.*, such as freedom, love and destruction, have since become very common when depicting robots within the science fiction genre. Isaac Asimov, a well-known Russian science fiction writer, helped to popularise robots this genre. Asimov published a collection of short stories on robots between 1938 and 1942 [42], and was the first to introduce the metallurgic robot commonly perceived today. In his 1942 short story *'Runaround'*, Asimov introduced the term *'robotics'*, which refers to the study of robots based on three fundamental laws. These laws govern a robot's behaviour, and have been widely cited within robotic literature as they are regarded as the ethical foundation for the field [43].

1. *"A robot may not injure a human being or, through interaction, allow a human being to come to harm"*

2. *"A robot must obey orders given to it by human beings, except where such orders would conflict with the first law"*

3. *"A robot must protect its own existence as long as such protection does not conflict with the first or second law"*

Since then, public interest in robotics has amplified and robots have become commonplace within science fiction, being portrayed as both friend (e.g. *Star Wars*, *Wall-E*, *Chappie*) and foe (e.g. *The Terminator*, *I, Robot*, *Ex Machina*). However, regardless of their moral compass, the robots depicted are highly advanced machines.

Figure 2.13: A scene from Karel Čapek's science fiction play R.U.R. showing three robots.
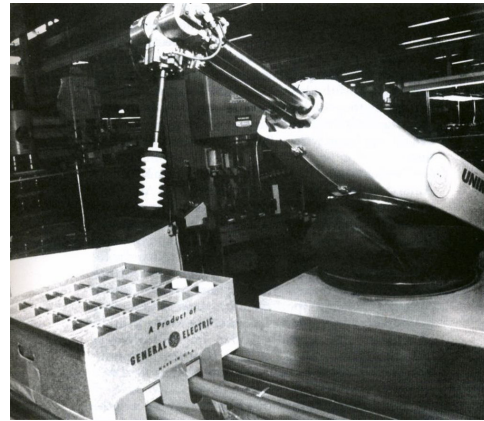
Figure 2.14: 'UNIMATE' - The first, fully automatic robot which was developed by General Motors and deployed in 1961.

This has led to a general misconception with regards to the current capability and intelligence of robots.

The first, fully automated robot, called *UNIMATE*, was built by General Motors in 1958 and deployed within the automotive sector in 1961. The robot was integrated along the assembly line as an automated die-casting mould robot which sequenced and stacked hot pieces of die-cast metal [44].

Since this introduction, automated robots have become an integral part of the industrial sector due to their suitability for repetitive, dangerous and high accuracy tasks. In addition, thanks to advancing technologies and increased public interest, robots have started to appear in other sectors such as the medical, aerospace, and domestic sectors. With greater mobility, versatility, and human-like characteristics [45], these robots can perform a wider range of operations and provide people with greater independence and quality of life. Accordingly, it is envisaged that the number of robots and their impact on day-to-day life will continue to grow over the coming years.

2.4.2   Industrial Robots

Within industry, robots are classified according to their mechanical configuration and workspace volume. As shown in Figure 2.15, there are five main types of industrial robot:

1. Articulated Robot: A robot whose arm has at least 3 rotary joints. Typically, operations performed by this type of robot include assembly, die casting, welding, and painting. Articulated robots are by far the most commonly used robot within industry (68% of market share in 2011 [46]).

2. SCARA Robot: A Selective Compliance Assembly Robot Arm (SCARA) which has two parallel rotary joints to provide compliance in a plane. Typical operations performed by this type of robot include part handling, palletising, and assembly.

3. Cylindrical Robot: A robot whose axes form a cylindrical coordinate system. Typical operations performed by this type of robot include assembly, part handling, and welding.

4. Linear Robot: Includes Cartesian and Gantry robots, and refers to robots that have three prismatic joints whose axes are coincident with a Cartesian coordinator. Typical operations performed by this type of robot include pick-and-place, adhesive application, machine tool loading, and part stacking.

5. Parallel Robot: A robot with a single base whose two or more arms have concurrent prismatic or rotary joints. Typical operations performed by this type of robot include simulation, high-accuracy alignment, and milling.

Since their introduction, industrial robots have played a crucial part in the increased productivity and output from the manufacturing sector (see Figure 2.16). This can be accredited to the inherent advantages of robots, such as their high speeds, levels of precision, repeatability, payload, and ability to operate continuously [1]. However, robot integration within manufacturing traditionally required significant investment due to their requirement for dedicated workspaces. This meant that
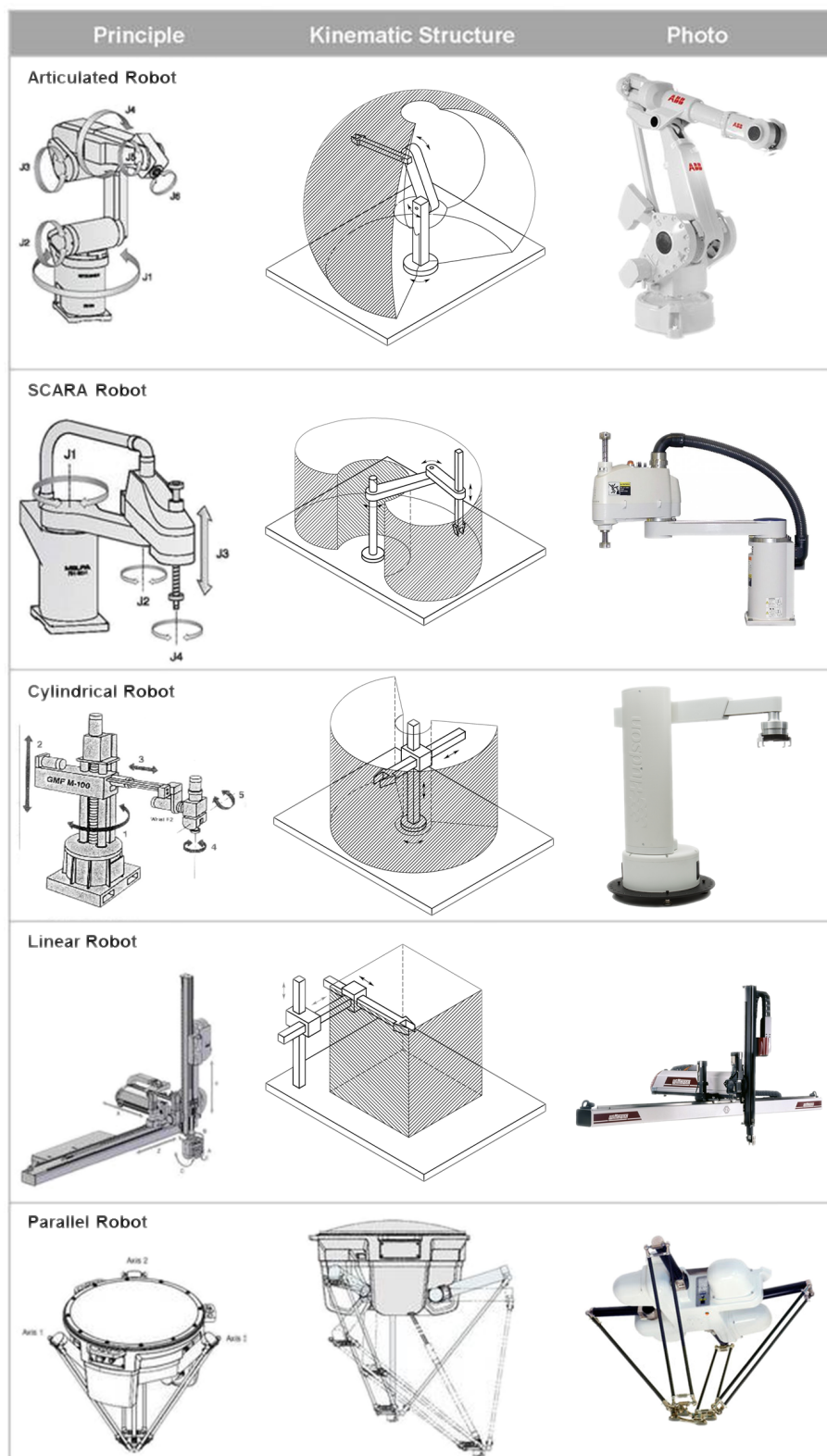
Figure 2.15: Types of industrial robot based on mechanical configuration (generated with reference to [45], [47]).
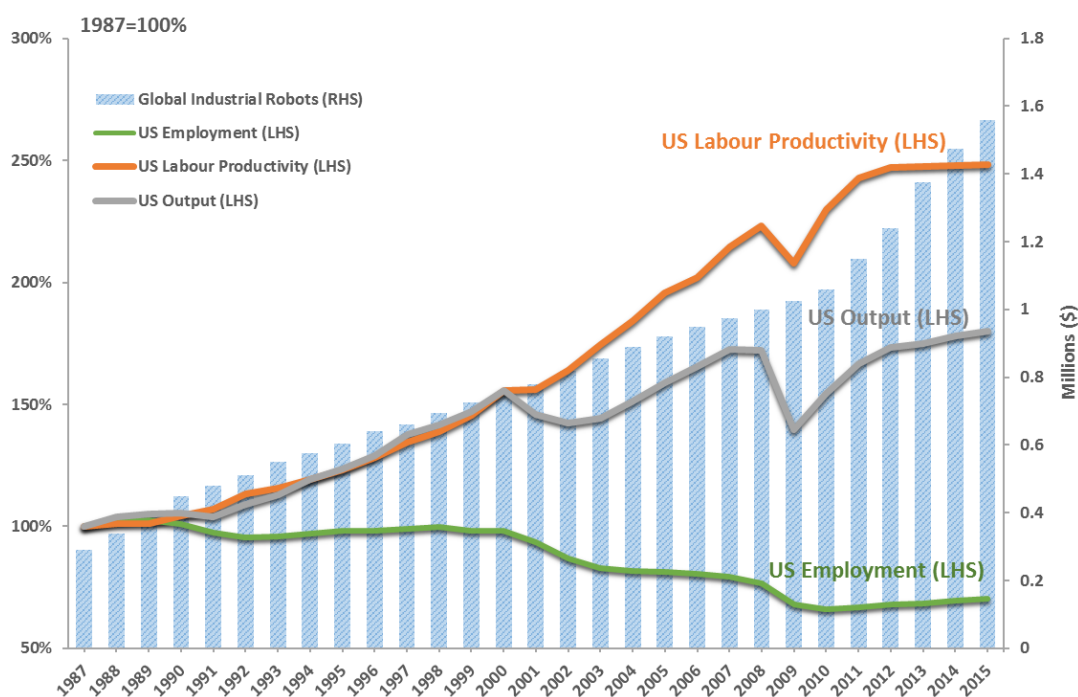
Figure 2.16: Global estimated operational stock of industrial robots combined with annual changes in U.S. manufacturing productivity, output, and employment between 1987 and 2015 (data from [48], [49]).

setup costs not only included the purchasing of expensive robotic systems, but also the redesigning the manufacturing process and the procuring of auxiliary equipment such as automated part feeders, safety cages, etc. Accordingly, industrial robots were initially used within large-scale manufacturing, and were particularly prominent within the automotive sector. This remains the case today, as the majority of industrial robots purchased are still deployed within this area (see Figure 2.17). This also accounts for the dominance of articulated and Cartesian robots, which are particularly useful within traditionally heavy industries.

However with the current manufacturing trends, there is a growing necessity for robots that are better suited to small-scale, flexible manufacturing. This is highlighted by recent funding initiatives and competitions [52]–[54], industrial action plans [1], [2], and the continued introduction of collaborative industrial robots [55].
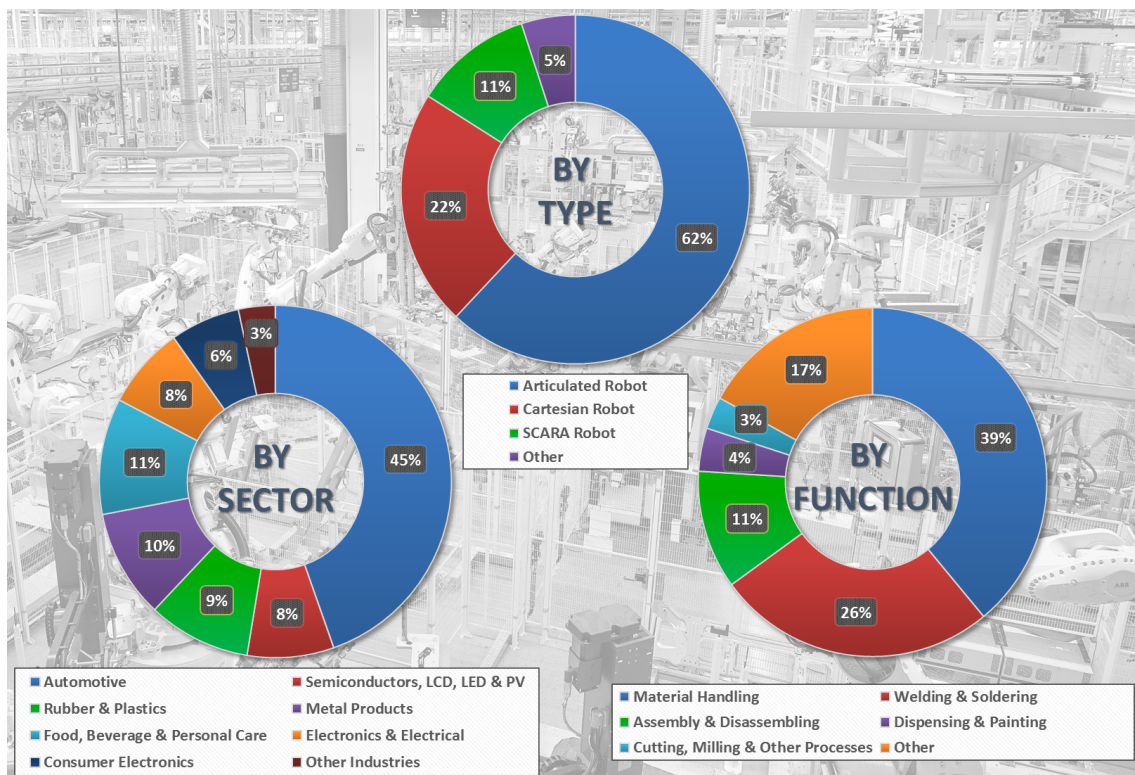
Figure 2.17: The world market for industrial robots by manufacturing sector, robot type, and robot function (data from [50], [51]).

2.4.3 Collaborative Robots

Collaborative industrial robots refer to those robotic systems that can share a workspace with humans. At present, collaborative robots only represent 5% of the global robots market, however forecasts predict that this figure will grow to 30% by 2018 [56]. This significant growth in the importance of collaborative robots is supported by estimated sales of collaborative robots, which is expected to increase tenfold from US $95 million to over US $1 billion between 2015 and 2020 (see Figure 2.18) [3].

These collaborative robots differ from traditional robots in that they prioritise performance parameters such as safety, dexterity, flexibility, ease-of-use, inexpensiveness, and throughput (speed of the full manufacturing process, which includes setup times, acquisition times, etc.) [58]. Inherent safety is of primary importance, as these robots must share a workspace with human co-workers. While a range of collaborative robots are commercially available [55], there is still significant research being conducted to improve the robot's performance in each of the metrics listed above.
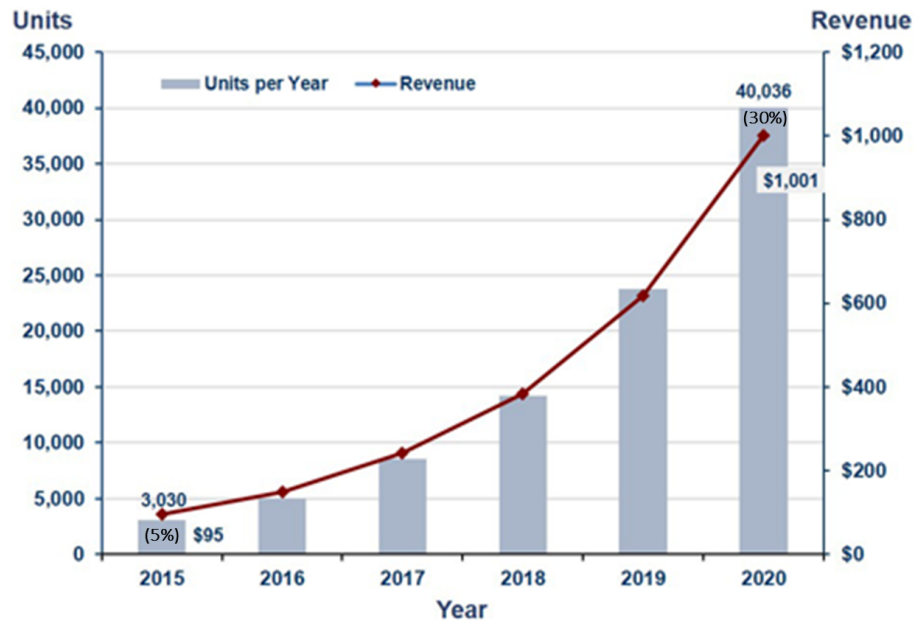
Figure 2.18: The estimated increase in collaborative robot sales between 2015 and 2020 (source: ABI Research [57]).

2.4.4 Robotics Research

There has been major investment in robotics over recent years thanks to increased public interest. This combined with advances in supporting technology such as actuation, sensing, and circuitry has allowed researchers to develop more advanced robotic systems that are better suited to flexible manufacturing.

2.4.4.1 Safety

As noted, a key area for collaborative robots is the area of safety, as robots working alongside humans should adhere to Asimov's first law and not harm their human co-workers. Accordingly, human-robot interaction (HRI) is an important area of focus within research. A collaborative robot is often made inherently safe through mechanical design, smart control or a combination of both. The former mitigates the severity of a collision by introducing passive compliance to the robot's mechanical structure. This is achieved by choosing softer materials, rounded surfaces, and incorporating back-drivable joints (e.g. series elastic actuators). The latter provides active compliance to ensure motions are both power and force limited. Sensing can also be used to prevent collisions by enabling the robot to react in real-time to its

surrounding environment. Research within this area included collision avoidance [59], prediction-based reactive control [60], and human centred motion-planning [61], [62]. The latter aids with HRI by selecting robot motions and poses that resemble those made by a human, which allows human co-workers to anticipate the robot's intent and react accordingly. This is particularly important during human-robot hand-overs, which is why methods have been developed to try to emulate a natural transition [63].

An alternative design approach is to reduce the weight of the robot in order to minimise its momentum during trajectories. However, the robot must still be capable of lifting equivalent payloads, which is why a robot's power-to-weight ratio is of interest within research. Stemming from this, actuators such as 'Smart Motors' and 'Air Muscles' have been developed [64]. The latter is the general term given to pneumatically driven artificial muscle actuators. These actuators were first developed in the 1950's by J.L. McKibben, and over recent years have become highly desirable in robotic applications thanks to their significant power to weight ratio of 400:1 [65]. To shift the weight of robotic end effectors further up the arm, robotic hands are being developed which are actuated via wire tendons rather than a gear array. While this is less desirable for power grasps, the removal of the actuators from the point of motion allows the robotic hand to more easily match the size and weight of a human hand [66], [67]. This is beneficial as it allows the robot hand to interact with tools already developed for humans, as shown in Figure 2.19.

The external actuator location of wire driven hands is also advantageous as it removes space limitations. Accordingly, there are fewer restrictions on the number of actuators, which means that the robot hand can more easily obtain a high number of degrees of freedom (DOF). For example, by moving its actuators to the wrist, the Shadow Dexterous Hand C6M was able to achieve 20 independent DOF [68]. In addition, the freed internal space facilitates sensor integration. As shown in Figure 2.20, this enables the hand to perform force controlled grasping which is particularly important when handling fragile objects within manufacturing.

Safety requirements within the field of industrial robots are defined within ISO 10218-1 and ISO 10218-2 (Robots and robotic devices - Safety requirements for
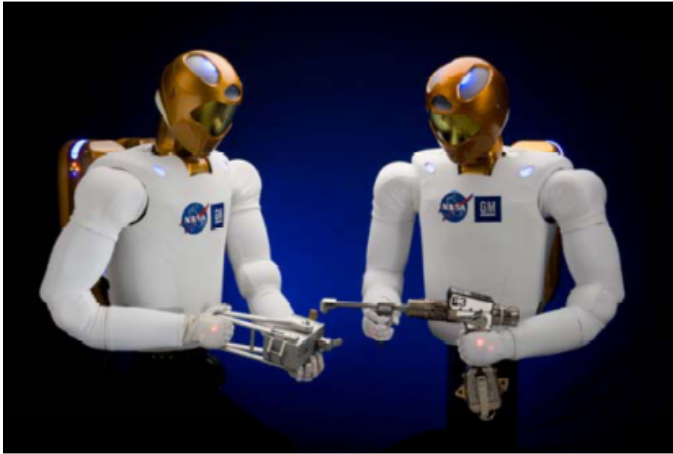
Figure 2.19: NASA's Robonaut 2 using hand tools (taken from [69]).

Figure 2.20: Shadow Dexterous Hand C6M gripping a light bulb (taken from [64]).

industrial robot - Part 1 and 2). Part 1 is for manufacturers of robots and outlines safety requirements of the manipulator, controller and their use. At this stage the robot is considered partly completed machinery. Part 2 is for the integrators of robotic systems, and outlines the safety requirements of the complete robotic system including the tooling, workpieces, surrounding environment, and safeguards. An integrated and installed robot is considered a complete machine. The standard was published in 2011, and was primarily developed for more traditional, large-scale industrial robots that are isolated from human co-workers.

SO 10218-1 is harmonised under the European Machinery Directive 2006/42/EC and it specifically states that a robot can be used for collaborative operation (i.e. without safety guards between the robot and the operator) if it is in compliance with Clause 5.10.5. This clause states that the robot must have sufficient power and force limiting by inherent design or control to ensure limited static and dynamic forces are imparted in contact events.

A technical specification ISO/TS 15066 (Robots and robotic devices - Collaborative robots) has since been released to specify the safety requirements for collaborative industrial robots and the work environment. While not a standard, this specification provides valuable guidance on risk assessment for the integrators of collaborative robots, discussing important considerations such as maximum robot speed, safety-rated sensing capabilities, power and force limiting capabilities, pain thresholds, and

operator control methods.

2.4.4.2   Throughput

Current industrial robots excel in large scale manufacturing as they can perform high volume tasks repetitively. Once the robot is set up, it can execute the operation(s) at speeds unobtainable by humans and thus has a favourable throughput. However, in small-scale manufacturing where changeovers are more frequent, the robot's setup time has a greater influence on its throughput. A more flexible robot will be able to react to changes in the production process with little downtime, while a less flexible robot will not. Hence, in order to have satisfactory throughput within flexible manufacturing, it is important that the robot have an inherent level of flexibility to minimise or negate setup times.

To try to develop more flexible industrial robots, a number of robotic hands have been developed which can perform a range of human hand motions at human-equivalent speeds e.g. the Barrett Hand [70] and the Keio Hand [71]. Robotic manipulators have also been developed, such as the hand-arm system used by the Ishikawa Watanabe Laboratory from the University of Tokyo (see Figure 2.21) [72]. This system can perform high-speed movements, with a maximum manipulator TCP velocity of $6\,ms^{-1}$ and a maximum finger velocity $1800\,deg/s$ [72]. In addition, the hand utilises a high-speed camera whose feedback and parallel control processing allows for a $1\,ms$ reaction time. This high-speed sensory-motor fusion allows the system to perform skilful manipulations and operate within unpredictable environments. While the system does not have the necessary payload capabilities for typical industrial applications, it shows the potential for robotic systems which can react in real-time to unexpected changes along a production line.

Effective control strategies are critical if a robotic system is to be adaptable. Manipulation control has seen significant advancement over recent years, which can be attributed to the addressing of three important engineering challenges [74]:

1. Optimal manipulation synthesis problem

2. Coordinated manipulation with finger gaiting

3. Real-time grasping force optimisation problem
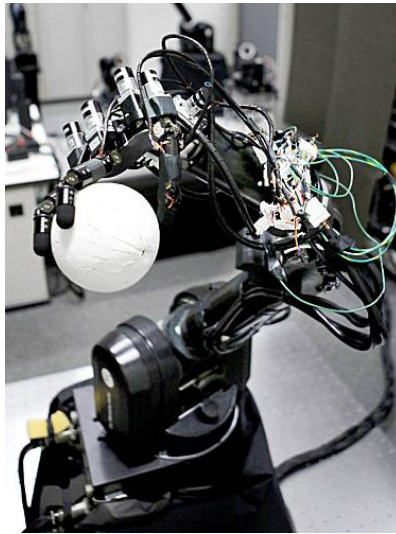
Figure 2.21: The high-speed hand-arm system used by the Ishikawa Watanabe Laboratory (taken from [73]).

As a result of this progression, more advanced control strategies are becoming available which mitigate previous design constraints within the area of robotic manipulation. For example, early robotic arms were designed with up to 6 DOF as the kinematics and computational analysis for such systems are well defined [75]. However, it is now possible to control higher DOF arm systems, which have more flexibility as the redundant DOF reduces singularity during task space motions. Other control strategies are being developed which provide real-time, reactive control during manipulation. This allows systems to interact with deformable object surfaces [76] and assess grasp stability during object contact [77]. This level of control is critical if robotic systems are to overcome uncertainties during grasping and manipulation. Following industrial trends, industrial robots will soon need be capable of overcoming uncertainties, such as the unknown objects or environments. Accordingly, more versatile control strategies have been developed within academia which focus on object detection and identification [78]–[80]. Mimicking humans, these strategies typically utilise vision-based systems which capture and process the robot's surrounding environment [81], [82]. By observing the environment during a robot's interaction, a vision system can assist in the detection and removal of individual objects from a pile [83]. This is achieved using local features and transform equations to determine if a single rigid motion explains the new state (see Figure 2.22).
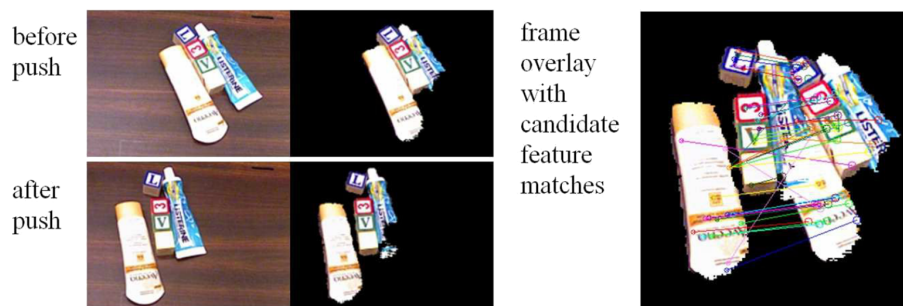
Figure 2.22: Interactive 'singulation' of an object from a pile (taken from [83]).

2.4.4.3   Dexterity

Robotic dexterity is an active research area that is considered important for enabling robotic adoption within flexible manufacturing [1], [84]. While it is acknowledged that dexterity will allow the robot to perform a greater range of skilful operations, there is still ambiguity as to what exactly the term encompasses. Consequently, it is currently difficult to define and measure dexterity, which has made it difficult to discuss the capability and track advancements within the area. To address this, the subsequent section is dedicated to defining dexterity and identifying its contributing factors.

2.5 Dexterity

To perform a structured and insightful analysis, dexterity will be examined from both human and robotic perspectives.

2.5.1 Human Dexterity

2.5.1.1 Overview & Definitions

Human dexterity is a very broad term which is surprisingly complex to fully define. In a general sense it can be considered as a measure of proficiency in manually completing tasks, however a more comprehensive definition requires much more thought.

In animals, dexterity is emergent from complex cognitive processes as well as complex environmental and sensorimotor interactions. The emergence of dexterity makes it challenging to quantitatively define. This is exemplified by Bernstein [4], who dedicates a book to its discussion and over four pages to its definition.

The dexterity of the human hand is often used as an indicator of overall dexterity, as shown by encyclopaedic definitions of the term [85]–[88] and the focus of human dexterity assessment tests [89]. These assessments further specify dexterity using two related terms; manual dexterity and fine motor dexterity. The former refers to the ability to perform controlled hand-arm manipulations of larger objects using gross motor grasp and release skills [89], [90], while the latter refers to the ability to perform skilful, rapid and controlled manipulations of small objects using in-hand manipulations [89], [90]. As fine motor dexterity predominantly requires use of the fingers, it can also be referred to as finger dexterity [90].

2.5.1.2 Contributing Factors

Dexterity is one of the four human psychophysical capabilities, meaning that it is dependent on elements of both physiology and psychology [4].

Due to these dependencies, dexterity is an ability which is only found in animals with a well-developed cortex [4]. This is emphasised by Wiesendanger [91] and Jeannerod [92] who link dexterity to neural processes such as cognition, learning,

memory, attention, and motivation. The requirement of these processes suggests that dexterity is an ability which develops with age as a human gains more experiences and knowledge (up to the point where age begins to inhibit motor functions) [4].

In addition to neural processes, human dexterity is dependent on the interaction of other fundamental human elements such as control and sensing [4], [91]. The dependence on sensing has been validated in [93], [94], where inhibitors to sensing such as finger numbness or wearing gloves caused a significant decrease to a person's dexterity assessment performance.

While the dexterity of humans is not necessarily superior to other species, it is often considered the case due to a human's natural problem solving ability [91]. In this sense, the essence of human dexterity is in *"finding a motor solution for any situation and in any condition"* [4]. From this it is clear that environmental interactions form a key part of human dexterity. Consequently, the demand for dexterity is observed to stem from the surrounding environment rather than the motions themselves i.e. even the most basic of movements can require a high level of dexterity in certain environments.

2.5.1.3 Assessments

Human dexterity assessment tests are employed in a wide range of applications when quantification of human dexterity is required e.g. assessing injured patients and rehabilitation progress, analysing job performance of employees, delivering evidence during compensation cases, etc. [89]. There are over twenty commercially available human dexterity assessment tests (HDAT) within the United States, fourteen of which have established psychometric properties (see Table 2.1) [89].

While the fourteen HDAT are each unique, it is observed that their procedure for assessing dexterity tends to be based on one of the following:

   i The grasping and transporting of blocks / large objects (generally to assess manual dexterity)

   ii The manipulation of pegs within a pegboard (generally to assess fine motor dexterity)

iii The performance of activities of daily living (ADL) (depends on the chosen
ADL, but generally to assess both manual and fine motor dexterity)

The categorisation of each HDAT is shown in Table 2.1. In addition to following
a similar procedure, all but one of the fourteen HDAT use timed measurements to
infer a level of dexterity. The remaining test incorporates quality of motion into its
assessment of dexterity. The use of time is advantageous as it simplifies measurement
methods, produces non-subjective quantitative results, and inherently captures the
contribution of influential factors such as speed, accuracy, and prehension pattern
choice [95].

Of the fourteen HDAT, Yancosek and Howell note that certain tests may be of
particular interest depending on the application. The most common application of
HDAT is within occupational therapy to track a patient's recovery during rehabilita-
tion. In this instance, HDAT which utilise ADL are particularly well suited as they
provide performance measurements relative to healthy humans and can be used to

Table 2.1: Breakdown of the 14 commercially available Human Dexterity Assessment
Tests (HDAT) based on their method for assessing dexterity. Type of dexterity
assessed taken from [89]. Images sourced online from the public domain [96]–[102].

Assessment Type	Abbreviation	Human Dexterity Assessment Test	Manual / Fine Motor Dexterity
Block Transfer Assessment	BBT	Box and Block Test	Manual Dexterity
	MMDT	Minnesota Manual Dexterity Test	Manual Dexterity
	MRMT	Minnesota Rate of Manipulation Test	Manual Dexterity
Pegboard Assessment	CDT	Crawford Small Parts Dexterity Test	Both
	GPT	Grooved Pegboard Test	Fine Motor Dexterity
	FDT	Functional Dexterity Test	Manual Dexterity
	NHP	Nine-Hole Peg Test	Fine Motor Dexterity
	OCFD	O'Connor Finger Dexterity Test	Both
	OCTD	O'Connor Tweezers Dexterity Test	Both
	PPT	Purdue Pegboard Test	Fine Motor Dexterity
Activities of Daily Living (ADL) Assessment	JHFT	Jebsen-Taylor Test of Hand Function	Both
	MPT	Moberg Pickup Test	Both
	SODA	Sequential Occupational Therapy Dexterity Assessment	Both
	WMFT	Wolf Motor Function Test	Manual Dexterity

(a) BBT   (b) MMDT   (c) MRMT   (d) CDT   (e) GPT   (f) FDT   (g) NHP

(h) OCFD   (i) OCTD   (j) PPT   (k) JHFT   (l) MPT   (m) SODA   (n) WMFT
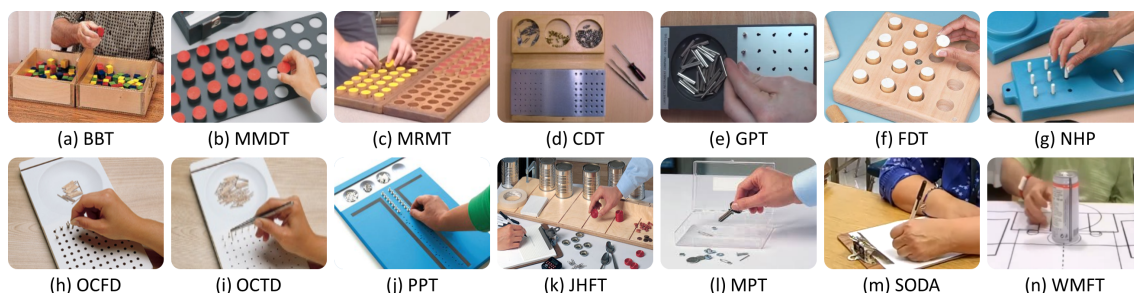
evaluate a patient's capability for independent living [103]. Alternatively, HDAT can be used to indicate a healthy person's level of dexterity e.g. to assess the manual and fine motor dexterity of an applicant for an assembly job. In this instance, manual dexterity can be captured by the BBT (unilateral) or the MRMT (bilateral), while fine motor dexterity can be captured by the PPT. The MRMT and PPT have been found to be good indicators of manual and fine motor dexterity [90], and have also been shown to have strong psychometric properties [89]. In more specialised cases, some of the other HDAT may be better suited. For example, the Morberg Pick-Up Test is the only assessment which assesses the influence of visual stimulus, while the O'Connor Tweezers Dexterity Test and Crawford Small Parts Dexterity Test assesses a subject's dexterity while using tools.

Another human dexterity assessment of interest is the Action Research Arm Test (ARAT), which is a reliable, validated assessment of arm motor status for stroke patients. This test, first described by Lyle in 1981, evaluates 19 tests of arm motor function, both distally and proximally. There are four subtests; Grasp, Grip, Pinch, and Gross Movement. Each test is given an ordinal score of 0, 1, 2, or 3, with higher values indicating better arm motor status. The total ARAT score is the sum of the 19 tests, and thus the maximum score is 57 [104]. The ARAT has been used in combination with the BBT within the Arm Amputee Program Cross Sectional Study to develop clinical tests to measure prosthetic use [105].

Within manufacturing, human dexterity can be assessed by considering the difficulty of manufacturing operations as there is a positive correlation between the difficulty of a manual assembly operation and its required dexterity. This has been validated by Sturges [33], who quantified the manual dexterity of an assembly using assembly difficulty factors. In addition, both assembly difficulty and dexterity are typically assessed using completion time, which shows their mutual dependence on time-related factors mentioned previously. As assembly difficulty is assessed within DFA methods, the use of these methods can therefore help to quantify the dexterity of different manufacturing operations.

2.5.2 Robot Dexterity

2.5.2.1 Overview & Definitions

Within the field of robotics, dexterity is defined in various ways depending on the application. For example robotic dexterity within industry has been associated with the ability of the robot to perform a diverse range of assembly operations without the need for custom fixtures or tool changes [106].

Many formal definitions of robotic dexterity focus on manipulative dexterity, which is approximately equivalent to human hand dexterity. Despite their intrinsic utility for tasks involving manipulation, definitions of dexterity pertaining to the hand alone are insufficient for many flexible manufacturing tasks that require consideration of the robot's global dexterity.

However since definitions of manipulative dexterity are subsumed under the spectrum of global dexterity, their examination remains relevant as it shows clear correlation with human dexterity. Manipulative dexterity has been reviewed in full by Bullock et al. [107], in which the authors draw attention to a number of definitions for the term:

- *"(The) capability of changing the position and orientation of the manipulated object from a given reference configuration to a different one, arbitrarily chosen within the hand workspace"* Bicchi [108],

- *"(The) process of manipulating an object from one grasp configuration to another"* Li et al. [109],

- *"(When) multiple manipulators, or fingers, cooperate to grasp and manipulate objects"* Okamura et al. [110],

- *"(The) kinematic extent over which a manipulator can reach all orientations"* Klein and Blaho [111],

- *"Skill in use of hands"* Sturges [112]

2.5.2.2   Contributing Factors

Often robotic systems are claimed to be dexterous due to their number of DOF or ranges of motion. However, the prominence of object manipulation in the definitions of robotic dexterity above emphasises its similarity to human dexterity and its dependence on both manual and fine motor dexterity. By extension, these definitions show that a robot's dexterity is not only dependent on the motions it can perform but on its sensing and control capabilities as well (equivalent to human sensorimotor requirements). In particular, robotic sensing has been identified as a key parameter when performing dexterous manipulations [110], which is analogous to observations within the human dexterity literature.

2.5.2.3   Assessments

In addition to assessing the performance of the overall system, a complete assessment of a robotic system's dexterity also includes the performance of its individual components which influence dexterity. Accordingly, there are typically two different benchmarking levels when assessing dexterity; component and system level benchmarking.

A number of robotic dexterity assessments and approaches have been developed which consider different components of a robotic system.

Kumar and Waldron define the *dexterous workspace* of a manipulator as the *"volume within which every point can be reached by a reference point on the manipulator hand with the hand in any desired orientation"* [113]. The authors proceed to define a numerically bounded and dimensionless dexterity index, which represents the manipulator's ability to achieve varying orientations at a given point ([113], summarised in [114]). In [115], manipulator dexterity is assessed along with safety using a developed safety and dexterity index (SD index). Here the authors quantify manipulative dexterity as a value between 0 and 1 using normalised evaluation factors derived from the robot's velocity, force, current joint configuration, and ability to avoid internal failure. However, these factors are local kinematic indices derived from the Jacobian and have inherent limitations due to their dependence on units, scale, and reference frame as identified in [114].

Performance metrics have been developed both formally through standards and informally by researchers who needed to evaluate their systems. The formal performance standards for industrial robots (ISO 9283 [116], ANSI/RIA R15.05) are old and cover only limited aspects of performance, mainly relating to point-to-point repeatability. Developed grasp taxonomies have been used to identify the more dexterous prehensile movements [117], and motion-centric taxonomies have been proposed which incorporate object contact and manipulation [118]. In the latter, dexterous manipulation is identified as the performance of in-hand manipulation, whereby the object is translated and/or rotated relative to the hand's coordinate system by use of the fingers. The consideration of prehensile motions allows manipulation strategies to be identified, and can be used to determine the dexterous operations within a given assembly. However, the taxonomies have not been adopted within industry as all finger motions must be analysed at each point in time and do not account for important factors such as integrated control or sensing.

Benchmarking tests to assess a robot hand's grasping ability were proposed by the European Robotics Research Network (EURON) [119], and these tests have since been incorporated into an assessment of underactuated hands [120]. However, these tests are limited to planar grasp cases and do not capture manipulation performance or other issues like object damage or positional deviations.

In [121], researchers outline a method for quantifying the *'Actuator Dexterity (AD)'* of a robotic hand using 48 evaluation criteria and a developed scoring method. A robotic hand is assigned a value of 0, 1, or 2 for each criteria depending on its performance in that area, and the overall AD score represents the *"extent to which various issues relating to actuation are addressed by the design approach...and the selected technologies."* While restricted to actuation within robotic hands, the combined numerical total and individual criteria scores allow for clear comparisons to be made.

Wright et al. [122] have proposed that a *"dexterity spectrum"* and *"design space framework"* can be used in the evaluation of dexterous robot hands and their selection within manufacturing. This spectrum qualitatively defines the dexterity of a robot hand by considering the system's suitability for a number of tasks of varying

complexity. Their framework builds on this spectrum by identifying mechanical design, control, and coordination-knowledge attributes to classify six robot hand and manufacturing task clusters. These attributes and clusters were to be developed and used to match robotic systems to manufacturing tasks as part of the ongoing research but results were never published.

Researchers have looked at capturing the overall dexterity of a robotic system by recording its performance during activities of daily living (ADL) [123]. This has mainly occurred within the domestic robotics areas, which means that chosen ADL typically stem from tasks commonly encountered around the home. For example, the European Commission 7th Framework project 'DEXMART' focused on benchmarking the dexterity of dual arm systems using ADL such as setting a table and opening/closing a bottle [123]. ADL have also been used to assess the effectiveness of prosthetic use in the Southampton Hand Assessment Procedure (SHAP) [124].

As summarised in [125], a number of object data sets have been developed to assist in the benchmarking of robotic systems. The purpose of these data sets is to encourage the standardisation of tests being conducted by various research groups in order to facilitate comparative analysis. Data sets have been developed for a range of areas such as simulation, object detection and grasp planning, but the Yale-CMU-Berkeley object and model set [125] is of particular interest as it focuses on robotic manipulation. Accordingly, objects with varying physical and surface properties are selected in addition to a number of widely used manipulation tests. However, the data set focuses more on objects found around the house and does not provide a comprehensive representation of objects found within industry. In general, the adoption of object data sets has been slow by research groups and as a result only a limited number of benchmarks and assessment protocols relating to dexterity have been developed to date which utilise any of these data sets.

Within manufacturing, robotic dexterity has previously been quantified by Sturges and Wright [126], who developed a mathematical model to calculate manipulative dexterity and capture its trade-off with power generation. This model of dexterity is defined by the number of kinematic degrees of freedom, the natural frequency of

the system and its resolution. However, the model is based on the human system as it makes use of an index of difficulty (ID) which is derived from human motor skills. This ID value indicates the relative effort needed for a given operation. In a subsequent paper, Sturges uses this link between dexterity and ID to develop a 'Design for Assembly' (DFA) calculator which numerically quantifies the manual dexterity of an assembly based on the difficulty of its operations [33]. This calculator estimates an ID value for acquisition and assembly scales taken from design for assembly the Boothroyd-Dewhurst DFA method and Xerox Corporation method. Individual ID values are given in seconds, and their combined total provides an estimate of the assembly's completion time. This total ID represents the manual dexterity of the assembly.

Robotic dexterity within manufacturing is also being considered by the Intelligent Systems Division at the National Institute of Standards and Technology (NIST), who are developing an assessment framework for robotic systems within manufacturing assembly [127]. As part of this body of research, the group have recently derived sixteen robotic actions from assembly taxonomies which they intend to use in the development of assembly-specific performance metrics [128]. These actions are described in detail in [128], but have been classified as follows:

1. Detect
2. Align
3. Pick up
4. Reposition
5. Insert
6. Slide
7. Retract
8. Transport
9. Place
10. Tool action
11. Hold
12. Fasten
13. Coordinate
14. Navigate
15. Track
16. Communicate

Having derived these actions, NIST are in the process of identifying the key robotic parameters and components required for each action which they intend to use to develop appropriate performance metrics. To date, the group have published grasping metrics and testing procedures for grasp cycle time, grasp efficiency, finger strength, grasp strength, in-hand manipulation, object pose estimation, slip resistance, touch sensitivity, finger force tracking, and sensor calibration [129].

2.6   Statistical Data & Tests

2.6.1   Data Types

Wihin research, the purpose of any experiment is to examine one or more variables. Variables refer to any characteristic that differs within a sample or population, and a variable can be measured, manipulated and controlled for. A response (or dependent) variable measures the outcome of a study, while an explanatory (or independent) variable explains or causes a change to the response variable [130]. In a typical experiment, independent variables are manipulated in order to observe their effect on a dependent variable. During measurement, variables can be generally classified as either categorical or continuous.

Categorical Variables: Categorical (or qualitative) variables are those which have a discrete number of possible outcomes (categories) during measurement. There are three major types of categorical variable; nominal, dichotomous, and ordinal [130]. Nominal variables are those which have two or more categories that do not have an intrinsic order e.g. blood group (A, B, AB, or O). A dichotomous variable is a nominal variable which only has two categories e.g. gender (male or female). Ordinal variables have two or more possible categories, but the categories have a hierarchy e.g. Likert scale (strongly disagree, disagree, neutral, agree, or strongly agree). In some cases, categorical variables with three or more outcomes can be dichotomised into a series of variables known as dummy variables or binary variables e.g. blood group (O or other).

Continuous Variables: Continuous (or quantitative) variables are those which are measured on a numerical scale covering a large range. Continuous variables can be further classified as either interval or ratio variables [130]. Interval variables are measured on a numerical scale in which the order and increments are known, consistent and measurable e.g. Celsius Scale ($40° - 30° = 30° - 20° = 10°$). Ratio variables are interval variables which have a clear definition of zero, the point when there is none of that variable e.g. weight.

Based on the above differentiation, it is useful to consider separate statistical tools when analysing categorical and continuous data.

2.6.2 Continuous Data Analysis

2.6.2.1 Kolmogorov-Smirnov Test

The two-sample Kolmogorov-Smirnov (KS) test is a hypothesis test that measures the maximum difference between two cumulative distributions and is commonly used to determine if two sets belong to the same population [131].

A hypothesis test has two opposing hypotheses; the null hypothesis H_0 and the alternative hypothesis H_a. In general, H_0 states that the samples were taken from the same population and differences in the sample data can be attributed to random sampling error. The null hypothesis represents the *"devil's advocate"* position, and data is tested to generate evidence against the null hypothesis. The alternative hypothesis states the opposite of H_0, and is the statement that the experiment is trying to prove. A hypothesis test will identify which statement (H_0 or H_a) is most likely, however the rejection of H_0 does not automatically mean the acceptance of H_a since a hypothesis test only tests the evidence against the null hypothesis. While rejection of H_0 may provide supporting evidence for H_a, it does not provide complete evidence for proving H_a. Hence, hypotheses are always falsified and never proven.

For most hypothesis tests, a p-value is calculated based on the sample data to determine if the null hypothesis can be rejected. The p-value corresponds to the probability of obtaining a difference at least as extreme as the one observed in the sample data, assuming the truth of the null hypothesis [132]. The p-value ranges from 0 to 1, where a small p-value indicates that the observed difference cannot be accounted for by random sampling errors and hence there is sufficient evidence to reject the null hypothesis for the full population.

The cut-off point for this distinction is known as the significance level (α), where p-values less than or equal to α provide *"statistically significant"* results [133]. While somewhat arbitrary, a significance level of 0.05 is the most widely used within academia [130]. However, since α represents the possibility that the null hypothesis will be incorrectly rejected, reducing α will increase the confidence in calculated

results.

The KS test is a non-parametric test (or distribution free method), which means that the test makes fewer and less stringent assumptions about the distribution of the data [134]. In contrast, parametric tests assume that the data arises from a distribution (a normal distribution is commonly assumed) which can be described by a number of parameters (mean, variance, etc.). Since non-parametric tests do not make these assumptions, they can be applied to all kinds of data which makes them more versatile than parametric tests. On the other hand, with correct assumptions parametric tests are more efficient and powerful. Accordingly, while the KS test is more versatile, it tends to be more conservative than other statistical tests i.e. it is less likely to incorrectly reject H_0 for the given significance level.

2.6.2.2   Detectable Difference

A commonly used parameter for describing a set of n continuous data points is the sample mean, $\bar{x}$:

$$\bar{x} = \frac{1}{n} \sum_{i=1}^{n} x_i \tag{2.4}$$

From which the sample spread can be defined using the variance (σ^2) or standard deviation (s) of the data set:

$$s^2 = \frac{1}{n-1} \sum_{i=1}^{n} (x_i - \bar{x})^2 \tag{2.5}$$

The true mean or population mean (μ) is the average of all elements in an entire population, and is usually an unknown constant [135]. Conversely, the sample mean ($\bar{x}$) varies during testing, and may or may not be close to the true mean depending on the sample size (n) and standard deviation (s). A confidence interval is used to relate the sample and true mean, and defines a range of values around the sample mean in which the true mean is likely to be located (with a given confidence level) [136]. The amount of random sampling error at this confidence level is known as the margin of error (E), which allows the true mean range to be defined as follows:

$$\mu = \bar{x} \pm E \tag{2.6}$$

For non-parametric testing, the margin of error can be related to the sample size (n) and standard deviation (s) by the equation:

$$n = 1.15 \left(\frac{s * z_{\alpha/2}}{E} \right)^2 \tag{2.7}$$

where $z_{\alpha/2}$ is the two-tailed z-score for a $(1 - \alpha)$ confidence. In non-parametric tests where the distribution shape is unknown, the sample size should be increased by 15% in order to ensure that sufficient data is gathered regardless of the distribution [137], [138].

Z-scores (or standard scores) are variable values transformed to zero mean and unit variance [131]. The larger the value of z, the less likely that the experimental result is due to chance. The two-tailed z-score is calculated by the equation:

$$z_{\alpha/2} = invNorm\left(1 - \frac{\alpha}{2}\right) \tag{2.8}$$

where invNorm is the inverse of the cumulative normal distribution function. The invNorm function can be calculated using statistical tools, but z-tables are also available [134]. From these, the two-tail z-score for a 0.05 significance level is $z_{0.025} = 1.96$.

When comparing two sample means, the margin of error determines if there is a detectable difference between the two sample means (see Figure 2.23). If a gap exists
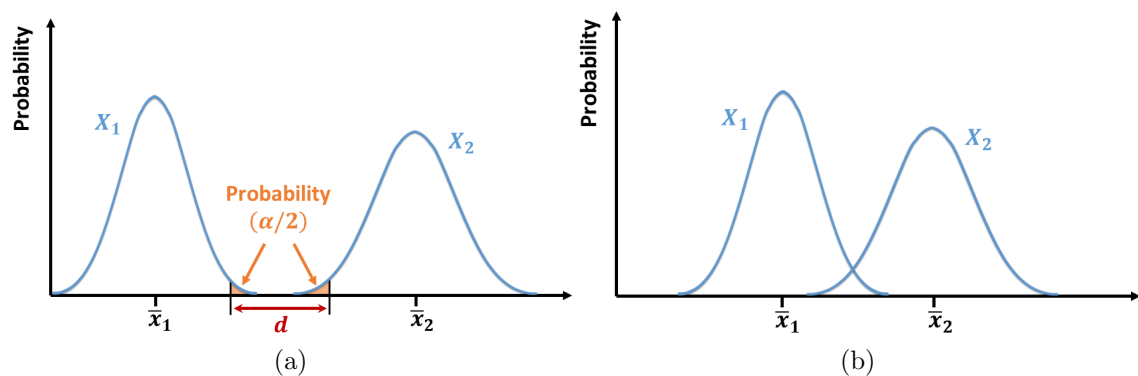
Figure 2.23: Comparison between two distributions, $X_1 = \bar{x}_1 \pm E_1$ and $X_2 = \bar{x}_2 \pm E_2$: (a) The sample means $\bar{x}_1$ and $\bar{x}_2$ differ by at least a value of d for the given confidence level α (b) The sample means $\bar{x}_1$ and $\bar{x}_2$ cannot be said to differ for the given confidence level.

between the two intervals, then there is a detectable difference between the two population means of at least that gap size. Conversely, there is not a detectable difference if the two intervals overlap. The threshold difference at which this occurs is known as the effect size. With reference to Equation 2.7, the effect size can be reduced by reducing the confidence level or increasing the sample number.

2.6.3 Categorical Data Analysis

2.6.3.1 Kolmogorov-Conover Test

The Kolmogorov-Conover (KC) test is an extension of the KS test, and is used to determine if two discontinuous data sets belong to the same population. The algorithms derived for this test are presented in [139], but in general the tests seek to test the hypothesis H_0,

$$H_0 : F(x) = H(x) \,\forall x, \tag{2.9}$$

where $F(x)$ is the cumulative distribution function under test and $H(x)$ is the hypothesised cumulative distribution function. For discrete distributions, KC is an exact statistical test (for one-sided testing) and nearly exact statistical test for the two-sided case. Unfortunately, KC becomes numerically unstable at sample sizes approximately greater than 40, limiting its usage. However, arbitrary precision arithmetic was implemented by researchers at NIST to enable the KC test to accurately analyse data sets with larger sample sizes [129].

2.6.3.2 Probability of Success

A simple, yet meaningful performance measure for categorical data is the probability of success (PS). Based on the number of independent trials n, number of successes m, and a chosen confidence level $CL \in \mathbb{R} : [0, 1]$, the theoretical probability of success $PS \in \mathbb{R} : [0, 1]$ can be calculated from the following inequality involving the binomial cumulative distribution function [140]:

$$BINCDF(m - 1, n, PS) \geq CL, \tag{2.10}$$

where PS is its minimum value to some precision while still satisfying Equation 2.10. The interpretation is straightforward for dichotomous data, where PS represents the likelihood of any single trial being a success. For ordinal data, the ordered ranking can be dichotomised by choosing a threshold rank at which the transition between success and failure occurs.

2.7 Summary

2.7.1 Key Findings

Manufacturing is a key contributor to a country's economy. However, due to global trends and issues such as globalisation, growing competition, reduced product life cycles, and greater consumer demands, it is an area which is seeing significant change. Flexibility and responsiveness to change are becoming important parameters, which is causing a shift within industry towards more flexible manufacturing methods.

Flexible manufacturing has traditionally favoured manual assembly over automation due to its dexterity requirements and low-volume production. However lightweight, collaborative industrial robots are being developed which differ from traditional industrial robots in that they prioritise metrics such as safety, ease-of-use, adaptability, and dexterity. These robots are better suited to flexible manufacturing, however their integration within the area has been stilted due to the lack of suitable performance metrics. While a number of robotic performance metrics are available, they were developed for traditional robots. Therefore, in order to facilitate the collaborative robots market to grow as expected, there is a strong need for the development of more relevant performance metrics.

In particular, the development of standardised metrics that capture robotic dexterity is of critical importance, as these metrics will help to determine the ability of a robotic system to perform within flexible manufacturing. However, ambiguity currently exists within the area of robotic dexterity, as seen by the qualitative and in-house measurements of the ability. Quantitative measurements that have been developed vary in their approach and in the components they consider, which has made it challenging to currently identify and compare the dexterity of different robotic systems.

From an analysis of human dexterity, it has been shown that dexterity is a sensori-motor capability that is dependent on the surrounding environment. Accordingly, the demand for robot dexterity is not in the motions themselves but in reacting to changes within the environment. This is an useful point to emphasise, as it means that definitions and measurements of robotic dexterity should be developed with the

surrounding environment in mind. Previous work has tended not to do this, opting instead to look at the overall dexterity of the robotic system. However, consideration of the surrounding environment is beneficial, as it allows robotic dexterity to be more easily quantified and measured.

Based on this fact, the development of a robotic dexterity framework within flexible manufacturing should first consider the range of possible operations within the area in order to identify their dexterous requirements. One possible way to achieve this is to make use of the Boothroyd-Dewhurst DFA method, which has developed classification tables that categorise manufacturing operations based on difficulty. From the identified positive correlation between operation difficulty and dexterity, the dexterous requirements within flexible manufacturing can potentially be captured by considering the B-D classification tables. This avenue will be explored in greater detail in Section 3.2.

2.7.2   Updated Research Objectives

As already outlined, this research aims to address the identified gap by developing a comprehensive assessment framework that captures the dexterity of industrial robotic systems and identifies their performance within flexible manufacturing. From examination of the literature, the research objectives presented in Section 1.2 can now be more explicitly defined. Accordingly, the primary objectives of this research are:

1. To examine current dexterity assessment approaches used within both human and robotic literature and identify their suitability for the assessment of robotic dexterity within flexible manufacturing. Both the benefits and limitations of using these assessments should be considered (Chapters 2 and 3).

2. To develop a set of dexterity assessment metrics that accurately capture the dexterity of a robotic system. While these metrics should build on previous work, they should be developed specifically for the assessment of industrial robots within flexible manufacturing environments. Any metrics developed

should require minimal a-priori information to ensure usability, and their accuracy should be validated through testing (Chapters 3 and 4).

3. To use the developed metrics to estimate the dexterous performance of different robotic systems within selected flexible manufacturing scenarios. The combination of these metrics should be clearly identified and should generate quantitative results that provide a true reflection of actual performance (Chapters 4 and 5).

4. To incorporate the set of metrics within an overall dexterity assessment framework that is comprehensive and simplifies the robot selection process within flexible manufacturing. In order to achieve this, the developed framework should facilitate the bidirectional matching of robotic systems and flexible manufacturing tasks (Chapter 3).

5. Combining the previous aims, to use the developed framework to estimate human and robotic performance within common flexible manufacturing tasks. This assessment should help to quantify the current gap between human and robotic dexterity and to highlight the usefulness of the framework as a selection tool within flexible manufacturing (Chapter 5).

Chapter 3

Research Framework

3.1   Research Methodology

Research methodologies are important as they ensure a structured approach to research that considers the rational, underlying assumptions, resources, limitations, and analysis of collected data [141], [142]. Accordingly, the use of research methodologies helps to promote the finding of a solution during an investigation, although this is not guaranteed. Research methods refer to the techniques and tools used to gather the data within the research study. The research methods employed will depend on adopted research methodology, but can be classified as either qualitative or quantitative depending on approach used.

Qualitative research is exploratory as it involves the investigation of culture, society, and behaviour to gain an understanding of underlying reasons, opinions, and motivations [143], [144]. This investigation provides an insight into the problem and the subjects being considered, which can be beneficial when developing hypotheses or identifying trends in people's behaviour and thought process. Qualitative research methods include individual interviews, focus groups, and observational studies.

Quantitative research is performed to quantify a problem through empirical investigation of quantitative properties and their relationships [145]. This research methodology typically involves the collection of measurable, numerical data that be statistically analysed to uncover trends and facts, but also includes the generation of models, theories, hypotheses, instruments, and/or measurement methods [145]. Quantitative research methods include surveys, interviews, and systematic observations.

To address the research objectives outlined in Section 2.7.2, this work adopted a design science research methodology [146] as presented in Figure 3.1. The design science research methodology promotes the construction, design, and evaluation of artefacts that solve a specific problem or research question [146]. While primarily used within information technology, the design science research methodology was particularly suited to this research, where the artefact being designed and developed was a robotic dexterity assessment framework. From Figure 3.1, a number of possible entry points exist within the methodology. To address all research objectives, this research started at the initial entry point before proceeding through the complete design science process.

By considering all six stages outlined within the design science research methodology, this work has adopted both qualitative and quantitative research methods. Initial research was based on theoretical studies, whereby prior work within the area of human and robotic dexterity was used identify and describe the problem area. Previous attempts to define and measure dexterity within both areas were considered through a qualitative evaluation of the literature (Chapter 2). From this analysis, a new framework was developed (Section 3.3). This framework built on previous studies by incorporating different strategies presented within the literature. These strategies are combined and expanded upon to generate a new approach and set of performance metrics that provide a comprehensive assessment of robotic dexterity
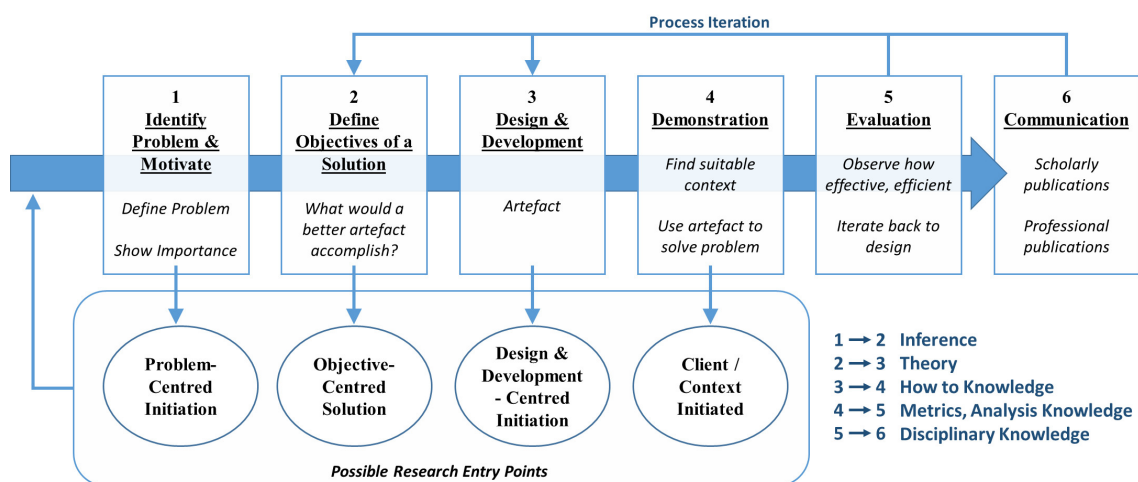
Figure 3.1: Design science research methodology, adapted from [146].

within flexible manufacturing.

Quantitative research was performed to validate the proposed framework and developed performance metrics. In particular, case study research was performed. This form of empirical research considers a specific event or set of related events in order to generate observations that help to explain the phenomenon of interest within the investigation [147]. Case study research is most commonly applied prospectively, and makes use of data from multiple sources including documentation, archival records, interviews, direct observation, participant observation, and physical artefacts [148], [149]. The tests outlined in Chapter 4 were conducted as case studies and the results presented in Chapter 5 were used to verify if the developed framework and metrics validated the core hypothesis.

3.2 Suitability of the B-D Method

Flexible manufacturing is currently dominated by small-scale, manual assembly lines. These assembly lines are typically optimised using DFA methods, which split the assembly into its constituent operations. A key requirement of a dexterity measurement system is that it should facilitate easy comparisons between robot and human performance. Accordingly, this work proposes that DFA methods present a logical starting point for identifying the dexterous requirements within flexible manufacturing.

It was shown in Section 2.5 that the dexterity is dependent on environmental interactions, sensorimotor feedback loops and cognitive processes. As existing human dexterity measurement techniques are based on data that is generated from observable behaviour and is independent of underlying causal mechanisms, it is suggested that existing human dexterity measurement techniques can be suitably extended to measure robot dexterity. By extending existing human dexterity measurement tools to describe robot-performance, the system is addressing the need for easy comparisons between robots and humans.

Of the available DFA methods, the Boothroyd-Dewhurst (B-D) DFA method is particularly suited for benchmarking the dexterity of robotic systems in a flexible manufacturing setting. Despite being a DFA tool, the B-D DFA method has an

established link as a dexterity measurement tool as its classification of operation difficulty has been shown to positively correlate to assembly dexterity (refer to discussion in Section 2.5.1.3). The manual handling and insertion tables used by this method encapsulate the diverse range of operations possible within the area and explicitly consider the properties of the object being handled (shape, size, symmetry, etc.). This completeness makes them well-suited for quantifying robotic performance requirements across the wide range of possible flexible manufacturing operations. Furthermore, because the B-D DFA method is so widely used in industry, its consideration during robot assessment simplifies robot selection and integration. To demonstrate the benefit of considering the B-D classification tables during the assessment of robot dexterity within flexible manufacturing, it is worth comparing their suitability against existing dexterity assessment approaches currently being utilised within industry and the research community. This comparison will address two elements that are particularly relevant when considering the dexterous requirements within flexible manufacturing:

- Operations: Examine how the operations defined within the B-D classification tables relate to those used within existing dexterity measurement methods by comparison with the fourteen established human dexterity assessment tests (HDAT).
- Objects: Examine how the objects covered by the B-D classification tables relate to other object datasets by comparison with the Yale-CMU-Berkeley (YCB) object dataset.

3.2.1   HDAT Comparison

The idea of using HDAT to assess robotic dexterity has intuitive appeal as they are currently used within flexible manufacturing to quantify a human operator's dexterity [89]. Accordingly, these tests may be familiar to those within industry, and their established levels of reliability and validity would ensure accuracy and comparability. The latter is particularly true, as robotic HDAT results could also be compared to human norm tables to determine the robot's dexterity relative to a

humans.

To determine their feasibility as robotic dexterity assessment tools within flexible manufacturing, the B-D classification tables will be used to identify the range of flexible manufacturing operations considered by the HDAT. To assist with this analysis, focus will be put on commercially available HDAT with established psychometric properties. As identified in Section 2.5.1, these HDAT can be categorised according to their testing procedure using three groups. One consequence of this commonality is that there is a tendency for repetition between HDAT. This is highlighted in Table 3.1, which summarises the operations and artefacts relevant to grasping and manipulation used by the fourteen HDAT.

Having identified these operations and items, the extent to which HDAT are applicable to the area of flexible manufacturing can be determined. Using the calculated B-D handling and insertion codes shown in Table 3.2, each HDAT operation can be mapped to its equivalent cell in the B-D handling and insertion tables. The complete mapping is given in Figure 3.2 and Figure 3.3.

From this mapping, it is clear that the fourteen HDAT only assess a limited number of the possible operations within flexible manufacturing. To highlight this, a summary of the handling and insertion operations captured by the HDAT is shown in Figure 3.4 and Figure 3.6 respectively. As the B-D tables represent the range of operations within flexible manufacturing, it can be surmised that the fourteen HDAT only assess 14 % of the possible handling operations and 11 % of the insertion operations within the area. In addition, those operations that are assessed tend to require low levels of dexterity due to the favourable object properties and handling situations. This is evident by the number of HDAT operations which map to cells with low completion times, as shown in Figure 3.5.

Accordingly, this study shows that HDAT are limited in their coverage of flexible manufacturing operations. The identification that the majority of operations within HDAT require low levels of dexterity is an interesting outcome, particularly since these tests are currently used within manufacturing to measure an operator's dexterity. Results from HDAT provide a relative level of dexterity, and thus it can be concluded that an operator's dexterous ability is currently derived from their performance

Table 3.1: HDAT operations which require object interaction and their corresponding objects. Item dimensions taken from HDAT documentation where possible, but otherwise estimated using standard values. Symmetry parameters (α and β) defined in Section 2.3.

HDAT	Operations Assessed	Object	Objects Handled Dimensions (mm)	Symmetry
BBT	Transfer blocks from a pile to the other side of box	Cube Block	25 (L) x 25 (W) x 25 (H)	$\alpha = 90°, \beta = 90°$
CDT	Transfer screws to threaded holes in a board and tighten with screwdriver	Screws	13 (L) x 4.1 (D)	$\alpha = 360°, \beta = 0°$
		Cylindrical Pin	17 (L) x 1.7 (D)	$\alpha = 180°, \beta = 0°$
	Using tweezers, transfer pins to holes in a board and add a collar	Collar	6.25 (L) x 5.3 (OD)	$\alpha = 180°, \beta = 0°$
FDT	Remove pegs from hole, flip by 180° then reinsert into hole	Cylindrical Peg	40 (L) x 22 (D)	$\alpha = 180°, \beta = 0°$
GPT	Transfer asymmetrical pegs to holes in a board Remove pegs from board and return to holder	Grooved Peg	25 (L) x 3 (D)	$\alpha = 180°, \beta = 360°$
JHFT	Write a short sentence Turn over index cards Simulate feeding using a spoon Stack checkers Pick up large light can Pick up large heavy can Pick up common small objects	Pencil / Pen	178 (L) x 7 (D)	$\alpha = 360°, \beta = 0°$
		Index Cards	76 (L) x 127 (W) x 0.3 (H)	$\alpha = 180°, \beta = 180°$
		Tablespoon	194 (L) x 38 (W) x 20 (H)	$\alpha = 360°, \beta = 360°$
		Checkers	6.35 (H) x 31.75 (D)	$\alpha = 180°, \beta = 0°$
		Cans	120 - 141 (L) x 66 - 81 (D)	$\alpha = 180°, \beta = 0°$
		Coins	1.5 (L) x 19 (D)	$\alpha = 180°, \beta = 0°$
		Bottle Cap	6.35 (L) x 25.4 (D)	$\alpha = 360°, \beta = 0°$
		Kidney Beans	15.8 (L) x 8 (D)	$\alpha = 360°, \beta = 180°$
		Paper Clip	25.4 (L) x 10 (W) x 1 (H)	$\alpha = 360°, \beta = 180°$
MPT	Transfer common small objects to a container Without a visual stimulus, transfer common small objects to a container	M7 Hex Nut	11 (W_{flats}) x 5.5 (L)	$\alpha = 180°, \beta = 60°$
		Nail	50 (L) x 2.2 (D)	$\alpha = 360°, \beta = 0°$
		Coins	1.5 - 2 (L) x 19 - 21 (D)	$\alpha = 180°, \beta = 0°$
		Screw	23 (L) x 4.7 (D)	$\alpha = 360°, \beta = 0°$
		M8 Wing Nut	32 (L) x 14.8 (W) x 13.8 (H)	$\alpha = 360°, \beta = 180°$
		Safety Pin	38 (L) x 1 (H)	$\alpha = 360°, \beta = 180°$
		Key	55 (L) x 25 (W) x 2.5 (H)	$\alpha = 360°, \beta = 360°$
		Washer	1 (L) x 14 (OD)	$\alpha = 180°, \beta = 0°$
		Paper Clips	25.4 - 50.8 (L) x 10 (W) x 1 (H)	$\alpha = 360°, \beta = 180°$
MRMT	Transfer blocks to holes in a board Transfer blocks to holes in a board, flipping during transition Remove blocks from hole, flip by 180°, then reinsert into hole	Cylindrical Peg	18 (L) x 37 (D)	$\alpha = 180°, \beta = 0°$
MMDT	Same as the MRMT	Cylindrical Peg	18 (L) x 37 (D)	$\alpha = 180°, \beta = 0°$
NHP	Transfer pegs to holes in a board Remove pegs from board and return to holder	Cylindrical Peg	32 (L) x 6.4 (D)	$\alpha = 180°, \beta = 0°$
OCFD	Transfer pins (three at a time) to holes in a board	Cylindrical Pin	25.4 (L) x 1.6 (D)	$\alpha = 180°, \beta = 0°$
OCTD	Using tweezers, transfer pins (one at a time) to holes in a board	Cylindrical Pin	25.4 (L) x 1.6 (D)	$\alpha = 180°, \beta = 0°$
PPT	Transfer pegs to holes in a board Transfer pegs to holes in a board and add a collar and two washers	Cylindrical Peg	25 (L) x 2.5 (D)	$\alpha = 180°, \beta = 0°$
		Washer	1 (L) x 9.5 (OD)	$\alpha = 180°, \beta = 0°$
		Collar	6 (L) x 5 (OD)	$\alpha = 180°, \beta = 0°$
SODA	Write a short sentence Pick up an envelope Pick up coins Hold the receiver of a telephone to one ear Unscrew cap from tube of toothpaste Squeeze toothpaste on a toothbrush Handle a spoon and knife Button a shirt or blouse Unscrew a large bottle Pour water in a glass	Pencil / Pen	178 (L) x 7 (D)	$\alpha = 360°, \beta = 0°$
		Envelope	220 (L) x 110 (W) x 1 (H)	$\alpha = 360°, \beta = 180°$
		Coins	1.5 - 2 (L) x 19 - 21 (D)	$\alpha = 180°, \beta = 0°$
		Telephone	210 (L) x 62 (W) x 68 (H)	$\alpha = 360°, \beta = 360°$
		Toothpaste Tube	145 (L) x 55 (W) x 35 (H)	$\alpha = 360°, \beta = 180°$
		Toothpaste Cap	13 (L) x 35 (D)	$\alpha = 360°, \beta = 0°$
		Toothbrush	180 (L) x 13 (W) x 27 (H)	$\alpha = 360°, \beta = 360°$
		Teaspoon	141 (L) x 25 (W) x 15 (H)	$\alpha = 360°, \beta = 360°$
		Knife	230 (L) x 20 (W) x 5 (H)	$\alpha = 360°, \beta = 360°$
		Shirt / Blouse	775 (L) x 553 (W) x 1 (H)	$\alpha = 360°, \beta = 360°$
		Button	2 (L) x 13 (D)	$\alpha = 180°, \beta = 0°$
		Large Bottle	203 (H) x 57.1 (D)	$\alpha = 360°, \beta = 0°$
		Bottle Cap	6.35 (L) x 25.4 (D)	$\alpha = 360°, \beta = 0°$
		Glass	85 (L) x 65 (D)	$\alpha = 360°, \beta = 0°$
WMFT	Pick up a can Pick up a pencil Pick up a paper clip Stack checkers Turn over index cards Turn a key in a lock Fold towel in half (twice) Lift a 3 lb basket to a bedside table	Can	120 (L) x 66 (D)	$\alpha = 180°, \beta = 0°$
		Pencil / Pen	178 (L) x 7 (D)	$\alpha = 360°, \beta = 0°$
		Paper Clip	50.8 (L) x 10 (W) x 1 (H)	$\alpha = 360°, \beta = 180°$
		Checkers	6.35 (H) x 31.75 (D)	$\alpha = 180°, \beta = 0°$
		Index Cards	76 (L) x 127 (W) x 0.3 (H)	$\alpha = 180°, \beta = 180°$
		Key	55 (L) x 25 (W) x 2.5 (H)	$\alpha = 360°, \beta = 360°$
		Face Towel	635 (L) x 381 (W)	$\alpha = 180°, \beta = 180°$
		Tote Basket	355.6 (L) x 216 (W) x 381 (H)	$\alpha = 360°, \beta = 180°$

One Hand

Parts can be grasped and manipulated by one hand without the aid of grasping tools			Parts are Easy to Grasp and Manipulate					Parts Present Handling Difficulties				
			Thickness > 2 mm			Thickness ≤ 2 mm		Thickness > 2 mm			Thickness ≤ 2 mm	
			Size > 15 mm	6mm ≤ Size < 15 mm	Size < 6mm	Size > 6 mm	Size ≤ 6 mm	Size > 15 mm	6mm ≤ Size < 15 mm	Size < 6mm	Size > 6 mm	Size ≤ 6 mm
			0	1	2	3	4	5	6	7	8	9
(α+β) < 360°	0		11	4		7						
360° ≤ (α+β) < 540°	1		10	1		2		1				
540° ≤ (α+β) < 720°	2		5			7						
(α+β) = 720°	3		6			1						

One Hand with Grasping Aids

Parts can be grasped and manipulated by one hand but only with the use of grasping tools

			Parts need Tweezers for Grasping and Manipulation								Parts need Standard Tools other than Tweezers	Parts need Special Tools for Grasping & Manipulation
			Parts can be Manipulated without Optical Magnification				Parts Require Optical Magnification for Manipulation					
			Parts are Easy to Grasp & Manipulate		Parts Present Handling Difficulties		Parts are Easy to Grasp & Manipulate		Parts Present Handling Difficulties			
			Thickness > 0.25 mm	Thickness ≤ 0.25 mm	Thickness > 0.25 mm	Thickness ≤ 0.25 mm	Thickness > 0.25 mm	Thickness ≤ 0.25 mm	Thickness > 0.25 mm	Thickness ≤ 0.25 mm		
			0	1	2	3	4	5	6	7	8	9
α ≤ 180°	0 ≤ β ≤ 180°	4	3									
	β = 360°	5										
α = 360°	0 ≤ β ≤ 180°	6										
	β = 360°	7										

Two Hands for Manipulation

Parts severely nest or tangle or are flexible but can be grasped and lifted by one hand (with the use of grasping tools if necessary)

		Parts Present No Additional Handling Difficulties					Parts Present Additional Handling Difficulties				
		α ≤ 180°			α = 360°		α ≤ 180°			α = 360°	
		Size > 15mm	6mm ≤ Size < 15mm	Size < 6mm	Size > 6mm	Size ≤ 6mm	Size > 15mm	6mm ≤ Size < 15mm	Size < 6mm	Size > 6mm	Size ≤ 6 mm
		0	1	2	3	4	5	6	7	8	9
	8	1			1						

Two Hands or Assistance Required for Large Size

Two hands, two persons, or mechanical assistance required for grasping and transporting parts

		Parts can be Handled by One Person without Mechanical Assistance									2 Persons or Mechanical Assistance Required for Parts Manipulation
		Parts do Not Severely Nest or Tangle and are Not Flexible								Parts Severely Nest or Tangle or are Flexible	
		Part Weight < 10 lb				Parts are Heavy (> 10 lb)					
		Parts are Easy to Grasp & Manipulate		Parts Present Handling Difficulties		Parts are Easy to Grasp & Manipulate		Parts Present Handling Difficulties			
		α ≤ 180°	α = 360°	α ≤ 180°	α = 360°	α ≤ 180°	α = 360°	α ≤ 180°	α = 360°		
		0	1	2	3	4	5	6	7	8	9
	9										

Figure 3.2: Handling operations required during the 14 HDAT as represented on the B-D manual handling tables. Colour intensity represents the performance frequency of each operation (range: 1 - 11). Those operations not assessed by HDAT are left blank.

Part Added but not Secured

			After assembly no holding down required to maintain orientation and location				Holding down required during subsequesnt processes to maintain orientation or location			
			Easy to align and position		Not easy to align or position		Easy to align and position		Not easy to align or position	
			No resistance to insertion	Resistance to insertion	No resistance to insertion	Resistance to insertion	No resistance to insertion	Resistance to insertion	No resistance to insertion	Resistance to insertion
			0	1	2	3	6	7	8	9
	Parts and associated tool (inc. hands) can easily reach the desired location	0	**22**	**1**						
Part and associated tool (inc. hands) cannot easily reach the desired location	Due to obstructed access OR restricted vision	1	**1**							
	Due to obstructed access AND restricted vision	2								

Left vertical label: Addition of any Part where neither the part itself nor any other part is finally secured immediately

Part Secured Immediately

			No screwing operation or plastic deformation immediately after insertion (snap/press fits)		Plastic defirmation immediately after insertion						Screw tightening immediately after insertion	
					Plastic bending or torsion				Rivetting or similar operation			
			Easy to align and position with no resistance to insertion	Not easy to align or position and/or resistance to insertion	Easy to align and position	Not easy to align or position		Easy to align and position	Not easy to align or position		Easy to align and position with no torsional resistance	Not easy to align or position and/or torsional resistance
						No resistance to insertion	Resistance to insertion		No resistance to insertion	Resistance to insertion		
			0	1	2	3	4	5	6	7	8	9
	Parts and associated tool (inc. hands) can easily reach the desired location and the tool can be operated easily	3		**1**							**1**	
Part and associated tool (inc. hands) cannot easily reach the desired location or tool cannot be operated easily	Due to obstructed access OR restricted vision	4										
	Due to obstructed access AND restricted vision	5										

Left vertical label: Addition of any Part where the part itself and/or other parts are being finally secured immediately

Separate Operation

		Mechanical Fastening processes (part(s) already in place but not secured immediately after insertion)				Non-mechanical fastening processes (part(s) already in place but not secured immediately after insertion)				Non-fastening processes	
		None or localized plastic deformation			Bulk plastic deformation (large proportion plastically deformed)	Metallurgical processes			Chemical processes (e.g. adhesive bolding)	Manipulation of parts or sub-assembly (e.g. orienting)	Other processes (e.g. liquid insertion)
		Bending or similar process	Rivetting or similar processes	Screw tightening or similar process		No additional material required (e.g. resistance)	Additional material added				
							Soldering processes	Weld / braze processes			
		0	1	2	3	4	5	6	7	8	9
Assembly processes where all solid parts are in place	9			**2**						**5**	

Figure 3.3: Insertion operations required during the 14 HDAT as represented on the B-D manual insertion tables. Colour intensity represents the performance frequency of each operation (range: 1 - 17). Those operations not assessed by HDAT are left blank.

Table 3.2: The B-D manual handling and insertion code(s) for each HDAT. Codes calculated using the B-D classification tables and the items and operations identified in Table 3.1.

HDAT	B − D Handling Code(s)	B − D Insertion Code(s)
BBT	'00'	'00'
CDT	'11'; '40'$_{\times 2}$	'00'; '38'
FDT	'00'	'98'
GPT	'20'	'00'; '02'
JHFT	'00'$_{\times 2}$; '03'; '10'$_{\times 2}$; '13'; '20'; '23'; '30'	'00'
MPT	'01'; '03'$_{\times 2}$; '10'$_{\times 2}$; '20'; '23'$_{\times 2}$; '30'	'00'; '10'
MRMT	'00'	'00'$_{\times 2}$; '98'
MMDT	'00'	'00'$_{\times 2}$; '98'
NHP	'00'	'00'$_{\times 2}$
OCFD	'03'	'00'
OCTD	'40'	'00'
PPT	'00'; '01'; '03'	'00'$_{\times 2}$
SODA	'03'; '10'$_{\times 5}$; '13'; '20'; '30'$_{\times 4}$; '38'	'00'; '01'; '31'; '92'; '98'
WMFT	00'$_{\times 2}$; '10'; '13'; '15'; '20'; '23'; '30'; '80'	'00'; '98'$_{\times 2}$
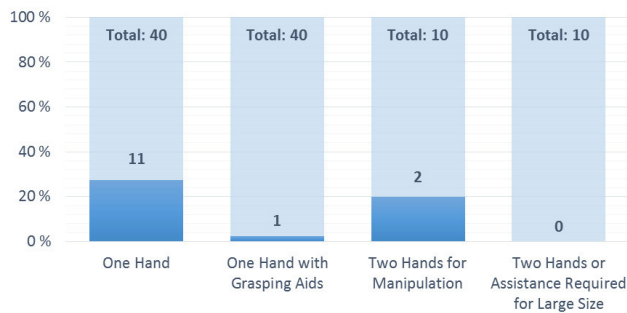
Figure 3.4: Number of operations within each B-D handling table that are considered by the 14 HDAT.
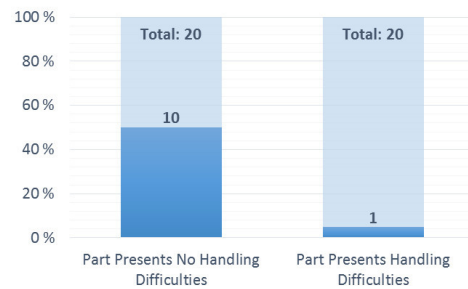
Figure 3.5: Number of one-handed B-D handling operations that are considered by the 14 HDAT.
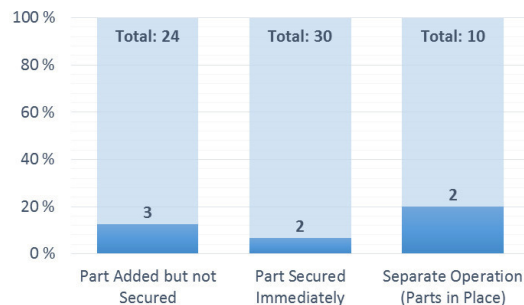
Figure 3.6: Number of operations within each B-D insertion table that are considered by the 14 HDAT.

relative to others within a narrow range of operations. While this association can be made when assessing human dexterity due to our natural ability to transfer skills between tasks, the same cannot be made when assessing robotic dexterity. Any assessment of robotic dexterity needs to be thorough, as robotic systems are much more susceptible to varying task and environmental conditions than humans.

Even when considering fourteen independent HDAT, their combined use does not offer as broad an analysis as the B-D classification tables. Consequently, the B-D classification tables are a more viable option for representing the dexterous operations within flexible manufacturing during robot assessment.

3.2.2   YCB Object Dataset Comparison

The YCB object and model set has been developed by researchers within the robotics community to *"facilitate benchmarking in robotic manipulation, prosthetic design and rehabilitation research"* [125]. The set incorporates a total of 73 objects which have sufficient variety to represent a wide range of aspects of the manipulation problem. These objects are mainly selected from daily life, which means that the dataset is particularly suited for assessments of robotic systems within the service robot industry. However, the dataset does include tools and other objects found within manufacturing, and so it is a viable option for those assessing industrial robotic systems. Accordingly, the B-D classification tables will be used to determine how comprehensively this object dataset represents those objects found within flexible manufacturing.

To reduce repetition, the full list of objects and their properties are given by the authors in [125]. Using this information and following the same approach as before, the handling of each YCB object has been classified and mapped to the B-D handling classification tables, as shown in Figure 3.7. Insertion codes are not calculated in this instance, as the YCB dataset defines the objects to be used during benchmarking but not the actual tests.

From summary of the results given in Figure 3.8 and Figure 3.9, it can be seen that the use of the YCB object dataset during robotic dexterity assessment will limit the number of flexible manufacturing operations which can be considered. Using the B-D

One Hand

Parts can be grasped and manipulated by one hand without the aid of grasping tools		Parts are Easy to Grasp and Manipulate					Parts Present Handling Difficulties				
		Thickness > 2 mm			Thickness ≤ 2 mm		Thickness > 2 mm			Thickness ≤ 2 mm	
		Size > 15 mm	6mm ≤ Size < 15 mm	Size < 6mm	Size > 6 mm	Size ≤ 6 mm	Size > 15 mm	6mm ≤ Size < 15 mm	Size < 6mm	Size > 6 mm	Size ≤ 6 mm
		0	1	2	3	4	5	6	7	8	9
$(α+β) < 360°$	0	21			1		2				
$360° ≤ (α+β) < 540°$	1	20			2		2				
$540° ≤ (α+β) < 720°$	2	14									
$(α+β) = 720°$	3	15								1	

One Hand with Grasping Aids

Parts can be grasped and manipulated by one hand but only with the use of grasping tools			Parts need Tweezers for Grasping and Manipulation								Parts need Standard Tools other than Tweezers	Parts need Special Tools for Grasping & Manipulation
			Parts can be Manipulated without Optical Magnification				Parts Require Optical Magnification for Manipulation					
			Parts are Easy to Grasp & Manipulate		Parts Present Handling Difficulties		Parts are Easy to Grasp & Manipulate		Parts Present Handling Difficulties			
			Thickness > 0.25 mm	Thickness ≤ 0.25 mm	Thickness > 0.25 mm	Thickness ≤ 0.25 mm	Thickness > 0.25 mm	Thickness ≤ 0.25 mm	Thickness > 0.25 mm	Thickness ≤ 0.25 mm		
			0	1	2	3	4	5	6	7	8	9
α ≤ 180°	0 ≤ β ≤ 180°	4										
	β = 360°	5										
α = 360°	0 ≤ β ≤ 180°	6										
	β = 360°	7										

Two Hands for Manipulation

Parts severely nest or are tangle but can be grasped and lifted by one hand (with the use of grasping tools if necessary)		Parts Present No Additional Handling Difficulties					Parts Present Additional Handling Difficulties				
		α ≤ 180°			α = 360°		α ≤ 180°			α = 360°	
		Size > 15mm	6mm ≤ Size < 15mm	Size < 6mm	Size > 6mm	Size ≤ 6mm	Size > 15mm	6mm ≤ Size < 15mm	Size < 6mm	Size > 6mm	Size ≤ 6 mm
		0	1	2	3	4	5	6	7	8	9
	8	1									

Two Hands or Assistance Required for Large Size

Two hands, two persons, or mechanical assistance required for grasping and transporting parts		Parts can be Handled by One Person without Mechanical Assistance								Parts Severely Nest or Tangle or are Flexible	2 Persons or Mechanical Assistance Required for Parts Manipulation
		Parts do Not Severely Nest or Tangle and are Not Flexible									
		Part Weight < 10 lb				Parts are Heavy (> 10 lb)					
		Parts are Easy to Grasp & Manipulate		Parts Present Handling Difficulties		Parts are Easy to Grasp & Manipulate		Parts Present Handling Difficulties			
		α ≤ 180°	α = 360°	α ≤ 180°	α = 360°	α ≤ 180°	α = 360°	α ≤ 180°	α = 360°		
		0	1	2	3	4	5	6	7	8	9
	9										

Figure 3.7: Potential handling operations that can be assessed using the YCB object dataset. Colour intensity represents the number of objects which map to each operation (range: 1 - 21). Those operations which cannot be assessed using objects from the YCB dataset are left blank.
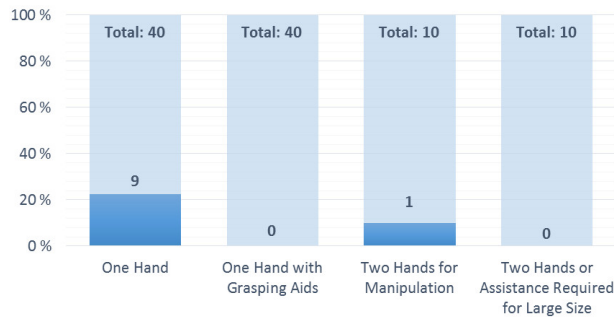
Figure 3.8: Number of operations within each B-D handling table that can be assessed using the YCB object dataset.
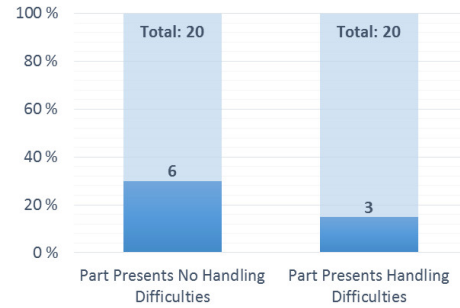
Figure 3.9: Number of one-handed B-D handling operations that can be assessed using the YCB object dataset.

classification system, many of the objects from the dataset have similar properties and can be handled using the same operation. As a result, only 10 % of all possible operations are considered when using all objects within the dataset. This does not diminish the usability of the YCB dataset, as it must be remembered that the set focuses on objects which are commonly encountered during daily living. However, it does highlight the need for considering more varied objects when assessing robotic dexterity within flexible manufacturing.

3.2.3   Comparison Outcome

While the range of operations and objects considered by the HDAT and YCB dataset have been shown to be limited when compared to the scope of the B-D classification tables, it is worth noting that the operations and objects that are considered represent those most commonly used within industry. This makes sense, as an optimised manufacturing process (from DFA analysis) will prioritise operations and objects that require lower levels of dexterity as they increase its efficiency. To highlight this, it has been noted that simple peg-in-hole operations account for 35% of all operations within industry [126]. Therefore, the use of HDAT and / or the YCB object dataset could provide a reasonable estimate of a robotic system's performance within selected assembly tasks. However, to perform a complete assessment of robotic dexterity within flexible manufacturing, the more challenging objects and operations identified by the B-D tables need to be considered.

3.3   Framework Proposal

A framework has been developed to provide a means of defining the dexterous capabilities of a robotic system and identifying the assembly operations that it can perform in a flexible manufacturing environment. It is foreseen that the adoption of such a framework would help facilitate direct comparisons between different robotic systems and further assist in quantifying the current state of robotic dexterity within manufacturing.

3.3.1   Robotic Dexterity - Updated Definition

At this stage, the preliminary definition of robotic dexterity provided in Chapter 2 can be updated in order to provide a more detailed definition that is specific to robotic systems within flexible manufacturing. From an analysis of the literature and the comparisons performed in Section 3.2, it can be concluded that the comprehensive nature of the B-D classification tables encapsulate the dexterous requirements within flexible manufacturing. Ergo, this work proposes that the dexterity of a robotic system within flexible manufacturing be defined as the ability of a robotic system to perform and adapt to the operations identified within the Boothroyd-Dewhurst classification tables in adequate time and in the presence of uncertainty.

Similar to other definitions of robotic dexterity presented in Section 2.5.2, this functional definition acknowledges the necessity for sensing and control by its reference to object manipulation. However, equally important is that the definition also accounts for the dexterous requirements that may arise from the surrounding environment. Based on this definition, a robot's dexterity is dependent on its ability to perform each B-D operation while overcoming the micro and macro level changes that occur within flexible manufacturing. This ability can be measured by considering a number of system-level performance metrics. These metrics will be discussed in Sections 3.4.2 and 3.4.3.

3.3.2   Framework Scope

Based on the updated definition of robotic dexterity, the framework considers a robotic system to include the robotic manipulator(s), end effector(s), controller(s), vision system(s), sensing system(s), and additional hardware/software required during grasping or manipulation. The framework is specifically for small-scale, flexible assemblies which require no part or tool acquisition outside of the assembly workspace. Accordingly, the robotic system does not need to be mobile, and components can be fixed within the environment if necessary. The positioning of the robotic manipulator within the environment is left to the user, but it should ideally be positioned to maximise the number of assembly operations contained within its dexterous workspace, as defined in Section 2.5.2.

The developed framework assesses the dexterity of a robotic system while performing benchtop assembly processes. This identification of a designated workspace helps to limit the scope of the framework to encourage an assessment of robotic dexterity that is more targeted and informative. Accordingly, the performance measures that are incorporated within the framework can be considered global indices [114] that represent the average performance of the robotic system within this region.

3.4   Framework Implementation

The developed framework can be applied in two key ways (see Figure 3.10). First, it provides a reliable means to define an assembly's dexterous requirements and identify the robot specifications necessary for assembly completion. This would simplify and improve the efficiency of the robot selection process. As an example, this use of the framework would be beneficial to a manufacturing company seeking to automate an existing manual assembly process. Second, the framework provides guidance for identifying the assembly processes achievable in scenarios where the robotic system to be used is predefined. This identification of assembly processes helps to capture the dexterous ability of a robotic system, and facilitates comparisons to be made between different robotic systems. As an example, this use of the framework would be beneficial to a robot supplier during marketing to highlight the potential within
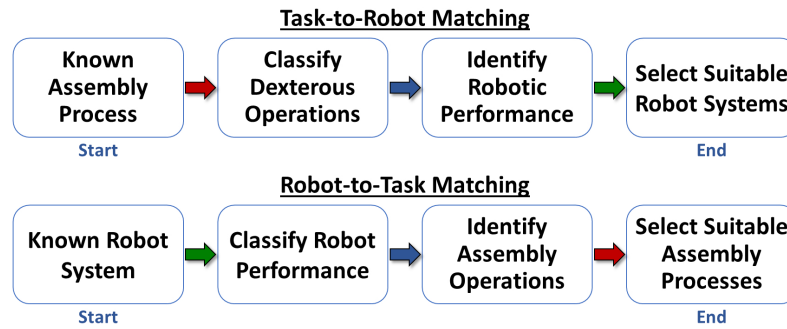
Figure 3.10: Developed framework can be used to identify the robotic systems suitable for a given assembly process, or equally to identify the assembly operations achievable by a given robotic system.
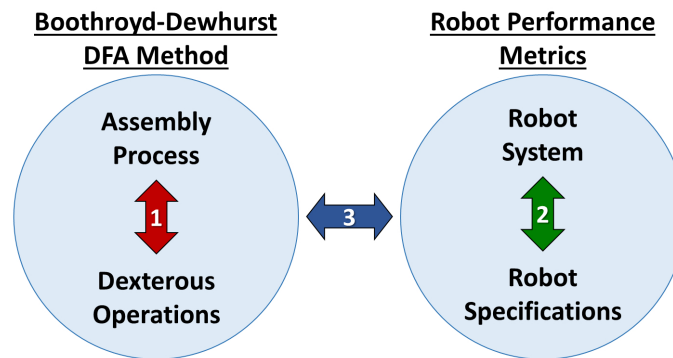
Figure 3.11: Framework incorporates three activities (labelled 1-3) to link robotic systems to flexible manufacturing operations and simplify selection within the area.

flexible manufacturing.

Regardless of the chosen direction, the developed framework incorporates the following three distinct activities (see Figure 3.11):

- *Activity 1:* Match a flexible manufacturing process to/from dexterous operations using the B-D classification tables

- *Activity 2:* Match a robotic system to/from robot specifications using robotic performance metrics

- *Activity 3:* Match the dexterous operations of a flexible manufacturing process to/from robot specifications

The execution of these activities helps to address the current difficulty in matching robotic systems to/from flexible manufacturing processes, as will be highlighted in the sections below.

3.4.1 Activity 1: Dexterous Requirements

During its optimisation of flexible manufacturing processes, the B-D DFA method utilises manual handling and insertion tables to classify the difficulty of operations within a manual assembly processes. Thanks to the positive correlation between assembly difficulty and dexterity, these tables also classify manual assembly operations based on the required dexterity. From Section 3.2, it has been shown that the range of operations and objects considered by these B-D classification tables is extensive and provides a good representation of those that may be encountered within flexible manufacturing. Accordingly, the B-D classification tables offer a very useful catalogue of possible operations within flexible manufacturing, and their inclusion within a dexterity assessment framework can help to ensure a thorough assessment of dexterity. From Section 2.3.2, Boothroyd and Dewhurst also developed classification tables for the analysis of high-speed and general-purpose (robotic) automation assemblies. However, these classification tables assume the use of traditional automation that require dedicated assembly lines and axillary equipment. Consequently, the tables are not well suited for the consideration of robotic systems within flexible manufacturing, as the environment requires a system to be capable of responding to macro- and/or micro-level changes in production. It is for this reason that flexible manufacturing is primarily performed by manual labour. Accordingly, the consideration of the B-D manual handling and insertion tables is better suited to this framework, as they identify the dexterous requirements that robotic systems must meet in order to become a viable choice for flexible manufacturing. This new application of the B-D manual classification tables is particularly useful, as it shows how the B-D DFA method can still be used when considering more modern robotic systems.

An advantage of using the B-D DFA method is that it is the most widely used DFA method. This means that the method is better known to those within industry, and is more likely to be used during initial design and optimisation of a flexible manufacturing process. Accordingly, the identification of the dexterous requirements (i.e. activity 1) may already be completed prior to the use of this framework, which would simplify the framework's implementation and encourage its use by those within industry. In addition, the B-D classification tables present an average human

completion time for each classified operation, which provide a means to reasonably estimate human performance without the need for task-specific testing and analysis. This is particularly useful within a robotic dexterity assessment framework, as it can be compared against calculated robotic performance in order to identify the most suitable choice for each flexible manufacturing operation.

3.4.2 Activity 2: Robotic Performance Metrics

Current robot specifications do not provide the necessary parameters to capture the dexterous performance of industrial robotic systems. This work proposes that a new set of performance metrics be developed to provide a more accurate indication of a robotic system's performance within flexible manufacturing. In particular, these metrics will capture the dexterous ability of a robotic system within the area by considering the dexterous requirements identified by the B-D classification tables. This ensures that the developed performance metrics account for all dexterous demands within flexible manufacturing.

In order to ensure a thorough assessment of the robotic system, both component-level and system-level metrics should be considered.

3.4.2.1 Component-Level Metrics

As the name suggests, component-level metrics relate to the individual components within a robotic system that have any influence on the system's performance of operations within the B-D tables. As noted earlier and reiterated by Biagiotti et al. in [150], robotic dexterity is dependent on the robot's mechanical design, sensory equipment, and control algorithms. Consequently, metrics which relate to these components should be considered within this framework.

With reference to the work performed by the Intelligent Systems Division at NIST (see Section 2.5.2.3), component-level metrics can be grouped according to sixteen assembly actions. This is beneficial as these actions can easily be mapped to B-D operations, which creates a direct link between developed performance metrics and assembly operations. To highlight this, a dependency table has been created which identifies the actions that influence each B-D handling and insertion operation. An

Table 3.3: Dependence of selected B-D handling and insertion operations on the sixteen actions identified by NIST (with reference to Figures 3.2 and 3.3).

	B-D Code	Detect	Align	Pick up	Reposition Object	Insert	Slide	Retract	Transport	Place	Tool Action	Hold	Fasten	Coordinate	Navigation	Track	Communications
Handling Code	'00'	1	1	1	0	0	0	0	1	0	0	1	0	1	0	0	1
	'09'	1	1	1	1	0	1	0	1	0	0	1	0	1	0	1	1
	'30'	1	1	1	1	0	0	0	1	0	0	1	0	1	0	1	1
	'39'	1	1	1	1	0	1	0	1	0	0	1	0	1	0	1	1
	'40'	1	1	1	1	0	0	0	1	0	1	1	0	1	0	1	1
	'49'	1	1	1	1	0	0	0	1	0	1	1	0	1	0	1	1
	'80'	1	1	1	1	0	1	0	1	0	0	1	0	1	0	1	1
	'89'	1	1	1	1	0	1	0	1	0	0	1	0	1	0	1	1
	'90'	1	1	1	1	0	0	0	1	0	0	1	0	1	0	1	1
	'99'	1	1	1	1	0	0	0	1	0	1	1	0	1	0	1	1
Insertion Code	'00'	1	1	0	1	1	0	1	0	1	0	1	0	1	0	1	1
	'09'	1	1	0	1	1	1	1	0	1	0	1	0	1	0	1	1
	'20'	1	1	0	1	1	0	1	0	1	0	1	0	1	0	1	1
	'29'	1	1	0	1	1	1	1	0	1	0	1	0	1	0	1	1
	'30'	1	1	0	1	1	0	1	0	1	0	1	1	1	0	1	1
	'39'	1	1	0	1	1	0	1	0	1	1	1	1	1	0	1	1
	'50'	1	1	0	1	1	1	1	0	1	0	1	1	1	0	1	1
	'59'	1	1	0	1	1	1	1	0	1	1	1	1	1	0	1	1
	'90'	1	1	0	1	0	1	1	0	0	1	1	1	1	0	1	1
	'99'	1	1	0	1	1	1	1	0	0	1	1	0	1	0	1	1

extract of this table is given in Table 3.3.

The use of component-level performance metrics that relate to each assembly action will help to ensure that a robot's dexterity is fully assessed and captured. However, a new set of performance metrics is required in order to achieve this, as metrics currently defined by suppliers are incomplete and do not provide a true reflection of performance. The development of a comprehensive and complete set of component-level performance metrics is beyond the scope of this work, however the first of these performance metrics are identified as part of this framework. These metrics have been identified using an inductive research approach, and provide a greater insight into the dexterity of robotic systems within flexible manufacturing when compared to supplier specifications. The developed component-level performance metrics include:

1. Grasp Region: The maximum area reachable by the fingers of an end effector

2. Grasp Cycle Time: The minimum time required for an end effector to achieve full closure from a known pre-grasp configuration and to return to the pre-grasp configuration [129]

3. Trajectory Time: The time required for a manipulator to complete a trajectory

in relation to the trajectory's distance

4. Communication Delay: Maximum delay during communication between a robot system and its control program

5. Insertion Search Time: The time required for a robotic system to find the correct insertion point in the presence of uncertainty

As will be shown in Chapter 5, this preliminary set of component-level performance metrics can be used to estimate the robot's performance within the align, pickup, transport and communicate assembly actions, which is sufficient to estimate a robotic system's dexterity in a range of B-D operations. The approach and method used to measure each of these robotic performance metrics will be outlined in Section 4.3.

3.4.2.2   System-Level Metrics

For a system to perform dexterous operations within manufacturing assembly, it is not only dependent on the performance of its individual components but also on their collaboration. As such, system-level metrics provide an insight into the performance of the overall system which will help to establish how the system will perform in real-life scenarios.

The measurement of system-level metrics requires the development of standard test methods and artefacts. Accordingly, the following system-level benchmarks are considered within this framework:

1. Modified Minnesota Rate of Manipulation Test
2. Peg Insertion Test

The former indicates the robotic system's ability to perform the gross manual dexterity operations typical within pick-and-place operations while the latter indicates the robotic system's ability to perform assembly operations that require a finer level of dexterity. Both tests make use of the following system-level performance metrics; initialisation time, probability of success (PS), and completion time. These metrics identify the robotic system's feasibility and capability, which will now be discussed in greater detail.

3.4.3 Activity 3: Dexterity Matching

The dexterity matching activity determines both the feasibility and capability of a robotic system for each B-D assembly operation.

3.4.3.1 System Feasibility

The feasibility of a robotic system indicates the likelihood that it will perform a B-D operation successfully, and its value is dependent on the system itself and the constraints of the operation. Performance metrics which relate to feasibility are compared to the requirements of the B-D operation. As an initial indicator, supplier specifications such as payload and reach can be used to determine if the robotic system can attempt the given operation. If it can, then additional performance metrics developed within the proposed framework can be combined in order to generate a probability of success (PS) value.

The PS value is bounded between 0 and 1, where 0 indicates that the system is not able to perform the given B-D operation, and 1 indicates that it can perform the operation with complete certainty. The PS value is dependent on the chosen robotic system and operation being considered, but can be estimated by combining developed component-level performance metrics. These performance metrics estimate the PS value for a given confidence level [140], which indicates the method's confidence in the accuracy of the results. A 95% confidence level will be employed within the developed framework, as this is commonly used within industry [151].

Calculating a PS value is particularly beneficial as it determines if a robot system has the necessary level of dexterity to overcome uncertainty and micro level changes during a flexible manufacturing process (e.g. disturbances in product geometry, unknown part orientation and presentation, etc.).

3.4.3.2 System Capability

The capability of a robotic system quantifies its suitability for a given B-D operation by estimating its initialisation time and completion time (CT). Combined, these metrics give an indication of the robotic system's throughput. Initialisation time refers to the time required to (re-)program a robot system before an operation can begin.

This metric does not consider the initial development of the control program(s), but rather focuses on the time required to (re-)teach a robotic system during integration. Initialisation time is an important metric as it identifies the robotic system's ability to adapt to macro level changes during a flexible manufacturing process (e.g. changes in product volume and mix).

Completion time (CT) refers to the time required to successfully complete operation in full. The metric incorporates all actions required to perform the operation including detection, alignment, acquisition, transportation, insertion, regrasping, etc. Time-related performance metrics are combined with operation information to give an accurate CT estimate. This numerical value is beneficial as it facilitates direct comparisons between robotic systems and human performance.

The capability of a robotic system provides a relative level of dexterity which can be combined with other cost metrics in order to determine the most suitable system for a flexible manufacturing process.

3.4.3.3 Operation - Performance Matching

A gap currently exists within industry as the dexterous performance of industrial robotic systems cannot easily be quantified within flexible manufacturing. Accordingly, the developed framework includes a dexterity matching activity which relates robotic system performance metrics to B-D operations. This facilitates robot-to-task matching based on dexterity, equivalent to that currently done with other parameters such as speed and payload.

This robot-to-task matching encourages the design and selection of better robotic systems within manufacturing. The framework identifies the component- and system-level performance necessary for an assembly operation, allowing manufacturers to construct robotic system structures which are optimal for their assembly based on dexterity and other metrics such as cost, reliability, and speed.

3.5   Performance Data Analysis

An important part of the developed framework is that data collected during the assessment of a robotic system is correctly analysed. This ensures that the performance of the robotic system is accurately captured and facilitates comparisons to be made between different robotic systems. Accordingly, a systematic approach to analysing the collected data is presented within this section.

With reference to Section 2.6, different statistical tools and algorithms are required depending on the variables being considered and the parameter(s) being analysed. As part of this framework, a minimum number of statistical tools are presented in order to reduce complexity but still provide meaningful results. Based on the system-level metrics proposed within this framework, these tools have been grouped according to the type of data being considered i.e. categorical and continuous data. Continuous data (results which are measured on a numerical scale covering a large range) can be analysed by using the two-sample Kolmogorov-Smirnov (KS) test and by calculating the detectable difference. The two-sample KS test determines acceptance or rejection of the null hypothesis (H_0), where H_0 states that the two data sets come from the same population. To complement the KS test, the detectable difference value quantifies the magnitude of any difference by measuring the minimum distance between the two population true mean ranges. A Matlab script has been developed as part of this work to implement both statistical tools. An example of the script is given in Appendix C. To note, a significance level of $\alpha = 0.05$ was used within the two-sample KS test.

Categorical data (results which only have a discrete number of possible outcomes) can be analysed by using the Kolmogorov-Conover (KC) test and by calculating the probability of success (PS) . The KC test is an extension of the KS test, and is used to determine if two discontinuous data sets belong to the same population. The PS is a performance measure that is used to identify the likelihood of achieving a given categorical rank. In contrast to the PS value outlined in Section 3.4.3, this value is calculated based on collected data, and is determined based on the number of independent trials, the number of successes, and the chosen confidence level. The

code for analysing categorical data using these statistical tools was taken from a software suite that has been made publicly available by researchers at NIST [129].

Chapter 4

Experimental Design and Methodology

4.1 Testing Overview

To illustrate the application of the developed framework, a number of sample scenarios have been considered. The selected scenarios are derived from typical manufacturing operations, and incorporate both handling and insertion operations. For each of the chosen scenarios, a level of uncertainty exists which make it difficult for traditional automation to perform the task. Flexible robotic systems appear to be a better option, however with current supplier specifications it is difficult to determine if their level of dexterity is sufficient to perform the tasks efficiently.

Accordingly, the developed framework will be used to systematically assess the dexterity of a number of robotic systems. This approach will utilise new metrics that better capture the dexterity of a robotic system and provide a more accurate estimate of their performance. The structured framework facilitates the comparison of different robotic systems and considers their viability relative to manual labour. To validate the developed performance metrics and estimated levels of dexterity, each scenario is replicated within a laboratory and performed by the different robotic systems. In order to ensure a satisfactory level of confidence in the collected results, the scenarios are repeated a minimum of 60 times by each robotic system. Collected data is compared to the performance estimated by the framework, but also provides an opportunity to perform cross-system comparisons using the suite of statistical tools outlined in Section 3.5.

4.2 Robotic Systems

Within the experiments described below, a range of robotic systems are used. These robotic systems are composed of a combination of the following components.

4.2.1 Robotic Manipulators

The robotic manipulators considered within this thesis and their relevant supplier specifications are presented in Table 4.1. Each robot manipulator is classified as a low payload, collaborative robot. Accordingly, these robots are designed to share human workspaces and perform smaller-scale operations such as pick-and-place, material handling, packaging, palletising, and assembly.

Of the chosen robotic manipulators, the KUKA LWR4, UR10, and UR5 are used throughout the developed framework, while the Baxter robot is only featured in later experimentation. This inclusion of the Baxter robot during testing facilitates additional comparisons to be made and highlights the scenarios' use as a benchmarking tool.

Table 4.1: Supplier specifications for the robotic manipulators considered, taken from [152]–[154] (* Repeatability not specified by supplier, but has been recorded in [155]).

Robot	DOF	Weight	Payload	Reach	Speed	Repeatability	Safety Features
Universal Robotics UR10	6	28.9 kg	10 kg	1300 mm	1 m/s	± 0.1 mm	Current Detection, 15 safety functions
Universal Robotics UR5	6	18.4 kg	5 kg	850 mm	1 m/s	± 0.1 mm	Current Detection, 15 safety functions
KUKA LWR4	7	16 kg	7 kg	790 mm	110-204 °/s	± 0.05 mm	Integrated joint torque sensors, streamlined housing, programmable compliance
Rethink Robotics Baxter Arm	7 (per arm)	75 kg (total)	2.3 kg (per arm)	1210 mm (per arm)	0.6 m/s (per arm)	± 2.9 - 3.3 mm * (per arm)	Series-elastic actuators, integrated force, sonar and camera sensors
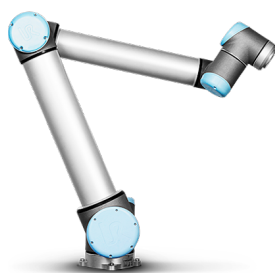
(a) KUKA LWR4 (b) UR10 (c) UR5 (d) Rethink Robotics Baxter
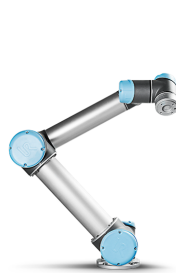
4.2.1.1   Universal Robotics UR10 & UR5

The Universal Robotics (UR) robots are 6 DOF robotic arms with embedded direct drive electromagnetic motors. The robots are controlled via a touch-screen PolyScope graphical user interface (GUI), which facilitates the easy programming of simple tasks through the recording of waypoints. The UR robot's motions are position controlled, which means that the arm moves to the desired position with the programmed velocity.

4.2.1.2   KUKA LWR4

The KUKA LWR4 is the fourth generation of the *"Lightweight Robot"* (LWR), which was developed in collaboration with the German Aerospace Centre (DLR). The robot arm is directly driven via motors with integrated joint torque sensors developed by DLR. The KUKA LWR4 has three controller options; position controller mode, gravity compensation mode, and compliance controller mode. In gravity compensation mode, the robot compensates for gravity and the weight of any load so that the arm can be moved with minimal forces. This mode is well suited when teaching the robot new waypoints. In compliance controller mode, the Cartesian compliance of robot's axes can be modified to suit a specific task. This mode is well suited for motions that require contact with the environment.

4.2.1.3   Rethink Robotics Baxter

Baxter is a 14-DOF dual arm collaborative industrial robot from Rethink Robotics. It is a humanoid robot with two arms, a torso, a LCD display face, and built in sonar and camera sensors for improved human interaction. The arms are driven by servo based series-elastic actuators, which provide passive compliance to their mechanical structure. The use of two arms allows Baxter to perform coordinated or dual manipulations unachievable by the other industrial robots considered.

4.2.2 Robotic End Effectors

The robotic end effectors considered within this work and their relevant supplier specifications are given in Table 4.2. Of these robotic end effectors, the Schunk KGG 80-30 gripper and the Robotiq 3-Fingered gripper are used throughout the developed framework, while the Allegro robotic hand is used in later benchmarking tests to facilitate additional cross-system comparisons.

4.2.2.1 Schunk KGG 80-30

The Schunk KGG 80-30 is a pneumatic parallel jaw gripper. Each finger can be custom engineered to suit the application, however the finger stroke length is limited to 15 *mm*. To note, the performance specifications of the gripper given in Table 4.2 are for the recommended operational pressure of 6 *bar*.

4.2.2.2 Robotiq 3-Fingered Gripper

The Robotiq 3-Fingered Gripper is an electrical industrial robot gripper. Each finger is under-actuated, meaning that it has fewer motors than its total number of joints. Under-actuation reduces cost and complexity while still allowing the gripper to perform shape-conforming grasps. The Robotiq 3-Fingered Adaptive gripper has

Table 4.2: Supplier specifications for the robotic end effectors considered, taken from [156]–[158].

End Effector	Type	Fingers	DOF	Weight	Fingertip Payload	Max Finger Speed	Repeatability
Schunk KGG 80-30	Pneumatic Parallel Jaw Gripper	2	1	0.25 kg	0.66 kg	300 mm/s	0.02 mm
Robotiq 3-Fingered Gripper	Underactuated Gripper	3	4	2.3 kg	2.5 kg	110 mm/s	0.05 mm
Allegro Hand	DC Motor Robotic Hand	4	16	1.09 kg	1.5 kg	545 °/s	NA

(a) Schunk KGG 80-30 Gripper   (b) Robotiq 3-Fingered Gripper   (c) Allegro Robotic Hand

four different grasp configurations; basic, wide, pinch, and scissor. The pinch grasp (shown in Table 4.2) is only considered within this framework, as this grip is best suited for the chosen flexible manufacturing scenarios.

4.2.2.3   Allegro Robotic Hand

The Allegro Hand is an electrical four-fingered robotic hand with 16 independent DOF and rotary joint encoders with a 0.002° resolution. This facilitates the performance of more complicated in-hand manipulations in addition to grasping operations, provided the use of an adequate, real-time control strategy.

For testing, the Allegro hand was modified by mounting three 6-axis force-torque transducers at the fingertips (see Figure 4.1). These sensors provided a touch-based, 6-DOF object pose estimation, 3D fingertip force, 3D fingertip normal force, and 3D fingertip centre of pressure. A manipulation controller and finger force controllers were developed to control the Cartesian pose of an object (see Figure 4.2). These controllers enabled impedance control when interacting with an object and the environment via finger Cartesian force control.

The integration and algorithms required to provide these sensing modalities and the custom manipulation controller were developed by Van Wyk and stem from his work in [159]. Accordingly, their discussion here is solely to provide the reader with some background on the robot hand used in later testing.
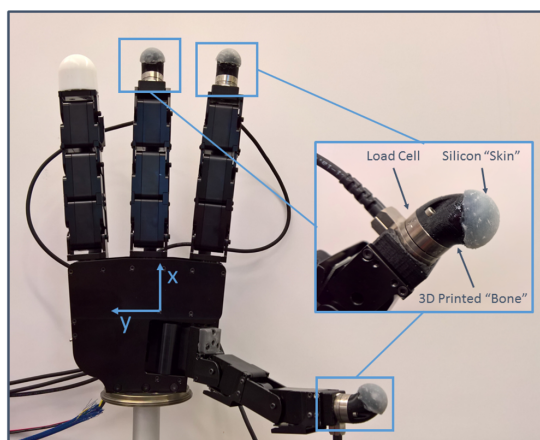
Figure 4.1: Allegro robotic hand with attached force-torque transducers.
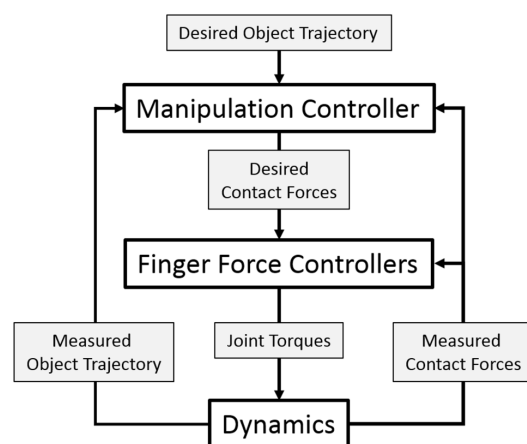
Figure 4.2: Multi-fingered manipulation control architecture.

4.2.3 Initialisation Approach

During testing, target locations within the environment were recorded using a number of different approaches.

4.2.3.1 Teach Programming

This approach was to teach the robot the target positions manually by dragging the robot manipulator to the desired locations and recording the robot's configuration at each point. Due to its simplicity, this form of programming is commonly used when interacting with collaborative robots within manufacturing. However, when precision is required, the robot's configuration may need to be fine-tuned using controlled motions via the robot's flex pendent. As each target location must be manually trained, this approach can be time consuming.

4.2.3.2 Simulated Vision Detection

During testing, simulated error can be added to target positions in order to indicate how the robotic system can deal with uncertainty during an operation. For simplicity, the positional uncertainty of a vision system can be represented by assuming a bivariate normal distribution with no correlation among variables (see Figure 4.3). A multivariate normal distribution is a generalisation of the univariate normal (Gaussian) distribution for two or more dimensions and is parametrised by its mean
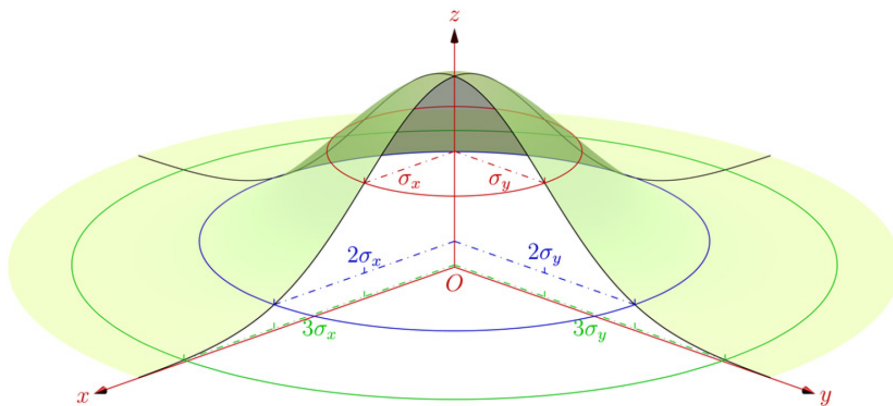
Figure 4.3: The probability distribution of a bivariate normal distribution with zero correlation and mean, showing the one, two and three standard deviation (σ) confidence regions. Taken from [160].

(μ), and covariance matrix (Σ). For a *n-dimensional* random vector x, the probability density function is given by [161]:

$$y = f_n(x, \mu, \Sigma) = \frac{1}{\sqrt{|\Sigma|(2\pi)^n}} e^{-\frac{1}{2}(x-\mu)'\Sigma^{-1}(x-\mu)} \tag{4.1}$$

where μ is a $(1 \ x \ n)$ vector and Σ is a $(n \ x \ n)$ symmetric positive definite matrix. The mean represents the expected value of the distribution and is therefore the central point of the probability distribution. The covariance matrix is analogous to the variance (σ^2) of a univariate normal distribution. The diagonal elements of Σ represent the variance for each variable, while the remaining elements represent the covariances between variables.

As noted, the variance is the square of the standard deviation (σ) and represents the spread of a distribution. A larger standard deviation means that the data points of the distribution tend to be further from the mean, and vice-versa. For a univariate normal distribution, the cumulative probability at distances of one, two and three standard deviations from the mean are 68.3%, 95.5%, and 99.7% (known as the *3-sigma rule*) [162]. For a bivariate normal distribution, these cumulative probabilities drop to 39.35%, 86.5% and 98.9% respectively [160].

The application of simulated perception error is beneficial for multiple reasons. First, its presence introduces stochasticity into a robot's performance data (many statistical tests assume sufficiently independent, uncorrelated samples). Furthermore, controlling the perception error allows for performance benchmarking by easily subjecting different robotic systems to the same perception errors, or subjecting one robotic system to various levels of perception error.

4.2.3.3   Cognex Vision System

To emulate a vision system used within manufacturing, a Cognex vision system and GigE (Gigabit Ethernet) camera were chosen for testing. Cognex provides hardware and software solutions to the wide range of vision requirements within industry. One such product is VisionPro, which is software environment that facilitates 2D, 3D, and multi-camera vision processing. The software includes a library of advanced vision tools which makes it particularly useful within industry for applications which require

inspection, detection, and guidance [163]. Accordingly, the VisionPro software was used to determine the target locations within the camera's field of view. The GigE camera used for image acquisition is summarised in Table 4.3.

During the execution of the vision detection system, the GigE camera was connected via an Ethernet cable and PCI frame grabber to a PC running the VisionPro software. This PC was connected to the internal network to facilitate communication between the VisionPro environment and the control programs of each robotic system. Communication was established on a separate thread to enable swift updates with a minimal hit to the control programs execution time. Within the VisionPro application, a number of tools were used in order to successfully detect the target location, including a colour extractor tool and blob tool (see Figure 4.4). The latter finds and filters blobs (or 2D shapes) within an image by identifying groups of pixels that fall into a designated grey-scale range.

With the GigE camera fixed within the environment, the camera was calibrated so that pixel locations could be converted to the required Cartesian coordinate system. This was achieved by performing a checkerboard calibration, as shown in Figures 4.5 and 4.6. During the calibration process, the checkerboard's horizontal and vertical lines was aligned to either the robot or world's X-Y coordinate system. By ensuring the checkerboard was placed on the table at the same height of the object being detected and knowing the side length of each square, the VisionPro checkerboard calibration tool could use the intersection points of the checkerboard to determine the (non-)linear transform between the camera and the real world. This transformation accounts for rotations and scaling, as well as optical and/or perspective distortion

Table 4.3: Supplier specifications for the Basler acA2000 GigE camera chosen for testing.

Basler acA2000 − 50gc Camera		
	Resolution	2046 x 1086
	Pixel Size	5.5 x 5.5
	Frame Rate	50 fps
	Pixel Depth	12 bits

(a) Input from GigE Camera

(b) Output from Colour Extractor

(c) Input to Colour Extractor

(d) Output from Blob Tool
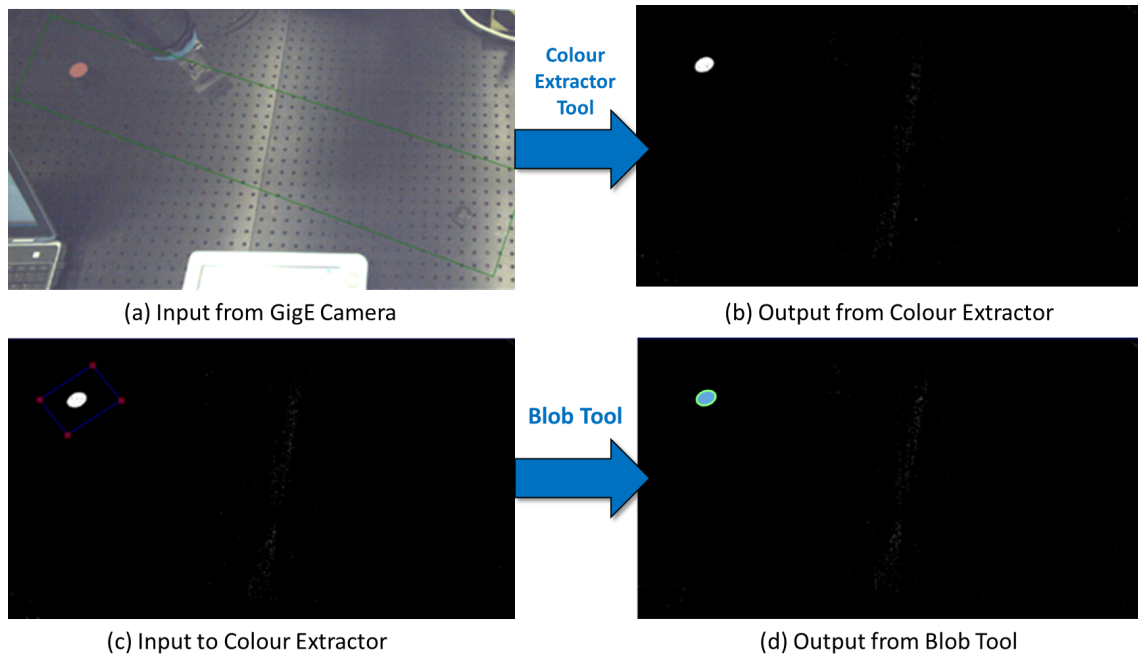
Figure 4.4: Image captured by the GigE camera being processed by VisionPro using the colour extractor tool and blob tool. In this instance the colour extractor tool (a) searches for red within the defined region, and (b) converts detected pixels white while setting remaining pixels to black, while the blob tool (c) searches for light blobs on a dark background within the defined region and (d) selects the most appropriate blob based on shape and area.

such as aspect and skew errors. Since errors accumulate as the distance from the calibration board increases, the accuracy of the transformation can be improved by ensuring that the calibration board fills a significant portion of the camera's field of view and is located in the area where detection is likely to occur.

To estimate the possible positional errors which arise from using the Cognex vision system, the system was calibrated to the world (as described above) and used to detect cylindrical blocks at thirteen known coordinates. During assessment, the accuracy of the vision system was determined by recording the trueness and precision of its measurements. From ISO 5725, trueness refers to closeness of agreement between the arithmetic mean of the test results and the reference value, while precision refers to the closeness of agreement between the test results [164], [165].

From testing, the Cognex vision system had high precision (with values less than $0.1\,mm$), but variable trueness depending on the block's location within the camera's field of view (see Table 4.4). Unsurprisingly, the camera's trueness decreased when
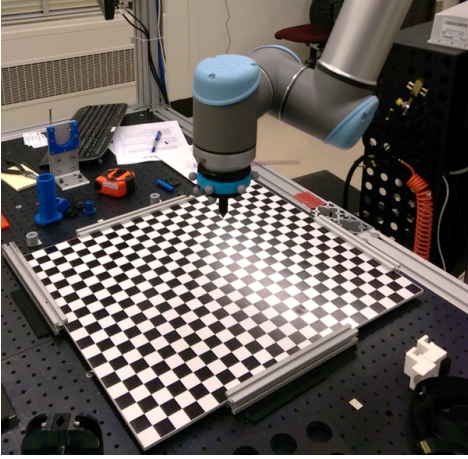
Figure 4.5: Positioning of calibration checkerboard within the robot's environment.
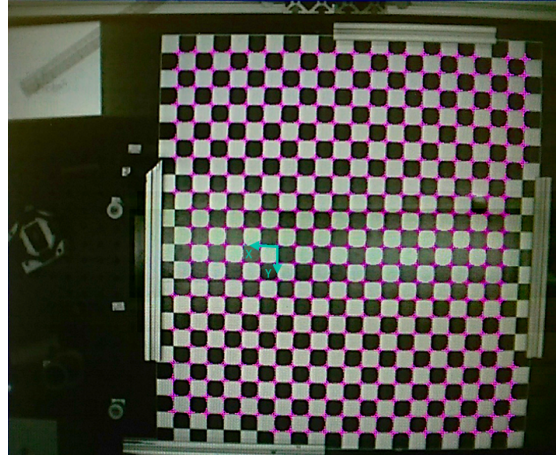
Figure 4.6: The VisionPro checkerboard tool detects the intersection points and uses the board's spacing distance, position, and orientation to transform pixel coordinates to world (or robot) coordinates.

Table 4.4: Trueness of the Cognex vision system during detection of cylindrical blocks at different world coordinates.

Position	World Coordinate		Recorded Position		Trueness	Position	World Coordinate		Recorded Position		Trueness
	X (mm)	Y (mm)	X (mm)	Y (mm)	(mm)		X (mm)	Y (mm)	X (mm)	Y (mm)	(mm)
1	-600	-300	-598.841	-298.934	-1.575	8	100	50	100.031	50.548	-0.549
2	-500	-250	-499.017	-249.046	-1.370	9	200	100	199.814	100.432	0.470
3	-400	-200	-399.170	-199.088	-1.233	10	300	150	299.587	150.229	0.472
4	-300	-150	-299.296	-149.245	-1.032	11	400	200	399.410	200.169	0.614
5	-200	-100	-199.504	-99.326	-0.837	12	500	250	499.270	250.049	0.732
6	-100	-50	-99.589	-49.364	-0.757	13	600	300	599.279	299.634	0.809
7	0	0	0.192	0.491	-0.527						

the block was further away from the camera's centre point due to an increase in perspective distortions. Accordingly, the performance of the Cognex vision system could be improved by repositioning the camera and/or performing a more meticulous calibration. However, this was not done as the purpose of this framework is not to estimate optimal performance but rather expected performance based on known parameters.

The positional error of the Cognex system across its field of view can be approximated using the recorded trueness values. Assuming the object to be detected is more likely to be located close the camera's centre point, the positional error can be represented by a normal distribution with a mean of $-0.37\,mm$ and a standard deviation of $0.87\,mm$.

4.2.3.4   Robot Registration

In selected tests, an alternative approach was used whereby the robot was registered to the world using the short hand-guiding methodology developed by researchers at NIST and presented in [166]. This methodology involves the guiding of the robot's tool centre point (TCP) to three predetermined poses within the world frame using target seats rigidly mounted to the workspace. Since the seats have known translations to the world origin, the recording of these poses allows for the generation of a transformation matrix which registers the robot to the world coordinate system. This robot registration approach allows for swift re-registration, which is important within flexible manufacturing as its changing environment requires more frequent alterations to the robotic system's workspace.

As shown in Figure 4.7, the error in using the short hand-guiding methodology is very much dependent on the chosen robotic manipulator and the distance of the target from the registration seats. However, from [166], the distribution of these errors can be represented by a normal distribution with a mean of $8.82\,mm$ and standard deviation of $4.85\,mm$ for the KUKA LWR4, and a mean of $4.64\,mm$ and standard deviation of $1.23\,mm$ for the UR10.
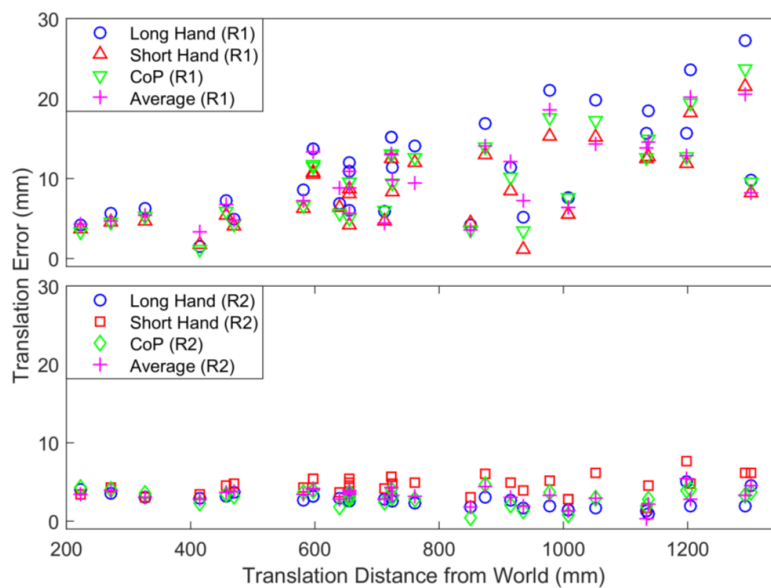
Figure 4.7: Translational error of the KUKA LWR4 (R1) and the UR10 (R2) as a function of the target's distance from the registration seats. Taken from [166].

4.2.3.5   Cognex + Registration

A final initialisation approach calibrated the Cognex vision system to the world coordinate system and used the robot registration approach to translate the world coordinates to the robot's coordinate system. Of those considered, this initialisation approach is best suited within flexible manufacturing processes that have shared and changing environments. Using this approach, multiple robots can share the same vision system, and can be quickly repositioned and recalibrated to the camera using the robot registration approach.

Since the Cognex vision system and robot registration approach are combined to determine the robot's coordinates, their positional errors amalgamate for this initialisation approach. For two independent normal distributions $X \sim \mathcal{N}(\mu_X, \sigma_X^2)$ and $Y \sim \mathcal{N}(\mu_Y, \sigma_Y^2)$, the combined probability distribution can be calculated [167]:

$$Z \sim \mathcal{N}(\mu_Z, \sigma_Z^2) = Z \sim \mathcal{N}(\mu_X + \mu_Y, \sigma_X^2 + \sigma_Y^2) \tag{4.2}$$

Accordingly, when the location of the target position is unknown the positional error of the Cognex + registration approach can be approximated using a normal distribution with a mean of $8.45 \, mm$ and standard deviation of $4.93 \, mm$ for the KUKA LWR4, and a mean of $4.27 \, mm$ and standard deviation of $1.5 \, mm$ for the UR10.

4.3   Performance Metrics

As part of the proposed framework, additional performance metrics have been developed to better estimate the robotic system's performance during handling and insertion operations. Methods were developed to record these performance metrics and were used on the robotic systems presented in Section 4.2. An outline of these performance metrics and the resulting performance of each robotic system is given in the following sections.

4.3.1   Grasp Region

For each end effector, a region can be defined which represents the space in which the end effector's fingers can reach. In other words, the grasp region is the maximum area reachable by the fingers of an end effector. This region is dependent on the end effector's configuration and can be determined directly from the supplier specifications. For the chosen robotic end effectors and configurations, the grasp regions shown in Figure 4.8 have been identified. This identification of this region is useful as it can be used to determine if an object can be grasped and the level of uncertainty which can be tolerated. This will be highlighted in Chapter 5.

(a) Schunk KGG 80-30 Gripper with finger configuration 1

(b) Schunk KGG 80-30 Gripper with finger configuration 2

(c) Robotiq 3-Fingered Gripper
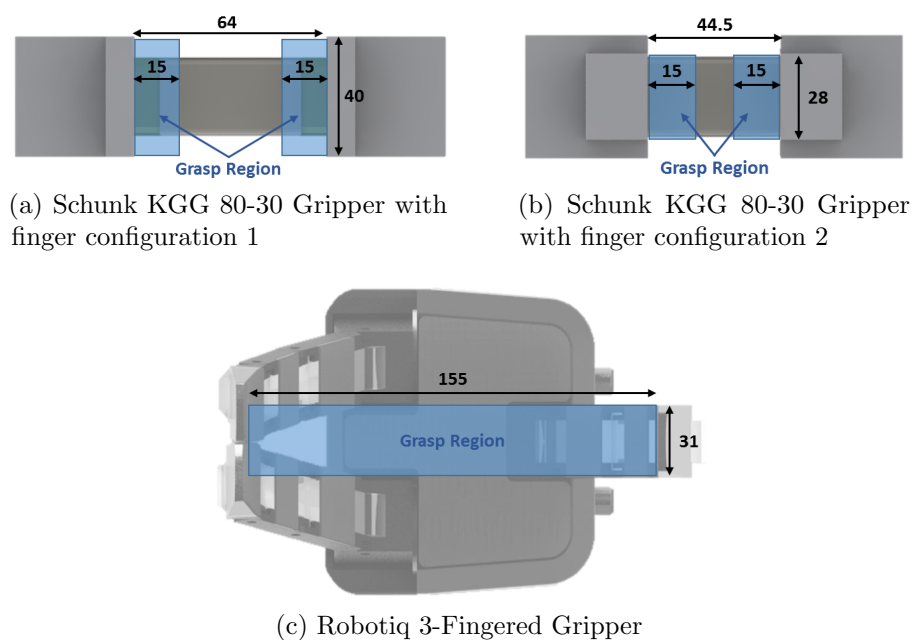
Figure 4.8: Grasp region of the chosen robotic end effectors.

4.3.2   Grasp Cycle Time

Grasp cycle time refers to the minimum time required for an end effector to achieve full closure from its default pre-grasp configuration and to return to the pre-grasp configuration [129].

As the Schunk KGG 80-30 gripper is a pneumatic gripper with only two states, its cycle time can be estimated by issuing an open and close command to the gripper and recording the time that elapses during execution. Using a 30 fps camera and simple video analysis, the cycle time of the Schunk KGG gripper was estimated to be $0.3\,s$ (see Figure 4.9). With reference to Section 4.2, this cycle time is three times larger than the expected time when using the supplier specifications of the gripper. Cycle time testing was performed with an air supply (operating pressure of $5.8 - 7.9\,bar$ and an output flow of $2.5\,CFM$) that met the nominal requirements of the Schunk gripper, which highlights the difficulty in attaining the performance quoted within supplier specification sheets.

A similar approach was used to measure the grasp cycle time of the Robotiq 3-Fingered Gripper, as shown in Figure 4.10. However, since the positions of each finger can be independently controlled, the grasp cycle time is dependent on the distance travelled by the fingers. Accordingly, multiple tests were performed in order to determine the relationship between grasp cycle time (t_{cycle}) and finger travel distance (d). With reference to Figure 4.11, the resulting relationship is linear and can be defined by the equation:

$$t_{cycle} = 0.0109d \tag{4.3}$$

The linear relationship suggests that the fingers move at a constant speed which equals the inverse of the slope. Since the cycle time incorporates both the opening and closing motion, the gripper's finger speed equals (2/0.0109) or $183.5\,mm/s$. Referring back to Section 4.2, this value is 75% of the specified finger speed which again highlights the limitations in using supplier specifications to estimate a robotic system's performance.

94
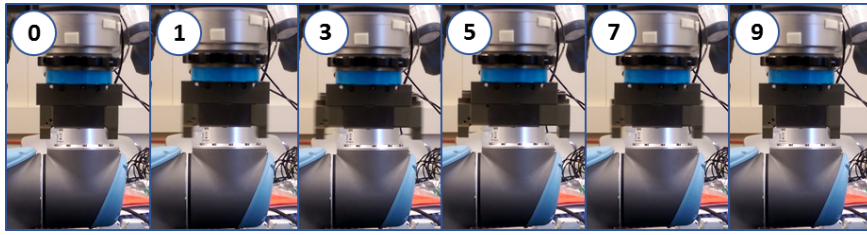
Figure 4.9: Selected frames from the opening and closing sequence of the Schunk KGG 80-30 gripper, where each frame is equal to 1/30 s.
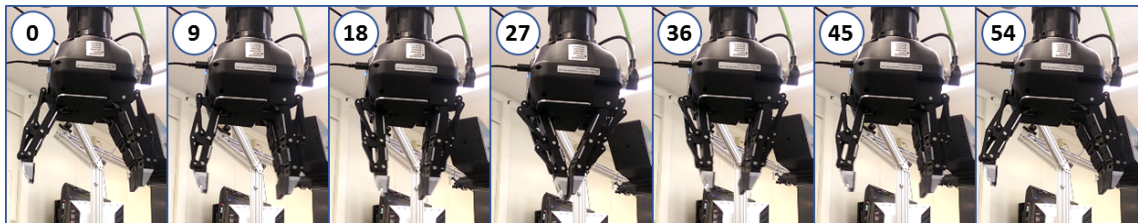
Figure 4.10: Selected frames from the opening and closing sequence of the Robotiq 3-Fingered Gripper, where each frame is equal to 1/30 s.
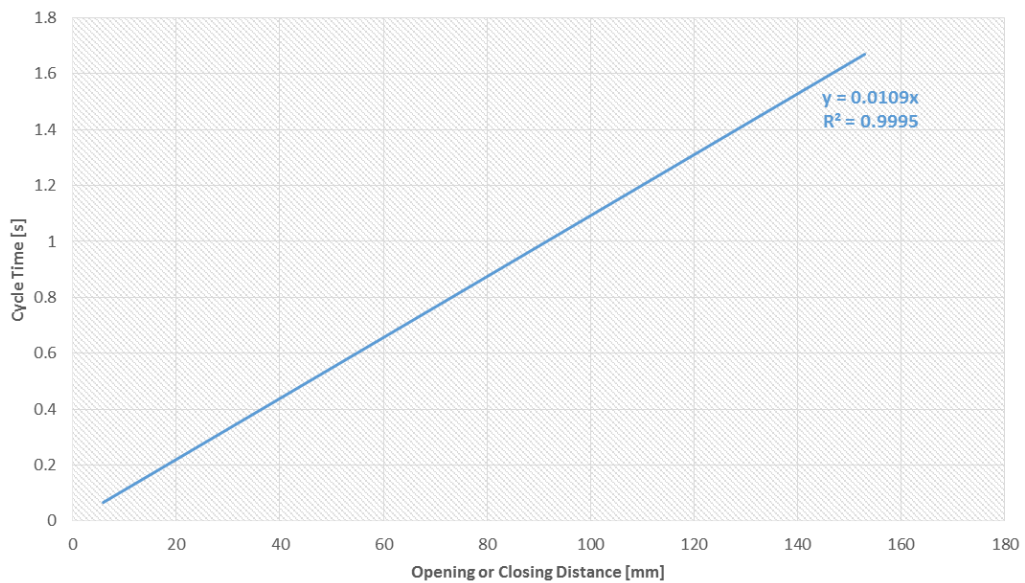
Figure 4.11: Cycle time of the Robotiq 3-Fingered Gripper when performing a pinch grasp.

4.3.3   Trajectory Completion Time

Trajectory completion time refers to the time required by a robotic manipulator to complete a linear trajectory. As it is dependent on the trajectory distance, this metric is defined with respect to the trajectory distance. The metric is specific to linear motions, as these motions are more controlled and predictable which is important for robotic manipulators that share a workspace with human co-workers. The relationship between completion time and trajectory distance can be estimated by considering the two point-to-point linear motion profiles presented in Figure 4.12. From these profiles, the equations of motion can be used to define the relationship between the trajectory distance (d_{traj}), the constant acceleration / deceleration ($\pm a$), the programmed velocity (v_{prog}), and the trajectory completion time (t_{traj}).
For short trajectories:

$$
\begin{aligned}
t_1 = t_2 &= \frac{t_{traj}}{2} \\
d_{traj} = d_1 + d_2 &= \frac{at_1^2}{2} + v_{traj}t_2 - \frac{at_2^2}{2} \\
d_{traj} = (at_1)(t_2) &= \frac{at_{traj}^2}{4} \\
t_{traj} &= \frac{2}{a^{0.5}}(d_{traj})^{0.5}
\end{aligned}
\tag{4.4}
$$

For long trajectories:

$$
\begin{aligned}
t_1 = t_3 &= \frac{v_{prog}}{a} \\
d_{traj} = d_1 + d_2 + d_3 &= \frac{at_1^2}{2} + v_{prog}t_2 + v_{prog}t_3 - \frac{at_3^2}{2} \\
d_{traj} = v_{prog}(t_{traj} - t_1 - t_3) + v_{prog}t_3 &= v_{prog}t_{traj} - \frac{2v_{prog}^2}{a} + \frac{v_{prog}^2}{a} \\
t_{traj} &= \frac{1}{v_{traj}}d_{traj} + \frac{v_{traj}}{a}
\end{aligned}
\tag{4.5}
$$

To distinguish between the two trajectories, a threshold distance (d_{thresh}) can be defined by considering a short trajectory motion where $v_{traj} = v_{prog}$. This gives:

$$
d_{thresh} = \frac{v_{prog}^2}{a}
\tag{4.6}
$$

(a) Short Trajectories   (b) Long Trajectories
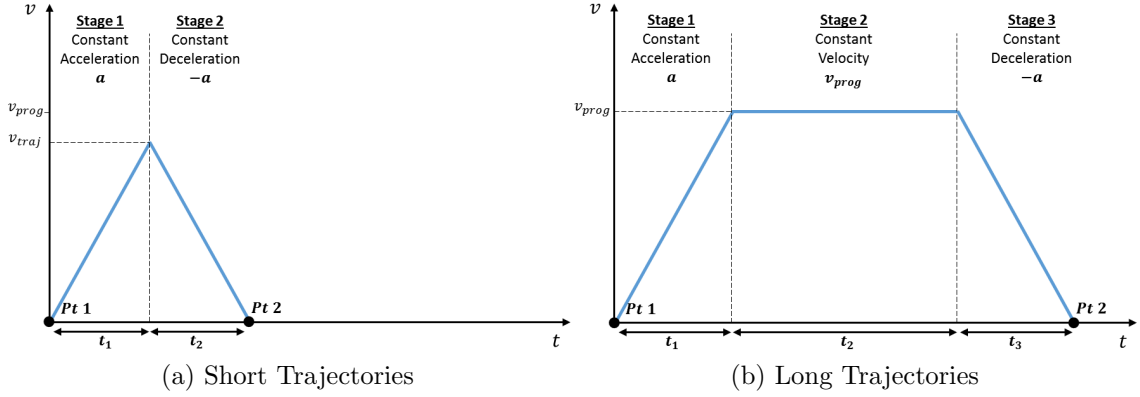
Figure 4.12: Motion profile of the robotic manipulators when performing a linear motion between points 1 and 2. Motion can be broken into stages, which are defined by the programmed velocity (v_{prog}), the constant acceleration / deceleration ($\pm\,a$), and the stage time (t_1,t_2,t_3). For short trajectories, the trajectory velocity (v_{traj}) is the maximum velocity achieved during the motion, which is less than v_{prog}.

For the UR robots, the default program velocity and acceleration were set to $1\,m/s$ and $1.2\,m/s^2$ respectively. Substituting these parameters into Equations 4.4 - 4.6 gives the following cases:

$$UR:\ t_{traj} = \begin{cases} 1.826(d_{traj})^{0.5} & \text{if } 0 < d_{traj} \leq 0.833\,m \\ d_{traj} + 0.833 & \text{if } d_{traj} > 0.833\,m \end{cases} \tag{4.7}$$

The above relationship can be represented by a power curve, which gives a consolidated estimate of the UR trajectory completion time. Converting the trajectory distance to mm, this power curve is described by the equation:

$$UR:\ t_{traj} = 0.0577(d_{traj})^{0.5} \tag{4.8}$$

For the KUKA LWR4 robot, it was found that the robot's motion attempts continually exceeded the velocity and acceleration limits set by the controller which resulted in the robot's failure. To overcome this, the program override value (POV) on the controller had to be reduced to 35%. The POV is specified as a percentage of the robot's programmed velocity, and limits the velocity of the robot during program execution. The reduction required was surprising, and it highlights a limitation of the controller's motion planner when executing longer trajectories. Since the KUKA LWR4 robot's path velocity and acceleration were set to $2\,m/s$ and $2\,m/s^2$, the

program velocity and acceleration were reduced to $0.7\,m/s$ and $0.7\,m/s^2$ respectively. In addition, it was noticed that the KUKA LWR4 was taking longer than expected to execute a trajectory. This delay was constant regardless of the trajectory distance, which indicated that it was a feature of the motion planner. The delay can be attributed to the additional time required by the motion planner to break each motion into the very small, intermediate steps required to ensure the TCP follows a linear motion. The delay was measured to be $0.12\,s$, which was combined with Equations 4.4 - 4.6 to give the following cases:

$$KUKA: \; t_{traj} = \begin{cases} 2.39(d_{traj})^{0.5} + 0.12 & \text{if } 0 < d_{traj} \leq 0.7\,m \\ 1.429 d_{traj} + 0.82 & \text{if } d_{traj} > 0.7\,m \end{cases} \tag{4.9}$$

The above relationship can be represented by a power curve with constant offset, which gives a consolidated estimate of the KUKA LWR4 trajectory completion time. Converting the trajectory distance to mm, this power curve is described by the equation:

$$KUKA: \; t_{traj} = 0.0756(d_{traj})^{0.5} + 0.12 \tag{4.10}$$

To determine their actual trajectory completion times, each robotic manipulator was timed as it performed trajectories of various distance. Each trajectory distance was repeated 20 to 40 times, and the recorded time was used to calculate the robot's average completion time for that trajectory distance. These recorded times were compared to the estimated trajectory completion times, and the results are shown in Figure 4.13.
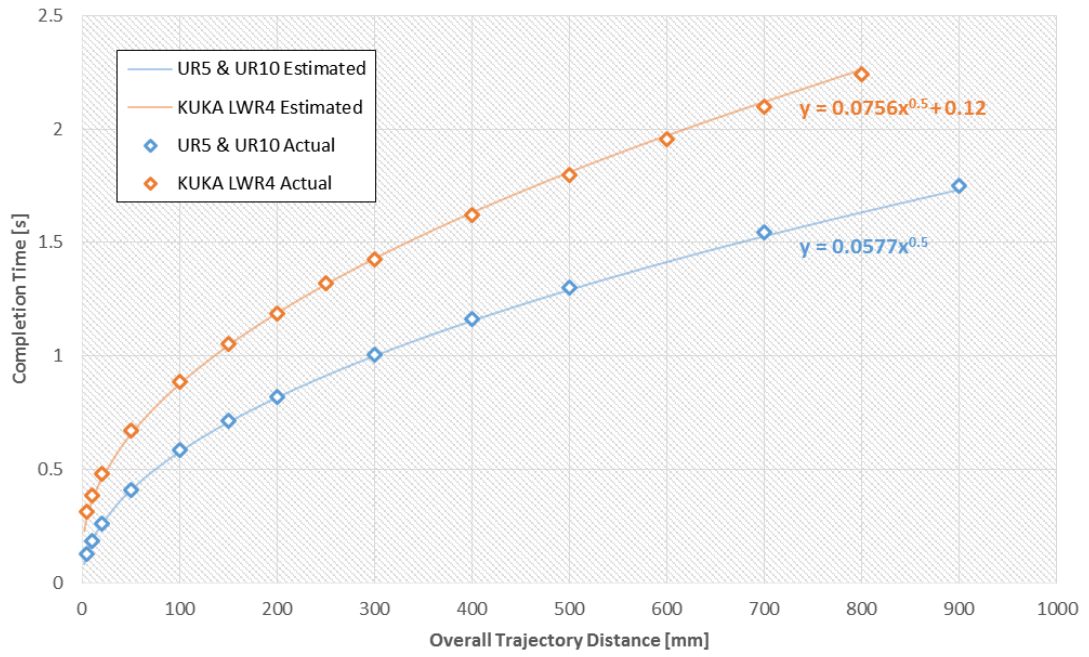
Figure 4.13: Comparison between the recorded completion times (discrete points) and the estimated completion times (continuous functions) of the KUKA LWR4 and UR robots in relation to trajectory distance.

4.3.4 Communication Delay

This metric refers to the maximum delay during communication between the robotic system and its control program. It is dependent on factors such as the communication protocol (e.g. transmission control protocol/internet protocol (TCP/IP), Ethernet/IP, EtherCAT, Modbus, etc.), communication bandwidth, communication latency, the type and size of data being transmitted, the transmission distance, the programming language, and the controllers read/write speeds.

During testing, a programming interface was used to provide integrated control of the various robotic systems. This minimised the reproduction of code for the different robotic systems and ensured coordination between the different components of the robotic system during task execution. To measure the communication delays between the programming interface and each robotic system, identical motion commands were executed using both the programming interface and the robot's local controller. The results from testing with the Robotiq 3-Fingered gripper and the robotic manipulators are shown in Figures 4.14 and 4.15 respectively. Since the Schunk KGG 80-30 gripper was controlled by setting a digital output pin, its communication delay was sufficiently small that it could be approximated as zero.

For the Robotiq 3-Fingered gripper, use of the programming interface still results in a linear relationship between finger travel distance and the gripper's cycle time. However, as Figure 4.14 identifies, there is a constant offset that equals the y-intercept of the programming interface's linear equation. As the cycle requires the execution of an open and close command, the communication delay when controlling the Robotiq 3-Fingered Gripper is equal to 0.1447 s.

With reference to Figure 4.15, the KUKA LWR4 robot has a relatively small and constant communication delay, while the UR robot's communication delay resembles that of a step function. The communication delay for the KUKA LWR4 equates to $0.028 \, s$ on average, while the communication delay for the UR robots range from 0 to $0.2 \, s$ within each $0.2 \, s$ interval. The reason for this is that the communication between the programming interface and the robot's local controller was limited to $5 \, Hz$, which was significantly lower than the UR robot's specified communication speed of $125 \, Hz$. A consequence of this low communication speed is that the
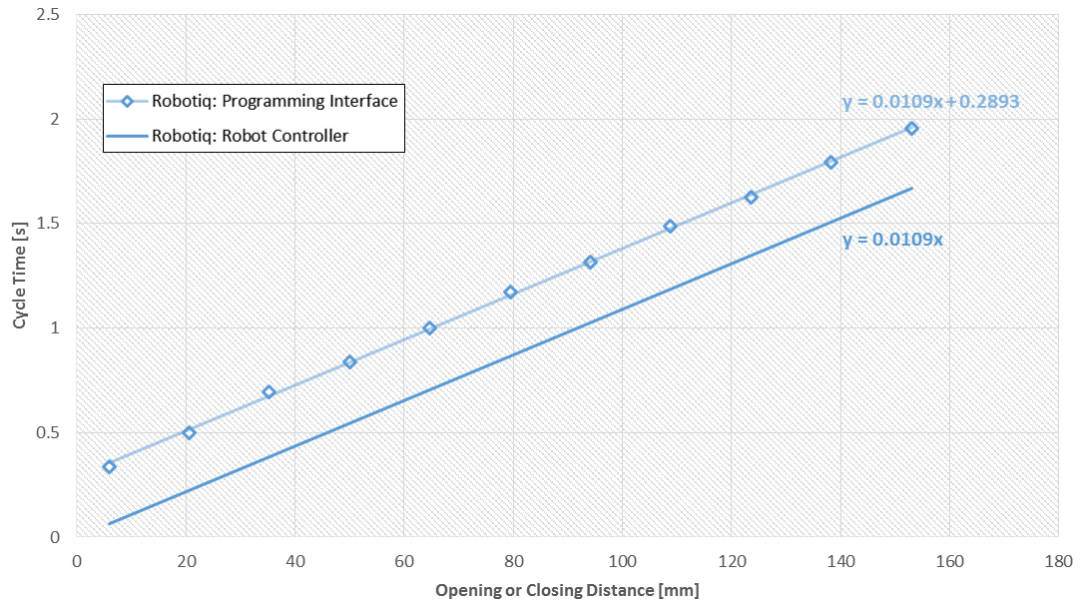
Figure 4.14: Cycle time of the Robotiq 3-Fingered Gripper performing a pinch grasp when using the robot's local controller and the programming interface. The constant offset $(0.2893\ s)$ is the communication delay between the programming interface and the robotic controller.
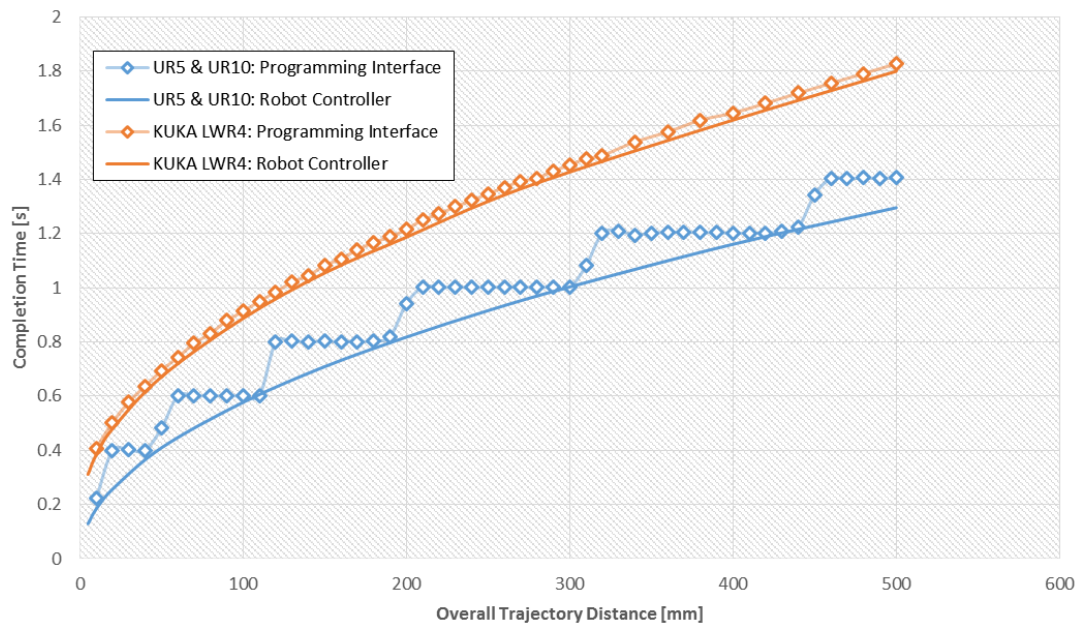
Figure 4.15: Comparison between the recorded completion times of the KUKA LWR4 and UR robots in relation to trajectory distance when the robot's local controller and the programming interface.

programming interface only receives updates on the robot's status every $0.2\,s$, which means that any trajectory completed within an interval isn't detected until the next update is received. Accordingly, the recorded completion time for the UR robots when using the programming interface can be described by a step function:

$$CT_{recorded} = \begin{cases} 0.2 & \text{if } 0.0 < t_{traj} \leq 0.2 \\ 0.4 & \text{if } 0.2 < t_{traj} \leq 0.4 \\ 0.6 & \text{if } 0.4 < t_{traj} \leq 0.6 \\ & etc. \end{cases} \tag{4.11}$$

where t_{traj} is the estimated trajectory completion time of the UR robots defined in Equation 4.8. The above step function is easily calculated by using a ceiling command within computer programs such as Microsoft Excel. Accordingly, the communication delay (t_{comm}) for the UR robots can be defined as follows:

$$t_{comm} = CEILING(t_{traj}, 0.2) - t_{traj} \tag{4.12}$$

To note, the communication delay and trajectory completion time of the UR robots are kept separate rather than using their combined completion time, as the communication delay will vary depending on the programming interface used. In addition, it's important to have a trajectory completion time which reflects the performance of the robotic manipulator only.

4.3.5 Insertion Search Time

Within flexible manufacturing, a robotic system may be required to overcome misalignment between a part and its receptacle during insertion. The most common example of this is a peg-in-hole insertion, which accounts for over 35% of all assembly operations [168]. It is therefore an area worth considering.

One common solution to misalignment during peg insertion is the inclusion of a remote centre compliance (RCC) between the robotic manipulator's wrist and the end effector. A RCC is a mechanical device which provides rotational and translational compliance to prevent lateral forces being exerted on the peg and causing jamming during insertion. However, a RCC is only useful when the peg and hole are adequately aligned for initial insertion to occur. For insertion operations with greater uncertainty, an additional or alternative option is for the robotic system to implement a search strategy when an insertion attempt is unsuccessful.

4.3.5.1 Search Region

To perform a search, the robotic system explores a designated space known as the search region. The size of this region is dependent on the level of uncertainty, but the region's boundary is typically optimised to minimise the region's size while still ensuring that it encloses the hole location. While the search region can be multi-dimensional, the two-dimensional case is used by peg insertion search strategies. To optimise a peg insertion search strategy, its search region can be discretised into a finite number of insertion points (see Figure 4.16) [169]. These points represent the possible insertion locations within the region, and are spaced optimally by setting the maximum distance between two points to equal the dimensionless insertion clearance (c) between the peg (of diameter d) and hole (of diameter D), where:

$$c = \frac{D - d}{D} \tag{4.13}$$

Using these identified insertion points, a robot's search path can be defined. A valid search path includes each point identified within the search region, as this ensures a successful insertion (assuming the search region and insertion points have been calculated correctly). However since the insertion could occur at any point along
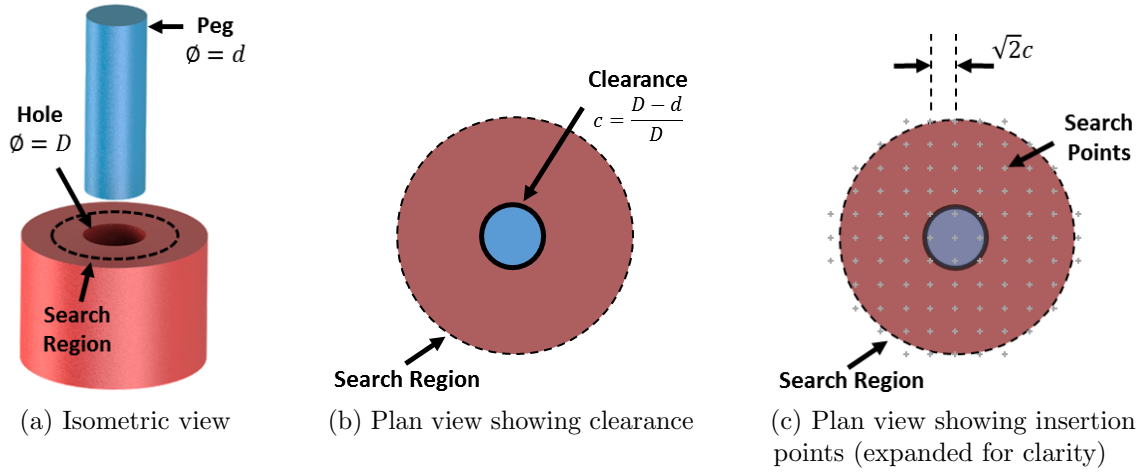
Figure 4.16: Discretisation of a search region into a finite number of points at which an insertion can occur. The spacing between these points is optimised by setting the diagonal distance to equal the insertion clearance c.

the search path, the time for the insertion is uncertain. To try to address this and minimise insertion times, optimised search paths are used. Three of these optimised search paths have been considered and are discussed below. The spiral and random search paths are commonly used within robotics, while the quasi-random search path has been developed as part of this work.

4.3.5.2 Spiral Search Routine

The spiral search is commonly used within industry as it is an optimised search routine for two-dimensional environments. It is particularly useful when the probability density of the hole's location follows a normal distribution within the search region, as the beginning of the spiral path can be located at the distribution's mean [170]. The most commonly used spiral search path follows an Archimedean spiral, which is the curve generated by moving away from a point at constant linear and angular velocity. In polar coordinates, an Archimedean spiral is defined by

$$r = a\theta \tag{4.14}$$

where a is a real number and corresponds to the distance between successive turnings. For a peg-in-hole operation, the spiral search path can be optimised by setting a to the insertion clearance, c (see Figure 4.18) [169].

4.3.5.3   Random Search Routine

The random search is a particularly simple yet effective search routine, as exemplified by its use by the majority of commercially available mobile robots [171]. The routine is well suited to peg insertions when the probability density of the hole's location is uniform within the search region. When performing this search routine during a peg insertion task, the robotic system attempts to insert the peg by following a path derived from uncorrelated, randomly generated waypoints within the defined search region. While this path is not optimised in terms of length, its distances between waypoints can be much larger which allows the robot to explore the region at a faster pace (see Figure 4.18).

4.3.5.4   Quasi-Random Search Routine

As noted, the quasi-random search routine was developed as part of this work. The routine effectively explores a region by utilising a quasi-random sequence to generate the search path waypoints. Stated simply, a quasi-random sequence fills a given space more uniformly than uncorrelated random points by sub-randomly generating points which minimise the maximum distance between all points [172]. While there are a number of quasi-random sequences, the Sobol' sequence was chosen. The Sobol' sequence is generated number-theoretically so that successive points fill the gaps in the previously generated distribution. For each component of the n-dimensional Sobol' sequence, numbers are generated between zero and one directly as binary fractions [172]. A detailed description of the Sobol' sequence is given in Appendix B. Considering the defined search region, a two-dimensional Sobol' sequence was used to generate the search path's waypoints (see Figure 4.17). The code for generating these waypoints is also given in Appendix B.

4.3.5.5   System Performance

As the above search strategies require the robot arm to be in impedance control, only the KUKA LWR4 robot arm was assessed using this metric. To capture the performance of the different search routines, a peg insertion test was performed with a dimensionless clearance, $c = 0.02$. This clearance is within the range experienced
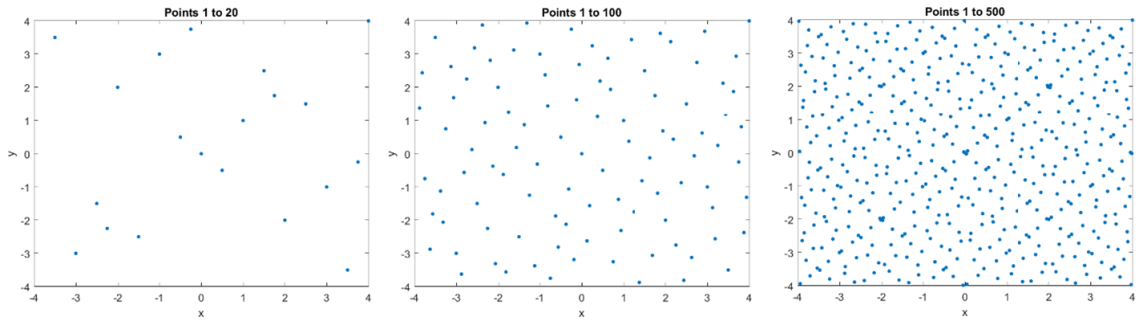
Figure 4.17: Points generated by the two dimensional Sobol' sequence within a 4 mm x 4 mm search region.
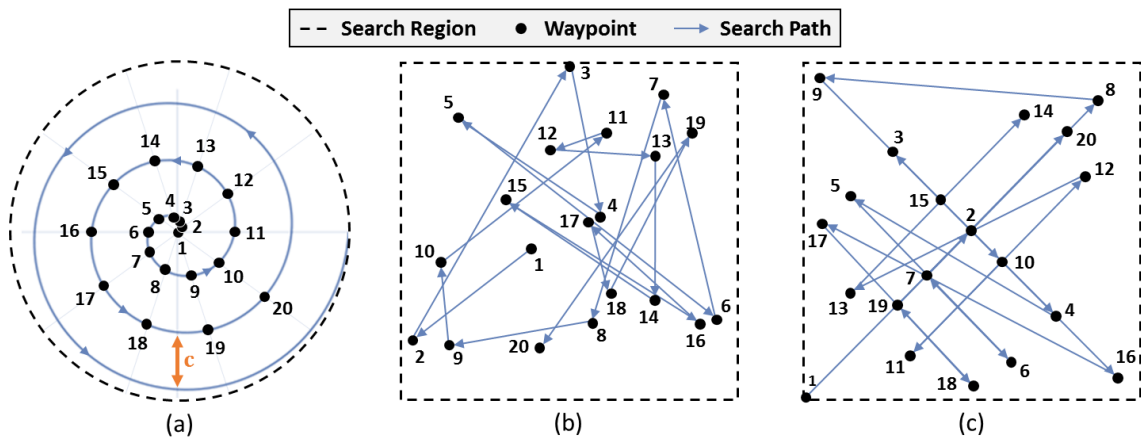
Figure 4.18: Search routines considered and an example of the first 20 robot waypoints used to generate the required path: (a) Spiral search where turning distance equals the insertion clearance, c (waypoints don't change between searches, turns enlarged for clarity) (b) Random search (waypoints vary between searches) (c) Quasi-random search (waypoints don't change between searches).

during manual assembly, and represents the point at which a human will start to have difficulties during insertion [29]. While the use of a single insertion clearance is adequate for comparing the performance of the different search routines, additional testing is needed to capture the influence of insertion clearance on a robot's insertion search time.

The true mean ranges of the robotic system's search time when using the spiral, random, and quasi-random search strategy at this insertion clearance are summarised in Figure 4.19. As shown, the mean time to perform each search and the margin of error is dependent on the initial positional error and the peg's chamfer design. In a typical manufacturing operation the part to be inserted will be chamfered, and the chamfer will be optimally designed so that its width is 0.1 times the peg diameter and

its angle is 45 degrees [29]. However, it was also useful to consider a non-chamfered peg as it provides an insight into each search strategy's ability to deal with more difficult insertions.

A notable observation from the graphs is the time required by the spiral search strategy to perform insertions with the non-chamfered peg. This is a feature of the implemented search strategy, which generates spiral waypoints based on the insertion clearance. However, when using the non-chamfered peg, the distance between successive turnings is set to equal the small clearance in order to ensure the hole is found, which greatly increases the strategy's search time as the initial positional error increases.
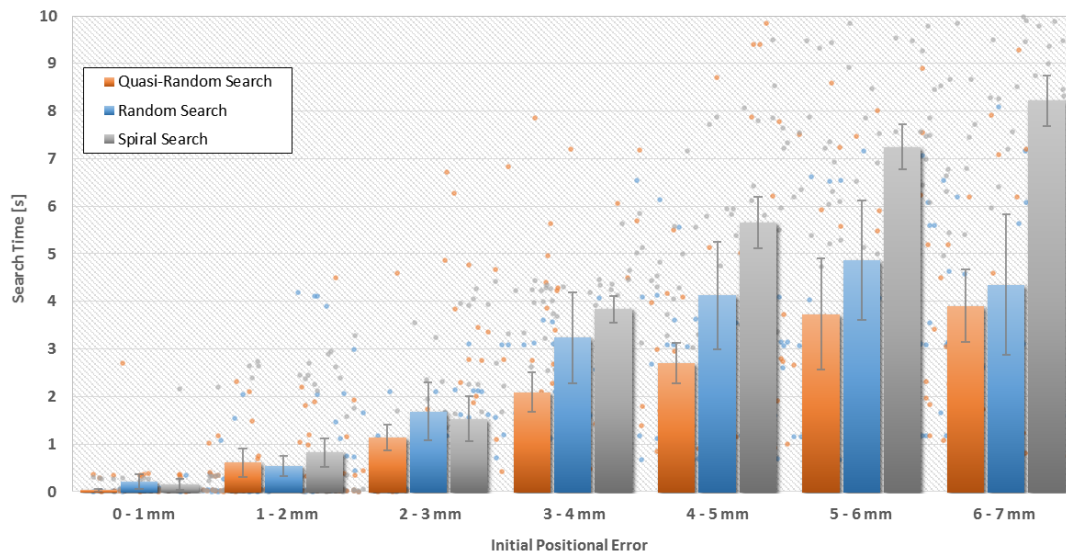
(a) Chamfered Peg
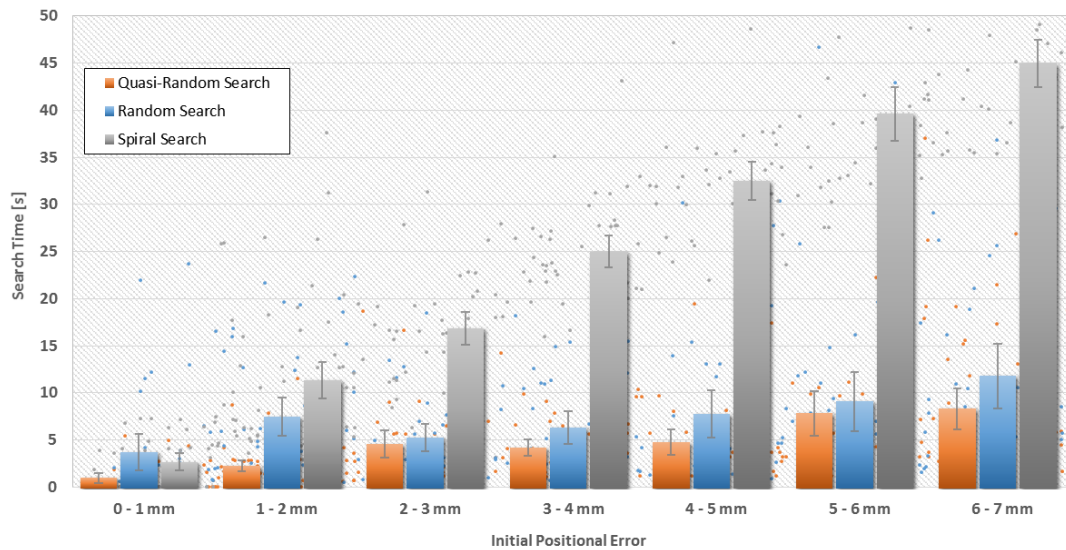
(b) Non-chamfered Peg

Figure 4.19: Peg insertion search times of the KUKA LWR4 when using the spiral, random and quasi-random search strategies. Graphs show the mean search time and 95% confidence interval error bars for each 1 mm increment.

4.4 Handling Scenario

4.4.1 Setup & Testing Overview

Handling operations are one of the fundamental operations that a robotic system will be required to perform. However, unlike traditional automated handling operations, those within flexible manufacturing may require the robotic system to overcome a greater level of uncertainty. As an example, consider the following scenario.

A manufacturing company is considering automating part of its assembly line. This company does not wish to modify the current assembly infrastructure (in a multistation layout) as the payback period for fixed automation would exceed the product's life cycle. The company is considering flexible automation, and wishes to compare the viability of selected robotic systems to human labour.

The assembly operation being considered is the handling operation shown in Figure 4.20. The operation requires an object to be grasped when it arrives at the workstation and transferred to an assembly bin. The two objects involved in this operation are shown in Figure 4.21. The objects will be face-up, but their orientation and position
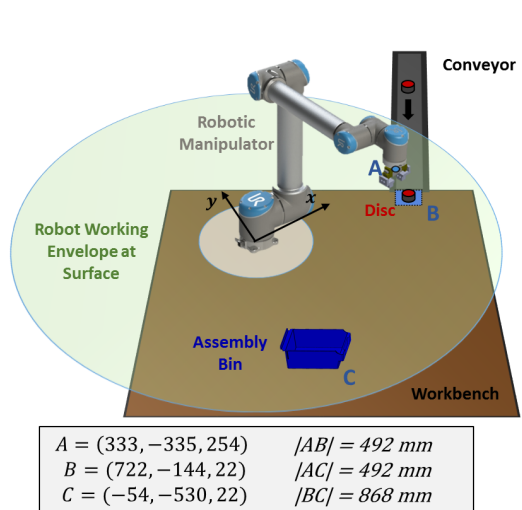
Figure 4.20: Layout of the handling operation showing the proposed location of a robotic system, which moves from its home position A to grasp the disc at position B and place it in the bin at position C. The coordinates are given in mm, and their values are taken from the real robot's coordinate system.

Figure 4.21: Chosen primitive objects and their classification within the B-D handling table based on their symmetry and size (given in mm).

upon arrival may vary.

Due to their shape and size, the handling of the cylindrical block and cuboid can be classified as a '00' and '10' B-D handling operation respectively. Referring back to Section 2.3.2, a B-D handling operation encompasses the approach, grasp, orientation, and transport of an object to its target location. The operation concludes when the grasped object has reached its target location, just prior to the performance of the subsequent action such as placing, mating, releasing, etc. Consequently, this scenario can be represented by a B-D handling operation and a release action. Since the latter requires minimal time, the B-D handling tables can be used to estimate the time required by human labour to perform this scenario.

The robotic systems being considered are summarised in Section 4.4.2. If selected, the robotic system must integrate with a programming interface currently used by the company. In addition, as the operation is within a shared environment, the robotic manipulator should perform linear Cartesian motions to increase their predictability for human co-workers.

4.4.2 Robotic Systems

With reference to Section 4.2, the robotic systems given in Table 4.5 were chosen for this scenario. The Schunk KGG 80-30 was equipped with parallel fingers, which could be attached in two different configurations to give the gripper dimensions shown in Figure 4.22.

As the object's location and orientation could vary, four different simulated errors were considered to determine the robotic system's ability to deal with uncertainty during the performance:

- **Simulated error, σ_2:** Noise in the X and Y directions were drawn from a normal distribution with zero mean and 2 mm standard deviation, and orientation error that follows a normal distribution with zero mean and 2° standard deviation.

- **Simulated error, σ_4:** Noise in the X and Y directions were drawn from a normal distribution with zero mean and 4 mm standard deviation, and

orientation error that follows a univariate normal distribution with zero mean and 4° standard deviation.

- **Simulated error, σ_6:** Noise in the X and Y directions were drawn from a normal distribution with zero mean and 6 mm standard deviation, and orientation error that follows a univariate normal distribution with zero mean and 6° standard deviation.

- **Simulated error, σ_8:** Noise in the X and Y directions were drawn from a normal distribution with zero mean and 8 mm standard deviation, and orientation error that follows a univariate normal distribution with zero mean and 8° standard deviation.

Table 4.5: Robotic systems considered for the handling operation.

Robotic System	Manipulator	End Effector	Initialisation Approach
UR5_KGG1_S	Universal Robotics UR5	Schunk KGG 80-30 (finger configuration 1)	Teach Programming + Simulated Error
UR5_KGG1_C			Cognex Vision System
UR5_KGG2_S	Universal Robotics UR5	Schunk KGG 80-30 (finger configuration 2)	Teach Programming + Simulated Error
UR5_KGG2_C			Cognex Vision System
UR5_RIQ_S	Universal Robotics UR5	Robotiq 3-Fingered Gripper	Teach Programming + Simulated Error
UR5_RIQ_C			Cognex Vision System
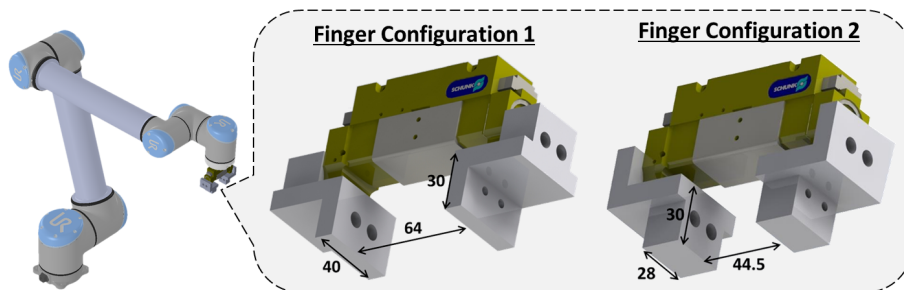
Figure 4.22: Schunk KGG 80-30 pneumatic gripper dimensions for finger configurations 1 & 2.

4.5 Pick-and-Place Scenario

4.5.1 Setup & Testing Overview

To assess the robotic system's ability to perform pick-and-place operations within a changing environment, the original Minnesota Rate of Manipulation Test (MRMT) [173] and a variant of the test were used.

The MRMT is a standardised human dexterity assessment test used to assess gross coordination and bilateral manual dexterity. The test is commonly used within industry to screen personnel for manual processes and within occupational therapy to assess injured patients and their rehabilitation progress. While the original MRMT has established reliability, validity and human norm tables [89], the commercial test currently available has replaced the original wooden artefacts with plastic versions that vary slightly in their dimensions. This suggests that new reliability, validity, and normative investigations using humans are required [174], [175], however it does not negate its usefulness as a robotic assessment tool.

The MRMT has five subtests; the placing test, turning test, displacement test, one-hand turning and placing test, and the two-hand turning and placing test. The displacement test evaluates how fast cylindrical blocks ($37\,mm$ diameter, $18\,mm$ height) can be transferred from one hole to another within a board ($5\,mm$ thick). The board contains sixty holes ($39\,mm$ diameter) in a $4\,x\,15$ linear pattern ($57\,mm$ bidirectional spacing). Fifty-nine blocks are used during the displacement test, which allows blocks to be sequentially transferred to the vacant hole. The test is typically repeated four times, and the combined completion time is compared to the norm tables presented in the examiner's manual [173] to determine the human's performance.

In order to obtain more meaningful results, a variant of the MRMT displacement test was created by researchers at NIST by substituting the MRMT board with a flat paper target (Figure 4.23). This paper target has the same layout as the MRMT board, but its flat profile and printed concentric circles of diameter 39 mm, 35 mm, 27 mm, 23 mm, and 19 mm increase the resolution of the recorded placement accuracy. As opposed to a simple pass-fail test, ordinal data can be collected by
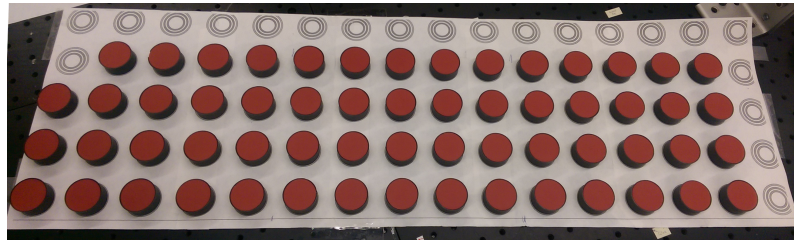
Figure 4.23: MRMT Displacement Test paper target variant.

| Concentric Circles | Zone 1 Accuracy: < 1 mm | Zone 2 Accuracy: < 3 mm | Zone 3 Accuracy: < 5 mm | Zone 4 Accuracy: < 7 mm | Zone 5 Accuracy: < 9 mm | Zone 6 Accuracy: < 19 mm |
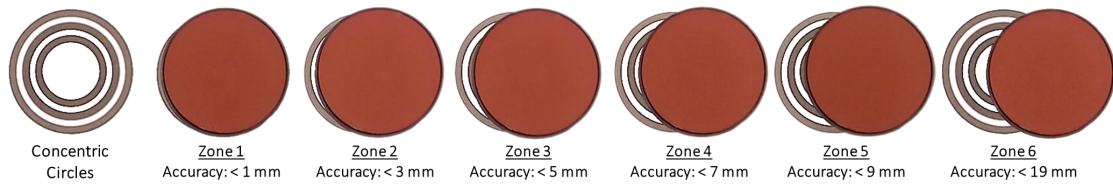
Figure 4.24: Zones defined by the MRMT Displacement Test variant to quantify placement accuracy.

recording the zone in which the disc lies after placement (Figure 4.24).

4.5.2   Robotic Systems

A number of robotic systems were chosen to perform the Minnesota Displacement Test and its variant. The systems were composed as outlined in Table 4.6.

Table 4.6: Robotic systems considered for the MRMT test.

Robotic System	Manipulator	End Effector	Initialisation Approach
UR10_KGG_T	Universal Robotics UR10	Schunk KGG 80-30	Teach Programming
UR10_KGG_C			Cognex Vision System
UR10_KGG_CR			Cognex + Registration
UR10_RIQ_T	Universal Robotics UR10	Robotiq 3-Fingered Gripper	Teach Programming
UR10_RIQ_C			Cognex Vision System
UR10_RIQ_CR			Cognex + Registration
UR10_AGO_CR	Universal Robotics UR10	Allegro Robotic Hand	Cognex + Registration
BAX_VAC_T	Rethink Robotics Baxter	Baxter Vacuum Gripper	Teach Programming

4.6 Insertion Scenario

4.6.1 Setup & Testing Overview

As noted, peg insertions account for up to 35% of all operations within assembly [168] and is an operation which a flexible robotic system should be able to perform. In particular, a flexible robotic system should be dexterous enough to compensate for misalignment during peg insertions that may occur within a flexible manufacturing environment.

To represent a typical peg-in-hole assembly task but facilitate repeated testing, the scenario was set up as shown in Figure 4.25. The holes are equally spaced 35 cm apart, which from Section 2.2.6 is the upper threshold for primary assembly processes. Hence, the approach and transfer distances compare to those currently within a manual assembly. The scenario initialises with two pegs placed into two holes. The goal is to cyclically transfer a peg into the next available hole.

The peg diameter, d, and hole diameter, D, give a dimensionless clearance, $c = (D - d)/D = 0.02$. This clearance corresponds to the insertion search time metric, and defines a sufficiently difficult insertion task as it is small enough to influence a human assembly worker's insertion time [29].

The peg insertion operation was performed using both a chamfered and non-chamfered peg. With reference to the B-D tables, the operation includes a B-D handling operation with code '00' and a B-D insertion operation. Due to the dimensionless clearance between the peg and hole, the insertion operation's classification was
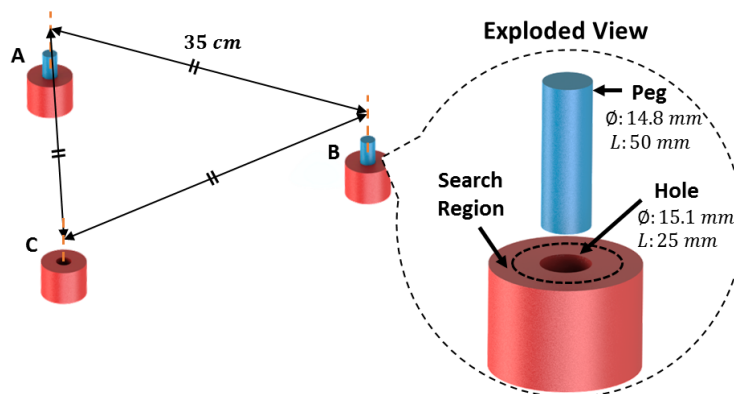
Figure 4.25: Peg insertion operation setup and design specifications.

dependent on the peg's chamfer design; use of the chamfered peg resulted in a '00' insertion operation, while use of the non-chamfered peg resulted in a '01' insertion operation. Similar to the handling operation, this deconstruction of the peg insertion task into B-D handing and insertion operations allows for human-level performance to be easily estimated.

4.6.2 Robotic Systems

Two tests were performed using the described peg insertion setup to assess the performance of different robotic systems, as summarised in Table 4.7.

The first test considered the performance of robotic systems using different search strategies. To accurately compare the performance of these systems, simulated perception error is used to intentionally misalign each insertion attempt. Noise in the X and Y directions were drawn from two distributions: a normal distribution with 1) zero mean and 1 mm standard deviation (σ_1), and 2) zero mean and 2 mm standard deviation (σ_2).

The LWR4_AGO_S$_f$ robotic system conducts this test with the hand actively controlling the pose of the peg using the sensing and control technology discussed in Section 4.2 while coordinating motions with the arm. During an insertion attempt, the hand initially tilts the peg approximately 35 degrees to induce peg-hole contact

Table 4.7: Robotic systems considered for the peg insertion task.

(a) Test 1: Assessment of different search strategies

Robotic System	Manipulator	End Effector	Initialisation Approach	Search Strategy
LWR4_AGO_S$_f$	KUKA LWR4	Allegro Hand	Teach Programming + Simulated Error	Active Force Control
LWR4_KGG_S$_s$	KUKA LWR4	Schunk KGG 80-30	Teach Programming + Simulated Error	Spiral
LWR4_KGG_S$_r$				Random
LWR4_KGG_S$_q$				Quasi-random

(b) Test 2: Assessment of different initialisation approaches

Robotic System	Manipulator	End Effector	Initialisation Approach	Search Strategy
LWR4_KGG_T$_q$	KUKA LWR4	Schunk KGG 80-30	Teach Programming	Quasi-random
LWR4_KGG_CR$_q$			Cognex + Registration	
LWR4_KGG_R$_q$			Registration	
LWR4_RIQ_T$_q$	KUKA LWR4	Robotiq 3-Fingered Gripper	Teach Programming	Quasi-random
LWR4_RIQ_CR$_q$			Cognex + Registration	
LWR4_RIQ_R$_q$			Registration	

force profiles that guide the preliminary alignment. Afterwards, the hand vertically re-aligns the peg with the hole, and the hand and arm insert the peg while minimising peg-hole contact forces and peg pose control error. This solution paradigm is quite feedback-intensive. The contact force on the peg was calculated by summing the measured (transformed) forces by all three force transducers. This resultant force was used in three ways during the insertion process: 1) detect initial contact between the peg and the hole, 2) guide initial alignment of tilted peg with hole, and 3) guide alignment of straightened peg with hole. In addition, the hand's estimate of the peg's orientation was used to help guide the alignment of the straightened peg with the hole.

The LWR4_KGG_S robotic systems conduct the peg insertion by coupling the arm's impedance properties with one of the three search routines discussed in Section 4.3. During a search, the peg remains stationary within the gripper while the robot arm is in Cartesian impedance control. The robot arm's stiffness and damping along the z-axis is reduced, and the robot attempts to position the peg $10\,mm$ below the surface of the block (see Figure 4.26). If the peg and hole are not aligned, a contact force is generated and maintained during each search routine until the peg and hole are aligned. At this point the robot's desired and measured positions match, and the control program identifies a successful insertion.

The second test considers the performance of robotic systems which are setup using different initialisation approaches, and highlights how the developed framework can be used to estimate the performance of different robotic systems. For uniformity, the same search strategy is used by these robotic systems during insertion. The initialisation approaches being considered include the teach programming (T), registration (R), and Cognex + registration (CR) approaches described in Section 4.2.3.
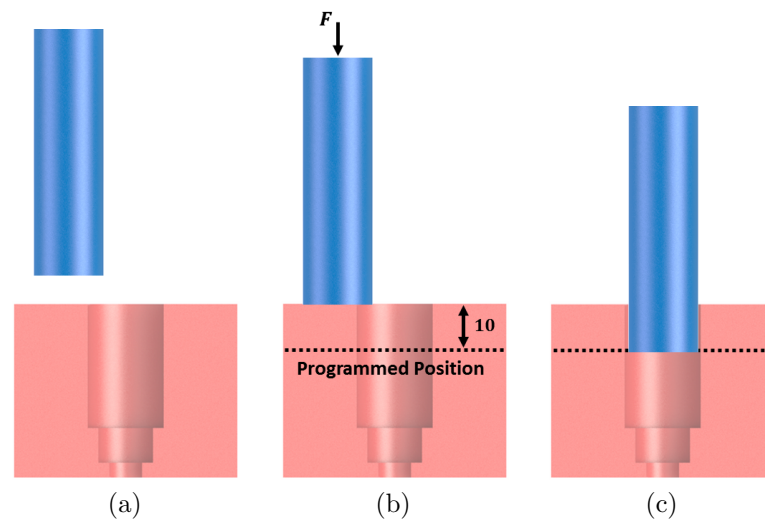
Figure 4.26: Cross section of the artefacts during an insertion by the LWR4_KGG system; (a) initial misalignment of peg and hole (b) programmed position not reached due to collision with surface, which generates a contact force, F (c) maintaining this contact force, a search strategy is implemented until a successful insertion is achieved (detected when the actual position equals the programmed position).

Chapter 5

Computational and Experimental Results

5.1 Results Overview

As noted, the developed framework allows users to follow a structured approach when evaluating a robotic system and provides a direct means for considering their viability relative to human labour. From Section 3.3, this evaluation involves the following three activities:

1. The breakdown of the scenario into its B-D handling and insertion operations. This helps to identify the performance metrics needed during the framework's implementation and provides an estimated human completion time for the scenario that can be used when considering the viability of the different robotic systems.

2. The identification of the assembly actions and corresponding performance metrics which relate to the scenario. A preliminary set of performance metrics have been developed in Section 4.3, and can be used instead of supplier specifications to estimate the robot's performance in each of the selected scenarios.

3. Determining the feasibility and capability of the robotic system in each scenario by calculating a probability of success (PS) and overall completion time (CT).

In the sections below, the developed framework is used to estimate the dexterity of robotic systems in each scenario. Actual testing is performed with each system,

and compared to the theoretical results in order to determine the usefulness of the developed framework. Tests are performed at least 60 times with each robotic system in order to ensure the collected data is representative of the system's actual performance. The chosen scenarios provide a platform for benchmarking robotic performance, and the statistical tools outlined in Section 3.5 are used to analyse and compare the collected data. When applicable, this analysis is performed using a 0.95 confidence level.

5.2   Handling Scenario

From Section 4.4, the handling scenario required the robotic system to grasp and transfer an object whose location could vary along a conveyor's width. The estimated performance of each robotic system was calculated using the developed framework, and compared to actual performance recorded during laboratory testing (see Figure 5.1). In this scenario, the completion time of each handling operation and the number of successful attempts were recorded. To note, the handling operation was only deemed successful if the object was successfully grasped and transported without the fingers of the robotic system making contact with the object during its approach.

(a)   (b)
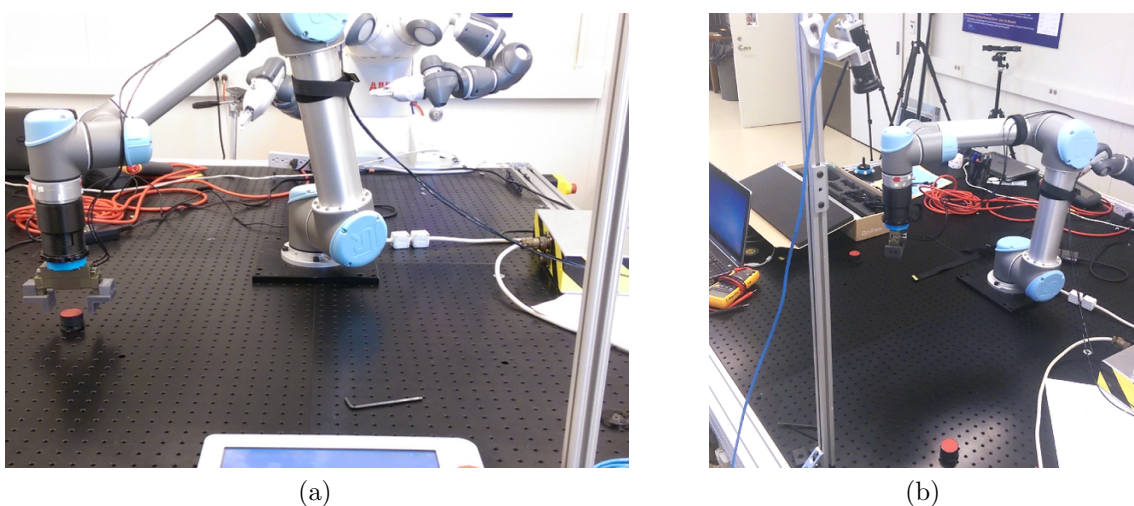
Figure 5.1: Actual testing of the handling scenario showing (a) the UR5_KGG1_C system approaching the cylindrical block, and (b) the location of the Cognex system within the environment.

5.2.1 Computational Results

5.2.1.1 Estimated Probability of Success

For each robotic system, the probability of successfully completing the handling operation can be estimated based on the robot's configuration, the object being grasped, and the estimated vision uncertainty.

Object Grasp Region   Using the end effector's grasp region defined and measured in Section 4.3, an object-specific grasp region can be calculated to determine if the positional uncertainty during the pick-up action can be absorbed by the robotic system. With reference to Section 4.4, the objects to be grasped include a cylindrical block and a cuboid. For the cylindrical block, the object grasp region can be determined using the block's diameter, as the robotic end effector can approach the block at any orientation. The calculated object grasp regions for the cylindrical disc are shown in Figure 5.2.

For the cuboid, the robotic system must approach the object at the correct orientation. This is particularly true for robotic systems that include the Schunk KGG 80-30 gripper, as its finger configuration and $30\,mm$ travel distance determines which side
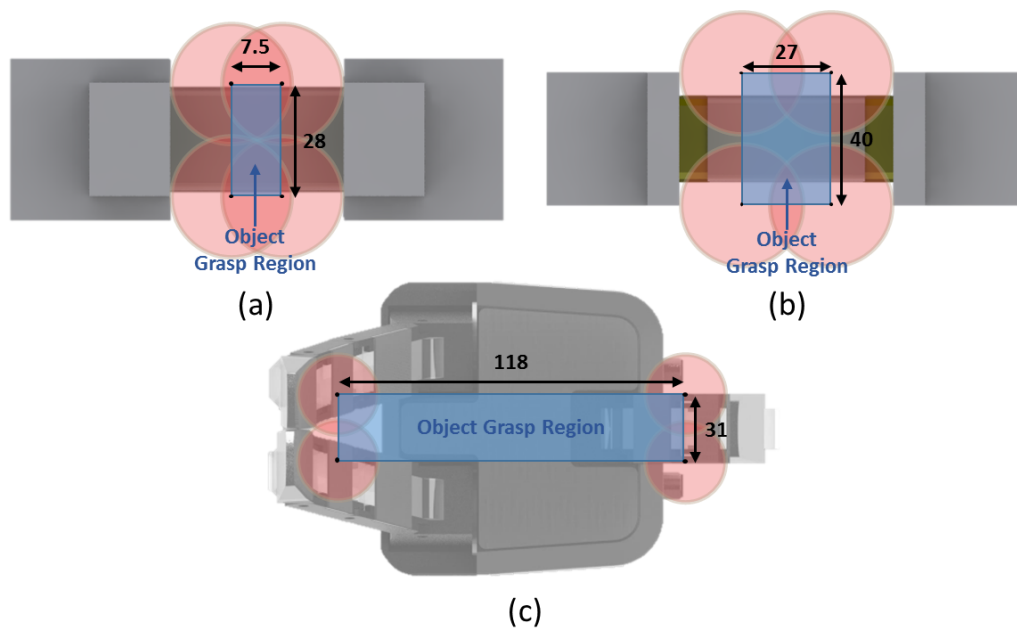
Figure 5.2: Calculated grasp region of the robotic end effectors when handling the disc.

of the cuboid should be grasped. Accordingly, orientation errors arising from the initialisation approach influence the object grasp region and should be accounted for. These orientation errors minimise the region in which a successful grasp is ensured, as an incorrect alignment can cause the fingers to collide with the object during a pick-up attempt. The reduction in the object grasp region is dependent on the level of orientation uncertainty. As an example, the object grasp regions for the cuboid and Schunk KGG 80-30 gripper have been calculated and shown in Figure 5.3.

In a similar manner, the reduced object grasp region was calculated for the Robotiq gripper. As Figure 5.3 illustrates, the magnitude of the rotational error determines the size of the reduced object grasp region. Knowing that the rotational error follows a univariate normal distribution, an average grasp region can be calculated using the rotational error $0.68\sigma_\theta$, where σ_θ is the standard deviation of this error.

With this reduced object grasp region, the probability of a successful grasp can be estimated by calculating the bivariate normal cumulative probability evaluated over the grasp region's area. Using the statistical toolbox within the MATLAB software, the PS value for each robotic system and object has been calculated and the results are summarised in Table 5.1.

Table 5.1: Estimated probability of success (PS) for varying degrees of uncertainty in the selected handling operation.

Robotic System	Grasp Region	Object	Object Grasp Region	Probability of Success (%)				
				σ_2	σ_4	σ_6	σ_8	Cognex
UR5-KGG1	15 x 40 mm (x2) *(with 34 mm gap)*	Disc	27 x 40 mm	100.00	99.93	97.47	89.72	100.00
		Cuboid	27 x 65 mm	100.00	99.81	95.50	85.84	100.00
UR5-KGG2	15 x 28 mm (x2) *(with 14.5 mm gap)*	Disc	7.5 x 28 mm	93.92	65.12	45.88	33.18	100.00
		Cuboid	19.5 x 65 mm	100.00	95.40	77.05	58.62	100.00
UR5-RIQ	155 x 31 mm	Disc	118 x 31 mm	100.00	99.99	99.02	94.73	100.00
		Cuboid	130 x 68 mm	100.00	100.00	100.00	99.99	100.00
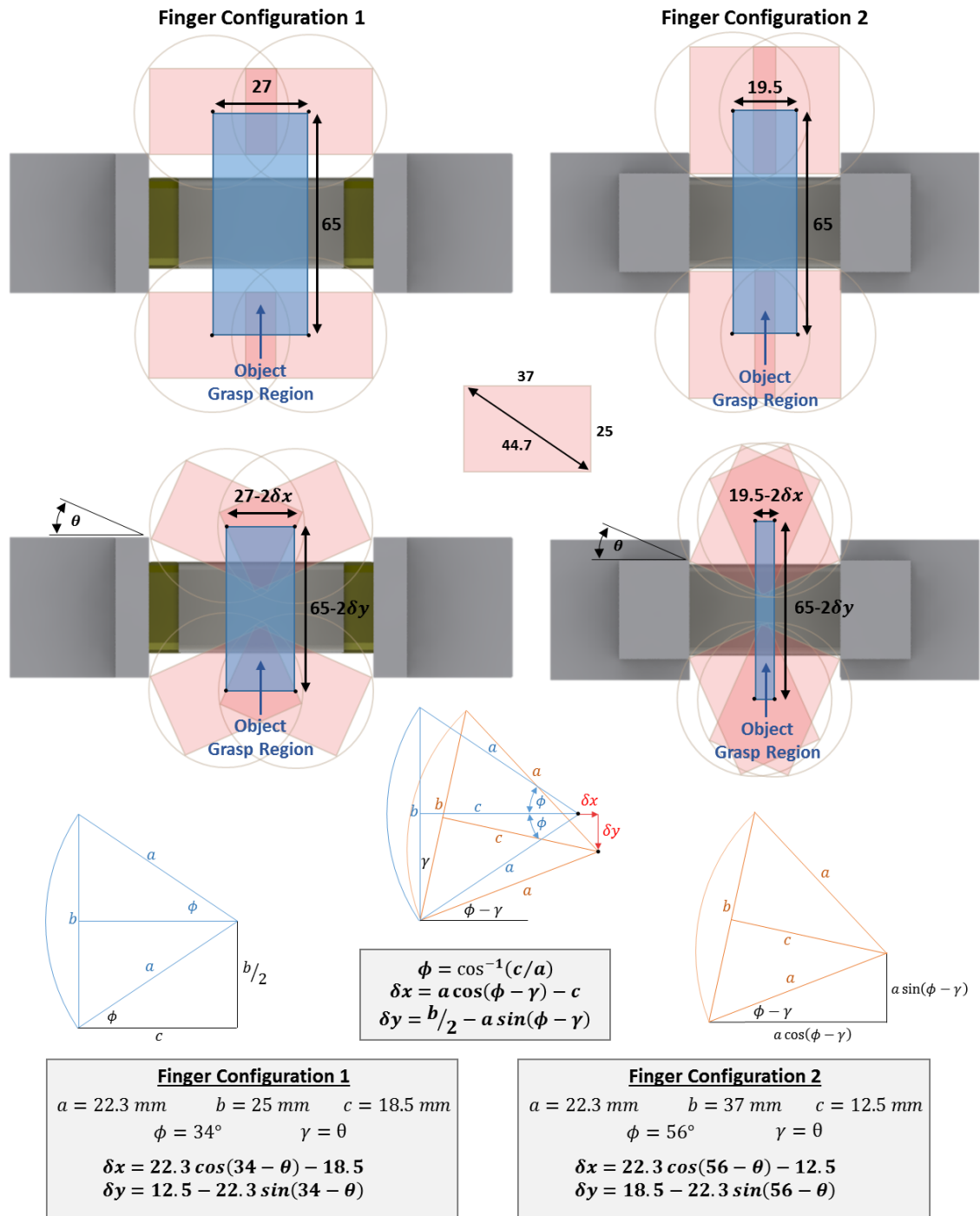
Figure 5.3: Calculated reduced grasp region of the Schunk KGG 80-30 gripper when handling the cuboid.

5.2.1.2   Estimated Completion Time

Since each action is performed sequentially in this handling operation, the overall completion time can be estimated by summing the time required for each relevant assembly action:

$$CT_{Total} = CT_{Align} + CT_{Pickup} + CT_{Transport} + CT_{Coordinate} \qquad (5.1)$$

For this operation, the robotic system's specified trajectory time and grasp cycle time can be used to estimate the robot's performance within the align, pickup, and transport actions. Equally, the communication delay metric can be used to estimate the robot's performance within the communication action.

Using the robot and object locations presented in Section 4.4 and choosing a reasonable approach clearance gives the following trajectory travel distances:

$$d_c = 17\,mm$$

$$d_a = 492\,mm$$

$$d_t = 868\,mm$$

To illustrate the use of a robot's performance metrics within Equation 5.1, the overall completion time of the UR5_KGG1_T robotic system is calculated below in full. A summary of the performance metrics recorded for this robotic system are given in Table 5.2. A similar approach is taken to estimate the performance of the other robotic systems, and the resulting completion times are presented in Table 5.3.

Table 5.2: Performance metrics of the UR5_KGG robotic system which relate to the chosen handling scenario.

Robot System Specification	Value	Robot System Specification	Value
Grasp Region	$30\,x\,40\,mm$	Grasp Cycle Time	$t_{cycle} = 0.3\,s$
Trajectory Completion Time	$t_{traj} = 0.0577\left(s_{traj}\right)^{0.5}$	Communication Delay	$t_{comm} = CEILING\left(t_{traj}, 0.2\right) - t_{traj}$

Overall completion time of the UR5_KGG1_T robotic system:

$$CT_{Align} = 0.0577(d_a)^{0.5} = 1.28 \ s$$

$$CT_{Pickup} = 0.0577(d_c)^{0.5} + (t_{cycle}/2) = 0.24 + 0.15 = 0.39 \ s$$

$$CT_{Transport} = 0.0577(d_c)^{0.5} + 0.0577(d_t)^{0.5} = 0.24 + 1.7 = 1.94 \ s$$

$$CT_{Coordinate} = t_{comm,1} + t_{comm,2} + t_{comm,3} + t_{comm,4}$$

$$= (1.4 - 1.28) + 2(0.4 - 0.24) + (1.8 - 1.7) = 0.54 \ s$$

$$CT_{Total} = CT_{Align} + CT_{Pickup} + CT_{Transport} + CT_{Coordinate}$$

$$CT_{Total} = 4.15 \ s$$

From Table 5.3, the chosen initialisation approach does not influence the estimated completion time for each Schunk KGG 80-30 gripper configuration as the gripper's cycle time is constant. However, since the cycle time of the Robotiq 3-fingered gripper is dependent on the travel distance of its fingers, the opening can be minimised to improve the gripper's performance. This opening gap is determined based on the level of uncertainty generated from the initialisation approach, which is why the simulated vision grasp time varies according to the standard deviation of the tested probability distributions.

Table 5.3: Estimated completion times of the different robotic systems for the selected handling operation.

Robot System	CT_{Align} (s)	CT_{Pickup} (s)	$CT_{Transport}$ (s)	$CT_{Coordinate}$ (s)	CT_{Total} (s)
UR5_KGG1_S	1.28	0.39	1.94	0.54	4.15
UR5_KGG1_C					
UR5_KGG2_S	1.28	0.39	1.94	0.54	4.15
UR5_KGG2_C					
UR5_RIQ_S	1.28	0.35 - 0.52	1.94	0.69	4.26 - 4.43
UR5_RIQ_C		0.4			4.26
LWR_KGG1_S	1.8	0.58	2.78	0.11	5.27
LWR_KGG1_C					

5.2.2 Experimental Results

5.2.2.1 Recorded Probability of Success

The probability of success (PS) during actual testing corresponded to the percentage of successful handling attempts. However, based on the chosen confidence level and number of iterations, the maximum PS value which could be determined from testing was 95.3% [140]. Hence, even if the robotic system performed all the handling iterations with a 100% success rate, the PS for the robotic system was recorded as 95.3%. For the given confidence level, recording a higher PS value would require more iterations e.g. a PS value of 0.99 can be recorded if the robotic system performs 299 successful iterations with no failures. The recorded PS value for the robotic systems when using the simulated and Cognex vision initialisation approach are given in Table 5.4. When unsuccessful handling iterations occurred during testing, the KC algorithm from Section 4.3 was used on the dichotomous data (pass/fail) data to determine the PS value.

From Table 5.4, the PS of the UR5_RIQ remained constant as the level of simulated uncertainty increased, while the PS of the UR5_KGG systems tended to decrease. Since a PS of 95.3% is the maximum that can be measured for 60 test iterations and a 95% confidence level, the UR5_RIQ was able to successfully complete each handling test without errors. This can be accredited to the gripper's ability to increase its finger gap to accommodate the larger levels of uncertainty.

Looking at the recorded PS for each UR5_KGG system, the UR5_KGG1 system was

Table 5.4: The recorded probability of success (PS) for each robotic system based on 60 handling iterations and a 0.95 confidence level. Due to the number of samples and the chosen confidence level, the maximum PS that could be determined was 95.3%.

Robot System	Object	Probability of Success (%)				
		σ_2	σ_4	σ_6	σ_8	Cognex
UR5_KGG1	Disc	95.3	90.1	95.3	95.3	95.3
	Cuboid	95.3	90.1	95.3	72.0	95.3
UR5_KGG2	Disc	85.7	49.4	42.9	42.9	95.3
	Cuboid	95.3	85.7	79.6	51.0	95.3
UR5_RIQ	Disc	95.3	95.3	95.3	95.3	95.3
	Cuboid	95.3	95.3	95.3	95.3	95.3

much more capable of dealing with uncertainty during the handling operation. This can be accredited to its more suitable finger design, which provided a large finger gap while still ensuring the objects could be grasped. When handling the cuboid, the UR5_KGG1 had comparable performance up until the simulated error σ_8. At this level of uncertainty, the additional rotational errors became sufficiently large to cause the corners of the cuboid to collide with the gripper upon approach.

For the UR5_KGG2 system, its smaller finger gap resulted in a poor PS when handling the disc at each simulated error. Its PS increased when handling the cuboid, as the gripper's design facilitated the system to grasp the object across its width. This could not be achieved by the UR5_KGG1, which highlights one trade-off between the different finger designs. The UR5_KGG2 finger design allowed the robot to grasp the object in any orientation, which would make the system preferable when it could achieve a similar PS e.g. when the system includes the Cognex vision system. However, since both systems are limited by a fixed finger stroke length of $15\,mm$, each system can only grasp a limited range of objects. Accordingly, both UR5_KGG systems are better suited to tasks where objects to be handled are known and similar in size.

5.2.2.2   Recorded Completion Time

The completion time (CT) of each iteration corresponds to the time taken for the robotic system to approach, orient, pick-up, and transport the object. A true mean was calculated based on the sample data, and the calculated values are given in Table 5.5.

Table 5.5: Calculated true mean value for each setup variation based on the recorded completion times.

Robot System	Object	Completion Time (s)				
		σ_2	σ_4	σ_6	σ_8	Cognex
UR5_KGG1	Disc	4.236 ± 0.008	4.233 ± 0.005	4.262 ± 0.014	4.255 ± 0.013	4.233 ± 0.002
	Cuboid	4.235 ± 0.006	4.233 ± 0.002	4.25 ± 0.012	4.251 ± 0.013	4.288 ± 0.014
UR5_KGG2	Disc	4.251 ± 0.013	4.252 ± 0.013	4.267 ± 0.014	4.269 ± 0.015	4.234 ± 0.003
	Cuboid	4.24 ± 0.008	4.238 ± 0.007	4.239 ± 0.009	4.245 ± 0.01	4.281 ± 0.015
UR5_RIQ	Disc	4.283 ± 0.004	4.293 ± 0.003	4.35 ± 0.001	4.406 ± 0.008	4.292 ± 0.003
	Cuboid	4.287 ± 0.009	4.292 ± 0.001	4.351 ± 0.001	4.401 ± 0.001	4.315 ± 0.012

With reference to Equation 2.7, the margin of error (E) recorded during the testing of each robotic system is low. From Table 5.5, the largest SE value was $0.063\,s$, which corresponds to a variance of $0.054\,s^2$. This suggests that the collected data points were relatively consistent for each robotic system. The variation present in each test can be accredited to the resolution of the measurements, which is sufficiently high that the measurand was influenced by the millisecond variations in the control program's execution and communication. In addition, this high resolution meant that the recorded CT was influenced by the small changes in approach and transport distances due to the varying positional error.

As an example, the different approach distances that result from a positive and negative error e_x are shown in Figure 5.4. While the distances are exaggerated for clarity, this example shows that the approach distances differ by:

$$|AC| = \sqrt{(x_1 + e_x - x_0)^2 + h^2}$$
$$|AD| = \sqrt{(x_1 - e_x - x_0)^2 + h^2}$$
$$|AC|^2 - |AD|^2 = 4e_x(x_1 - x_0)$$

From these equations, it can be seen that for a non-trivial solution, the two distances differ by a magnitude which is dependent on the error distance and the distance between the robots home position and the pick position. As shown, the distances become equal when either the error is zero (no positional uncertainty) and when the pick position is directly below the home position.

Using the collected data and the calculated true mean ranges, a version of the MATLAB code presented in Appendix C can be used to determine the outcome of the two-sample KS test and the detectable difference between the collected data sets (refer back to Figure 2.23). The resulting comparisons are given in Table 5.6 and Table 5.7.

From these cross-system comparisons, it is clear that CT of the UR5_RIQ differs from the other two systems for all simulated errors. This difference is first identified by the KS test, whose rejection suggests that their data sets are not from the same population. In addition, there is a detectable difference between the CT true means.
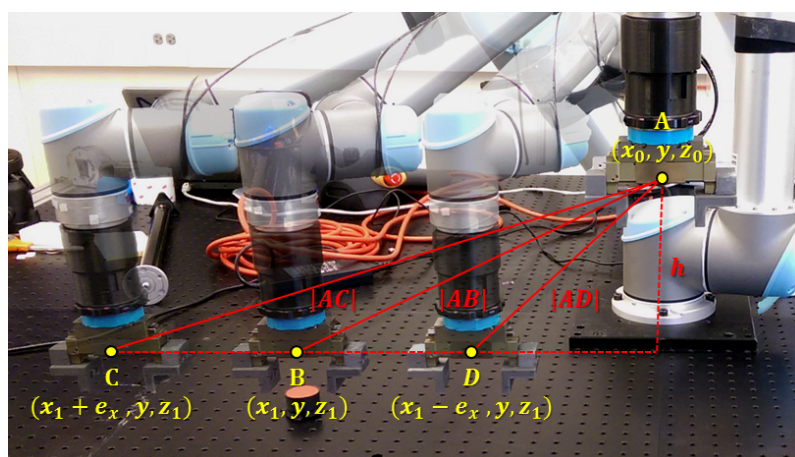
Figure 5.4: One-dimensional positional error $\pm e_x$ applied to the robot's pick-up location, which results in approach distances $|AC|$ and $|AD|$.

This difference is noted to depend on the simulated error, increasing from at least $0.02\,s$ for simulated error σ_2 to $0.11\,s$ for simulated error σ_8. This increase in CT can be explained by the longer grasp time, which is a consequence of the increased gripper opening due to the greater level of uncertainty. From this comparison, it can be seen that the CT of the UR5_RIQ is comparable to the UR5_KGG when testing with low errors, as the Robotiq gripper can reduce its finger gap to minimise its closing time. However, this difference in CT only gets larger as the uncertainty increases, as the UR5_RIQ increases its finger gap while Schunk KGG gripper's gap remains constant.

The performance of the three robotic systems when using the Cognex vision system differs from the simulated error tests. As presented in Table 5.6, there is a notable difference between the performances of each system when handling the disc and cuboid. The CT when handling the cuboid has a larger sample mean and margin of error, which implies a greater variance in the recorded results. Both increases can be explained by the additional time required for the vision system to detect and communicate the cuboid's orientation, and the subsequent tool rotation which varied between test iterations. Due to the increased variance, the performance of UR5_RIQ relative to the UR5_KGG systems becomes less obvious when considering the cuboid and the Cognex vision system.

Table 5.6: Comparison of the different robotic systems for each initialisation approach. A positive detectable difference (in seconds) between the system's true mean completion times differ by at least that value. Rejection (1) of the null hypothesis (H_0) suggests that the data sets do not belong to the same population at the 5% significance level.

(a) Simulated Vision, σ_2

Detectable Difference	UR5_KGG1		UR5_KGG2		UR5_RIQ	
	Disc	Cuboid	Disc	Cuboid	Disc	Cuboid
UR5_KGG1 Disc		-0.01	0.00	-0.01	0.05	0.05
UR5_KGG1 Cuboid	-0.01		0.00	0.00	0.06	0.06
UR5_KGG2 Disc	0.00	0.00		-0.01	0.02	0.02
UR5_KGG2 Cuboid	-0.01	0.00	-0.01		0.05	0.05
UR5_RIQ Disc	0.05	0.06	0.02	0.05		0.00
UR5_RIQ Cuboid	0.05	0.06	0.02	0.05	0.00	

KS Test	UR5_KGG1		UR5_KGG2		UR5_RIQ	
	Disc	Cuboid	Disc	Cuboid	Disc	Cuboid
UR5_KGG1 Disc		0	1	0	1	1
UR5_KGG1 Cuboid	0		1	0	1	1
UR5_KGG2 Disc	1	1		1	1	1
UR5_KGG2 Cuboid	0	0	1		1	1
UR5_RIQ Disc	1	1	1	1		0
UR5_RIQ Cuboid	1	1	1	1	0	

(b) Simulated Vision, σ_4

Detectable Difference	UR5_KGG1		UR5_KGG2		UR5_RIQ	
	Disc	Cuboid	Disc	Cuboid	Disc	Cuboid
UR5_KGG1 Disc		-0.01	-0.02	0.00	0.07	0.07
UR5_KGG1 Cuboid	-0.01		-0.01	-0.01	0.09	0.09
UR5_KGG2 Disc	-0.02	-0.01		0.00	0.07	0.07
UR5_KGG2 Cuboid	0.00	-0.01	0.00		0.10	0.10
UR5_RIQ Disc	0.07	0.09	0.07	0.10		0.00
UR5_RIQ Cuboid	0.07	0.09	0.07	0.10	0.00	

KS Test	UR5_KGG1		UR5_KGG2		UR5_RIQ	
	Disc	Cuboid	Disc	Cuboid	Disc	Cuboid
UR5_KGG1 Disc		0	0	1	1	1
UR5_KGG1 Cuboid	0		1	0	1	1
UR5_KGG2 Disc	0	1		1	1	1
UR5_KGG2 Cuboid	1	0	1		1	1
UR5_RIQ Disc	1	1	1	1		0
UR5_RIQ Cuboid	1	1	1	1	0	

(c) Simulated Vision, σ_6

Detectable Difference	UR5_KGG1		UR5_KGG2		UR5_RIQ	
	Disc	Cuboid	Disc	Cuboid	Disc	Cuboid
UR5_KGG1 Disc		-0.01	-0.02	0.00	0.07	0.07
UR5_KGG1 Cuboid	-0.01		-0.01	-0.01	0.09	0.09
UR5_KGG2 Disc	-0.02	-0.01		0.00	0.07	0.07
UR5_KGG2 Cuboid	0.00	-0.01	0.00		0.10	0.10
UR5_RIQ Disc	0.07	0.09	0.07	0.10		0.00
UR5_RIQ Cuboid	0.07	0.09	0.07	0.10	0.00	

KS Test	UR5_KGG1		UR5_KGG2		UR5_RIQ	
	Disc	Cuboid	Disc	Cuboid	Disc	Cuboid
UR5_KGG1 Disc		0	0	1	1	1
UR5_KGG1 Cuboid	0		1	0	1	1
UR5_KGG2 Disc	0	1		1	1	1
UR5_KGG2 Cuboid	1	0	1		1	1
UR5_RIQ Disc	1	1	1	1		0
UR5_RIQ Cuboid	1	1	1	1	0	

(d) Simulated Vision, σ_8

Detectable Difference	UR5_KGG1		UR5_KGG2		UR5_RIQ	
	Disc	Cuboid	Disc	Cuboid	Disc	Cuboid
UR5_KGG1 Disc		-0.02	-0.01	-0.01	0.13	0.13
UR5_KGG1 Cuboid	-0.02		-0.01	-0.02	0.13	0.14
UR5_KGG2 Disc	-0.01	-0.01		0.00	0.11	0.12
UR5_KGG2 Cuboid	-0.01	-0.02	0.00		0.14	0.14
UR5_RIQ Disc	0.13	0.13	0.11	0.14		0.00
UR5_RIQ Cuboid	0.13	0.14	0.12	0.14	0.00	

KS Test	UR5_KGG1		UR5_KGG2		UR5_RIQ	
	Disc	Cuboid	Disc	Cuboid	Disc	Cuboid
UR5_KGG1 Disc		0	0	0	1	1
UR5_KGG1 Cuboid	0		1	0	1	1
UR5_KGG2 Disc	0	1		1	1	1
UR5_KGG2 Cuboid	0	0	1		1	1
UR5_RIQ Disc	1	1	1	1		0
UR5_RIQ Cuboid	1	1	1	1	0	

(e) Cognex Vision

Detectable Difference	UR5_KGG1		UR5_KGG2		UR5_RIQ	
	Disc	Cuboid	Disc	Cuboid	Disc	Cuboid
UR5_KGG1 Disc		0.04	0.00	0.03	0.05	0.07
UR5_KGG1 Cuboid	0.04		0.04	-0.02	-0.01	0.00
UR5_KGG2 Disc	0.00	0.04		0.03	0.05	0.07
UR5_KGG2 Cuboid	0.03	-0.02	0.03		-0.01	0.01
UR5_RIQ Disc	0.05	-0.01	0.05	-0.01		0.01
UR5_RIQ Cuboid	0.07	0.00	0.07	0.01	0.01	

KS Test	UR5_KGG1		UR5_KGG2		UR5_RIQ	
	Disc	Cuboid	Disc	Cuboid	Disc	Cuboid
UR5_KGG1 Disc		1	0	1	1	1
UR5_KGG1 Cuboid	1		1	0	1	1
UR5_KGG2 Disc	0	1		1	1	1
UR5_KGG2 Cuboid	1	0	1		1	1
UR5_RIQ Disc	1	1	1	1		1
UR5_RIQ Cuboid	1	1	1	1	1	

Table 5.7: Comparison of the different initialisation approaches for each robotic system. A positive detectable difference (in seconds) between the system's true mean completion times differ by at least that value. Rejection (1) of the null hypothesis (H_0) suggests that the data sets do not belong to the same population at the 5% significance level.

(a) UR5_KGG1

Detectable Difference		σ_2		σ_4		σ_6		σ_8		Cognex	
		Disc	Cuboid	Disc	Cuboid	Disc	Cuboid	Disc	Cuboid	Disc	Cuboid
σ_2	Disc		-0.01	-0.01	-0.01	0.00	-0.01	0.00	-0.01	-0.01	**0.03**
	Cuboid	-0.01		-0.01	-0.01	**0.01**	0.00	0.00	0.00	-0.01	**0.03**
σ_4	Disc	-0.01	-0.01		-0.01	**0.01**	0.00	0.00	0.00	-0.01	**0.04**
	Cuboid	-0.01	-0.01	-0.01		**0.01**	0.00	**0.01**	0.00	0.00	**0.04**
σ_6	Disc	0.00	**0.01**	**0.01**	**0.01**		-0.01	-0.02	-0.01	**0.01**	0.00
	Cuboid	-0.01	0.00	0.00	0.00	-0.01		-0.02	-0.02	0.00	**0.01**
σ_8	Disc	0.00	0.00	0.00	**0.01**	-0.02	-0.02		-0.02	**0.01**	**0.01**
	Cuboid	-0.01	0.00	0.00	0.00	-0.01	-0.02	-0.02		0.00	**0.01**
Cognex	Disc	-0.01	-0.01	-0.01	0.00	**0.01**	0.00	**0.01**	0.00		**0.04**
	Cuboid	**0.03**	**0.03**	**0.04**	**0.04**	0.00	**0.01**	**0.01**	**0.01**	**0.04**	

KS Test		σ_2		σ_4		σ_6		σ_8		Cognex	
		Disc	Cuboid	Disc	Cuboid	Disc	Cuboid	Disc	Cuboid	Disc	Cuboid
σ_2	Disc		0	0	0	**1**	0	**1**	**1**	0	**1**
	Cuboid	0		0	0	**1**	0	**1**	0	0	**1**
σ_4	Disc	0	0		0	**1**	0	**1**	0	0	**1**
	Cuboid	0	0	0		**1**	0	**1**	0	0	**1**
σ_6	Disc	**1**	**1**	**1**	**1**		0	0	0	**1**	**1**
	Cuboid	0	0	0	0	0		0	0	0	**1**
σ_8	Disc	**1**	**1**	**1**	**1**	0	0		0	**1**	**1**
	Cuboid	**1**	0	0	0	0	0	0		**1**	**1**
Cognex	Disc	0	0	0	0	**1**	0	**1**	**1**		**1**
	Cuboid	**1**	**1**	**1**	**1**	**1**	**1**	**1**	**1**	**1**	

(b) UR5_KGG2

Detectable Difference		σ_2		σ_4		σ_6		σ_8		Cognex	
		Disc	Cuboid	Disc	Cuboid	Disc	Cuboid	Disc	Cuboid	Disc	Cuboid
σ_2	Disc		-0.01	-0.03	-0.01	-0.01	-0.01	-0.01	-0.02	0.00	0.00
	Cuboid	-0.01		-0.01	-0.01	**0.01**	-0.02	**0.01**	-0.01	-0.01	**0.02**
σ_4	Disc	-0.03	-0.01		-0.01	-0.01	-0.01	-0.01	-0.02	0.00	0.00
	Cuboid	-0.01	-0.01	-0.01		**0.01**	-0.01	**0.01**	-0.01	-0.01	**0.02**
σ_6	Disc	-0.01	**0.01**	-0.01	**0.01**		0.00	-0.03	0.00	**0.02**	-0.02
	Cuboid	-0.01	-0.02	-0.01	-0.01	0.00		**0.01**	-0.01	-0.01	**0.02**
σ_8	Disc	-0.01	**0.01**	-0.01	**0.01**	-0.03	**0.01**		0.00	**0.02**	-0.02
	Cuboid	-0.02	-0.01	-0.02	-0.01	0.00	-0.01	0.00		0.00	**0.01**
Cognex	Disc	0.00	-0.01	0.00	-0.01	**0.02**	-0.01	**0.02**	0.00		**0.03**
	Cuboid	0.00	**0.02**	0.00	**0.02**	-0.02	**0.02**	-0.02	**0.01**	**0.03**	

KS Test		σ_2		σ_4		σ_6		σ_8		Cognex	
		Disc	Cuboid	Disc	Cuboid	Disc	Cuboid	Disc	Cuboid	Disc	Cuboid
σ_2	Disc		0	0	0	**1**	0	**1**	0	0	**1**
	Cuboid	0		0	0	**1**	0	**1**	0	0	**1**
σ_4	Disc	0	0		**1**	0	0	**1**	0	**1**	**1**
	Cuboid	0	0	**1**		**1**	0	**1**	0	0	**1**
σ_6	Disc	**1**	**1**	0	**1**		**1**	0	**1**	**1**	0
	Cuboid	0	0	0	0	**1**		**1**	0	0	**1**
σ_8	Disc	**1**	**1**	**1**	**1**	0	**1**		**1**	**1**	0
	Cuboid	0	0	0	0	**1**	0	**1**		0	**1**
Cognex	Disc	0	0	**1**	0	**1**	0	**1**	0		**1**
	Cuboid	**1**	**1**	**1**	**1**	0	**1**	0	**1**	**1**	

(c) UR5_RIQ

Detectable Difference		σ_2		σ_4		σ_6		σ_8		Cognex	
		Disc	Cuboid	Disc	Cuboid	Disc	Cuboid	Disc	Cuboid	Disc	Cuboid
σ_2	Disc		-0.01	0.00	0.00	0.06	0.06	0.11	0.11	0.00	0.02
	Cuboid	-0.01		-0.01	-0.01	0.05	0.05	0.10	0.10	-0.01	0.01
σ_4	Disc	0.00	-0.01		0.00	0.05	0.05	0.10	0.10	-0.01	0.01
	Cuboid	0.00	-0.01	0.00		0.06	0.06	0.10	0.11	0.00	0.01
σ_6	Disc	0.06	0.05	0.05	0.06		0.00	0.05	0.05	0.05	0.02
	Cuboid	0.06	0.05	0.05	0.06	0.00		0.05	0.05	0.05	0.02
σ_8	Disc	0.11	0.10	0.10	0.10	0.05	0.05		0.00	0.10	0.07
	Cuboid	0.11	0.10	0.10	0.11	0.05	0.05	0.00		0.10	0.07
Cognex	Disc	0.00	-0.01	-0.01	0.00	0.05	0.05	0.10	0.10		0.01
	Cuboid	0.02	0.01	0.01	0.01	0.02	0.02	0.07	0.07	0.01	

KS Test		σ_2		σ_4		σ_6		σ_8		Cognex	
		Disc	Cuboid	Disc	Cuboid	Disc	Cuboid	Disc	Cuboid	Disc	Cuboid
σ_2	Disc		0	1	1	1	1	1	1	1	1
	Cuboid	0		1	1	1	1	1	1	1	1
σ_4	Disc	1	1		0	1	1	1	1	0	1
	Cuboid	1	1	0		1	1	1	1	0	1
σ_6	Disc	1	1	1	1		0	1	1	1	1
	Cuboid	1	1	1	1	0		1	1	1	1
σ_8	Disc	1	1	1	1	1	1		0	1	1
	Cuboid	1	1	1	1	1	1	0		1	1
Cognex	Disc	1	1	0	0	1	1	1	1		1
	Cuboid	1	1	1	1	1	1	1	1	1	

Comparing the performance the UR5_KGG1 and UR5_KGG2 systems show that there is little difference in the recorded CT between the two Schunk fingers for each initialisation approach and object. The KS test suggests that some of the data sets do not belong to the same population, but there is no detectable difference when considering the true means of each test. The KS test detects a difference between the two systems when handling the disc at simulated error σ_2 and σ_4. Referring to Table 5.5, the sample means and variances recorded for these tests do suggest that they do not belong to the same sample, but the variance is sufficiently large that there is no detectable difference between their true means. As both approaches compare the data sets using a 0.05 significance level, there is a 5% risk that either test is incorrect. Accordingly, the comparison of these data sets could be performed with a lower significance in order to increase the confidence in the calculated results. However, this was not required here, as the conflicting results only suggest that the difference between the collected results, if any, is marginal since the CT was recorded with a resolution of 0.001 s.

From this comparison, it can be concluded that there is minimal difference between the recorded CT of the UR5_KGG1 and UR5_KGG2 systems. The lack of a significant detectable difference between each test shows that the system's CT was independent of the Schunk's finger configuration, the object being grasped, and the level of

uncertainty. While not unexpected, this comparison confirms the consistency of the interface and program that was used to control each system.

5.2.2.3   Experimental Summary

From the recorded PS and CT values, the performance of each robotic system is dependent on the level of uncertainty present. Of the robotic systems considered, the UR5_RIQ system provides greater flexibility as it can increase its finger gap to accommodate larger positional errors. While this flexibility comes at the price of higher CT, the robotic system is the better choice for the given handling scenario due to the object's positional uncertainty along the width of the conveyor system. Alternatively, a vision system could be introduced within the environment. While this increases the initial investment required during setup, its introduction ensures that the three robotic systems could perform the handling operation without any failures. With vision, the UR5_KGG systems may be a better choice thanks to their lower CT when compared to UR5_RIQ system. Of the two finger designs, the UR5_KGG2 would be better suited to the given scenario as it is not limited to a specific orientation when grasping the cuboid. However, if more objects were introduced to the given scenario, it is likely that the UR5_RIQ system would be required as the UR5_KGG systems are limited to objects which can be grasped by the KGG gripper's fixed finger stroke length of $15\,mm$.

5.2.3 Handling Scenario Discussion

5.2.3.1 Computational vs. Experimental Results

A summary of the estimated and recorded CT and PS values is given in Table 5.7. For the sake of comparison, an average recorded CT is presented for each robotic system based on its performance across each initialisation approach. This simplification helps to identify the performance of the developed framework, and was deemed acceptable due to the proximity of the sample means and the low variability in the recorded values.

Comparing the estimated and recorded CT, it can clearly be seen that the developed framework provides an accurate approach to estimating a robotic system's performance. As opposed to supplier specifications which assume optimal performance, the developed performance metrics provide a true reflection of the robotic system's performance which results in estimated CT that are within $0.1\ s$ (2.5%) of the recorded CT.

If using supplier specifications, an estimate could be obtained by using the quoted manipulator tool speed and gripper closing time, but the resulting estimate would be significantly less accurate. As an example, the supplier specifications of the UR5_KGG1 system can be used to give an estimated CT of $2.14\ s$. This estimate is calculated using the UR5 robot's maximum tool speed of $1\ ms_{-1}$, the Schunk KGG 80-30 gripper's closing time of $0.025\ s$, and assuming that the manipulator executes each trajectory with a phase of constant acceleration, constant velocity and constant deceleration. The latter allows the equations of motion to be used to estimate the CT of each trajectory using the equation $CT_{traj} = 1.5(s_{traj})/v_{max}$, where s_{traj} is the

Table 5.7: Comparison between the estimated and recorded performance of each robotic system. To improve the clarity of the table, an average completion time is calculated from the testing of each robotic system.

Robot System	Object	Completion Time (s)		Probability of Success (%)									
		Estimated	Actual	σ_2		σ_4		σ_6		σ_8		Cognex	
				Estimated	Actual	Estimated	Actual	Estimated	Actual	Estimated	Actual	Estimated	Actual
UR5-KGG1	Disc	4.15	4.24	100.00	95.30	99.93	90.10	97.47	95.30	89.72	95.30	100.00	95.30
	Cuboid	4.15	4.25	100.00	95.30	99.81	90.10	95.50	95.30	85.84	72.00	100.00	95.30
UR5-KGG2	Disc	4.15	4.25	93.92	85.70	65.12	49.40	45.88	42.90	33.18	42.90	100.00	95.30
	Cuboid	4.15	4.25	100.00	95.30	95.40	85.70	77.05	79.60	58.62	51.00	100.00	95.30
UR5-RIQ	Disc	4.26 - 4.43	4.28 - 4.41	100.00	95.30	99.99	95.30	99.02	95.30	94.73	95.30	100.00	95.30
	Cuboid	4.26 - 4.43	4.29 - 4.40	100.00	95.30	100.00	95.30	100.00	95.30	99.99	95.30	100.00	95.30

Table 5.8: Overall disparity between the estimated and recorded probability of success values. A positive and negative value correspond to an overestimation and underestimation by the developed framework.

Robot System	Object	Estimation Error (%)				
		σ_2	σ_4	σ_6	σ_8	Cognex
UR5-KGG1	Disc	4.70	9.83	2.17	-5.58	4.70
	Cuboid	4.70	9.71	0.20	13.84	4.70
UR5-KGG2	Disc	8.22	15.72	2.98	-9.72	4.70
	Cuboid	4.70	9.70	-2.55	7.62	4.70
UR5-RIQ	Disc	4.70	4.69	3.72	-0.57	4.70
	Cuboid	4.70	4.70	4.70	4.69	4.70

linear trajectory distance and v_{max} is the specified manipulator tool speed.

From Table 5.7, the accuracy of the estimated PS varies for each robotic system and initialisation approach. To improve clarity, the difference between the estimated and actual PS values are summarised in Table 5.8. Within this table, positive and negative differences correspond to overestimations and underestimations by the developed framework. Estimations within 5% of the recorded PS are shaded out as they were deemed satisfactory considering the sensitivity of the recorded data.

As noted, the number of test iterations influence the maximum PS which can be determined from the collected data for a given confidence level. To balance the time spent testing with the usefulness of the collected results, 60 test iterations were performed with each robotic system. Assuming no failures, this number of iterations allowed for a maximum PS of 95.3% to be recorded given the chosen 95% confidence level. Accordingly, the maximum PS recorded during testing and presented within Table 5.7 is 95.3%. However, since these tests had no failures, their PS is comparable to the higher estimated PS values.

As the actual PS value represents the maximum probability of success which can be determined with 95% confidence based on 60 iterations, its calculated value is conservative and should be lower than the estimated PS in the majority of cases. This is identified in Table 5.8, which shows that the developed framework overestimates the robotic system's performance in 26 of the 30 tests. Looking at the instances when the developed framework underestimated performance, two of the estimations were within 2.6% of the recorded PS, while three underestimations occurred when handling the disc with simulated perception error σ_8. Since the perception errors were constant across systems, this suggests that the 60 positional errors generated

for σ_8 were slightly more conservative with few data points from the outer portion of the distribution curve.

Conversely, the recorded PS for the simulated perception error σ_4 were continually lower than estimated across systems, which suggests that the generated positional errors included a higher proportion of outliers and points close to the distribution's upper and lower tail. In addition, these larger overestimations can be accounted for by the sensitivity of the recorded PS value to errors. Due to the number of test iterations, a single error during the handling scenario causes the recorded PS to drop from 95.3% to 90.1%. While this sensitivity could be reduced by performing more test iterations, it was accepted so that testing would not require a significant time investment.

Overall, the proximity of the estimated PS and CT to actual recorded values highlights the potential of the developed framework. Its decomposition of the handling scenario into actions and its use of developed robot metrics provides a structured evaluation method that provides an accurate CT estimation. PS estimations are satisfactorily close considering the number of test iterations performed, and provide a good indication of a robotic system's ability to perform the operation at different levels of uncertainty. This allows an informed decision to be made based on the robotic system and handling operation being considered.

5.2.3.2 Boothroyd-Dewhurst Comparison

Based on its setup, the handling scenario presents no handling difficulties and so can be identified as a B-D operation with handling code '00' for the disc and '10' for the cuboid (refer back to Figure 2.10). Accordingly, a human operator can handling the disc and cuboid in an average time of 1.13 s and 1.5 s respectively.

Using the developed framework, the UR5_KGG systems are estimated to perform the operation in 4.15 s, while the UR5_RIQ system is estimated to take between 4.26 s and 4.43 s depending on the level of uncertainty. Assuming a Cognex vision system is available, the outcome of the framework's evaluation indicates that either UR5_KGG system would be the best choice for the given handling scenario. However, the estimated CT of these systems is 2.76 to 3.67 times slower than the average

human completion time. This information can be combined with other cost metrics to determine if the benefits of using an automated system (increased working hours, reduced operation costs, etc.) outweigh its shortcomings (high set-up costs, reduced flexibility, etc.). In this instance, the potential loss in workstation throughput makes the robotic systems considered unsuitable when compared to human performance.

If the deployment of a robotic system is desired, the use of the developed framework allows for the identification of better system structures from its analysis of performance within each assembly action. In this scenario, the motions of the robotic manipulator account for the majority of the estimated CT. Accordingly, a robotic manipulator better suited to the trajectory distances could be selected (using the trajectory time metric), or the operation layout could be modified to minimize these distances. The framework identifies communication delays as the second biggest contributor to the estimated CT, and so increasing the communication frequency between the computer and controller would also produce noticeable improvements in the robotic system's performance.

5.3 Pick-and-Place Scenario

From Section 4.5, the MRMT is a standardised human dexterity test which can be used to represent a typical pick-and-place assembly task. The MRMT is a development of the handling scenario that provides a greater insight into the performance of a robotic system within this area. While the original MRMT displacement test uses a board, more meaningful results can be generated by using paper targets instead. Both approaches were used during testing, as shown in Figure 5.5.

5.3.1 Computational Results

Similar to the handling scenario, the dexterous performance of the robotic system can be estimated by calculating the system's probability of success and task completion time.

5.3.1.1 Estimated Probability of Success

For the original MRMT, the PS corresponds to the probability that the robotic system will successfully transfer the cylindrical blocks from one hole to another within the board. The use of the board allows the pick-and-place operation to be considered a simple handling operation, as the blocks can be dropped into the hole without requiring accurate placement.

(a)	(b)
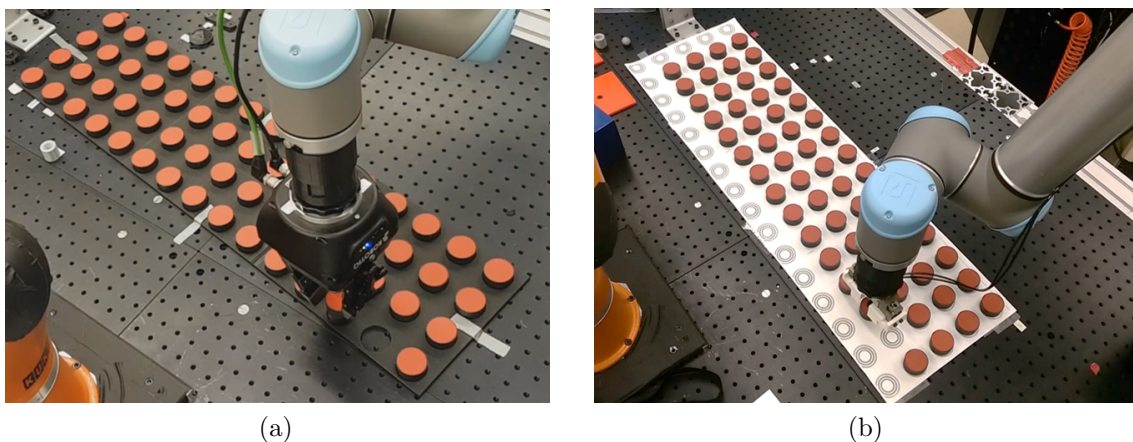
Figure 5.5: Pick-and-place testing of (a) the UR10_RIQ system using the original MRMT displacement test and (b) the UR10_AGO system using the MRMT displacement test variant.

In this scenario, the estimated PS is calculated from the level of uncertainty present, which is dependent on the employed initialisation approach. For the teach programming approach, the uncertainty is dependent on the operator. However, assuming a competent trainer and sufficient teaching time, the positional error can be approximated as the robotic manipulator's specified repeatability. From Table 4.1 this is equal to $0.01\,mm$ for the UR10 robot manipulator. With reference to Section 4.2.3, the positional error when using the Cognex system has been approximated by a normal distribution with a mean of $-0.37\,mm$ and standard deviation of $0.87\,mm$, while the positional error for the Cognex + registration has been approximated by a normal distribution with a mean of $4.27\,mm$ and standard deviation of $1.5\,mm$. Using the object grasp regions already calculated for these robotic systems, the estimated level of uncertainty is sufficiently small for each initialisation approach to ensure a successful handling of each disc. Accordingly, the PS was calculated to determine the likelihood of a successful placement of the block. For the original MRMT, this corresponded to the probability that the block would be successfully transferred to a hole within the board. From observation, the elevated board and its hole dimensions accommodated insertion inaccuracies of up to $5\,mm$. For the MRMT displacement test variant, the estimated PS was calculated for each placement accuracy zone and corresponded to the probability that the robotic system would place the disc within that accuracy zone. Using the estimated uncertainty generated by each initialisation approach, the PS for each robotic system was calculated. These values are presented in Table 5.9.

Table 5.9: Estimated probability of success (PS) for each of the robotic systems during the original MRMT Test and the MRMT test variant.

Robotic System	MRMT Handling PS (%)	Original MRMT Insertion PS (%)	MRMT Variant Insertion PS (%)				
			Zone 1 (0 – 1 mm)	Zone 2 (0 – 3 mm)	Zone 3 (0 – 5 mm)	Zone 4 (0 – 7 mm)	Zone 5 (0 – 9 mm)
UR10_KGG_T UR10_RIQ_T	100.0	100.0	100.0	100.0	100.0	100.0	100.0
UR10_KGG_C UR10_RIQ_C	100.0	100.0	70.8	99.9	100.0	100.0	100.0
UR10_KGG_CR UR10_RIQ_CR	100.0	76.8	2.6	27.5	76.8	98.0	100.0

5.3.1.2   Estimated Completion Time

For both versions of the Minnesota displacement test, the estimated CT can be determined by considering the completion time of each handling and insertion action:

$$CT_{Total} = CT_{Align} + CT_{Pickup} + CT_{Transport} + CT_{Coordinate} + CT_{Place} + CT_{Retract} \quad (5.2)$$

Considering the setup of the MRMT presented in Section 4.5, the transfer distance is equal to $57\,mm$, while the alignment distance (d_a) is either equal to $108\,mm$ or $80.6\,mm$ depending on the location of the next block within the board's $4\,x\,15$ linear pattern. The clearance distance (d_c) remains constant throughout the test, and is set to $25\,mm$. From Equation 4.12, the coordinate time of the UR robot is dependent on the trajectory distance. Following the same approach as used to estimate the CT of the handling scenario, the CT for the full Minnesota displacement test and its variant (4 runs of 59 = 236 pick-and-place operations) can be estimated by summing the estimated CT of each individual pick-and-place operation. The calculated CT values are summarised in Table 5.10.

5.3.2   Experimental Results

As noted in Section 4.5, testing was performed using the original MRMT board and a paper target variant. In both cases, the test was arbitrary positioned within the robot's workspace and secured to the environment. The block positions were calculated using the chosen initialisation approach, and this time was recorded as the system's initialisation time. The robot system then performed the complete MRMT displacement test, and the completion time and number of successful transfers were

Table 5.10: Estimated completion times of the different robotic systems for the MRMT displacement test and its variant.

Robotic System	Single Operation Completion Time (s)							Total Completion Time (s)			
	$CT_{Align,1}$	$CT_{Align,2}$	CT_{Pickup}	$CT_{Transport}$	CT_{Place}	$CT_{Retract}$	$CT_{Coordinate}$	$CT_{Handling,1}$	$CT_{Handling,2}$	CT_{Total}	$CT_{Per\,Block}$
MRMT Original											
UR10_KGG	0.60	0.52	0.44	0.72	0.15	0.00	0.39	2.30	2.22	531.26	2.25
UR10_RIQ	0.60	0.52	0.34	0.72	0.05	0.00	0.68	2.40	2.32	554.48	2.35
MRMT Variant											
UR10_KGG	0.60	0.52	0.44	0.72	0.44	0.29	0.61	3.10	2.73	687.75	2.91
UR10_RIQ_T	0.60	0.52	0.34	0.72	0.34	0.29	0.90	3.20	2.83	710.97	3.01
UR10_RIQ_C	0.60	0.52	0.40	0.72	0.40	0.29	0.90	3.31	2.94	736.69	3.12
UR10_RIQ_CR	0.60	0.52	0.45	0.72	0.45	0.29	0.90	3.42	3.05	762.42	3.23

recorded for each run.

In addition to the robotic systems considered within the previous section, the MRMT test and its variant were used to assess the performance of the Baxter robot and the Allegro robotic hand (see Figure 5.6). This testing was conducted by researchers Rick Norcross and Karl Van Wyk from NIST, and their results have been included here to show the potential for using the MRMT as a benchmarking tool within robotics research.

The results of all robotic systems during the original MRMT displacement test and its variant are presented in Tables 5.11 and 5.12.

5.3.2.1   Recorded Initialisation Time

From Tables 5.11 and 5.12, there is a significant difference between the initialisation times of the robotic systems. Unsurprisingly, the teach programming takes the longest time, as the pick-and-place positions have to be taught by manually moving the robot to the four corner positions. Three different robotic systems were initialised using teach programming; the BAX_VAC_T, the UR10_KGG_T, and the UR10_RIQ_T system. The BAX_VAC_T system required the least amount of training time as there was no benefit to accurately recording corner positions because of the robotic manipulator's inherent compliance and low repeatability. The initialisation time of the BAX_VAC_T system during the original test and its variant was 64 s and 141 s respectively. This increase in initialisation time can be accounted for by the added difficulty in aligning the robot with the flat target positions.
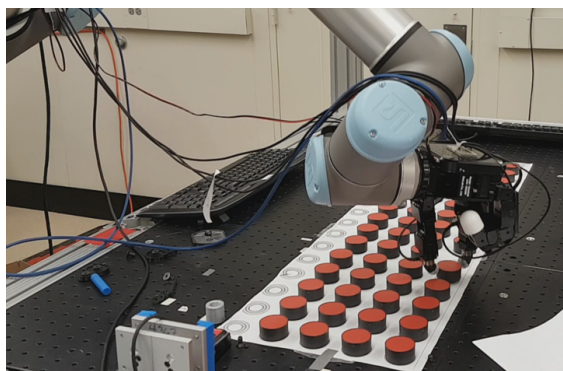
Figure 5.6: Additional testing using the MRMT and its variant to assess the performance of the LWR4_AGO system.

Table 5.11: Robotic system performance during the MRMT displacement test. Probability of success (PS) calculated for a 95% confidence level.

Robotic System	Placement Zone	Accuracy Range	Successful Placements					Probability of Success (%)	Initialisation Time (s)	Completion Time (s)	
			Run 1	Run 2	Run 3	Run 4	Combined			CT_{Total}	$CT_{Per\ Block}$
UR10_KGG_T	1	0 - 5 mm	59	59	59	59	236	98.75	570	516	2.19
UR10_RIQ_T	1	0 - 5 mm	59	59	59	59	236	98.75	294	530.3	2.25
BAX_VAC_T	1	0 - 5 mm	43	45	42	50	180	71.20	64	2141	9.1
	2	0 - 10 mm	58	57	58	58	231	95.50			
	3	0 - 20 mm	59	59	59	59	236	98.75			
UR10_KGG_C	1	0 - 5 mm	59	59	59	59	236	98.75	7.2	517	2.19
UR10_RIQ_C	1	0 - 5 mm	59	59	59	59	236	98.75	10.4	527.4	2.23
UR10_AGO_CR	1	0 - 5 mm	59	59	59	59	236	98.75	3.8	500.2	2.12

Table 5.12: Robotic system performance during the MRMT displacement test variant. Probability of success (PS) calculated for a 95% confidence level.

Robotic System	Placement Zone	Accuracy Range	Successful Placements					Probability of Success (%)	Initialisation Time (s)	Completion Time (s)	
			Run 1	Run 2	Run 3	Run 4	Combined			CT_{Total}	$CT_{Per\ Block}$
UR10_KGG_T	1	0 - 1 mm	24	26	35	31	116	43.6	450	677.2	2.87
	2	0 - 3 mm	59	59	59	59	236	98.8			
UR10_RIQ_T	1	0 - 1 mm	56	55	53	55	219	89.2	241	680.3	2.88
	2	0 - 3 mm	59	59	59	59	236	98.8			
BAX_VAC_T	1	0 - 1 mm	6	4	2	10	22	6.3	141	2954	12.52
	2	0 - 3 mm	25	26	24	26	101	37.3			
	3	0 - 5 mm	42	42	40	41	165	64.6			
	4	0 - 7 mm	53	54	50	49	206	83.1			
	5	0 - 9 mm	58	58	56	55	227	93.4			
	6	0 - 19 mm	59	59	59	59	236	98.8			
UR10_KGG_C	1	0 - 1 mm	10	6	4	4	24	7.1	9	675.9	2.86
	2	0 - 3 mm	53	52	57	53	215	87.4			
	3	0 - 5 mm	59	59	59	59	236	98.8			
UR10_RIQ_C	1	0 - 1 mm	40	38	40	38	156	60.6	9.5	705.8	2.99
	2	0 - 3 mm	59	59	59	59	236	98.8			
UR10_RIQ_CR	1	0 - 1 mm	5	11	14	8	38	12.2	8.2	776.8	3.29
	2	0 - 3 mm	42	45	50	58	195	78.0			
	3	0 - 5 mm	59	59	59	59	236	98.8			
UR10_RIQ_CR (Rotated)	1	0 - 1 mm	12	13	12	14	51	17.2	6.6	774.2	3.28
	2	0 - 3 mm	34	34	35	36	139	53.3			
	3	0 - 5 mm	48	48	48	48	192	76.6			
	4	0 - 7 mm	57	57	57	59	230	95.0			
	5	0 - 9 mm	59	59	59	59	236	98.8			
UR10_AGO_CR	1	0 - 1 mm	4	4	6	7	21	6.0	4.65	675.6	2.86
	2	0 - 3 mm	27	29	33	27	116	43.6			
	3	0 - 5 mm	47	48	52	48	195	78.0			
	4	0 - 7 mm	57	59	58	59	233	96.7			
	5	0 - 9 mm	59	59	59	59	236	98.8			

The initialisation time of the UR10_KGG_T system during the original test and its variant was 570 s and 450 s. These times are larger than the initialisation times of the UR10_RIQ_T (294 s and 241 s respectively), which seems unusual since both systems use the same robotic manipulator. However, the two robotic systems were initialised by different researchers, which was intentionally done to highlight the initialisation time's dependence on the adopted teaching approach and the attentiveness of the programmer. Regardless of the programmer, the two systems differ from the BAX_VAC_T system in that they required less time to initialise during the MRMT displacement test variant. The reason for this that the target positions

(a) Original MRMT Displacement Test   (b) MRMT Displacement Test Variant
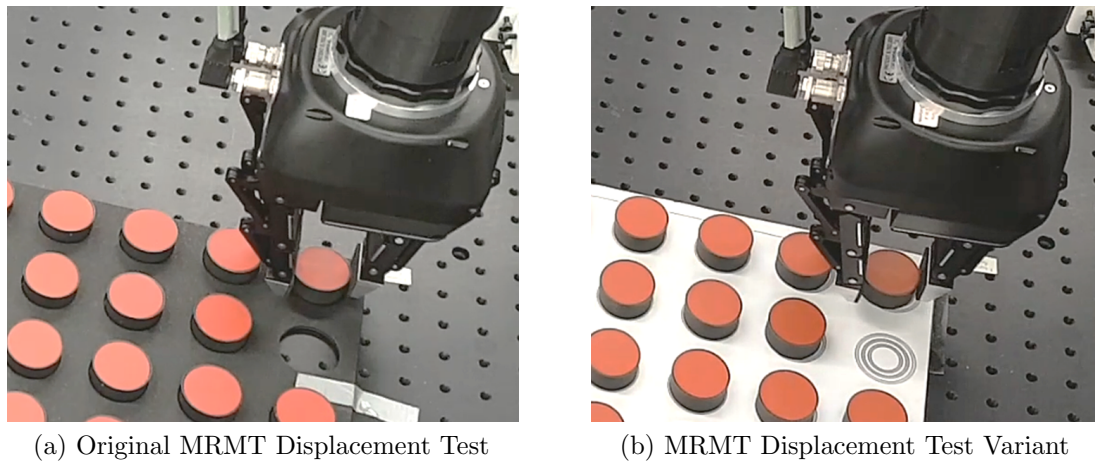
Figure 5.7: The teaching of corner positions when using the UR10 robotic manipulator takes less time during the MRMT displacement test variant as it's easier to determine when the robot is aligned with the printed concentric circles.

are recorded with greater accuracy, and the printed concentric circles provide a better visual guide during alignment than the hole (see Figure 5.7).

Regardless of teaching time being considered, there is a significant reduction in initialisation time when using the Cognex system or the Cognex + registration system. For both initialisation approaches, a camera is used to detect the block locations. This detection time determines the robot's initialisation time, as the camera is mounted within the environment and is already calibrated to the required coordinate system. While actual detection by the vision system could occur in under $50\,ms$, the initialisation time of the robotic system varied between $4.65\,s$ and $10.4\,s$ as time was allotted to ensure the vision system was running correctly and a reliable connection had been established. The larger initialisation times occurred when the robotic arm had to be moved out the camera's field of view before detection could occur.

The recorded initialisation times help to identify the increased flexibility that a vision system provides. Looking at initialisation times of the UR10 manipulator, the use of a vision system reduces the robot's initialisation time by at least 96%. This significant reduction in initialisation time is highly desirable within flexible manufacturing processes, as the changing environment will require robots to be reprogrammed more frequently.

143

5.3.2.2 Recorded Probability of Success

A PS value was calculated based on the number of successful transfers achieved by each robotic system. Similar to the handling scenario, this PS was calculated from Equation 2.10 with a 0.95 confidence level. However, since the complete MRMT displacement test involves 236 pick-and-place iterations, the maximum PS which can be determined for the given confidence level is 98.75%.

For the original MRMT displacement test, the PS corresponded to the probability of a successful block transfer to a hole in the board. However, based on observations, additional placement zones could be defined for the less accurate systems. These zones were defined based on the blocks position relative to the hole, as shown in Figure 5.8. For the MRMT displacement test variant, the PS was calculated for each placement zone. These zones allowed the placement accuracy to be recorded with greater resolution, which provided a greater insight into the performance of the different robotic systems.

Looking at the recorded PS values in Table 5.11, the results of the original MRMT test provide little insight into the placement accuracy of the different robotic systems. Since the pick-and-place operation tended to be successful if the block was placed within $5mm$ of the hole, the majority of robotic systems could perform the test without any failures. The one exception is the BAX_VAC_T system, whose low repeatability and compliant actuation resulted in larger placement errors. Accordingly, the original MRMT displacement test may be useful for comparing the performance of robotic
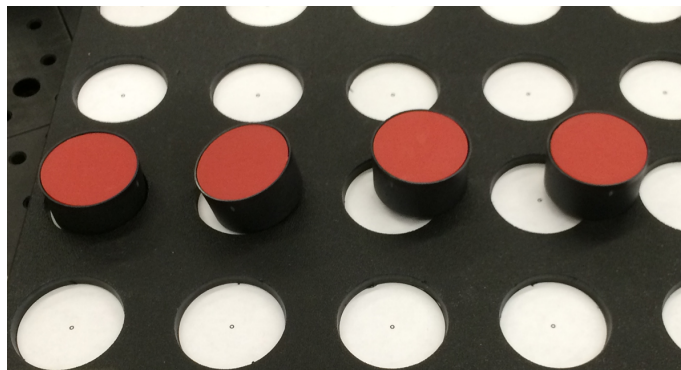
Figure 5.8: Placement accuracy zones which can be defined for the original MRMT displacement test based on the block's position relative to the target hole.

systems with low repeatability, but in the majority of cases is only useful for CT comparisons.

From Table 5.12, the MRMT displacement test variant is able to differentiate between the placement accuracy of the different robotic systems. From the recorded PS values, the UR10_KGG_T, UR10_RIQ_T, and UR10_RIQ_C systems were all able to achieve a placement accuracy of less than $3\,mm$. It is unsurprising that the teach programming approach produced the most accurate placements, as their positional errors should be minimal. In fact, it was expected that these systems would be able to achieve a higher placement accuracy, but it was noticed that the blocks momentarily stuck to the gripper's fingers during some release attempts. In addition, the flat targets did not prevent block movement as the blocks were released by the gripper.

Comparing the robotic system's PS for each initialisation approach, it can be seen that UR10_RIQ system had a higher probability for more accurate placements. This can be accounted for by the gripper's flat fingers, which allowed the robotic system to absorb positional errors that were parallel to the gripper's fingers (see Figure 5.9). Therefore, aligning the Robotiq gripper with the direction of maximum error could improve the robotic system's placement accuracy. This is highlighted by the recorded PS values for the UR10_RIQ_CR system, which performed the MRMT test twice using gripper orientations that differed by 90 degrees. When rotated, the placement accuracy of the UR10_RIQ_CR system decreased, and became more dependent on the block's location relative to the registration target seats. This is illustrated in Figure 5.10, which shows the placement zones achieved by the two systems during a single run.
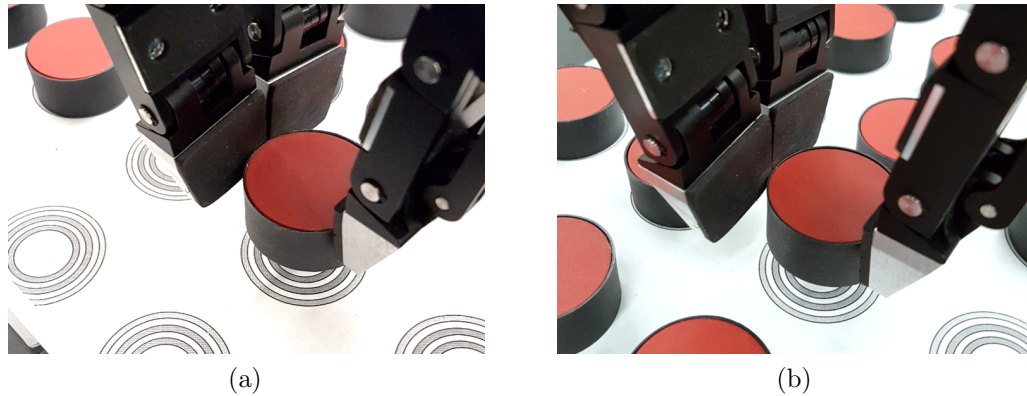
Figure 5.9: Ability of the Robotiq gripper to absorb errors when aligned parallel to the direction of maximum error. As shown in (b), the cylindrical block can be grasped off centre which means that errors in this direction are negated during placement.
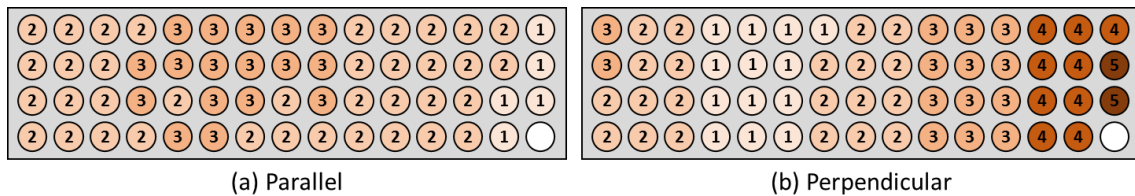
Figure 5.10: Comparison between the recorded placement zones of the UR10_RIQ_-CR during a single run when the Robotiq gripper is aligned (a) parallel and (b) perpendicular to the direction of maximum error.

5.3.2.3   Recorded Completion Time

The recorded CT_{Total} presented in Tables 5.11 and 5.12 correspond to the time required by each robotic system to perform the four runs of the complete MRMT displacement test. This overall time was recorded as it facilitates direct comparisons with established human norm tables that have been developed for the original MRMT displacement test. In addition, the sample mean, $CT_{Per\ Block}$, was calculated by dividing CT_{Total} by the total number of iterations (236). The sample mean is presented instead of the true mean range, as the high number of iterations and low variability generated margin of errors of less than $0.001\ s$. The $CT_{Per\ Block}$ is a useful representation of a robotic system's performance, and will be used in Section 5.3.3. From the tabulated data, the original MRMT displacement test required less time to complete than the MRMT displacement test variant as the latter required the block to be placed on the paper target. This placement introduced two additional

waypoints and motions per pick-and-place operation, which increased the robotic system's execution time and communication delay.

The BAX_VAC_T system takes at least 3.8 times longer than the other robotic systems tested, requiring a CT of 2141 s for the original MRMT displacement test and a CT of 2954 s for the MRMT displacement test variant. This large CT is a consequence of the Baxter's compliant actuation and low repeatability which meant that the robotic arm required time to settle at each waypoint. In addition, these attributes of the robot arm meant that multiple grasping attempts were sometimes required when the vacuum gripper did not align with the surface of the block.

The CT of the UR10_KGG and UR10_RIQ systems was relatively consistent across the different initialisation approaches, as these approaches did not have a significant impact on the execution program. The one exception was the UR10_RIQ_CR system, which required the gripper's gap to be increased to accommodate the larger uncertainty when using the Cognex + registration initialisation approach. To note, since the gripper gap of the UR10_KGG system was fixed, it was unable to complete the MRMT displacement test when using the Cognex + registration initialisation approach.

Of the robotic systems, the UR10_AGO_CR system performed both tests with the lowest CT, achieving a CT of 500.2 s for the original test and 675.6 s for the test variant. This system utilised force-torque transducers that were mounted at the fingertips of the Allegro hand to detect when its fingers made contact with the cylindrical block. Using a nominal sensing and control rate of 333 Hz, this system could therefore perform efficient grasps that did not waste time exerting unnecessary forces on the block.

5.3.2.4   Experimental Summary

Combining the initialisation times, PS, and CT values recorded during the MRMT displacement test variant gives an interesting insight into the performance of each robotic system. While the BAX_VAC_T system can be initialised faster than the other taught robotic systems, its poor PS and CT values suggest that it is not well suited to the chosen scenario. The UR10_KGG_T and UR10_RIQ_T systems have a relatively good CT and a high PS for the smaller accuracy ranges, but their large initialisation time would only make them a viable option in high-volume, low-variability scenarios.

Of the remaining systems, those which use the Cognex initialisation approach tend to operate at a higher CT and PS for a given accuracy zone, which makes these systems a better choice for flexible manufacturing environments in which the robotic manipulator can be fixed. The UR10_RIQ_CR and the UR10_AGO_CR systems have a lower PS of achieving an accurate placement, but this drop in accuracy may be acceptable for the increased flexibility that the Cognex + registration system provides. In addition, the UR10_AGO_CR has the lowest CT, which makes it a particularly attractive choice for pick-and-place operations within flexible manufacturing processes as the Allegro hand has the potential to perform a wider range of B-D operations thanks to its force-based control and in-hand manipulation capabilities.

5.3.3 Pick-and-Place Scenario Discussion

5.3.3.1 Computational vs. Experimental Results

The estimated and actual performance of each robotic system can be compared in order to consider the strength of the developed assessment framework. Accordingly, the estimated and recorded PS and CT values for each MRMT test and robotic system have been summarised in Table 5.13.

Looking at the PS values of the original MRMT test, it can be seen that the estimated and actual values are as expected. The robotic systems performed the test without any failures, which for 236 pick-and-place iterations corresponds to PS of at least 98.75% for the 0.95 confidence level.

For the MRMT variant, the estimated PS values became less accurate, particularly for the smaller placement zones. One reason for this is the unexpected performance of the robotic systems during the MRMT variant test, which can be identified by the poor performance of the robotic systems that were initialised using teach programming. These robotic systems should be capable of achieving placement accuracies close to $0.01\,mm$, but during the MRMT variant the systems were only able to place the blocks within $3\,mm$ of the target. As noted in the previous section,

Table 5.13: Comparison between the estimated and recorded PS and CT of each robotic system during the original MRMT and the MRMT variant.

Robotic System	Placement Zone	Accuracy Range	Probability of Success (%)			CT_{Total} (s)			$CT_{Per\,Block}$ (s)		
			Estimated	Actual	Difference	Estimated	Actual	Difference	Estimated	Actual	Difference
MRMT Original											
UR10_KGG_T	1	0 - 5 mm	100.00	98.75	1.25	531.26	516.00	15.26	2.25	2.19	0.06
UR10_KGG_C	1	0 - 5 mm	100.00	98.75	1.25	531.26	517.00	14.26	2.25	2.19	0.06
UR10_RIQ_T	1	0 - 5 mm	100.00	98.75	1.25	554.48	530.30	24.18	2.35	2.25	0.10
UR10_RIQ_C	1	0 - 5 mm	100.00	98.75	1.25	554.48	527.40	27.08	2.35	2.23	0.11
MRMT Variant											
UR10_KGG_T	1	0 - 1 mm	100.00	43.60	56.40	687.75	677.20	10.55	2.91	2.87	0.04
	2	0 - 3 mm	100.00	98.75	1.25						
UR10_KGG_C	1	0 - 1 mm	70.78	7.10	63.68	687.75	675.90	11.85	2.91	2.86	0.05
	2	0 - 3 mm	99.87	87.40	12.47						
	3	0 - 5 mm	100.00	98.75	1.25						
UR10_RIQ_T	1	0 - 1 mm	100.00	89.20	10.80	710.97	680.30	30.67	3.01	2.88	0.13
	2	0 - 3 mm	100.00	98.75	1.25						
UR10_RIQ_C	1	0 - 1 mm	70.78	60.60	10.18	736.69	705.80	30.89	3.12	2.99	0.13
	2	0 - 3 mm	99.87	98.75	1.12						
UR10_RIQ_CR	1	0 - 1 mm	2.63	12.20	-9.57	762.42	776.80	-14.38	3.23	3.29	-0.06
	2	0 - 3 mm	27.47	78.00	-50.53						
	3	0 - 5 mm	76.78	98.75	-21.97						
UR10_RIQ_CR (Rotated)	1	0 - 1 mm	2.63	17.20	-14.57	762.42	774.20	-11.78	3.23	3.28	-0.05
	2	0 - 3 mm	27.47	53.30	-25.83						
	3	0 - 5 mm	76.78	76.60	0.18						
	4	0 - 7 mm	98.04	95.00	3.04						
	5	0 - 9 mm	99.97	98.75	1.22						

this decrease in placement accuracy can be accounted for by the tendency of the block to stick to the gripper's fingers upon release and by the flat targets which allowed the block to move.

The positional errors from the Cognex and the Cognex + registration systems are estimated within the framework using a normal distribution. The actual errors are dependent on a number of factors, such as the relative locations of the equipment and the calibration of the systems, but a normal distribution was selected as it provides a simple means for estimating general performance without requiring specific setup information. However, as these normal distributions were generated based on the system's average performance within its workspace, the positional errors are acknowledged to be approximate.

As discussed in Section 5.3.2, the higher PS achieved by the UR10_RIQ system when compared UR10_KGG system can be accounted for by the Robotiq's ability to absorb positional errors thanks to its flat fingers. When testing with the UR10_RIQ_C and UR10_RIQ_CR system, the gripper was orientated so that its fingers were parallel to the direction of maximum error. This removed the effect of this error, which explains why the recorded PS values of the UR10_RIQ_C and UR10_RIQ_CR are higher than the estimated performance. However, this favourable orientation of the gripper is not guaranteed, which is why testing was also performed with the gripper rotated by 90 degrees. In this case, the UR10_RIQ_CR performs similar to the expected performance, but still achieves higher PS values thanks to its absorption of the positional errors in the other direction.

Looking at the estimated and recorded CT values, it can be seen that the structured framework provides an accurate estimate of each pick-and-place operation. This was expected, as the pick-and-place operation within the original MRMT and its variant are similar to the handling scenario considered in the previous section. The developed framework allows for a more accurate estimate of the robotic systems performance than possible using supplier specifications. If using the latter, the robot's optimal performance would have to be assumed which for the UR10_KGG system would give a $CT_{Per\ Block}$ of $0.4\,s$ for the original MRMT and $0.44\,s$ for the MRMT variant (making the same assumptions as before). Using the developed

performance metrics, the framework estimates a $CT_{Per\ Block}$ that are within $0.13\,s$ (4.5%) of the recorded CT. However, since the same operation is repeated 236 times, the estimation errors accumulate to $30.89\,s$ (4.5%) for CT_{Total}. This accumulation of estimation errors during repetitive tasks is unfavourable but is a consequence of any estimation method. The developed framework ensures that this effect is minimised by providing an accurate estimate for each pick-and-place operation, which illustrates its benefit over current estimation approaches.

5.3.3.2   Boothroyd - Dewhurst Comparison

Since the original MRMT displacement test allows the block to be dropped into the hole, each pick-and-place operation can be classified as a B-D handling operation with handling code '00'. However, for the MRMT displacement test variant, the block must be carefully placed within the concentric circles and so each pick-and-place operation must also include a B-D insertion operation with insertion code '00'. From the B-D handling and insertion tables shown previously in Figures 2.10 and 2.12, each pick-and-place operation within the original MRMT displacement test and the MRMT displacement test variant can be estimated to take a human $1.13\,s$ and $2.63\,s$ to complete on average. This corresponds to an overall CT of $266.68\,s$ for the original MRMT displacement test, and an overall CT of $620.68\,s$ for the MRMT displacement test variant.

For the original MRMT displacement test, this B-D estimated human CT can be compared to the MRMT's established human norm tables. From these tables, the 50th percentile four-test completion time for human subjects is $189\,s$. The B-D tables estimated a CT of $266.68\,s$, which is just outside the human range presented within these norm tables. In this case, the B-D tables overestimate the time required to perform each pick-and-place operation because of the operation's short alignment and transfer distance. While this overestimation is only $0.33\,s$ per operation, the same operation is repeated 236 times and so the errors amalgamate to give a total error of $77.68\,s$. This highlights a potential drawback of the B-D tables when considering repetitive tasks, but may not be an issue within assemblies that require a range of operations as the B-D tables have an equal chance of overestimating and

underestimating performance. Regardless, the primary reason for using the B-D tables is their ability to easily estimate a human's performance in any manufacturing scenario. Since this requires generalisations to be made, the difference between the B-D estimated time and the actual human range corresponding to this test is acceptable.

Using the developed framework, the estimated CT of each robotic system can be compared to the human estimated CT in order to determine the most suitable choice for the given scenario. For the original MRMT displacement test, an average human operator is estimated to complete the task in 266.68 s, which is 50% lower than the estimated CT of the UR10_KGG systems (531.26s) and 52% lower than the estimated CT of the UR10_RIQ systems (554.48 s). This time difference is significant, but can be overcome by robotic systems thanks to their ability to operate continuously. Accordingly, the robotic systems that were considered in this scenario may be a viable option, depending on other cost metrics such as initialisation, production volume, etc.

For the MRMT displacement test variant, the difference between human and robotic performance is much less, as a human operator requires more time to accurately place the blocks. The estimated human completion time is 620.68 s, which is only 10% lower than the estimated CT of the UR10_KGG systems (687.75 s) and 13% to 19% lower than estimated CT of the UR10_RIQ systems (710.97 to 762.42 s). In this scenario, one of the robotic systems is likely the best choice. As discussed in the preceding section, the most suitable robotic system is dependent on the required placement accuracy and the manufacturing environment. However, assuming the task is to be performed as part of a flexible manufacturing process, the UR10_RIQ_C or UR10_AGO_CR would be the best robotic systems of those considered.

5.4   Insertion Scenario

Based on the test setup described in Section 4.6, estimated and actual performance of the different robotic systems was determined. To record actual performance, the test was setup in the laboratory as shown in Figure 5.11.

5.4.1   Computational Results

5.4.1.1   Estimated Probability of Success

In this scenario, the robotic systems are able to overcome misalignment during a peg insertion attempt by performing one of the search strategies discussed in Chapter 4. These strategies ensure a successful insertion provided the hole is located within the designated search region and sufficient time is allocated for the search.

For the first test, which compares the performance of the different search strategies, the size of the search region can be defined based on the simulated perception error. As the perception error follows a bivariate normal distribution with zero mean, the radius of the search region, is set to 4σ, where σ is the standard deviation of the perception error being tested. By letting the robotic system search until the hole is found, this search region ensure a PS of 99.97% [160]. While a larger area could have been defined to increase the PS, it would negatively impact the system's CT as the hole would occupy a smaller proportion of the search region.

For the second test, which compares the performance of the different initialisation

(a)   (b)
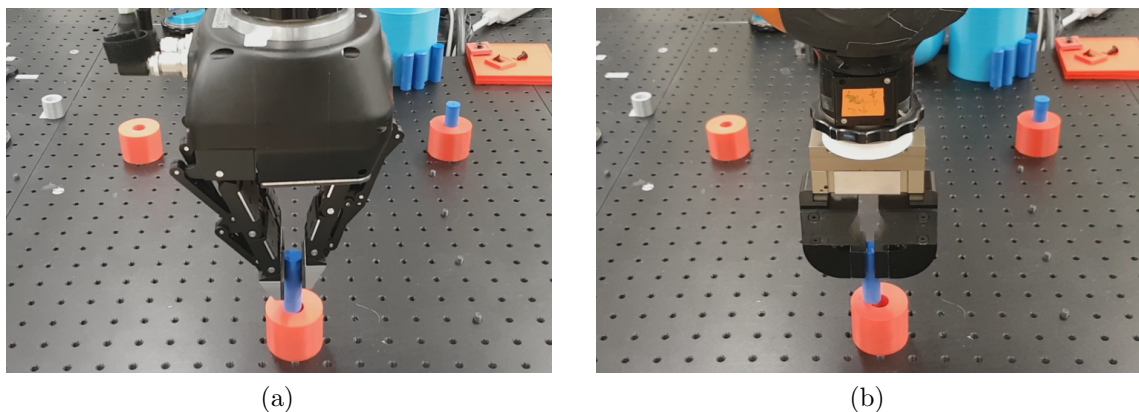
Figure 5.11: Actual testing of the insertion scenario using (a) the LWR4_RIQ system and (b) the LWR4_KGG system.

approaches, the size of the search region can be defined based on the accuracy of the initialisation approach. Since the positional errors which arise from these initialisation approaches tend to have low variability but constant bias, an area that contains the bidirectional accuracy of the initialisation approach is adequate. Setting this search region area and again allowing the robotic system to search until the hole is found generates an estimated PS of 100% for these tests.

5.4.1.2   Estimated Completion Time

As noted, this scenario involves a B-D handling operation with code '00' and an insertion operation with code '00' when using the chamfered peg and '01' when using the non-chamfered peg. Accordingly, the robotic system's CT can be estimated by considering its performance during both operations.

Handling Operation   Similar to the previous scenario, the time required to complete the handling operation can be estimated by breaking the operation into the relevant assembly actions and summing the time required for each relevant assembly action:

$$CT_{Handling} = CT_{Align} + CT_{Pickup} + CT_{Transport} + CT_{Coordinate} \qquad (5.3)$$

As before, the grasp cycle time, trajectory time, and communication delay metrics can be used to estimate the CT of each action. To reduce repetition the calculation of these times is omitted, but the resulting CT are given in Table 5.14. To note, in this scenario the alignment distance (d_a) and transport distance (d_t) both equal $300\,mm$, while the clearance distance d_c is equal to $35\,mm$ in order to account for insertion and retraction of the peg.

Insertion Operation   Similar to the handling operation, the time required to complete the insertion operation can be estimated by breaking the operation into its assembly actions and estimating the robot's performance during each action. For this scenario, the insertion time can be estimated as follows:

$$CT_{Insertion} = CT_{Detect} + CT_{Reposition} + CT_{Place} + CT_{Retract} + CT_{Coordinate} \qquad (5.4)$$

The insert action corresponds to the actual act of inserting the peg, and is estimated by considering the insertion trajectory time and the cycle time of the end effector. The cycle time of the KGG gripper is $0.3\ s$, but the cycle time of the Robotiq 3-Fingered gripper is dependent on the chosen opening / closing gap. This gap was set to $25\ mm$, which corresponds to a cycle time of $0.272\ s$. This generates the following insert times:

$$CT_{Place,KGG} = (0.0756(d_c)^{0.5} + 0.12) + (t_{cycle}/2) = 0.567 + 0.15 = 0.72\ s$$

$$CT_{Place,RIQ} = (0.0756(d_c)^{0.5} + 0.12) + \frac{0.0109(25)}{2} = 0.567 + 0.137 = 0.7\ s$$

The time to retract can easily be calculated by subbing the retract distance into the trajectory completion time metric derived for the KUKA LWR4. However, in this scenario it was decided that the insertion operation would be complete once the peg was released by the end effector. Accordingly, the retract time is set to zero.

The coordinate CT is calculated using the recorded communication delay between the programming interface and the robot controller. For the KUKA LWR4 robot arm, the average communication delay was calculated to be 0.028 per command. Since only one motion of the arm is executed during the insertion operation, the coordinate CT for the LWR4_KGG systems is 0.028. For the LWR4_RIQ systems this time increases to $0.17\ s$ due to the communication delay between the programming interface and gripper.

For the insertion operation, the detection time corresponds to the time required by the robotic system to detect a successful insertion. This time is a feature of the initialisation approach, and in this scenario it encapsulates the time required for the robot to switch from position to impedance control, determine if its actual position matches the programmed position after an insertion attempt (refer to Figure 4.26), and to return to position control. This time was indirectly determined by considering the testing performed to generate the search time metric, and was approximated as $CT_{Detect} = 0.52\ s$.

The reposition action is required when the peg and hole are misaligned and its

CT corresponds to the robotic system's search time before a successful insertion is detected. The search time of the KUKA LWR4 has been estimated in Section 4.2.3, and its value varies significantly depending on the implemented search strategy, the magnitude of the misalignment, and the peg's chamfer design.

The expected positional error of each robotic system and the graphs in Section 4.2.3 can be used to give an approximate time for each search strategy and peg design. For the first test which uses simulated error σ_1 and σ_2, the expected error can be conservatively estimated to equal two standard deviations, as 86.5% of the actual errors should fall within this band. For the second test, the teach programming approach should not require any searches, as the actual hole positions are taught by hand. For the registration approach, the expected positional error can be estimated by considering the hole's distance from the registration target seats. Since this distance averaged $330\,mm$ for the three holes, Figure 4.7 can be used to give an estimated positional error of $4.0\,mm$. Using this value and the mean Cognex error of $-0.37\,mm$ gives an approximated Cognex + registration positional error of $3.63\,mm$. Using Figure 4.19, the expected positional errors can be used to provide an estimated reposition CT for each system configuration. These CT values and the overall insertion CT are given in Table 5.14 (b).

Table 5.14: Estimated completion times of the different robotic systems during performance of the peg insertion scenario.

(a) Handling Completion Time

Robotic System	CT_{Align} (s)	CT_{Pickup} (s)	$CT_{Transport}$ (s)	$CT_{Coordinate}$ (s)	$CT_{Handling}$ (s)
LWR4_KGG_S					
LWR4_KGG_T					
LWR4_KGG_R	1.43	0.72	2.00	0.11	4.26
LWR4_KGG_CR					
LWR4_RIQ_T					
LWR4_RIQ_R	1.43	0.69	2.00	0.26	4.37
LWR4_RIQ_CR					

(b) Insertion Completion Time

Robotic System	Perception Error (mm)	CT_{Detect} (s)	CT_{Place} (s)	$CT_{Coordinate}$ (s)	Chamfered Peg		Non-Chamfered Peg	
					$CT_{Reposition}$ (s)	$CT_{Insertion}$ (s)	$CT_{Reposition}$ (s)	$CT_{Insertion}$ (s)
Test 1 – Search Strategies								
LWR4_KGG_S$_s$					0.83 ± 0.31	2.1 ± 0.31	11.51 ± 2.06	12.78 ± 2.06
LWR4_KGG_S$_r$	σ_1	0.52	0.72	0.03	0.56 ± 0.23	1.83 ± 0.23	7.64 ± 2.09	8.91 ± 2.09
LWR4_KGG_S$_g$					0.62 ± 0.31	1.89 ± 0.31	2.4 ± 0.58	3.67 ± 0.58
LWR4_KGG_S$_s$					3.84 ± 0.29	5.11 ± 0.29	25.16 ± 1.77	26.43 ± 1.77
LWR4_KGG_S$_r$	σ_2	0.52	0.72	0.03	3.24 ± 1	4.51 ± 1	6.46 ± 1.79	7.73 ± 1.79
LWR4_KGG_S$_g$					2.1 ± 0.44	3.37 ± 0.44	4.36 ± 0.95	5.63 ± 0.95
Test 2 – Initialisation Approaches								
LWR4_KGG_T$_q$	≈ 0.01				0.00	1.27	0.00	1.27
LWR4_KGG_R$_q$	≈ 4.00	0.52	0.72	0.03	2.1 ± 0.44	3.37 ± 0.44	4.36 ± 0.95	5.63 ± 0.95
LWR4_KGG_CR$_q$	≈ 3.63				2.1 ± 0.44	3.37 ± 0.44	4.36 ± 0.95	5.63 ± 0.95
LWR4_RIQ_T$_q$	≈ 0.01				0.00	1.38	0.00	1.38
LWR4_RIQ_R$_q$	≈ 4.00	0.52	0.70	0.17	2.1 ± 0.44	3.48 ± 0.44	4.36 ± 0.95	5.74 ± 0.95
LWR4_RIQ_CR$_q$	≈ 3.63				2.1 ± 0.44	3.48 ± 0.44	4.36 ± 0.95	5.74 ± 0.95

(c) Total Completion Time

Robotic System	Perception Error (mm)	$CT_{Handling}$ (s)	Chamfered Peg		Non-Chamfered Peg	
			$CT_{Insertion}$ (s)	CT_{Total} (s)	$CT_{Insertion}$ (s)	CT_{Total} (s)
Test 1 – Search Strategies						
LWR4_KGG_S$_s$			2.1 ± 0.31	6.35 ± 0.31	12.78 ± 2.06	17.03 ± 2.06
LWR4_KGG_S$_r$	σ_1	4.26	1.83 ± 0.23	6.08 ± 0.23	8.91 ± 2.09	13.16 ± 2.09
LWR4_KGG_S$_g$			1.89 ± 0.31	6.14 ± 0.31	3.67 ± 0.58	7.92 ± 0.58
LWR4_KGG_S$_s$			5.11 ± 0.29	9.36 ± 0.29	26.43 ± 1.77	30.68 ± 1.77
LWR4_KGG_S$_r$	σ_2	4.26	4.51 ± 1	8.76 ± 1	7.73 ± 1.79	11.98 ± 1.79
LWR4_KGG_S$_g$			3.37 ± 0.44	7.62 ± 0.44	5.63 ± 0.95	9.88 ± 0.95
Test 2 – Initialisation Approaches						
LWR4_KGG_T$_q$	≈ 0.01		1.27	5.52	1.27	5.52
LWR4_KGG_R$_q$	≈ 4.00	4.26	3.37 ± 0.44	7.62 ± 0.44	5.63 ± 0.95	9.88 ± 0.95
LWR4_KGG_CR$_q$	≈ 3.63		3.37 ± 0.44	7.62 ± 0.44	5.63 ± 0.95	9.88 ± 0.95
LWR4_RIQ_T$_q$	≈ 0.01		1.38	5.75	1.38	5.75
LWR4_RIQ_R$_q$	≈ 4.00	4.37	3.48 ± 0.44	7.85 ± 0.44	5.74 ± 0.95	10.11 ± 0.95
LWR4_RIQ_CR$_q$	≈ 3.63		3.48 ± 0.44	7.85 ± 0.44	5.74 ± 0.95	10.11 ± 0.95

5.4.2 Experimental Results - Search Strategy

For the first test, the insertion scenario was used to assess the performance of robotic systems using three different search strategies; spiral search (S_s), random search (S_r), quasi-random search (S_q). The insertions were performed at two defined levels of perception error (σ_1 and σ_2), and the numerical results are presented in Table 5.15. In addition, the developed insertion scenario was used to assess the performance of the Allegro robotic hand when using an active force control (S_f) search strategy (see Figure 5.12). This testing was performed by Karl Van Wyk at NIST, and has been included here for comparisons and as an example of the scenario's potential use as a benchmarking tool within robotics research.

5.4.2.1 Recorded Probability of Success

The PS for each robotic system was calculated based on the number of failed insertion attempts. As presented in Table 5.15, each LWR4_KGG_S system successfully inserted both the chamfered and non-chamfered pegs without any failures and so had a PS of 95.3% (based on the number of test iterations and chosen confidence level). The LWR4_AGO_S_f system had either three or four failures during each insertion test, which corresponded to a PS of 85.7% and 83.6% respectively.

Based on its number of failed insertion attempts, the PS values of the LWR4_-
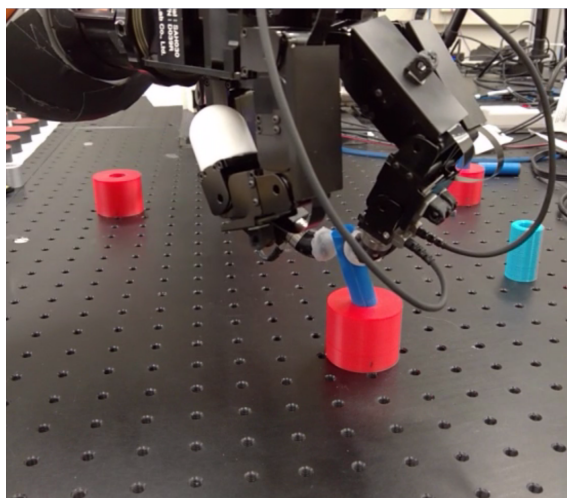
Figure 5.12: Additional testing with the LWR4_AGO_S_f system that used an active force-controlled search strategy to locate the hole and complete a peg insertion.

Table 5.15: Robotic system performance during the insertion scenario with simulated perception error σ_1 and σ_2. Values calculated based on 60 test iterations and for a 0.95 confidence level.

Robot System	Chamfer Design	Probability of Success (%)		Perception Error, σ_1			Perception Error, σ_2		
		σ_1	σ_2	$CT_{Handling}$ (s)	$CT_{Insertion}$ (s)	CT_{Total} (s)	$CT_{Handling}$ (s)	$CT_{Insertion}$ (s)	CT_{Total} (s)
LWR4_KGG_S$_s$		95.3	95.3	4.566 ± 0.005	2.227 ± 0.267	6.793 ± 0.266	4.568 ± 0.006	3.957 ± 0.595	8.525 ± 0.593
LWR4_KGG_S$_r$	Chamfered	95.3	95.3	4.568 ± 0.006	2.152 ± 0.232	6.719 ± 0.231	4.545 ± 0.05	3.529 ± 0.674	8.073 ± 0.681
LWR4_KGG_S$_q$	Peg	95.3	95.3	4.563 ± 0.037	1.452 ± 0.155	6.014 ± 0.161	4.55 ± 0.009	3.191 ± 0.638	7.741 ± 0.639
LWR4_AGO_S$_f$		85.7	83.6	4.719 ± 0.005	10.391 ± 0.965	14.96 ± 0.941	4.718 ± 0.006	19.828 ± 3.376	24.396 ± 3.263
LWR4_KGG_S$_s$		95.3	95.3	4.567 ± 0.005	7.195 ± 0.971	11.762 ± 0.971	4.586 ± 0.053	37.129 ± 5.424	41.715 ± 5.425
LWR4_KGG_S$_r$	Non-Chamfered	95.3	95.3	4.589 ± 0.024	8.008 ± 2.101	12.597 ± 2.098	4.583 ± 0.007	15.617 ± 5.546	20.199 ± 5.547
LWR4_KGG_S$_q$	Peg	95.3	95.3	4.563 ± 0.038	3.115 ± 0.806	7.677 ± 0.811	4.579 ± 0.008	8.203 ± 1.924	12.782 ± 1.924
LWR4_AGO_S$_f$		83.6	85.7	4.72 ± 0.005	11.697 ± 1.789	16.267 ± 1.728	4.719 ± 0.005	18.311 ± 2.884	22.88 ± 2.81

AGO_S$_f$ system were statistically different from all variants of the LWR4_KGG_S system and perception errors. This was determined using the KC test discussed in Section 2.6.3. From the KC test, a system must have 3 or more failures during 60 insertion attempts in order to have statistically different performance when compared to a system that successfully completed all insertions (at the 5% significance level). To note, additional failures or a larger number of test iterations would have to be performed in order to see a significant difference between the LWR4_AGO_S$_f$ and LWR4_KGG_S systems at a higher confidence level.

5.4.2.2   Recorded Completion Time

The completion time (CT) of each robotic system during the different stages of the insertion scenario have been recorded and the results are summarised within Table 5.15. From this table, it can be seen that there is minimal difference between the recorded $CT_{Handling}$ values, as there was no uncertainty during the handling operation and all systems used the same robotic manipulator and handling strategy. Accordingly, the main focus of this section will be on the recorded $CT_{Insertion}$ values. Similar to the approach used in Section 5.2, the CT of the different robotic systems can be compared by using the collected data and the MATLAB code in Appendix C. This code compares the true mean ranges and passes the data sets through the two-sample KS test in order to determine statistical significance. The results are summarised in Table 5.16.

During insertion of the chamfered peg with perception error σ_1, there is a detectable

difference in the true mean ranges for the majority of robotic systems. The exception is the LWR4_KGG_S$_s$ and LWR4_KGG_S$_r$ systems, whose sample means are sufficiently close to cause their true mean intervals to overlap. This is validated by the results of the KS test, which accepts the null hypothesis (H_0) when comparing the two data sets (where H_0 states that the two data sets belong to the same population). From the magnitude of the detectable differences, it can be noted that the LWR4_KGG_S$_s$, LWR4_KGG_S$_r$ and LWR4_KGG_S$_q$ systems perform the peg insertion in a similar CT, but that the quasi-random search strategy outperforms the spiral and random search strategy by at least $0.35\,s$ and $0.31\,s$ respectively. The LWR4_AGO_S$_f$ system requires the longest insertion time, with a mean CT that is at least $7.82\,s$ longer than the LWR4_KGG_S$_q$ system.

For the chamfered peg and perception error σ_2, the KS test identifies that the distribution of each system's performance data was statistically different. These preliminary indicators suggest that there is an increased chance of detecting a difference in sample means or variances (though this is not guaranteed). Looking at the true mean ranges, there is only a detectable difference between the LWR4_AGO_-S$_f$ system and the other LWR4_KGG_S systems. This detectable difference is large, ranging between $11.9\,s$ and $12.62\,s$ depending on the chosen LWR4_KGG_S system. There is no detectable difference between mean CT of the remaining systems, which can be accredited to the proximity of their sample means combined with the larger margin of error (and variance) due to the higher uncertainty.

Looking at the non-chamfered insertions with perception errors σ_1, the KS test again identifies statistically significant differences between all data distributions. Considering the true mean ranges, the LWR4_KGG_S$_q$ system had a detectably lower CT compared to the other robotic systems. This also occurred when analysing the chamfered peg results (for the same perception error), but the magnitude of the difference is larger in this instance due to additional insertion difficulty. With the non-chamfered peg, the quasi-random search strategy outperforms the spiral and random search strategy by at least $2.30\,s$ and $1.99\,s$ respectively. The LWR4_AGO_-S$_f$ system performs comparatively better for the chamfered peg, and there is no detectable difference between its true mean range and the true mean range of the

Table 5.16: Comparison of the different search strategies when inserting the (a) chamfered and (b) non-chamfered peg. A positive detectable difference (in seconds) between the system's true mean completion times differ by at least that value. Rejection (1) of the null hypothesis (H_0) suggests that the data sets do not belong to the same population at the 5% significance level.

(a) Chamfered Peg

Detectable Difference		Perception Error, σ_1 (s)				Perception Error, σ_2 (s)			
		LWR4_KGG_S$_s$	LWR4_KGG_S$_r$	LWR4_KGG_S$_q$	LWR4_AGO_S$_f$	LWR4_KGG_S$_s$	LWR4_KGG_S$_r$	LWR4_KGG_S$_q$	LWR4_AGO_S$_f$
Perception Error σ_1	LWR4_KGG_S$_s$		-0.42	0.35	6.93	0.87	0.36	0.06	13.96
	LWR4_KGG_S$_r$	-0.42		0.31	7.04	0.98	0.47	0.17	14.07
	LWR4_KGG_S$_q$	0.35	0.31		7.82	1.76	1.25	0.95	14.84
	LWR4_AGO_S$_f$	6.93	7.04	7.82		4.87	5.22	5.60	5.09
Perception Error σ_2	LWR4_KGG_S$_s$	0.87	0.98	1.76	4.87		-0.84	-0.47	11.90
	LWR4_KGG_S$_r$	0.36	0.47	1.25	5.22	-0.84		-0.97	12.25
	LWR4_KGG_S$_q$	0.06	0.17	0.95	5.60	-0.47	-0.97		12.62
	LWR4_AGO_S$_f$	13.96	14.07	14.84	5.09	11.90	12.25	12.62	

KS Test		Perception Error, σ_1 (s)				Perception Error, σ_2 (s)			
		LWR4_KGG_S$_s$	LWR4_KGG_S$_r$	LWR4_KGG_S$_q$	LWR4_AGO_S$_f$	LWR4_KGG_S$_s$	LWR4_KGG_S$_r$	LWR4_KGG_S$_q$	LWR4_AGO_S$_f$
Perception Error σ_1	LWR4_KGG_S$_s$		0	1	1	1	1	1	1
	LWR4_KGG_S$_r$	0		1	1	1	1	1	1
	LWR4_KGG_S$_q$	1	1		1	1	1	1	1
	LWR4_AGO_S$_f$	1	1	1		1	1	1	1
Perception Error σ_2	LWR4_KGG_S$_s$	1	1	1	1		1	1	1
	LWR4_KGG_S$_r$	1	1	1	1	1		1	1
	LWR4_KGG_S$_q$	1	1	1	1	1	1		1
	LWR4_AGO_S$_f$	1	1	1	1	1	1	1	

(b) Non-Chamfered Peg

Detectable Difference		Perception Error, σ_1 (s)				Perception Error, σ_2 (s)			
		LWR4_KGG_S$_s$	LWR4_KGG_S$_r$	LWR4_KGG_S$_q$	LWR4_AGO_S$_f$	LWR4_KGG_S$_s$	LWR4_KGG_S$_r$	LWR4_KGG_S$_q$	LWR4_AGO_S$_f$
Perception Error σ_1	LWR4_KGG_S$_s$		-2.26	2.30	1.74	23.54	1.90	-1.89	7.26
	LWR4_KGG_S$_r$	-2.26		1.99	-0.20	21.60	-0.04	-3.83	5.32
	LWR4_KGG_S$_q$	2.30	1.99		5.99	27.78	6.15	2.36	11.51
	LWR4_AGO_S$_f$	1.74	-0.20	5.99		18.22	-3.42	-0.22	1.94
Perception Error σ_2	LWR4_KGG_S$_s$	23.54	21.60	27.78	18.22		10.54	21.58	10.51
	LWR4_KGG_S$_r$	1.90	-0.04	6.15	-3.42	10.54		-0.06	-5.74
	LWR4_KGG_S$_q$	-1.89	-3.83	2.36	-0.22	21.58	-0.06		5.30
	LWR4_AGO_S$_f$	7.26	5.32	11.51	1.94	10.51	-5.74	5.30	

KS Test		Perception Error, σ_1 (s)				Perception Error, σ_2 (s)			
		LWR4_KGG_S$_s$	LWR4_KGG_S$_r$	LWR4_KGG_S$_q$	LWR4_AGO_S$_f$	LWR4_KGG_S$_s$	LWR4_KGG_S$_r$	LWR4_KGG_S$_q$	LWR4_AGO_S$_f$
Perception Error σ_1	LWR4_KGG_S$_s$		1	1	1	1	1	1	1
	LWR4_KGG_S$_r$	1		1	1	1	1	1	1
	LWR4_KGG_S$_q$	1	1		1	1	1	1	1
	LWR4_AGO_S$_f$	1	1	1		1	1	1	1
Perception Error σ_2	LWR4_KGG_S$_s$	1	1	1	1		1	1	1
	LWR4_KGG_S$_r$	1	1	1	1	1		0	1
	LWR4_KGG_S$_q$	1	1	1	1	1	0		1
	LWR4_AGO_S$_f$	1	1	1	1	1	1	1	

LWR4_KGG_S$_r$ system. However, the LWR4_AGO_S$_f$ still requires at least 5.99 s longer to perform the insertion than the LWR4_KGG_S$_q$ system.

For the non-chamfered peg with perception error σ_2, the KS test identifies statistically significant differences in the majority of data distributions. The exception is the LWR4_KGG_S$_r$ and LWR4_KGG_S$_q$ systems for perception error σ_2. This outcome suggests that the two data sets belong to the same population, which may be surprising considering the apparent difference in their sample mean and variance. However, this outcome is supported by the lack of a detectable difference between the two system's true mean ranges. In addition to these two systems, the comparison

of the true mean ranges shows that there is no detectable difference between the CT of the LWR4_KGG_S$_r$ and the LWR4_AGO_S$_f$ systems. This can again be accounted for by the larger margin of error (and variance) caused by the higher perception error and the non-chamfered peg.

Looking at the robotic system's sensitivity to perception error can provide an insight into the robotic system's robustness. From the KS test, there is a statistically significant difference between the performance data of all systems. For the chamfered peg, the mean CT of each system increases sufficiently between perception error σ_1 and σ_2 for a detectable difference to be observed. This difference is most notable for the LWR4_AGO_S$_f$ system, whose mean CT increases by at least $5.09\,s$ between perception error σ_1 and σ_2. The remaining systems have a relatively small detectable difference of less than $1.00\,s$. This indicates that their search strategies were less sensitive to perception error when using the chamfered-peg.

For the non-chamfered peg, there is no detectable difference between the mean CT of the LWR4_KGG_S$_r$ system between perception error σ_1 and σ_2. This can be accounted for by the random nature of the search strategy, which caused a large variance in performance which consequently increased the interval of the true mean range. The non-chamfered peg amplified this effect, as it became less likely that the peg would find the hole during each generated search path. Contrary to the chamfered peg results, the LWR4_AGO_S$_f$ system is least sensitive to perception error when inserting the non-chamfered peg with a minimum detectable mean CT difference of $1.94\,s$. This suggests that the search strategy employed by the LWR4_AGO_S$_f$ system is better suited for the insertion of non-chamfered pegs. A particularly notable observation from the mean CT differences is the $23.54\,s$ increase in the LWR4_KGG_S$_s$ system's insertion time between perception error σ_1 and σ_2. This is a consequence of the implemented spiral search strategy, which defined the distance between successive turnings based on the insertion clearance and chamfer design in order to ensure the hole was found. For the non-chamfered peg, this distance was much smaller which meant that the search strategy took much longer to transverse the larger offsets generated by perception error σ_2.

5.4.2.3   Experimental Summary

The performance of the different search strategies has been compared by considering their PS and CT. From this comparison, the LWR4_AGO_S$_f$ system was noted to have a detectably lower PS which would likely make it an unsuitable choice for the given scenario. The remaining systems perform each insertion test without failure, which from the number of test iterations indicates a minimum PS of 95.3% for the 0.95 confidence level. However, from CT comparisons, the LWR4_KGG_S$_q$ is best suited for the given scenario as the quasi-random search strategy is shown to statistically outperform the other insertion strategies. The robotic system has the lowest mean CT and margin of error in all tests, which indicates the search strategy's suitability regardless of peg chamfer design and perception error.

However the comparable performance of the LWR4_AGO_S$_f$ system and its low sensitivity to perception error is promising as the system offers greater reconfigurability and force feedback control which may make it beneficial in other scenarios. For example, LWR4_AGO_S$_f$ system emitted less than $0.5\,N$ of force between the peg and hole at all times during the insertion operation. This reduced wear-and-tear, as illustrated by Figure 5.13 which compares the condition of the pegs after the completion of all testing. Accordingly, robotic systems that perform similarly to LWR4_AGO_S$_f$ are likely to be more attractive for those applications that require the regulation of operation forces or the preservation of surface finishes. Furthermore,
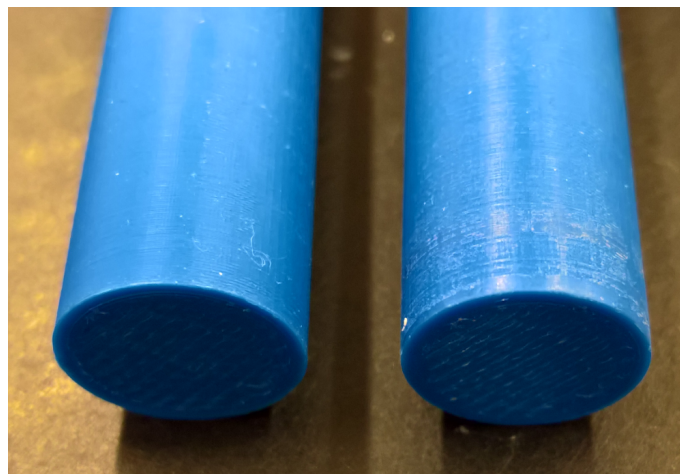
Figure 5.13: The surface condition of a peg after testing over a period with the LWR4_AGO_S$_f$ system (left) and the LWR4_KGG_S systems (right).

the LWR4_AGO_S$_f$ system includes the multi-fingered Allegro hand, which allows the system to adapt more easily to the range of B-D operations that may be encountered during flexible manufacturing processes.

5.4.3 Experimental Results - Initialisation Approach

For the second test, the insertion scenario was used to assess the performance of robotic systems using three different initialisation approaches; teach programming (T), registration (R), and Cognex + registration (CR). Based on the experimental results from the first test, each robotic system used the quasi-random search strategy when misalignment occurred during insertion. As this test was considering different initialisation approaches, the time required to initialise each system was recorded in addition to PS and CT. The resulting experimental results are presented in Table 5.17.

5.4.3.1 Recorded Initialisation Time

There is a significant difference between the time required by each initialisation approach to determine the three target hole locations prior to testing. The teach programming approach requires the longest time $(335\,s)$, as the target positions had to be manually taught by moving the robotic manipulator to each hole location. In addition, time was required for the robotic system to grasp a peg, which was used during teaching to ensure that the hole positions were recorded with higher accuracy. The registration approach required an initialisation time of $52.5s$ in order to determine the world coordinates of the three holes and input their values within the robot's control program. In this case it was assumed that the location of each hole within the environment was initially unknown, but if their locations were known then the initialisation time could be further reduced.

For the Cognex + registration approach, the three hole world coordinates are detected

Table 5.17: Robotic system performance within the insertion scenario when using different initialisation approaches. Values calculated based on 60 test iterations and for a 0.95 confidence level.

Robotic System	Probability of Success (%)	Initialisation Time (s)	Chamfered Peg			Non-Chamfered Peg		
			$CT_{Handling}$ (s)	$CT_{Insertion}$ (s)	CT_{Total} (s)	$CT_{Handling}$ (s)	$CT_{Insertion}$ (s)	CT_{Total} (s)
LWR4_KGG_T$_q$		335	4.549 ± 0.005	1.172 ± 0.005	5.721 ± 0.007	4.551 ± 0.004	1.181 ± 0.004	5.732 ± 0.004
LWR4_KGG_R$_q$	95.3	52.5	4.584 ± 0.004	1.239 ± 0.016	5.823 ± 0.016	4.546 ± 0.008	3.799 ± 0.53	8.344 ± 0.533
LWR4_KGG_CR$_q$		4.1	4.519 ± 0.004	2.225 ± 0.397	6.745 ± 0.395	4.521 ± 0.003	4.157 ± 0.449	8.678 ± 0.451
LWR4_RIQ_T$_q$		335	4.646 ± 0.008	1.214 ± 0.018	5.861 ± 0.02	4.648 ± 0.007	1.257 ± 0.016	5.905 ± 0.019
LWR4_RIQ_R$_q$	95.3	52.5	4.645 ± 0.006	3.212 ± 0.491	7.858 ± 0.491	4.649 ± 0.009	6.763 ± 0.955	11.412 ± 0.956
LWR4_RIQ_CR$_q$		4.1	4.639 ± 0.006	3.678 ± 0.395	8.317 ± 0.397	4.647 ± 0.009	6.415 ± 1.226	11.062 ± 1.227

by a GigE camera mounted within the environment and transmitted directly to the robot's control program. As this is all done automatically, the initialisation time of the Cognex + registration approach is 4.1 s. Similar to the MRMT test, this initialisation time is not reflective of the vision system's optimal performance, which can detect the hole locations in under 50 ms, but is indicative of the time required to set up a connection with the Cognex camera and ensure that the three holes are being correctly detected.

The recorded initialisation time provides an insight into the flexibility of the three initialisation approaches. From these times, it is clear that Cognex + registration approach offers the greater flexibility, as its initialisation time is 98.8% and 92.2% lower than that of the teach programming and registration approaches. This low initialisation time can help to minimise downtime during a changeover, which makes the initialisation approach particularly suited to flexible manufacturing processes. However, this system does require the integration of a vision system within the environment, which may not be desired or financially viable. If this is the case, the registration approach is a good alternative, as the approach is inexpensive but still has an initialisation time which is 84.3% lower than that of the teach programming approach.

5.4.3.2 Recorded Probability of Success

Using the quasi-random search strategy, the robotic systems were able to compensate for misalignment and ensure each insertion was successful. Accordingly, the robotic systems completed the 60 insertions with no failed attempts, which resulted in each system having a PS of 95.3% when using the 0.95 confidence level. Since each system had an equal PS, the KC test detected no difference between any of the robotic systems.

5.4.3.3 Recorded Completion Time

Similar to the previous scenarios, the recorded performance data and true mean ranges can be used to determine if there is a statistical difference between the performances of the different robotic systems. Since this test included different

Table 5.18: Comparison of the different initialisation approaches when inserting the (a) chamfered and (b) non-chamfered peg. A positive detectable difference (in seconds) between the system's true mean completion times differ by at least that value. Rejection (1) of the null hypothesis (H_0) suggests that the data sets do not belong to the same population at the 5% significance level.

(a) Chamfered Peg

Detectable Difference	LWR4_KGG_T_q	LWR4_KGG_R_q	LWR4_KGG_CR_q	LWR4_RIQ_T_q	LWR4_RIQ_R_q	LWR4_RIQ_CR_q
LWR4_KGG_T_q		0.08	0.62	0.11	1.64	2.19
LWR4_KGG_R_q	0.08		0.51	0.00	1.53	2.08
LWR4_KGG_CR_q	0.62	0.51		0.47	0.23	0.78
LWR4_RIQ_T_q	0.11	0.00	0.47		1.49	2.04
LWR4_RIQ_R_q	1.64	1.53	0.23	1.49		-0.43
LWR4_RIQ_CR_q	2.19	2.08	0.78	2.04	-0.43	

KS Test	LWR4_KGG_T_q	LWR4_KGG_R_q	LWR4_KGG_CR_q	LWR4_RIQ_T_q	LWR4_RIQ_R_q	LWR4_RIQ_CR_q
LWR4_KGG_T_q		1	1	1	1	1
LWR4_KGG_R_q	1		1	1	1	1
LWR4_KGG_CR_q	1	1		1	1	1
LWR4_RIQ_T_q	1	1	1		1	1
LWR4_RIQ_R_q	1	1	1	1		1
LWR4_RIQ_CR_q	1	1	1	1	1	

(b) Non-Chamfered Peg

Detectable Difference	LWR4_KGG_T_q	LWR4_KGG_R_q	LWR4_KGG_CR_q	LWR4_RIQ_T_q	LWR4_RIQ_R_q	LWR4_RIQ_CR_q
LWR4_KGG_T_q		2.08	2.49	0.15	4.72	4.10
LWR4_KGG_R_q	2.08		-0.65	1.89	1.58	0.96
LWR4_KGG_CR_q	2.49	-0.65		2.30	1.33	0.71
LWR4_RIQ_T_q	0.15	1.89	2.30		4.53	3.91
LWR4_RIQ_R_q	4.72	1.58	1.33	4.53		-1.83
LWR4_RIQ_CR_q	4.10	0.96	0.71	3.91	-1.83	

KS Test	LWR4_KGG_T_q	LWR4_KGG_R_q	LWR4_KGG_CR_q	LWR4_RIQ_T_q	LWR4_RIQ_R_q	LWR4_RIQ_CR_q
LWR4_KGG_T_q		1	1	1	1	1
LWR4_KGG_R_q	1		1	1	1	1
LWR4_KGG_CR_q	1	1		1	1	1
LWR4_RIQ_T_q	1	1	1		1	1
LWR4_RIQ_R_q	1	1	1	1		1
LWR4_RIQ_CR_q	1	1	1	1	1	

robotic end effectors which influenced handling times, the overall CT of the robotic systems were considered. The detectable difference between the true mean ranges and the outcome of the two-sample KS tests are summarised in Table 5.18.

In all cases, the KS test rejects the null hypothesis at the 5% significance level which indicates that there is a statistical difference between data distributions of each robotic system. This suggests that there is an increased chance of detecting a difference in sample means or variances (but this is not guaranteed).

Looking at the true mean ranges, there is a detectable difference between the LWR4_-KGG and LWR4_RIQ systems for each registration approach. The closest difference occurs when using teach programming, as both systems are able to successfully insert the chamfered and non-chamfered peg on their first attempt. In this instance, the peg insertion scenario is similar to the pick-and-place scenarios considered earlier, which showed that KGG gripper can outperform the Robotiq gripper with a slightly lower CT. Accordingly, the mean CT of the LWR4_KGG_T$_q$ system is detectably lower than the mean CT of the LWR4_RIQ_T$_q$ system, with a minimum difference of $0.11\ s$ and $0.15\ s$ for the chamfered and non-chamfered peg.

When using other two initialisation approaches, the detectable difference between the systems is larger because the LWR4_RIQ system requires more time to insert the peg. One reason for this is the difference in finger design between the Schunk and Robotiq gripper. The former had fingers which centred the peg within the gripper, while the latter had flat fingers. As identified in Section 5.3, the Robotiq's flat fingers can absorb positional errors and increase accuracy during pick-and-place operations. However, in this case, the off-centre location of the peg will offset the quasi-random's search path and consequently influence the robotic systems insertion time. In addition, the flat profile of the fingers allowed the peg to rotate during a search from the resultant surface contact forces, which tended to delay the finding of the hole.

For the registration approach, the mean CT of the LWR4_KGG_R$_q$ system is detectably lower than the mean CT of the LWR4_RIQ_R$_q$ system, with a minimum difference of $1.53\ s$ and $1.58\ s$ for the chamfered and non-chamfered peg. For the Cognex + registration approach, the LWR4_KGG_CR$_q$ system outperforms the LWR4_RIQ_CR$_q$ system by at least $0.78\ s$ and $0.71\ s$ respectively. While the non-chamfered peg requires a higher CT, this relatively constant difference between the two systems across all initialisation approaches is attributable to the structured nature of the quasi-random search strategy, which successively searches smaller and smaller gaps until the hole is found.

Looking at the difference between the initialisation approaches, the LWR4_KGG and LWR4_RIQ systems have a detectably lower CT when initialised using teach

programming. This is unsurprising, as the teach programming approach provides sufficient accuracy to ensure a successful insertion without the need for searching. However, as already noted, this accuracy is achieved at the expense of higher initialisation times.

From testing with the chamfered peg, the teach programming approach outperforms the registration and Cognex + registration approaches by a minimum of $0.08\,s$ and $0.62\,s$ when considering the LWR4_KGG system or by $1.49\,s$ and $2.04\,s$ when considering the LWR4_RIQ system. The proximity of the LWR4_KGG_T$_q$ and LWR4_KGG_R$_q$ system is due to the finger design of the KGG gripper. These fingers centred the peg within the gripper during pick-up, which was sufficient to allow the LWR4_KGG_R$_q$ system to insert the majority of the chamfered pegs first time. The larger detectable difference in the LWR4_RIQ system's mean CT is a result of its higher search time, which is a consequence of the peg's off-centre location and rotation during execution of the search.

For the non-chamfered peg, the teach programming approach outperforms the registration and Cognex + registration approaches by a minimum of $2.08\,s$ and $2.49\,s$ when considering the LWR4_KGG system or by $4.53s$ and $3.91s$ when considering the LWR4_RIQ system. The difference between the initialisation systems is more notable in this case as the non-chamfered peg requires a more accurate alignment before insertion can occur. As noted, the LWR4_RIQ_T$_q$ system inserts all non-chamfered pegs first time, but the LWR4_RIQ_R$_q$ and LWR4_RIQ_CR$_q$ systems require a longer search time, which is why their differences are notably larger than the LWR4_KGG systems.

In the majority of cases, there is no detectable difference between the true mean ranges of the robotic systems using the registration approach and the Cognex + registration approach. The one exception is the LWR4_KGG system when inserting the chamfered peg, as the centring of the peg within the gripper and the forgiving nature of the chamfered peg allowed LWR4_KGG_R$_q$ system to insert the majority of pegs first time. For the remaining systems, a search strategy was required and the resulting increase in its margin of error (and variance) made their true mean ranges indistinguishable.

5.4.3.4   Experimental Summary

As the recorded PS of all systems was 95.3%, the robotic system's throughput can be used to determine the suitability of each initialisation approach. From the recorded results, the teach programming approach is able to perform the scenario with the lowest CT, as the hole locations can be taught with greater accuracy to ensure first time insertions. However, this approach requires an initialisation time of 335 s, which is much larger than the other two approaches considered. Accordingly, teach programming is better suited to high-volume, low variability tasks in which its reduction in operation CT overcomes its high initialisation time.

Both the registration approach and the Cognex + registration approach result in larger CT, but reduce the robotic system's initialisation time. This suggests that the two systems are better suited to flexible manufacturing processes, where frequent operation changeovers will increase the impact of a robotic system's initialisation time on its throughput. Of the two systems, the Cognex + registration approach has an initialisation time of only 4.1 s, which is 92.2% lower than the registration initialisation time. Looking at CT, it is difficult to differentiate between the two initialisation approaches. The only statistically significant difference between the two approaches was during chamfered peg insertion, where the mean CT of the LWR4_KGG_R$_q$ system was at least 0.51 s lower than the mean CT of the LWR4_-KGG_CR$_q$ system. In the remaining tests, the recorded means suggested that the registration approach outperformed the Cognex + registration approach, but this cannot be determined using the 0.95 certainty level. To overcome this, more test iterations could be performed or the certainty level could be reduced.

From testing with the LWR4_KGG and LWR4_RIQ systems, the mean CT of the LWR4_KGG system is detectably lower than the LWR4_RIQ system for each initialisation approach, which indicates suitability of the LWR4_KGG system for this insertion scenario. However, as noted before, the LWR4_RIQ system can more easily adapt to different objects and operations, which may make it a preferable choice if the reduction in CT can be tolerated.

5.4.4 Insertion Scenario Discussion

5.4.4.1 Computational vs. Experimental Results

Again, the estimated and actual performance of each robotic system can be compared in order to consider the strength of the developed assessment framework. In this scenario, the consideration of PS is superfluous as the LWR4_KGG and LWR4_RIQ systems performed all insertions without failure. Accordingly, this section will focus on the comparison of estimated and recorded CT. For clarity, these values are presented side-by-side in Table 5.19.

Looking first at the handling operation, it can be seen that the framework's estimation of the robotic system's CT is relatively close to the measured true mean range. For the LWR4_KGG and LWR4_RIQ systems, the handling time is underestimated by $0.28\,s$ (6.2%) and $0.27\,s$ (5.8%) on average. While this estimation error is satisfactory, it is higher than those experienced when estimating the handling times in the previous two scenarios. The reason for this was found to be a result of the KUKA LWR4's control program, which had additional verifications during the execution of each motion command that were not accounted for in the manipulator's trajectory speed. From Table 5.19, the major estimation errors occur during insertion operations that required the implementation of a search strategy. When the robotic system did not need to search to find the hole, the estimated insertion CT was relatively close to the recorded CT, as shown by the LWR4_KGG_T$_q$ and LWR4_RIQ_T$_q$ systems. For these two systems, the framework overestimated the system's mean CT by $0.085\,s$ and $0.107\,s$. This switch from underestimation to overestimation can be accounted for by the framework's inclusion of an approximated detect time, CT_{Detect}, when estimating CT_{Insert}.

For the remaining insertions, the framework estimates a CT using the insertion search time metric presented in Section 4.3.5. To maintain generality, this metric defines a search time for each strategy based on the magnitude of the expected positional error. However, since the direction of the positional error also has a significant impact on the search time, the average search times calculated for each $1\,mm$ error increment are approximate (refer back to Figure 4.19). Accordingly, the estimated CT is only meant as an approximation of actual performance, which is satisfactory due to the

Table 5.19: Comparison between the estimated and recorded CT of each robotic system for (a) the chamfered and (b) the non-chamfered peg insertion scenario.

(a) Chamfered Peg

Robotic System	Perception Error (mm)	$CT_{Handling}$ (s)		$CT_{Insertion}$ (s)		CT_{Total} (s)		Detectable Difference
		Estimated	Actual	Estimated	Actual	Estimated	Actual	
Test 1 – Search Strategies								
LWR4_KGG_S$_s$			4.566±0.005	2.1±0.31	2.227±0.267	6.35±0.31	6.793±0.266	-0.13
LWR4_KGG_S$_r$	σ_1	4.26	4.568±0.006	1.83±0.23	2.152±0.232	6.08±0.23	6.719±0.231	**0.18**
LWR4_KGG_S$_q$			4.563±0.037	1.89±0.31	1.452±0.155	6.14±0.31	6.014±0.161	-0.35
LWR4_KGG_S$_s$			4.568±0.006	5.11±0.29	3.957±0.595	9.36±0.29	8.525±0.593	-0.05
LWR4_KGG_S$_r$	σ_2	4.26	4.545±0.05	4.51±1	3.529±0.674	8.76±1	8.073±0.681	-0.99
LWR4_KGG_S$_q$			4.55±0.009	3.37±0.44	3.191±0.638	7.62±0.44	7.741±0.639	-0.95
Test 2 – Initialisation Approaches								
LWR4_KGG_T$_q$	≈ 0.01		4.549±0.005	1.27	1.172±0.005	5.52	5.721±0.007	**0.19**
LWR4_KGG_R$_q$	≈ 4.00	4.26	4.584±0.004	3.37±0.44	1.239±0.016	7.62±0.44	5.823±0.016	**1.35**
LWR4_KGG_CR$_q$	≈ 3.63		4.519±0.004	3.37±0.44	2.225±0.397	7.62±0.44	6.745±0.395	**0.04**
LWR4_RIQ_T$_q$	≈ 0.01		4.646±0.008	1.38	1.214±0.018	5.75	5.861±0.02	**0.09**
LWR4_RIQ_R$_q$	≈ 4.00	4.37	4.645±0.006	3.48±0.44	3.212±0.491	7.85±0.44	7.858±0.491	-0.92
LWR4_RIQ_CR$_q$	≈ 3.63		4.639±0.006	3.48±0.44	3.678±0.395	7.85±0.44	8.317±0.397	-0.37

(b) Non-Chamfered Peg

Robotic System	Perception Error (mm)	$CT_{Handling}$ (s)		$CT_{Insertion}$ (s)		CT_{Total} (s)		Detectable Difference
		Estimated	Actual	Estimated	Actual	Estimated	Actual	
Test 1 – Search Strategies								
LWR4_KGG_S$_s$			4.567±0.005	12.78±2.06	7.195±0.971	17.03±2.06	11.762±0.971	**2.23**
LWR4_KGG_S$_r$	σ_1	4.26	4.589±0.024	8.91±2.09	8.008±2.101	13.16±2.09	12.597±2.098	-3.62
LWR4_KGG_S$_q$			4.563±0.038	3.67±0.58	3.115±0.806	7.92±0.58	7.677±0.811	-1.15
LWR4_KGG_S$_s$			4.586±0.053	26.43±1.77	37.129±5.424	30.68±1.77	41.715±5.425	**3.84**
LWR4_KGG_S$_r$	σ_2	4.26	4.583±0.007	7.73±1.79	15.617±5.546	11.98±1.79	20.199±5.547	**0.88**
LWR4_KGG_S$_q$			4.579±0.008	5.63±0.95	8.203±1.924	9.88±0.95	12.782±1.924	**0.03**
Test 2 – Initialisation Approaches								
LWR4_KGG_T$_q$	≈ 0.01		4.551±0.004	1.27	1.181±0.004	5.52	5.732±0.004	**0.21**
LWR4_KGG_R$_q$	≈ 4.00	4.26	4.546±0.008	5.63±0.95	3.799±0.53	9.88±0.95	8.344±0.533	**0.06**
LWR4_KGG_CR$_q$	≈ 3.63		4.521±0.003	5.63±0.95	4.157±0.449	9.88±0.95	8.678±0.451	-0.19
LWR4_RIQ_T$_q$	≈ 0.01		4.648±0.007	1.38	1.257±0.016	5.75	5.905±0.019	**0.14**
LWR4_RIQ_R$_q$	≈ 4.00	4.37	4.649±0.009	5.74±0.95	6.763±0.955	10.11±0.95	11.412±0.956	-0.60
LWR4_RIQ_CR$_q$	≈ 3.63		4.647±0.009	5.74±0.95	6.415±1.226	10.11±0.95	11.062±1.227	-1.22

large uncertainty that exists when implementing a search strategy. This uncertainty is exemplified by the large variance during actual testing.

To consider the framework's performance, the minimum detectable difference between the estimated and actual CT_{Total} of each robotic system has been calculated and included in Table 5.19. Similar to before, a negative value implies that there is no detectable difference between the estimated and actual true mean ranges as the intervals overlap. For the chamfered peg, it can be seen that the framework provides an estimated CT which is close to the recorded CT. The largest detectable difference is from the initialisation approach testing, where the framework overestimates the CT of the LWR4_KGG_R$_q$ system by 1.35 s. This can be accredited to the centring

of the peg within the gripper, which allowed the system to perform the insertions without searching (as noted earlier). The remaining detectable differences between estimated and actual CT_{Total} are less than $0.2\,s$, which is satisfactory considering the variance that searching introduces.

For the non-chamfered peg, the framework overestimates the CT of the LWR4_-KGG_S_s by at least $2.23\,s$ for perception error σ_1, but underestimates the CT of the same system by at least $3.84\,s$ for perception error σ_2. These larger detectable differences can be accounted for by the non-chamfered peg, as its insertion times are larger and more sensitive to the initial positional error. In addition, the performance data set of the LWR4_KGG_S_s system for perception error σ_2 was noted to contain a few outliers. These outliers had insertion times of over $90\,s$, which raised the recorded sample mean and variance. The framework also underestimates the CT of the other two systems for perception error σ_2. The largest of these is for the LWR4_KGG_S_r system, where the estimated CT is lower than the actual CT by at least $0.88\,s$. This difference can again be accounted for by outliers in the experimental data, as well as the unpredictable nature of the random search strategy.

Overall the developed framework provides a structured approach to estimating the performance of the robotic systems. The estimated CT is less accurate at larger positional errors as the performance of the search strategies becomes less predictable, but is still within an acceptable range to provide an insight into the robotic system's capabilities.

5.4.4.2 Boothroyd - Dewhurst Comparison

As noted, this peg insertion scenario includes the handling and insertion of a chamfered and non-chamfered peg. The peg's size, geometry, and physical properties do not introduce any difficulties, and so the handling of the peg can be classified as a B-D handling operation with code '00'. From Figure 2.10, this type of operation can be performed by a human in $1.13\,s$ on average.

The estimated human insertion time is dependent on the peg's chamfer design. From Section 4.6, the diameter of the peg and hole give a dimensionless clearance of 0.02. This clearance does not impact a human's insertion time when using a chamfered peg,

but is sufficiently tight to cause difficulties when inserting a non-chamfered peg [29]. Accordingly, the insertion of the chamfered and non-chamfered peg can be classified as B-D insertion operations with codes '00' and '01'. From Figure 2.12, these codes correspond to an average human insertion time of 1.5 s and 2.5 respectively.

Based on these times, a human can perform the insertion scenario in 2.63s when using the chamfered peg or 3.63 s when using the non-chamfered peg. Using the developed framework, these human completion times can be compared to the estimated CT of each robotic system to determine the most suitable choice for this scenario. From Table 5.19, the robotic systems that are initialised using teach programming are estimated to achieve the lowest CT, with the LWR4_KGG_T$_q$ and LWR4_RIQ_T$_q$ systems having an estimated CT of 5.52 s and 5.75 s for both pegs. Considering the ability of a robotic system to operate continuously, these times are close enough to the estimated human times to be considered for the given scenario. However, as discussed previously, teach programming requires a large initialisation time which negatively impacts the robotic system's throughput during low-volume production. Accordingly, the LWR4_KGG_T$_q$ and LWR4_RIQ_T$_q$ systems are unsuited for this scenario if it is part of a flexible manufacturing process.

The other two initialisation approaches have lower initialisation times which make them better suited to changing environments. However, their estimated times are 2.7 to 3.0 times larger than the estimated human times, which makes their selection over human operators less discernible. As noted before, other cost metrics such as operation costs, initial setup costs, and production volumes would need to be considered in order to determine the most suitable choice for the scenario.

Chapter 6

Conclusions and Future Work

6.1   Dexterity within Manufacturing

From examination of the literature, this work has identified that the demand for robotic dexterity stems from the surrounding environment. Accordingly, this work proposes that robotic dexterity within flexible manufacturing can be captured by considering the dexterous requirements within the area. While the focus on this area limits its scope, the clearly defined environment allows robotic dexterity to be more easily measured and quantified.

Within flexible manufacturing, an assembly's layout, parts and operations are typically optimised using DFA methods. Of these methods, the Boothroyd-Dewhurst (B-D) DFA method is the most well-established and widely used. The B-D DFA method is currently used to improve the efficiency of a manual assembly process, but this work has identified the potential for using their classification tables when considering robotic dexterity within manufacturing.

The handling and insertion tables defined within the B-D DFA method identify the range of possible operations within flexible manufacturing. From the analysis and comparison to other dexterity assessments presented within this work, these tables have been shown to comprehensively capture the dexterous requirements within flexible manufacturing. Ergo, this work proposes that the dexterous ability of a robotic system within flexible manufacturing be represented by the ability of the robotic system to perform the operations identified within the B-D classification tables.

6.2   Developed Assessment Framework

The presented framework incorporates three distinct activities that capture the dexterous capabilities of a robotic system and identify the operations it can perform within a flexible manufacturing environment. The first activity identifies the range of dexterous requirements within flexible manufacturing through consideration of the B-D classification tables. The second activity involves the matching of a robotic system to robot specifications using robotic performance metrics (and vice versa). These performance metrics were developed as part of this work based on the dexterous requirements identified by the B-D classification tables. Consequently, the developed metrics provide a greater insight into the dexterous ability of industrial robotic systems when compared to supplier specifications. The third activity involves the matching of the classified dexterous operations to robotic performance metrics (and vice versa). This activity determines both the feasibility and capability of a robotic system for each dexterous operation, and simplifies robot selection within the area by directly relating robotic performance to a classification system commonly used within manufacturing.

The developed framework provides a comprehensive approach to assessing dexterity within flexible manufacturing. By linking the range of dexterous operations within manufacturing to the dexterous capabilities of the robotic system, the framework overcomes a current challenge by simplifying the robot selection process. In addition, the structured nature of the framework and its set of developed performance metrics facilitates the direct comparison of different robotic systems which helps to quantify the current state of robotic dexterity within manufacturing.

6.3   Computational vs Experimental Results

To demonstrate its application, the developed framework and metrics were used to estimate the dexterity of different robotic systems within three flexible manufacturing scenarios by calculating a probability of success (PS) value and an overall task completion time (CT). These computational results were then validated by performing actual testing with each robotic system and scenario variation.

In all scenarios, the developed framework produced estimations that were close to real-life performance and superior to those generated from supplier specifications. This highlights the potential for the developed framework and its structured evaluation approach, as the accuracy of these estimations is critical in a sector whose key drivers include reliability and throughput.

Through use of the framework and the data analysis methods presented, manufacturers can accurately compare human and robot performance and acquire statistically significant conclusions. This facilitates the making of informed decisions during manufacturing system selection i.e. whether the benefits of using an automated system (increased working hours, reduced operation costs, etc.) outweigh its shortcomings (higher set-up costs, reduced flexibility, etc.). In addition, the ability to accurately compare human and robot performance helps to quantify the current gap and to identify the areas in which collaborative robotic systems need to improve before becoming a viable option for each operation within a flexible manufacturing environment.

6.3.1 Handling Scenario

From use of the developed framework, a PS value could be calculated for each robotic system and uncertainty level. The estimated values not only confirmed the importance of a vision system at higher levels of uncertainty, but also identified the positional uncertainty at which the use of a vision system becomes critical. This critical point is dependent on the manufacturer's required system performance, but a value of 0.95 is the standard within statistical analysis and has been adopted here. By comparing the estimated CT values to those within original B-D handling table (see Figure 2.10), this work identified the relative performance of the robotic systems to human labour. The robotic systems assessed were estimated to take 2.7 to 3.7 times longer than the average human completion time of $1.13\,s$. This loss in workstation throughput would be unacceptable within a real manufacturing scenario which makes each of the considered robotic systems an impractical choice for this handling operation.

However the developed framework identifies the actions which have the biggest

influence on the robotic system's CT, and so can be used to identify a better robotic system structure. In this scenario, the motions of the robotic manipulator account for the majority of the estimated CT, which means that a robotic manipulator better suited to the given trajectory distances could be selected (from the trajectory time metric). Furthermore, a programming interface with a higher communication frequency would help to reduce communication delays and improve the robotic system's performance. Combining these improvements, an alternative robotic system could be identified by the framework which has an estimated CT that rivals human performance.

6.3.2 Pick-and-Place Scenario

The original Minnesota Rate of Manipulation Test (MRMT) and its variant have been proposed as two benchmarking tests which provide a simple method for assessing and comparing the performance of batch pick-and-place operations by robotic systems within a changing environment. Of the initialisation approaches considered, the teach programming approach was shown to have the highest PS for an accurate placement, but required long initialisation times. From comparisons to the Cognex and the Cognex + registration programming approaches, this work has identified that the inclusion of vision can reduce a robotic system's initialisation time by over 96%. This helps to quantify the increased flexibility that a vision system provides and its importance within flexible manufacturing. In addition, these benchmarking tests have helped to identify a limitation in using series elastic actuators for pick-and-place operations that require high fidelity as the recorded CT of the Baxter robot arm (9.1 to 12.5 $s/block$) was significantly larger than that of the UR10 manipulator (2.2 to 3.3 $s/block$).

Comparison of the estimated and recorded robotic CT (Table 5.13) shows that the developed framework is able to accuracy estimate the true performance of a robotic system during a pick-and-place scenario. The breakdown of the scenario into individual actions and use of developed metrics provided a more accurate estimation of CT than currently possible using supplier specifications. This is particularly important within batch production, as initial estimation errors will amalgamate due

to repetition of the same operations.

Through use of the developed framework, it was estimated that the chosen robotic systems take at least 2 times longer than an average human worker to complete the original MRMT but only 1.1 to 1.2 times longer to complete the MRMT variant due to its requirement for more careful and accurate placements. This proximity in CT advocates the selection of a robotic system for this scenario, however it should be combined with the initialisation time and estimated PS values in order to determine if the robotic system has a satisfactory level of dexterity to perform the batch pick-and-place operation based on its changeover frequency and required placement accuracy.

For validation, the average human completion times presented within the B-D tables were compared to the original MRMT's established norm tables. This showed that the B-D tables overestimated the single-run CT by 19.45 s (41 %). While significant, the estimate is sufficiently close considering the versatility of the B-D tables to estimate completion times for all operations within flexible manufacturing. It is also worth noting that the accuracy of B-D estimations are more likely to improve when considering a range of operations due to its equal likelihood of overestimating and underestimating performance. The B-D tables form a key part of the developed framework, so it is encouraging that their estimated CT values are comparable to normative data.

6.3.3   Peg Insertion Scenario

Within the peg insertion scenario, each robotic system performed a search strategy in order to correctly align the peg and hole at varying levels of uncertainty. This flexibility ensured a high PS, but had a notable impact on the robotic system's CT values. From the results presented in Table 5.19, the magnitude and variance of this impact was dependent on the level of uncertainty and the search strategy implemented. The spiral search was most sensitive to uncertainty due to its structured search path, but may be favourable within manufacturing as its performance is predictable. Conversely, the random search strategy was less sensitive to uncertainty but had greater variance in recorded CT values.

Taking the benefits of both search strategies, a new quasi-random search strategy was developed within this work. This strategy incorporated the Sobol' sequence, which ensured an efficient but structured generation of search points within the search region. From experimentation, the developed quasi-random search strategy was shown to achieve the best performance, enabling the robotic system to quickly converged on the hole location in a more predictable manner.

The merits of a sensory-rich and complex multi-fingered control strategy were also identified within this scenario. The approach was least sensitive to uncertainty, and could perform the peg-in-hole insertion at a level that was competitive to the other systems considered. This makes the strategy a viable option, particularly in insertion tasks which require careful insertion, as the strategy limited peg-hole forces to 0.5 N or less.

Using the developed framework, estimated robot completion times were compared to expected human completion times. From this comparison, it was clear that the chosen robotic systems would only be a viable option for peg insertions with low levels of uncertainty. While the high PS values indicated that the robotic systems are dexterous enough to perform the operation, their increased CT and sensitivity at higher levels of uncertainty confirmed that they do not have the necessary level of dexterity to provide comparable performance to human operators. This outcome justifies the selection of human operators for peg insertion tasks within flexible manufacturing.

6.4 Concluding Remarks

As industrial robots become more important within flexible manufacturing, there is pressing need to clearly define and measure robotic dexterity. To address this challenge, a new framework has been developed to capture and assess robotic dexterity within flexible manufacturing. By utilising classification tables from a DFA method commonly used within industry, this framework ensures a comprehensive assessment that promotes and simplifies robotic integration within the area.

Using the developed framework, the dexterity of a robotic system can be quantified by considering the range of B-D operations it can perform and its performance within these operations. A new set of performance metrics is required in order to achieve this, as current supplier specifications and metrics do not provide a true or comprehensive representation of the robotic system's performance. The first of these performance metrics have been developed and presented within this work, and provide the necessary information to capture the dexterity of a robotic system during a number of B-D operations.

Based on these performance metrics and to demonstrate the framework's application, the dexterity of various robotic systems was considered during three different scenarios. These scenarios are representative of those most commonly encountered within manufacturing and so present a logical starting point for the framework. The feasibility and capability of the robotic systems was calculated using the identified performance metrics, and the PS and CT values derived from these metrics was shown to closely align with actual performance. These measures provided an insight into the dexterity of the robotic system, and thanks to the framework's incorporation of the B-D tables could be directly compared to human performance in order to identify the level of dexterity that would justify a robot's selection for each scenario. Accordingly, the presented framework provides a structured approach to assessing robotic dexterity within flexible manufacturing. The developed performance metrics provide estimations of robot dexterity that closely match real-life performance, illustrating the framework's enhanced performance when compared to current assessment approaches and identifying its potential as a dexterity assessment tool.

6.5 Recommendations for Future Work

While the results and analysis presented within this thesis have demonstrated the potential of the developed framework for assessing dexterity within flexible manufacturing, many opportunities still remain for the continued expansion of the framework. This section presents some of these possible directions.

1. *B-D Operations:* Initial testing has validated the strength of the developed framework within selected scenarios, but there are many more B-D operations that can still be analysed. While these operations may be less common within manufacturing, their consideration will be more beneficial as the additional operations require different levels of dexterity. As noted within this work, the B-D operations classified by the B-D tables capture the range of dexterous requirements within flexible manufacturing, so the consideration of more operations will result in a more comprehensive assessment framework.

   While current robotic systems have struggled in the scenarios considered, the use of the B-D tables within the developed framework provides plenty of opportunities for extending the scope of the framework. An additional benefit in using the B-D tables is that they classify operations according to difficulty, which provides a natural order to the expansion. As the performance of robotic systems within flexible manufacturing increases, operations with increasing difficulty can be considered to provide a more detailed insight into the dexterity of the robotic system.

   Based on the operations considered within this work, a natural progression would be to consider a B-D handling operation with codes '20' ($CT = 1.8\,s$) or '30' ($CT = 1.95\,s$), which would capture the robot's ability to handle more asymmetrical shapes. Alternatively, handling operations with codes '01' ($CT = 1.43\,s$) or '02' ($CT = 1.88\,s$) could be considered to give an insight into the robotic system's ability to deal with smaller objects. Within the area of insertion, a natural progression would be to consider fastening operations, such as the most basic snap/press fit with insertion code '30' ($CT = 2.0\,s$) or screw tightening with insertion code '38' ($CT = 6.0\,s$).

2. *Performance Metrics:* To expand the framework and consider more difficult operations, a more comprehensive set of performance metrics would need to be developed. The performance metrics developed within this framework were satisfactory for estimating the dexterity of the robotic systems within the chosen scenarios, but additional metrics would be required when considering additional operations in order to maintain the framework's estimation accuracy.

   The selection of subsequent performance metrics would depend on the next B-D operations being considered. For example, metrics such as *object pose estimation* and *slip resistance* would provide an insight into a robot's ability to handle more asymmetrical and smaller shapes, while *touch sensitivity* and *in-hand manipulation* metrics would help to determine its ability during different insertion operations. Regardless, the developed metrics need to be clearly defined and measured using standardised methods if they are to be a useful addition to the developed framework.

3. *Robotic Systems:* A worthwhile progression of the work presented within this thesis is to use the developed framework to assess the dexterity of additional robotic systems. While a number of robotic systems were assessed here, they only represent a small portion of those possible within flexible manufacturing.

   The developed performance metrics provide a true reflection of a robotic system's performance, and can be used to accurately estimate the dexterity of the robotic system when performing the most popular manufacturing operations. Accordingly, it would be beneficial to analyse more robotic systems using the developed framework in order to obtain more meaningful indicators of dexterity. The performance metrics and test methods discussed within the framework would facilitate both cross-system and within-system comparisons, and the proposed data analysis approaches would ensure statistically significant results. This would help to identify robotic systems and structures that are particularly suited to the dexterous operations within flexible manufacturing, and would subsequently help to distinguish the current state-of-the-art within industrial robotics.

4. *Robotic Sectors:* While the focus of this thesis was on the assessment of robotic dexterity within flexible manufacturing, the presented work could aid in the development of other dexterity assessments within robotics. The in-depth discussion of dexterity and its contributing factors is not specific to dexterity within flexible manufacturing, and the identified importance of the surrounding environment can be used by other researchers to develop a dexterity assessment that is better suited to their target application.

While the B-D tables stem from the manufacturing sector, the tables can potentially be used to classify operations within other sectors. The use of the B-D tables in this way is new to the robotics sector, but the advantages presented within this work should emphasise their merit. The tables provide an easy way to deconstruct a task into fundamental operations and to estimate human performance, which should be appealing to other researchers.

The performance metrics developed within this framework are not restricted to manufacturing and can be used to more accurately represent the performance of other, non-industrial robotic systems. Accordingly, the metrics can be incorporated within other dexterity assessment frameworks and combined with additional metrics to determine the feasibility and capability of different robotic systems. This is particularly true for those performance metrics which relate to the pick-and-place operation, as this type of operation is required within the majority of robotic sectors.

Bibliography

[1]   Robotics Technology Consortium, "A Roadmap for US Robotics From Internet to Robotics (2016 Edition)," Tech. Rep., 2016, pp. 1–109.

[2]   Ad-hoc Industrial Advisory Group (AIAG), "Factories of the Future Ppp Strategic Multi-Annual Roadmap," European Commission, Tech. Rep., 2010, pp. 13–17. DOI: 10.2777/98640.

[3]   F. Tobe, "Why Co-Bots Will Be a Huge Innovation and Growth Driver for Robotics Industry," *IEEE Spectrum*, 2015. [Online]. Available: http://spectrum.ieee.org/automaton/robotics/industrial-robots/collaborative-robots-innovation-growth-driver (visited on 10/31/2016).

[4]   N. A. Bernstein, "Dexterity and Its Development," in *On dexterity and its development*, M. L. Latash and M. T. Turvey, Eds., Lawrence Erlbaum Associates, 1996, ch. 1, pp. 3–246, ISBN: 0805816461. DOI: 10.1007/s13398-014-0173-7.2. arXiv: 9809069v1 [arXiv:gr-qc].

[5]   European Commission Eurostat, "Employment growth and activity branches - annual averages," 2014. [Online]. Available: http://ec.europa.eu/eurostat/web/products-datasets/-/lfsi_grt_a (visited on 10/05/2016).

[6]   U.S. Bureau of Labor Statistics, "Employment by major industry sector," 2015. [Online]. Available: http://www.bls.gov/emp/ep_table_201.htm (visited on 10/05/2016).

[7]   Forfás Ireland, "Forfás Annual Report 2012," Tech. Rep., 2012. [Online]. Available: https://djei.ie/en/Publications/Forfas-Annual-Report-2012.html.

[8]   Department of Jobs Enterprise and Innovation, "Manufacturing Guide - An Overview of Government Supports for Manufacturing in Ireland," Dublin, Ireland, Tech. Rep., 2015, p. 60. [Online]. Available: https://www.djei.ie/en/Publications/Manufacturing-Guide1.html.

[9]   Forfás Ireland, "Making it in Ireland: Manufacturing 2020," Tech. Rep., 2013. [Online]. Available: https://www.djei.ie/en/Publications/Making-it-in-Ireland-Manufacturing-2020.html.

[10]   Industrial Development Authority (IDA) Ireland, "Horizon 2020 - IDA Ireland Strategy," Dublin, Ireland, Tech. Rep., 2010.

[11]   IDA Ireland, "Winning: Foreign Direct Investment 2015-2019," Tech. Rep., 2015. [Online]. Available: http://www.idaireland.com/docs/publications/ida_strategy_final.pdf.

[12] Central Statistics Office (CSO) Ireland, "Statistics," [Online]. Available: http://www.cso.ie/en/statistics/ (visited on 10/19/2016).

[13] Department of Jobs Enterprise and Innovation, "The Science Budget 2014-2015," Tech. Rep. November, 2015, p. 204. [Online]. Available: https://www.djei.ie/en/Publications/The-Science-Budget-2014-2015.html.

[14] Forfás Ireland, "State Investment in Research and Development 2011-2012," Tech. Rep., 2012. [Online]. Available: http://edepositireland.ie/handle/2262/70202.

[15] Central Statistics Office (CSO) Ireland, "Business Demography Report," Tech. Rep., 2014. [Online]. Available: http://www.cso.ie/en/releasesandpublications/er/bd/businessdemography2014/.

[16] R. Singh, *Introduction to Basic Manufacturing Process and Workshop Technology.* New Age International (P) Ltd., Publishers, 2006, p. 506, ISBN: 9788122423167.

[17] Evolubox, "Evolubox Flexible Assembly Unit Advantages," 2015. [Online]. Available: http://www.evolubox.net/en/advantages/ (visited on 11/06/2016).

[18] M. P. Groover, "Automation," *Encyclopaedia Britannica*, 2017. [Online]. Available: https://www.britannica.com/technology/automation/Manufacturing-applications-of-automation-and-robotics (visited on 05/16/2017).

[19] J. N. Pires, A. Loureiro, and G. Bölmsjo, *Welding robots: Technology, system issues and applications.* 2006, pp. 1–180, ISBN: 1852339535. DOI: 10.1007/1-84628-191-1.

[20] A. Kurtoglu, "Flexibility analysis of two assembly lines," *Robotics and Computer-Integrated Manufacturing*, vol. 20, no. 3, pp. 247–253, 2004, ISSN: 07365845. DOI: 10.1016/j.rcim.2003.10.011.

[21] M Mori and M Fujishima, "Changeable and reconfigurable manufacturing systems," in, H. ElMaraghy, Ed., Springer Science & Business Media, 2008, ISBN: 9781848820678.

[22] Y. P. Gupta and S. Goyal, "Flexibility of manufacturing systems: Concepts and measurements," *European Journal of Operational Research*, vol. 43, no. 2, pp. 119–135, 1989, ISSN: 03772217. DOI: 10.1016/0377-2217(89)90206-3.

[23] D. Gerwin, "Manufacturing Flexibility: A Strategic Perspective," *Management Science*, vol. 39, no. 4, pp. 395–410, 1993, ISSN: 0025-1909. DOI: 10.1287/mnsc.39.4.395.

[24] D. M. Upton, "The Management of Manufacturing Flexibility," *California Management Review*, vol. 36, no. 2, pp. 72–89, 1994, ISSN: 0008-1256. DOI: 10.2307/41165745.

[25] M. Jonsson, "On manufacturing technology as an enabler of flexibility: Affordable reconfigurable tooling and force-controlled robotics," PhD thesis, Linköping University Electronic Press, 2013.

[26]   H.-P. Wiendahl, H. A. ElMaraghy, P. Nyhuis, M. F. Zäh, H.-H. Wiendahl, N. Duffie, and M. Brieke, "Changeable manufacturing-classification, design and operation," *CIRP Annals-Manufacturing Technology*, vol. 56, no. 2, pp. 783–809, 2007.

[27]   N. Slack, "The Flexibility of Manufacturing Systems," *International Journal of Operations & Production Management*, vol. 7, no. 4, pp. 35–45, 1987, ISSN: 0144-3577. DOI: 10.1108/eb054798.

[28]   E. Tempelman, H. Sherchiff, and B. Ninader van Eyben, *Manufacturing and Design: Understanding the Principles of How Things Are Made*. Elsevier, 2014, p. 310, ISBN: 978-0-08099-922-7.

[29]   G. Boothroyd, P. Dewhurst, and W. A. Knight, *Product Design for Manufacture and Assembly, Third Edition*. 2010, p. 709, ISBN: 1420089277.

[30]   B. Lotter, *Manufacturing assembly handbook*. Butterworths, 1989, p. 395, ISBN: 9780408035613.

[31]   I. Mašín, "A comparison of dfa methods for manual assembly," in *Modern Methods of Construction Design*, Springer, 2014, pp. 265–271, ISBN: 978-3-319-05203-8. DOI: 10.1007/978-3-319-05203-8_38.

[32]   P. Leaney and G. Wittenberg, "Design for assembling: The evaluation methods of hitachi, boothroyd and lucas," *Assembly Automation*, vol. 12, no. 2, pp. 8–17, 1992. DOI: 10.1108/eb004359.

[33]   R. H. Sturges, "A quantification of manual dexterity: the design for an assembly calculator," *Robotics and Computer Integrated Manufacturing*, vol. 6, no. 3, pp. 237–252, 1989, ISSN: 07365845. DOI: 10.1016/0736-5845(89)90044-6.

[34]   C. Favi and M. Germani, "From product architecture to assembly sequence: a method to develop conceptual Design for Assembly based on interface analysis," in *Enabling Manufacturing Competitiveness and Economic Sustainability: Proceedings of the 4th International Conference on Changeable, Agile, Reconfigurable and Virtual production (CARV2011), Montreal, Canada, 2-5 October 2011*, A. H. ElMaraghy, Ed., Berlin, Heidelberg: Springer Berlin Heidelberg, 2012, pp. 209–214, ISBN: 978-3-642-23860-4. DOI: 10.1007/978-3-642-23860-4_34.

[35]   D. L. M. de Almeida and J. C. E. Ferreira, "Analysis of the Methods Time Measurement (MTM) methodology through its application in manufacturing companies," *Flexible Automation and Intelligent Manufacturing*, no. 6, 2009. DOI: 10.13140/RG.2.1.2826.1927.

[36]   J. L. Mathieson, B. a. Wallace, and J. D. Summers, "Assembly time modelling through connective complexity metrics," *International Journal of Computer Integrated Manufacturing*, vol. 25, no. 12, pp. 1160–1172, 2012, ISSN: 0951-192X. DOI: 10.1080/0951192X.2012.684706.

[37]   D. Braha and O. Maimon, *A mathematical theory of design: foundations, algorithms and applications*. Springer Science & Business Media, 2013, vol. 17, ISBN: 9781475728729.

[38] D. E. Whitney, "Chapter 15: Design for Assembly and Other Ilities," in *Mechanical Assemblies: Their Design, Manufacture, and Role in Product Development*, Oxford University Press, 2004, pp. 379–391, ISBN: 978-0-19-515782-6.

[39] G Boothroyd, *Assembly automation and product design*, 2nd edition. CRC Press, 2005, p. 512, ISBN: 9781574446432.

[40] M. E. Moran, "Rossum's universal robots: not the machines," *Journal of endourology / Endourological Society*, vol. 21, no. 12, pp. 1399–1402, 2007, ISSN: 0892-7790. DOI: 10.1089/end.2007.0104.

[41] J. Horáková and J. Kelemen, "Artificial living beings and robots: One root, variety of influences," *Artificial Life and Robotics*, vol. 13, no. 2, pp. 555–560, 2009, ISSN: 14335298. DOI: 10.1007/s10015-008-0502-z.

[42] N. G. Hockstein, C. G. Gourin, R. A. Faust, and D. J. Terris, "A history of robots: From science fiction to surgical robotics," *Journal of Robotic Surgery*, vol. 1, no. 2, pp. 113–118, 2007, ISSN: 18632483. DOI: 10.1007/s11701-007-0021-2.

[43] E. G. Christoforou and A. Müller, "R.U.R. Revisited: Perspectives and Reflections on Modern Robotics," *International Journal of Social Robotics*, vol. 8, no. 2, pp. 237–246, 2016, ISSN: 18754805. DOI: 10.1007/s12369-015-0327-6.

[44] B. J. Challacombe, M. S. Khan, D. Murphy, and P. Dasgupta, "The history of robotics in urology," *World Journal of Urology*, vol. 24, no. 2, pp. 120–127, 2006, ISSN: 07244983. DOI: 10.1007/s00345-006-0067-1.

[45] B. Siciliano, L. Sciavicco, L. Villani, and G. Oriolo, *Robotics: Modelling, Planning and Control*, Springer, Ed., ser. Advanced Textbooks in Control and Signal Processing. Springer, 2009, p. 632, ISBN: 9781846286414. DOI: 10.1007/978-1-84628-642-1.

[46] Robotics Business Review, "Small-payload Robots Fastest Growing Market 2013 to 2016," 2012. [Online]. Available: https://www.roboticsbusinessreview.com/small_payload_robots_fastest_growing_market_2013_to_2016/ (visited on 10/18/2016).

[47] H. Formoe, "Types of Industrial Robots," *BotArc*, 2010. [Online]. Available: http://botarc.blogspot.ie/2010/09/types-of-industrial-robots.html (visited on 05/16/2016).

[48] U.S. Bureau of Labor Statistics, "U.S. Bureau of Labor Statistics," [Online]. Available: https://www.bls.gov/ (visited on 09/30/2016).

[49] BofA Merrill Lynch Global Investment Strategy, "Creative Disruption," Tech. Rep. April, 2015, p. 27. [Online]. Available: https://www.bofaml.com (visited on 10/10/2016).

[50] T. Harbert, "Robot Renaissance Could Boost U.S. Electronics Manufacturing," *Electronics360*, October, 2013. [Online]. Available: http://electronics360.globalspec.com/article/3102/robot-renaissance-could-boost-u-s-electronics-manufacturing (visited on 10/19/2016).

[51] B. Ma, S. Nahal, and F. Tran, "Thematic Investing: Robot Revolution Global Robot and AI Primer," BofA Merrill Lynch Group, Tech. Rep. November, 2015. [Online]. Available: https://www.bofaml.com (visited on 10/10/2016).

[52] National Science Foundation, "National Robotics Initiative," [Online]. Available: https://www.nsf.gov/funding/pgm_summ.jsp?pims_id=503641 (visited on 09/01/2016).

[53] Rockin, "RoCKIn@Work," [Online]. Available: http://rockinrobotchallenge. eu/work.php (visited on 09/08/2016).

[54] Amazon Robotics, "Amazon Picking Challenge 2016," [Online]. Available: http://amazonpickingchallenge.org/ (visited on 09/08/2016).

[55] M. Bélanger-Barrette, *Collaborative Robot Ebook*, 6th edition. Robotiq, 2015. [Online]. Available: http://blog.robotiq.com/collaborative-robot-ebook.

[56] International Data Corporation (IDC), "IDC Unveils its Top 10 Predictions for Worldwide Robotics for 2017 and Beyond," 2016. [Online]. Available: https://www.idc.com/getdoc.jsp?containerId=prAP42000116 (visited on 12/20/2016).

[57] T. M. Anandan, "The Business of Automation, Betting on Robots," *Robotic Industries Association*, 2016. [Online]. Available: https://www.robotics.org/ content-detail.cfm/Industrial-Robotics-Industry-Insights/The-Business-of-Automation-Betting-on-Robots/content_id/6076 (visited on 07/06/2016).

[58] J. Payne, "Rodney Brooks speaking at the CMU Robotics Institute," *Robohub*, 2012. [Online]. Available: http://robohub.org/rodney-brooks-speaking-at-the-cmu-robotics-institute/ (visited on 03/28/2014).

[59] A. Dietrich, T. Wimböck, H. Täubig, A. Albu-Schaffer, and G. Hirzinger, "Extensions to reactive self-collision avoidance for torque and position controlled humanoids," in *Proceedings - IEEE International Conference on Robotics and Automation*, 2011, pp. 3455–3462, ISBN: 9781612843865. DOI: 10.1109/ICRA. 2011.5979862.

[60] N. Najmaei and M. R. Kermani, "Prediction-based reactive control strategy for human-robot interactions," *2010 IEEE International Conference on Robotics and Automation*, pp. 3434–3439, 2010. DOI: 10.1109/ROBOT.2010.5509179.

[61] E. a. Sisbot and R. Alami, "A Human-Aware Manipulation Planner," *IEEE Transactions on Robotics*, vol. 28, no. 5, pp. 1045–1057, 2012, ISSN: 1552-3098. DOI: 10.1109/TRO.2012.2196303.

[62] F. Zacharias, C. Schlette, F. Schmidt, C. Borst, J. Rossmann, and G. Hirzinger, "Making planned paths look more human-like in humanoid robot manipulation planning," *2011 IEEE International Conference on Robotics and Automation*, pp. 1192–1198, 2011. DOI: 10.1109/ICRA.2011.5979553.

[63] J. Aleotti, V. Micelli, and S. Caselli, "Comfortable robot to human object hand-over," *2012 IEEE RO-MAN: The 21st IEEE International Symposium on Robot and Human Interactive Communication*, pp. 771–776, 2012. DOI: 10.1109/ROMAN.2012.6343845.

[64] Shadow Robot Company, "Shadow Dexterous Hand C6P6 Technical Specification," 2010. [Online]. Available: http://www.shadowrobot.com/products/dexterous-hand/ (visited on 11/18/2012).

[65] P. Scarfe and E. Lindsay, "Air Muscle Actuated Low Cost Humanoid Hand," *International Journal of Advanced Robotic Systems*, vol. 3, no. 1, p. 1, 2006, ISSN: 1729-8806. DOI: 10.5772/5745.

[66] H. Kawasaki, T. Komatsu, and K. Uchiyama, "Dexterous anthropomorphic robot hand with distributed tactile sensor: Gifu hand ii," *IEEE/ASME Transactions on Mechatronics*, vol. 7, no. 3, pp. 296–303, 2002. DOI: 10.1109/TMECH.2002.802720.

[67] J. Ueda, Y. Ishida, M. Kondo, and T. Ogasawara, "Development of the NAIST-hand with vision-based tactile fingertip sensor," in *Proceedings - IEEE International Conference on Robotics and Automation*, vol. 2005, 2005, pp. 2332–2337, ISBN: 078038914X. DOI: 10.1109/ROBOT.2005.1570461.

[68] Shadow Robot Company, "Shadow Dexterous Hand Technical Specification," Tech. Rep. January, 2013, pp. 1–14. [Online]. Available: http://www.shadowrobot.com/wp-content/uploads/shadow_dexterous_hand_technical_specification_E1_20130101.pdf (visited on 04/08/2014).

[69] M. A. Diftler, J. S. Mehling, M. E. Abdallah, N. A. Radford, L. B. Bridgwater, A. M. Sanders, R. S. Askew, D. M. Linn, J. D. Yamokoski, F. A. Permenter, B. K. Hargrave, R. Platt, R. T. Savely, and R. O. Ambrose, "Robonaut 2 - The first humanoid robot in space," in *Proceedings - IEEE International Conference on Robotics and Automation*, vol. 1, 2011, pp. 2178–2183, ISBN: 9781612843865. DOI: 10.1109/ICRA.2011.5979830.

[70] W. Townsend, "The BarrettHand grasper - programmably flexible part handling and assembly," *The International Journal of Industrial Robot*, vol. 27, no. 3, pp. 181–188, 2000, ISSN: 0143-991X. DOI: 10.1108/01439910010371597.

[71] A. Deshpande, Z. Xu, M. Weghe, and B. Brown, "Mechanisms of the Anatomically Correct Testbed Hand," *IEEE/ASME Transactions on Mechatronics*, vol. 18, no. 1, pp. 238–250, 2011. [Online]. Available: http://ieeexplore.ieee.org/xpls/abs_all.jsp?arnumber=6032103.

[72] T. Senoo, Y. Yamakawa, S. Mizusawa, A. Namiki, M. Ishikawa, and M. Shimojo, "Skillful manipulation based on high-speed sensory-motor fusion," *2009 IEEE International Conference on Robotics and Automation*, pp. 1611–1612, 2009, ISSN: 1050-4729. DOI: 10.1109/ROBOT.2009.5152852.

[73] Boston Globe Media Partners LLC., "Unique and strange robots from Japan," 2016. [Online]. Available: http://archive.boston.com/business/technology/gallery/humanoidrobots/ (visited on 10/31/2016).

[74] H. Liu, "Exploring human hand capabilities into embedded multifingered object manipulation," *IEEE Transactions on Industrial Informatics*, vol. 7, no. 3, pp. 389–398, 2011, ISSN: 15513203. DOI: 10.1109/TII.2011.2158838.

[75] C. Yu, M. Jin, and H. Liu, "An analytical solution for inverse kinematic of 7-DOF redundant manipulators with offset-wrist," *2012 IEEE International Conference on Mechatronics and Automation*, pp. 92–97, 2012. DOI: 10.1109/ ICMA.2012.6282813.

[76] S. Patil, J. van den Berg, and R. Alterovitz, "Motion planning under uncertainty in highly deformable environments," in *Proceedings of Robotics: Science and Systems*, Los Angeles, CA, USA, 2011, pp. 241–248, ISBN: 9780262517799. DOI: 10.15607/RSS.2011.VII.033.

[77] Y. Bekiroglu, J. Laaksonen, J. A. Jorgensen, V. Kyrki, and D. Kragic, "Assessing grasp stability based on learning and haptic data," *IEEE Transactions on Robotics*, vol. 27, no. 3, pp. 616–629, 2011, ISSN: 15523098. DOI: 10.1109/TRO.2011.2132870.

[78] A. Hermann, Z. Xue, S. W. Ruhl, and R. Dillmann, "Hardware and software architecture of a bimanual mobile manipulator for industrial application," in *2011 IEEE International Conference on Robotics and Biomimetics*, 2011, pp. 2282–2288, ISBN: 978-1-4577-2138-0. DOI: 10.1109/ROBIO.2011.6181638.

[79] J. A. Alcazar and L. G. Barajas, "Dexterous robotic hand grasping method for automotive parts," in *10th IEEE-RAS International Conference on Humanoid Robots, Humanoids 2010*, 2010, pp. 282–287, ISBN: 9781424486885. DOI: 10. 1109/ICHR.2010.5686824.

[80] J. Z. Zheng, S. De La Rosa, and A. M. Dollar, "An investigation of grasp type and frequency in daily household and machine shop tasks," *2011 IEEE International Conference on Robotics and Automation*, pp. 4169–4175, 2011. DOI: 10.1109/ICRA.2011.5980366.

[81] B. Cohen, S. Chitta, and M. Likhachev, "Search-based planning for dual-arm manipulation with upright orientation constraints," *2012 IEEE International Conference on Robotics and Automation*, pp. 3784–3790, 2012. DOI: 10.1109/ ICRA.2012.6225008.

[82] B. Bäuml, F. Schmidt, T. Wimböck, O. Birbach, A. Dietrich, M. Fuchs, W. Friedl, U. Frese, C. Borst, M. Grebenstein, O. Eiberger, and G. Hirzinger, "Catching flying balls and preparing coffee: Humanoid Rollin' Justin performs dynamic and sensitive tasks," in *Proceedings - IEEE International Conference on Robotics and Automation*, 2011, pp. 3443–3444, ISBN: 9781612843865. DOI: 10.1109/ICRA.2011.5980073.

[83] L. Chang, J. R. Smith, and D. Fox, "Interactive singulation of objects from a pile," in *Proceedings - IEEE International Conference on Robotics and Automation*, 2012, pp. 3875–3882, ISBN: 9781467314039. DOI: 10.1109/ICRA. 2012.6224575.

[84] J. Falco, J Marvel, and E. Messina, "A roadmap to progress measurement science in robot dexterity and manipulation," *NIST Interagency/Internal Report (NISTIR) - 7993*,

[85]   Oxford University Press, "Dexterity," in *The Oxford English dictionary: Creel-duzepere*, J. A. Simpson and E. S. C. Weiner, Eds., 2nd edition, Clarendon Press, 1989, p. 1144, ISBN: 0198612168.

[86]   G. N. Garmonsway and J. Simpson, "Dexterity," in *The Penguin English dictionary*, 3rd edition, Allen Lane, 1979, ISBN: 0713901993.

[87]   P. B. Gove, "Dexterity," in *Webster's Third New International Dictionary of the English Language*, unabridged, Springfield, Massachusetts: Merriam-Webster Inc., 1981, ISBN: 9780877792017.

[88]   Collins, "Dexterity," in *Collins English dictionary and thesaurus*, 3rd edition, London : William Collins; HarperCollins, 2007, ISBN: 9780007252084.

[89]   K. E. Yancosek and D. Howell, "A narrative review of dexterity assessments.," *Journal of hand therapy : official journal of the American Society of Hand Therapists*, vol. 22, no. 3, 258–69; quiz 270, 2009, ISSN: 0894-1130. DOI: 10.1016/j.jht.2008.11.004.

[90]   E. A. Fleishman and G. D. Ellison, "A factor analysis of fine manipulative tests," *Journal of Applied Psychology*, vol. 46, no. 2, pp. 96–105, 1962, ISSN: 1939-1854. DOI: 10.1037/h0038499.

[91]   M Wiesendanger, "Manual dexterity and the making of tools - an introduction from an evolutionary perspective," *Experimental brain research*, vol. 128, no. 1-2, pp. 1–5, 1999, ISSN: 0014-4819. DOI: 10.1007/s002210050810.

[92]   M. Jeannerod, "The cognitive neuroscience of action.," *Trends in Cognitive Sciences*, vol. 1, p. 238, 1997, ISSN: 1548-5943 (Print). DOI: 10.1146/annurev.clinpsy.1.102803.143959.

[93]   M. a. M. Berger, A. J. Krul, and H. a. M. Daanen, "Task specificity of finger dexterity tests," *Applied Ergonomics*, vol. 40, no. 1, pp. 145–147, 2009, ISSN: 00036870. DOI: 10.1016/j.apergo.2008.01.014.

[94]   R. S. Dahiya and M. Valle, "Tactile Sensing for Robotic Applications," in *Sensors, Focus on Tactile, Force and Stress Sensors*, J. G. Rocha and S. Lanceros-Mendez, Eds., InTech, 2008, pp. 289–304, ISBN: 978- 953-7619-31-2. DOI: 10.5772/6627.

[95]   C. Backman, S. C. D. Gibson, and J. Parsons, "Assessment of Hand Function: The Relationship between Pegboard Dexterity and Applied Dexterity," *Canadian Journal of Occupational Therapy*, vol. 59, no. 4, pp. 208–213, 1992, ISSN: 0008-4174. DOI: 10.1177/000841749205900406.

[96]   Patterson Medical, "Dexterity and Sensory Assessments," 2015. [Online]. Available: http://www.pattersonmedical.com/app.aspx?cmd=get_subsections&id=57784 (visited on 12/10/2015).

[97]   North Coast Medical Inc., "Hand and Dexterity Evaluation," 2015. [Online]. Available: https://www.ncmedical.com/categories/Hand--Dexterity_12839559.html (visited on 12/10/2015).

[98]   University of Alabama at Birmingham, "Minnesota Rate of Manipulation two-hand turning and placing subtest," 2014. [Online]. Available: https://www.youtube.com/watch?v=Y-xYTsrOc0A (visited on 12/10/2015).

[99] S.I. Instruments, "Dexterity Testing," 2013. [Online]. Available: https://www.youtube.com/watch?v=C7Ciu2b0ApQ (visited on 12/10/2015).

[100] Graduate Institute of Rehabilitation Counseling, National Taiwan Normal University, "Assessment tools / aids," 2015. [Online]. Available: http://www.girc.ntnu.edu.tw/page2/super_pages.php?ID=page201 (visited on 12/10/2015).

[101] C. Oberle, "Modified Wolf Motor Function Test Rating," 2015. [Online]. Available: http://www.youtube.com/watch?v=MsfrGauYHfc (visited on 12/10/2015).

[102] C. Marcus, "9 Hole Peg Test, Jebsen Test of Hand Function, part 1," 2011. [Online]. Available: http://www.youtube.com/watch?v=DWz-Tvi8i-Q (visited on 12/10/2015).

[103] M. Kimmerle, L. Mainwaring, and M. Borenstein, "The functional repertoire of the hand and its application to assessment," *American Journal of Occupational Therapy*, vol. 57, no. 5, pp. 489–498, 2003, ISSN: 02729490. DOI: 10.5014/ajot.57.5.489.

[104] M. McDonnell, "Action research arm test.," *The Australian journal of physiotherapy*, vol. 54, no. 3, p. 220, 2008, ISSN: 00049514. DOI: 10.1016/S0004-9514(08)70034-5.

[105] MedStar National Rehabilitation Hospital, "Arm Amputee Program - Cross Sectional Study," 2014. [Online]. Available: http://armamputee.org/cross-sectional (visited on 01/15/2014).

[106] J. M. Hollerbach, "Workshop on the Design and Control of Dextrous Hands," Massachusetts Institute of Technology, Tech. Rep., 1982. [Online]. Available: http://hdl.handle.net/1721.1/5688.

[107] I. M. Bullock, R. R. Ma, and A. M. Dollar, "A hand-centric classification of human and robot dexterous manipulation," *IEEE Transactions on Haptics*, vol. 6, no. 2, pp. 129–144, 2013, ISSN: 19391412. DOI: 10.1109/TOH.2012.53.

[108] A. Bicchi, "Hands for dexterous manipulation and robust grasping: A difficult road toward simplicity," *IEEE Transactions on Robotics and Automation*, vol. 16, no. 6, pp. 652–662, 2000, ISSN: 1042296X. DOI: 10.1109/70.897777.

[109] Z. Li, J. F. Canny, and S. Sastry, "On motion planning for dexterous manipulation. I. The problem formulation," *IEEE International Conference on Robotics and Automation*, no. 3, pp. 775–780, 1989. DOI: 10.1109/ROBOT.1989.100078.

[110] A. M. Okamura, N. Smaby, and M. R. Cutkosky, "An Overview of Dexterous Manipulation," *IEEE International Conference on Robotics and Automation*, vol. 1, no. April, 255–262 vol.1, 2000, ISSN: 1050-4729. DOI: 10.1109/ROBOT.2000.844067.

[111] C. A. Klein and B. E. Blaho, "Dexterity Measures for the Design and Control of Kinematically Redundant Manipulators," *The International Journal of Robotics Research*, vol. 6, no. 2, pp. 72–83, 1987, ISSN: 0278-3649. DOI: 10.1177/027836498700600206.

[112]   R. Sturges, "A Quantification of Machine Dexterity Applied to an Assembly Task," *The International Journal of Robotics Research*, vol. 9, no. 3, pp. 49–62, 1990, ISSN: 0278-3649. DOI: 10.1177/027836499000900303.

[113]   A Kumar and K. J. Waldron, "The Workspaces of a Mechanical Manipulator," *Journal of Mechanical Design*, vol. 103, no. 3, p. 665, 1981, ISSN: 10500472. DOI: 10.1115/1.3254968.

[114]   S. Patel and T. Sobh, "Manipulator Performance Measures - A Comprehensive Literature Survey," *Journal of Intelligent and Robotic Systems: Theory and Applications*, pp. 1–24, 2014, ISSN: 09210296. DOI: 10.1007/s10846-014-0024-y.

[115]   S. Jeong and T. Takahashi, "Unified evaluation index of safety and dexterity of a human symbiotic manipulator," *Advanced Robotics*, vol. 27, no. 5, pp. 393–405, 2013, ISSN: 0169-1864. DOI: 10.1080/01691864.2013.763745.

[116]   International Organization for Standardization, "Manipulating industrial robots - Performance criteria and related test methods (ISO 9283:1998)," *UNE EN ISO 9283:1998*, 1998.

[117]   M. Cutkosky, "On grasp choice, grasp models, and the design of hands for manufacturing tasks," *Robotics and Automation, IEEE Transactions on*, vol. 5, no. 3, 1989. DOI: 10.1109/70.34763.

[118]   I. M. Bullock and A. M. Dollar, "Classifying human manipulation behavior," in *IEEE International Conference on Rehabilitation Robotics*, vol. 2011, 2011, p. 5 975 408, ISBN: 9781424498628. DOI: 10.1109/ICORR.2011.5975408.

[119]   European Robotics Research Network (EURON), "Benchmarking Initiative: Manipulation and Grasping," 2008. [Online]. Available: http://www.euron.org/activities/benchmarks/grasping (visited on 12/14/2013).

[120]   G. Kragten, "Underactuated hands: Fundamentals, performance analysis and design," Doctoral Thesis, TU Delft, Delft University of Technology, 2011, ISBN: 9789461690913.

[121]   M. a. Saliba and C. Ellul, "Dexterous actuation," *Mechanism and Machine Theory*, vol. 70, pp. 45–61, 2013, ISSN: 0094114X. DOI: 10.1016/j.mechmachtheory.2013.06.012.

[122]   P. Wright, J. Demmel, and M. Nagurka, "The Dexterity of Manufacturing Hands," *Robotics Research DSC*, vol. 14, no. ASME Winter Annual Meeting, pp. 157–163, 1989.

[123]   European Commission, "Deliverable D6.2 - Report on the experimental results," European Commission, Tech. Rep., 2012. [Online]. Available: http://www.dexmart.eu/fileadmin/dexmart/public_website/downloads/216239_D6-2_Report_on_experimental_results.pdf.

[124]   P. J. Kyberd, A. Murgia, M. Gasson, T. Tjerks, and C. Metcalf, "Case studies to demonstrate the range of applications of the Southampton Hand Assessment Procedure," *The British Journal of Occupational Therapy*, vol. 72, no. 5, pp. 212–218, 2009, ISSN: 03080226.

[125] B. B. Calli, A. Walsman, A. Singh, and S. Srinivasa, "Benchmarking in Manipulation Research: Using the YaleCMUBerkeley Object and Model Set," *IEEE Robotics and Automation Magazine*, no. September, pp. 36–52, 2015. DOI: 10.1109/MRA.2015.2448951.

[126] R. H. Sturges and P. K. Wright, "A quantification of dexterity," *Robotics and Computer Integrated Manufacturing*, vol. 6, no. 1, pp. 3–14, 1989, ISSN: 07365845. DOI: 10.1016/0736-5845(89)90080-X.

[127] National Institute of Standards and Technology (NIST), "Performance Assessment Framework for Robotic Systems," EN-US, 2014. [Online]. Available: http://www.nist.gov/el/isd/ms/pafrs.cfm (visited on 09/10/2014).

[128] M. Shneier, E. Messina, C. Schlenoff, F. Proctor, T. Kramer, and J. Falco, "Measuring and Representing the Performance of Manufacturing Assembly Robots," *NISTIR 8090*, vol. November, 2015. DOI: 10.6028/NIST.IR.8090.

[129] National Institute of Standards and Technology (NIST), "Performance Metrics and Benchmarks to Advance the State of Robotic Grasping," 2014. [Online]. Available: https://www.nist.gov/programs-projects/performance-metrics-and-benchmarks-advance-state-robotic-grasping (visited on 09/17/2016).

[130] Lund Research Ltd., "Understanding the Different Types of Variable in Statistics," *Laerd Statistics*, 2013. [Online]. Available: https://statistics.laerd.com/statistical-guides/types-of-variable.php (visited on 10/20/2016).

[131] B. Everitt, *The Cambridge Dictionary of Statistics*, 9. 2013, vol. 53, pp. 1689–1699, ISBN: 9788578110796. DOI: 10.1017/CBO9781107415324.004. arXiv: arXiv:1011.1669v3.

[132] PennState Eberly College of Science, "Review of Basic Statistical Concepts," *Pennsylvania State University*, 2016. [Online]. Available: https://onlinecourses.science.psu.edu/statprogram/review_of_basic_statistics (visited on 10/05/2016).

[133] J. Frost, "Understanding Hypothesis Tests: Significance Levels (Alpha) and P values in Statistics," *Minitab*, 2015. [Online]. Available: http://blog.minitab.com/blog/adventures-in-statistics-2/understanding-hypothesis-tests:-significance-levels-alpha-and-p-values-in-statistics (visited on 10/10/2016).

[134] ISixSigma, "Hypothesis Testing," 2014. [Online]. Available: https://www.isixsigma.com/tools-templates/hypothesis-testing/ (visited on 10/10/2016).

[135] S. Surbhi, "Difference Between Sample Mean and Population Mean," 2016. [Online]. Available: http://keydifferences.com/difference-between-sample-mean-and-population-mean.html (visited on 10/10/2016).

[136] T. Hill and P. Lewicki, "Statistics : Methods and Applications," in *StatSoft Inc.* Vol. 1, StatSoft, Inc., 2007, pp. 1–719, ISBN: 1884233597. DOI: 10.1016/B978-0-323-03707-5.50024-3.

[137] GraphPad Software Inc., "GraphPad Statistics Guide," 2015. [Online]. Available: http://www.graphpad.com/guides/prism/6/statistics/index.htm?stat_more_about_confidence_interval.htm (visited on 04/18/2016).

[138]   E. Lehmann, "Nonparametrics: Statistical methods based on ranks," *Prentice Hall New Jersey*, p. 463, 1998, ISSN: 00033472. DOI: 10.1016/0003-3472(79) 90214-8.

[139]   W. J. Conover, "A Kolmogorov Goodness-of-Fit Test for Discontinuous Distributions," *Journal of the American Statistical Association*, vol. 67, no. 339, pp. 591–596, 1972, ISSN: 0162-1459. DOI: 10.1080/01621459.1972.10481254.

[140]   D. Gilliam, S. Leigh, A. Rukhin, and W Strawderman, "Pass-fail testing: Statistical requirements and interpretations," *J. Res. Nat. Inst. Stand. Technol.*, vol. 114, no. 3, pp. 195–199, 2009, ISSN: 1044677X.

[141]   K. G. Wilson, "Some notes on theoretical constructs: Types and validation from a contextual behavioral perspective," *Revista Internacional de Psicología y Terapia Psicológica*, vol. 1, no. 2, pp. 205–215, 2001.

[142]   L. Cohen, L. Manion, and K. Morrison, *Research methods in education*, 7th edition. Routledge, 2013, ISBN: 978-0415583350.

[143]   J. Hogan, P. Dolan, and P. Donnelly, "Introduction: Approaches to Qualitative Research," *Approaches to Qualitative Research: Theory and Its Practical Application*, pp. 1–8, 2009. [Online]. Available: http://arrow.dit.ie/cgi/viewcontent.cgi?article=1013{\&}context=buschmarbk.

[144]   S. Wyse, "What is the Difference between Qualitative Research and Quantitative Research?," 2011. [Online]. Available: https://www.snapsurveys.com/blog/what-is-the-difference-between-qualitative-research-and-quantitative-research/.

[145]   O. Foley, "Information quality and diverse information systems situations," PhD thesis, Dublin City University, 2011.

[146]   K. Peffers, T. Tuunanen, M. A. Rothenberger, and S. Chatterjee, "A Design Science Research Methodology for Information Systems Research," *Journal of Management Information Systems*, vol. 24, no. 3, pp. 45–77, 2007, ISSN: 0742-1222. DOI: 10.2753/MIS0742-1222240302.

[147]   P. D. Bromley, "Academic contributions to psychological counselling. 1. a philosophy of science for the study of individual cases," *Counselling psychology quarterly*, vol. 3, no. 3, pp. 299–307, 1990.

[148]   D. M. Zucker, "How to do case study research," *Teaching Research Methods in the Humanities and Social Sciences*, vol. 2, 2009. [Online]. Available: http://scholarworks.umass.edu/nursing_faculty_pubs/2.

[149]   R. K. Yin, *Case study research: Design and methods*, 5th edition. SAGE publications, 2013, ISBN: 9781452242569.

[150]   L Biagiotti, F Lotti, C Melchiorri, and G Vassura, "How Far Is the Human Hand? A Review on Anthropomorphic Robotic End-effectors Basic concepts," p. 21, 2004.

[151]   P. Hunter, "Margin of Error and Confidence Levels Made Simple," 2010. [Online]. Available: https://www.isixsigma.com/tools-templates/sampling-data/margin-error-and-confidence-levels-made-simple/ (visited on 10/02/2016).

[152]   Universal Robots, [Online]. Available: https://www.universal-robots.com (visited on 10/20/2016).

[153]   R. Bischoff, J. Kurth, G. Schreiber, R. Koeppe, A. Albu-Schäffer, A. Beyer, O. Eiberger, S. Haddadin, A. Stemmer, G. Grunwald, *et al.*, "The kuka-dlr lightweight robot arm-a new reference platform for robotics research and manufacturing," in *Robotics (ISR), 2010 41st international symposium on and 2010 6th German conference on robotics (ROBOTIK)*, VDE, 2010, pp. 1– 8.

[154]   Rethink Robotics, "Baxter," [Online]. Available: http://www.rethinkrobotics. com/baxter (visited on 10/20/2016).

[155]   K. Chen, "Application of the ISO 9283 standard to test repeatability of the Baxter robot," PhD thesis, University of Illinois, 2015.

[156]   SCHUNK GmbH & Co., "KGG 80-30," [Online]. Available: https://schunk. com/de_en/gripping-systems/product/2739-0303060-kgg-80-30 (visited on 10/21/2016).

[157]   Robotiq, "3 Finger Adaptive Robotic Gripper," [Online]. Available: http: //robotiq.com/products/industrial-robot-hand (visited on 10/21/2016).

[158]   SimLab, "Allegro Hand," [Online]. Available: http://www.simlab.co.kr/ Allegro-Hand.htm (visited on 10/21/2016).

[159]   K. V. Wyk, "Grasping and Manipulation Force Control for Coordinating Multi-Manipulator Robotic Systems with Proprioceptive Feedback," PhD thesis, University of Florida, 2014, pp. 1–208.

[160]   B. Wang, W. Shi, and Z. Miao, "Confidence analysis of standard deviational ellipse and its extension into higher dimensional Euclidean space," *PLoS ONE*, vol. 10, no. 3, pp. 1–17, 2015, ISSN: 19326203. DOI: 10.1371/journal.pone. 0118537.

[161]   MathWorks, "Multivariate Normal Distribution," 2016. [Online]. Available: https://uk.mathworks.com/help/stats/multivariate-normal-distribution. html (visited on 09/12/2016).

[162]   G. Upton and I. Cook, *A Dictionary of Statistics*. Oxford University Press, 2008, p. 512, ISBN: 978-0-19-954145-4. DOI: 10.1093/acref/9780199541454.001. 0001.

[163]   Cognex, "VisionPro Machine Vision Software," 2016. [Online]. Available: http://www.cognex.com/ (visited on 04/02/2016).

[164]   ISO, "Accuracy (trueness and precision) of measurement methods and results - Part 1: General principles and definitions," vol. 1998, pp. 30–31, 1994.

[165]   A. Menditto, M. Patriarca, and B. Magnusson, "Understanding the meaning of accuracy, trueness and precision," *Accreditation and Quality Assurance*, vol. 12, no. 1, pp. 45–47, 2007, ISSN: 09491775. DOI: 10.1007/s00769-006-0191-z.

[166]   J. A. Marvel and K. V. Wyk, "Simplified Framework for Robot Coordinate Registration for Manufacturing Applications," *2016 IEEE International Symposium on Assembly and Manufacturing (ISAM)*, DOI: 10.1109/ISAM.2016. 7750718.

[167]   M. Ribeiro, "Gaussian probability density functions: Properties and error characterization," Institute for Systems and Robotics, Lisboa, Portugal, Tech. Rep., 2004, pp. 1–30. [Online]. Available: http://hans.fugal.net/comps/ papers/ribeiro_2004.pdf.

[168]   J. L. Nevins and D. E. Whitney, "Robot assembly research and its future applications," in *Computer Vision Sensor-Based Robots*, G. G. Dodd and L. Rossol, Eds., Warren, Michigan: Plenum Press, 1979, pp. 275 –322, ISBN: 978-1-4613-3029-5. DOI: 10.1007/978-1-4613-3027-1.

[169]   S. Chhatpar and M. Branicky, "Search strategies for peg-in-hole assemblies with position uncertainty," *Proceedings 2001 IEEE/RSJ International Conference on Intelligent Robots and Systems*, vol. 3, pp. 1465–1470, 2001. DOI: 10.1109/IROS.2001.977187.

[170]   D. Deiterding, Jan; Hendrich, "Probability-Based Robot Search Paths," in *Advances in Robotics Research*, Springer, 2008, pp. 31–42.

[171]   M. A. Habib, M. S. Alam, and N. H. Siddique, "Optimizing coverage performance of multiple random path-planning robots," *Paladyn*, vol. 3, no. 1, pp. 11–22, 2012, ISSN: 2080-9778. DOI: 10.2478/s13230-012-0012-5.

[172]   W. H. Press, S. A. Teukolsky, W. T. Vetterling, and B. P. Flannery, "Quasi-(that is, Sub-) Random Sequences," in *Numerical Recipes in C: The Art of Scientific Computing*, 2nd edition, Cambridge University Press, 1992, ch. 7, pp. 309 –315, ISBN: 0521431085.

[173]   G. Betts, "Minnesota Rate of Manipulation Test: Examiner's Manual," Tech. Rep., 1946.

[174]   L. R. Surrey, K. Nelson, C. Delelio, D. Mathie-Majors, N. Omel-Edwards, J. Shumaker, and G. Thurber, "A comparison of performance outcomes between the Minnesota Rate of Manipulation Test and the Minnesota Manual Dexterity Test.," *Work (Reading, Mass.)*, vol. 20, no. 2, pp. 97–102, 2003, ISSN: 1051-9815.

[175]   J. MacDermid, "Outcome Measurement in Upper Extremity Practice," in *Rehabilitation of the Hand and Upper Extremity, 2-Volume Set: Expert Consult*, T. M. Skirven, A. L. Osterman, J. Fedorczyk, and P. C. Amadio, Eds., 6th edition, Elsevier Mosby, 2011, pp. 194–205, ISBN: 0323081266.

[176]   K. Al-Saleh, "Predetermined time systems," *King Saud University*, pp. 1–21, 2008. [Online]. Available: http://faculty.ksu.edu.sa/alsaleh/Pages/ 441(DesignandMeasurementofWork).aspx (visited on 06/05/2016).

[177]   P. Bratley and B. L. Fox, "ALGORITHM 659: implementing Sobol's quasirandom sequence generator," *ACM Transactions on Mathematical Software*, vol. 14, no. 1, pp. 88–100, 1988, ISSN: 00983500. DOI: 10.1145/42288.214372.

[178]   S. Joe and F. Y. Kuo, "Notes on generating Sobol' sequences," 2008. [Online]. Available: http://web.maths.unsw.edu.au/$\sim$fkuo/sobol/joe-kuo-notes.pdf (visited on 08/14/2016).

Appendix A

MTM-1 Basic Movement Tables

The currently valid version of the *MTM* system's *MTM-1* metric card is the *MTM-Data-Card 101 A*, 1955 edition, of the U.S. and Canada MTM Association. Within this system, there are five fundamental motions identified:

1. Reach

2. Grasp

3. Move

4. Position

5. Release

A.1 Reach

The movements of an empty hand to the object (equivalent to approach action). The time of this movement is influenced by the length of motion, the object, and surrounding conditions. These factors give rise to five reach cases:

- Case A: Reach to object in fixed location or in other hand

- Case B: Reach to single object in location which may vary slightly

- Case C: Reach to object jumbled with other objects in a group

- Case D: Reach to a very small object or where accurate grasp is required

- Case E: Reach to indefinite location to get hand in position for next motion / body balance / out of way.

Also, there are two addition cases depending on the requirement for hand motion:

- Case A: Hand in motion at the start or end of reach

- Case B: Hand in motion at the start and end of reach

Table A.1: Normal time values for MTM-1 motion element 'Reach' [176].

Distance Moved in Inches	Time TMU				Hand in Motion	
	A	B	C or D	E	A	B
3/4 or less	2.0	2.0	2.0	2.0	1.6	1.6
1	2.5	2.5	3.6	2.4	2.3	2.3
2	4.0	4.0	5.9	3.8	3.5	2.7
3	5.3	5.3	7.3	5.3	4.5	3.6
4	6.1	6.4	8.4	6.8	4.9	4.3
5	6.5	7.8	9.4	7.4	5.3	5.0
6	7.0	8.6	10.1	8.0	5.7	5.7
7	7.4	9.3	10.8	8.7	6.1	6.5
8	7.9	10.1	11.5	9.3	6.5	7.2
9	8.3	10.8	12.2	9.9	6.9	7.9
10	8.7	11.5	12.9	10.5	7.3	8.6
12	9.6	12.9	14.2	11.8	8.1	10.1
14	10.5	14.4	15.6	13.0	8.9	11.5
16	11.4	15.8	17.0	14.2	9.7	12.9
18	12.3	17.2	18.4	15.5	10.5	14.4
20	13.1	18.6	19.8	16.7	11.3	15.8
22	14.0	20.1	21.2	18.0	12.1	17.3
24	14.9	21.5	22.5	19.2	12.9	18.8
26	15.8	22.9	23.9	20.4	13.7	20.2
28	16.7	24.4	25.3	21.7	14.5	21.7
30	17.5	25.8	26.7	22.9	15.3	23.2
Additional per inch over 30 inches	0.4	0.7	0.7	0.6		

A.2 Grasp

The motion used to obtain one or more objects, bringing it under control. The grasp movement is mainly influenced by the object's properties, giving rise to five grasp cases:

- Case A: Pick-up

- Case B: Re-grasp

- Case C: Transfer

- Case D: Select

- Case E: Contact

Table A.2: Normal time values for MTM-1 motion element 'Grasp' [176].

Type of Grasp	Case	Time TMU	Description	
Pick-UP	1A	2.0	Any size object by itself, easily grasped.	
	1B	3.5	Object very small or lying close against a flat surface.	
	1C1	7.3	Diameter Larger than ½"	Interference with Grasp on bottom and one side of nearly cylindrical object.
	1C2	8.7	Diameter 1/4" to 1/2"	
	1C3	10.8	Diameter Less than 1/4"	
Regrasp	2	5.6	Change grasp without relinquishing control.	
Transfer	3	5.6	Control transferred from one hand to the other.	
Select	4A	7.3	Larger than 1 x1 x1	Object jumbled with other objects so that search and select occur.
	4B	9.1	1/4 x1/4 x1/8 to 1 x1 x1	
	4C	12.9	Smaller than 1/4 x1/4 x1/8	
Contact	5	0	Contact, Sliding, or Hook Grasp.	

A.3 Move

Similar to the reach movement only that the hand is now holding the object (equivalent to transport action). The time required for this movement is influenced by the length of motion, the nature of the destination, and the object's properties (e.g. weight factor). These factors give rise to three move cases:

- Case A: Move object to other hand or against stop

- Case B: Move object to an approximate or indefinite location

- Case C: Move object to an exact location

As with reach, the move movement has an additional case if hand movement is required at the start or end of the motion. Also, depending on the object's weight, there may be a dynamic factor and static constant added to the movements' completion time.

Table A.3: Normal time values for MTM-1 motion element 'Move' [176].

Distance moved in Inches	Time TMU				Wt. Allowance		
	A	B	C	Hand In Motion B	Wt. (lb). Up to	Dynamic Factor	Static Constant TMU
¾ OR LESS	2.0	2.0	2.0	1.7	2.5	1.00	0
1	2.5	2.9	3.4	2.3			
2	3.6	4.6	5.2	2.9	7.5	1.06	2.2
3	4.9	5.7	6.7	3.6			
4	6.1	6.9	8.0	4.3	12.5	1.11	3.9
5	7.3	8.0	9.2	5.0			
6	8.1	8.9	10.3	5.7	17.5	1.17	5.6
7	8.9	9.7	11.1	6.5			
8	9.7	10.6	11.8	7.2	22.5	1.22	7.4
9	10.5	11.5	12.7	7.9			
10	11.3	12.2	13.5	8.6	27.5	1.28	9.1
12	12.9	13.4	15.2	10.0			
14	14.4	14.6	16.9	11.4	32.5	1.33	10.8
16	16.0	15.8	18.7	12.8			
18	17.6	17.0	20.4	14.2	37.5	1.39	12.5
20	19.2	18.2	22.1	15.6			
22	20.8	19.4	23.8	17.0	42.5	1.44	14.3
24	22.4	20.6	25.5	18.4			
26	24.0	21.8	27.3	19.8	47.5	1.50	16.0
28	25.5	23.1	29.0	21.2			
30	27.1	24.3	30.7	22.7			
Additional	0.8	0.6	0.85		TMU per inch over 30 inches		

A.4   Position

The motions required to align, orient and mate two objects (equivalent to the insertion action), where the motions are too minor to be classified separately. The time required to position is dependent on the case of fit (tolerance), insertion symmetry (symmetric, semi-symmetric, non-symmetric), and ease of handling.

Table A.4: Normal time values for MTM-1 motion element 'Position' [176].

Class of Fit	Symmetry	Easy to Handle	Difficult to Handle
1 Loose	S	5.6	11.2
	SS	9.1	14.7
	NS	10.4	16.0
2 Close	S	16.2	21.8
	SS	19.7	25.3
	NS	21.0	26.6
3 Exact	S	43.0	48.6
	SS	46.5	52.1
	NS	47.8	53.4
Supplementary Rule for Surface Alignment			
P1SE per alignment: >1/16 1/4		P2SE per alignment: 1/16	

A.5 Release

The discharging of control of an object by the hand. This movement has two cases:

- Case 1: Normal release by opening of fingers

- Case 2: Contact release where the release begins and is completed the instant the following reach movement begins

Table A.5: Normal time values for MTM-1 motion element 'Release' [176].

Case	Time TMU	Description
1	2.0	Normal release performed by opening fingers as independent motion
2	0	Contact Release

Appendix B

Sobol' Sequence

The description of the Sobol' sequence and its underlying equations presented in this section are based on the work in [172], [177], [178].

For each component of the n-dimensional Sobol sequence, numbers are generated between zero and one directly as binary fractions of length w bits [172]. For the kth component of the sequence ($0 < k \leq n$), these numbers are generated using a set of w special binary fractions $V_{i,k}$, $i = 1, 2, ..., w$ known as *direction numbers*.

The direction numbers $V_{i,k}$ differ for each component of the n-dimensional Sobol sequence, and are based on a different primitive polynomial over the integers modulo 2 (a polynomial whose coefficients are either 0 or 1 and which generates a maximal length shift register sequence). For the kth component of the sequence, a primitive polynomial P of degree q_k is defined:

$$P = x^{q_k} + a_{1,k}x^{q_k-1} + a_{2,k}x^{q_k-2} + ... + a_{q_k-1,k}x + 1 \tag{B.1}$$

where the coefficients $a_{1,k}, a_{2,k}, ..., a_{q_k-1,k}$ are either 0 or 1 and the coefficient $a_{q_k,k}$ equals 1 since P is primitive. From this a sequence of positive integers $M_{i,j}$ can be defined by the q_k-term recurrence relation:

$$M_{i,k} = 2a_{1,k}M_{i-1,k} \oplus 2^2 a_{2,k}M_{i-2,k} \oplus ... \oplus 2^{q_k-1}a_{q_k-1,k}M_{i-q_k+1,k} \oplus 2^{q_k}M_{i-q_k,k} \oplus M_{i-q_k,k}$$

$$\tag{B.2}$$

where $\oplus$ is the bitwise *exclusive or* operator, *XOR*. The starting values of $M_{1,k}$, $M_{2,k}$, ..., $M_{q_k,k}$ can be chosen freely provided each $M_{i,k}$ is odd and less than $2, 2^2, ..., 2^{q_k}$

respectively.

From this sequence of positive integers, the direction numbers V_i are given by:

$$V_{i,k} = \frac{M_{i,k}}{2^i} \qquad i = 1, 2, ..., w \tag{B.3}$$

As a short example of its execution, consider the primitive polynomial with degree $q_k = 3$, $a_{1,k} = 0$ and $a_{2,k} = 1$ is:

$$x^3 + x + 1 \tag{B.4}$$

The corresponding recurrence for this primitive polynomial is:

$$M_{i,k} = 4M_{i-2,k} \oplus 8M_{i-3,k} \oplus M_{i-3,k} \tag{B.5}$$

Starting with $M_{1,k} = 1$, $M_{2,k} = 3$, and $M_{3,k} = 7$ (whose values are odd and less than 2,4, and 8 respectively), Equation B.5 can be used to calculate $M_{4,k} = 5$, $M_{5,k} = 7$, $M_{6,k} = 43$, etc. For clarity, the calculation for $M_{4,k}$ is done by long-hand below.

$$M_{4,k} = 4M_{2,k} \oplus 8M_{1,k} \oplus M_{1,k}$$

$$M_{4,k} = 12 \oplus 8 \oplus 1$$

$$M_{4,k} = (1100)_2 \oplus (1000)_2 \oplus (0001)_2 = (0101)_2 \qquad in\ binary$$

$$M_{4,k} = 5$$

These values give the direction numbers:

$$V_{1,k} = 1/2 = (0.1)_2 \qquad\qquad V_{2,k} = 3/4 = (0.11)_2$$

$$V_{3,k} = 7/8 = (0.111)_2 \qquad\qquad V_{4,k} = 5/16 = (0.0101)_2$$

$$V_{5,k} = 7/32 = (0.00111)_2 \qquad\qquad V_{6,k} = 43/64 = (0.101011)_2$$

$$etc.$$

Using the original method, the jth number of the kth component of the Sobol sequence is generated by the equation:

$$X_{j,k} = b_1 V_{1,k} \oplus b_2 V_{2,k} \oplus ... \tag{B.6}$$

where $(...b_3b_2b_1)_2$ is the binary representation of j. However, a more computationally efficient approach has been developed by Antonov and Saleev. In this variant, the jth number of the kth component of the Sobol sequence is generated by the equation:

$$X_{j,k} = g_1V_{1,k} \oplus g_2V_{2,k} \oplus ... \tag{B.7}$$

where $(...g_3g_2g_1)_2$ is the Gray code representation of j. The Gray code, or reflected binary code (RBC), is a binary numeral system where two successive values $G(j)$ and $G(j+1)$ differ in only one bit position. The Gray code for j, $G(j)$, is obtained from a bitwise XOR of the binary representation of j and a version of j that has been right-shifted by one bit position i.e.

$$G(j) = (...g_3g_2g_1)_2 = (...b_3b_2b_1)_2 \oplus (...b_4b_3b_2)_2 \tag{B.8}$$

e.g. The Gray code for 43 is calculated as follows:

$$G(43) = (101011)_2 \oplus (010101)_2 = (111110)_2$$

Using the properties of the Gray code and Equation B.7, the $(j+1)^{st}$ number of the kth component of the Sobol sequence, $X_{j+1,k}$, can be determined by performing an bitwise XOR of $X_{j,k}$ and a single $V_{i,k}$, where i corresponds to the position of the rightmost zero bit in the binary representation of j, which is the bit that changes between $G(j)$ and $G(j+1)$.

$$X_{j+1,k} = X_{j,k} \oplus V_{i,k} \tag{B.9}$$

Continuing the previous example, the first four numbers of the kth component of the Sobol sequence are:

$$X_{0,k} = 0$$

$$\curvearrowright$$

$$j = 0 = (0)_2 \qquad i = 1$$

$$X_{1,k} = X_{0,k} \oplus V_{1,k} = (0.0)_2 \oplus (0.1)_2 = (0.1)_2 \qquad \textit{in binary}$$

$$X_{1,k} = 1/2 = 0.5$$

$$\curvearrowright$$

$$j = 1 = (1)_2 \qquad i = 2$$

$$X_{2,k} = X_{1,k} \oplus V_{2,k} = (0.1)_2 \oplus (0.11)_2 = (0.01)_2 \qquad \textit{in binary}$$

$$X_{2,k} = 1/4 = 0.25$$

$$\curvearrowright$$

$$j = 2 = (10)_2 \qquad i = 1$$

$$X_{3,k} = X_{2,k} \oplus V_{1,k} = (0.01)_2 \oplus (0.10)_2 = (0.11)_2 \qquad \textit{in binary}$$

$$X_{3,k} = 3/4 = 0.75$$

$$\curvearrowright$$

$$j = 3 = (11)_2 \qquad i = 3$$

$$X_{4,k} = X_{3,k} \oplus V_{3,k} = (0.110)_2 \oplus (0.111)_2 = (0.001)_2 \qquad \textit{in binary}$$

$$X_{4,k} = 1/8 = 0.125$$

$$\textit{etc.}$$

The code for generating the two-dimensional Sobol' sequence is given below, and is based on the multi-dimensional Sobol' sequence code given in [172].

```c
void sobseq(double *x, double *y, int init)
//Generates a Sobol sequence of random numbers; returns as the vector x[1..n] the↩
     next values from n of these sequences
//int n: number of pseudo random numbers to generate
//x[]: stores array of pseudo random numbers
//Modified from "Numerical Recipes in C" (https://www2.units.it/ipl/students_area↩
    /imm2/files/Numerical_Recipes.pdf)
{
  int j, k, l;
  unsigned long i, im, ipp;
  static float fac;
  static unsigned long in, ix[3], *iu[MAXBIT + 1];
  static unsigned long mdeg[3] = {0,1,2};
  static unsigned long ip[3] = { 0,0,1};
  static unsigned long iv[2*MAXBIT + 1] = ↩
      {0,1,1,1,1,1,1,3,1,3,3,1,1,5,7,7,3,3,5,15,11,5,15,13,9};

  if (init==0) {  //Initialize the generator the first time the function is ↩
      called
    for (k = 1; k <= 2; k++)
      ix[k] = 0;
    in = 0;
    if (iv[1] != 1)
      return;
    fac = 1.0 / (1L << MAXBIT);
    for (j = 1, k = 0; j <= MAXBIT; j++, k += 2)
      iu[j] = &iv[k];
    //To allow both 1D and 2D addressing.
    for (k = 1; k <= 2; k++) {
      for (j = 1; j <= mdeg[k]; j++)
        iu[j][k] <<= (MAXBIT - j);
      //Stored values only require normalization.
      for (j = mdeg[k] + 1; j <= MAXBIT; j++) {
        //Use the recurrence to get other values.
        ipp = ip[k];
        i = iu[j - mdeg[k]][k];
        i ^= (i >> mdeg[k]);
        for (l = mdeg[k] - 1; l >= 1; l--) {
          if (ipp & 1)
            i ^= iu[j - l][k];
          ipp >>= 1;
          }
          iu[j][k] = i;
        }
      }
    }
  //Calculate the pair of numbers in the 2D Sobol Sequence
  im = in++;
  for (j = 1; j <= MAXBIT; j++) { //Find the rightmost zero bit.
    if (!(im & 1)) break;
    im >>= 1;
  }
  if (j > MAXBIT)
    printf("MAXBIT too small in sobseq");
  im = (j - 1)*2;
  ix[1] ^= iv[im + 1];
  ix[2] ^= iv[im + 2];
  *x = (double)(ix[1] * fac);
  *y = (double)(ix[2] * fac);
}
```

Appendix C

MATLAB Code for Analysing Continuous Data

This appendix provides an example of the MATLAB code used to perform the two-sample KS Test and to calculate the detectable difference between multiple datasets that were recorded during testing. In this instance, the MATLAB code is used to compare six different datasets, which are loaded in from the excel file *'Recorded_Results.xlsx'*. The results of each comparison i.e. the KS test outcome and the calculated detectable difference, are stored within cell arrays during the program's execution and subsequently exported to their corresponding sheet within the excel file *'Data_Analysis_Results.xlsx'*.

```matlab
clear all; close all;

save = true; %Save calculations to file
num = 6; %Number of test iterations
h_table = cell(num,num); %Table to store results of KS test
true_means = zeros(num, 2); %Mean and tolerable error of each test
true_means_table = cell(num,num); %Table to store detectable distances

data = cell(1,num); %Cell for storing recorded test data

%Read in recorded data (60 test iterations in this example)
data{1} = xlsread('Recorded_Results.xlsx','Sheet 1','A1:A60');
data{2} = xlsread('Recorded_Results.xlsx','Sheet 1','B1:B60');
data{3} = xlsread('Recorded_Results.xlsx','Sheet 1','C1:C60');
data{4} = xlsread('Recorded_Results.xlsx','Sheet 1','D1:D60');
data{5} = xlsread('Recorded_Results.xlsx','Sheet 1','E1:E60');
data{6} = xlsread('Recorded_Results.xlsx','Sheet 1','F1:F60');

%Calculate true mean and tolerable error
for i = 1:num
    if isempty(data{i})
        continue;
    else
        true_means(i,1) = mean(data{i});
        sd = std(data{i});
        true_means(i,2) = (sd*1.96*sqrt(1.15)) ./ sqrt(length(data{i}));
    end
end

%Comparisons between two tests
for i = 1:num
    for j = 1:num
        %Do not compare a test against itself (or against no data)
        if isempty(data{i}) || isempty(data{j}) || i ==j
            continue;
        else
            %KS Result
            h_table{i,j} = kstest2( data{i}, data{j},'alpha', 0.05);
            %Determine distance between true means ranges
            if true_means(i,1) > true_means(j,1)
                true_means_table{i,j} = (true_means(i,1) - true_means(i,2)) - (←
                    true_means(j,1) + true_means(j,2));
            else
                true_means_table{i,j} = (true_means(j,1) - true_means(j,2)) - (←
                    true_means(i,1) + true_means(i,2));
            end
        end
    end
end

%Save calculated results to excel file
if save
    xlswrite('Data_Analysis_Results.xlsx',h_table,'h','A1')
    xlswrite('Data_Analysis_Results.xlsx',true_means,'true_means','A1')
    xlswrite('Data_Analysis_Results.xlsx',true_means_table,'detectable_difference←
        ','A1')
end
```